CELLULAR FUSION IN THE MOUSE INTESTINE

by

Anne Elizabeth Powell

A DISSERTATION

Presented to the Department of Cell and Developmental Biology

And the Oregon Health and Science University

School of Medicine

In partial fulfillment of the requirements for the degree of

Doctor of Philosophy

April 2010

School of Medicine
Oregon Health & Science University

CERTIFICATE OF APPROVAL

This is to certify that the Ph.D. dissertation of

Anne Elizabeth Powell

has been approved

Mentor/Advisor

Committee Chair

Member

Member

Member

Member

Member

TABLE OF CONTENTS

LIST OF FIGURES

CHAPTER 1

CHAPTER 2

CHAPTER 3

CHAPTER 4

APPENDIX 1

APPENDIX 2

APPENDIX 3

LIST OF TABLES

CHAPTER 2

CHAPTER 3

APPENDIX 2

APPENDIX 3

ABBREVIATIONS

5-ASA	5-Aminosalicylic acid
ACD	Asymmetric cell division
ALCAM	Activated leukocyte cell adhesion molecule
APC/Apc	Adenomatous Polyposis Coli
APC	Allophycocyanin
aPKC	Atypical protein kinase C
BMDCs	Bone marrow derived cells
Bmp	Bone morphogenetic protein
Brat	Brain tumor
BrdU	5-Bromo-2-deoxyuridine
β-gal	beta-galactosidase
β-NF	beta-naphthoflavone
CBC cell	Crypt-base columnar cell
CLP	Common Lymphoid Progenitor
CMP	Common Myeloid Progenitor
CRC	Colorectal cancer
Cre	Cre-recombinase
CSC	Cancer stem cell
CT	Cycle threshold
Cy3	Indocarbocyanine
Cy5	Indodicarbocyanine
DAB	Diaminobenzidine
Dgl	Discs-large
DSI	Distal Small Intestine
DSS	Dextran sodium sulfate
DTT	Dithiothreitol
EDTA	Ethylenediaminetetraacetic acid
eGFP	Enhanced Green Fluorescent Protein
EMT	Epithelial-to-mesenchymal transition
ESA	Epithelial Surface Antigen
FACS	Fluorescence Activated Cell Sorting
FISH	Fluorescent *in situ* hybridization
FITC	Fluorescein
GALT	Gut-associated lymphatic tissue
γ–IR	Gamma irradiation
Gapdh	Glyceraldehyde 3-phosphate dehydrogenase
GFP	Green Fluorescent Protein
H&E	Hematoxylin and Eosin
HBSS	Hank's Buffered Saline Solution
HUGL-1	Human homologue of lgl-1
IEL	Intraepithelial lymphocyte
IHC	Immunohistochemistry
IL-1β	Interleukin-1β
IL-10	Interleukin-10

Ins	Inscutable
FACS	Fluorescence-activated cell sorting
Fz	Frizzled
Lgl	Lethal giant larvae
Lgr-5	Leucine-rich-repeat-containing G-protein-coupled receptor 5
Mchr1	Melanin-concentrating hormone receptor 1
Min/MIN	Multiple Intestinal Neoplasia
Mira	Miranda
mRNA	Messenger Ribonucleic Acid
Msi-1	Musashi-1
PBS	Phosphate Buffered Saline
PCR	Polymerase Chain Reaction
PE	Phycoerythrin
PI	Propidium iodide
Pins	Partner of Inscutable
Pros	Prospero
PSI	Proximal small intestine
qRT-PCR	Quantitative reverse transcriptase polymerase chain reaction
Scrib	Scribble
sFRP	Secreted Frizzled-related protein
SI	Small intestine
Std	Standard deviation
TA-cell	Transient amplifying cell
WBM	Whole bone marrow
WT	Wild-type
X-gal	bromo-chloro-indolyl-galactopyranoside

ACKNOWLEDGEMENTS

First I'd like to thank my thesis mentor, Missy, for her guidance throughout the process of pursuing my Ph.D. She has always been tremendously supportive and helpful, while teaching me to think critically and independently. Thank you, as well, to the members of the Wong lab present during my time here: Dr. Paige Davies, John Swain, Dr. Adria Dismuke, Trevor Levin, Christine Glynn, Dr. Alain Silk, Dr. Eric Anderson and Dr. Marcus Monroe- you made coming to work every day a lot of fun. Thank you, as well, for your scientific contributions to this dissertation.

Thank you to two other scientific mentors- Dr. Chuck Kunert and Dr. Jan Christian. Chuck, you have shown me what it means to be a tremendous mentor and teacher. As my professor and advisor at Concordia, you also have the distinction of being solely responsible for my interest in pursuing a Ph.D. Thank you for the opportunity you gave me. And to Jan- thank you for being my first scientific mentor and allowing me to pursue undergraduate research in your lab, nearly 9 years ago, where I first discovered what it is to really love bench science, even when it doesn't love you back. Thank you as well, for being the chairwoman of my Ph.D. thesis committee and supporting my research and development as a scientist in that capacity for the last 6 years.

. Thank you to my committee members: Dr, Jan Christian, Dr. Phil Streeter, Dr. Brian Johnstone, Dr. Caroline Enns and Dr. John Brigande. Thank you for your constructive comments and suggestions in helping to shape and guide my

Ph.D. over the last 6 years. This body of work would not be what it is today without your academic contributions. I am a better scientist for having your influence throughout my graduate career.

Thank you to my fellow graduate members of the Program for Molecular and Cellular Biosciences: Deanne Tibbitts, Christina Lorentz, Kirsten Verhein, Carole Kuehl, Bridget Robinson, Xiaoli Zhang, Abhinav Sinha, Damian Curtis, Tom Keck, Chang Liu, Paul Wille and Kristin Sauter. Many of you are the closest friends I have made. All of you made this experience tremendous. There is not a class better than this one. I am sure of it.

Thank you also, to my family who shaped the framework for who I am as a person today. Thank you for teaching me to be honest, inquisitive and persistent to a fault- little did you know you were instilling the 3 traits imperative to any good scientist. A very special thank you to my mom, who used every last penny she had, as a single mom, to send me to private school when I was very young and thereby affording me the best education possible in town. I still believe that is the very reason I am as successful as I have been.

Lastly and most importantly, thank you to my husband Brendon, who commuted 90 minutes every day just so that I could be closer to lab and not have to be the one to commute. You have been there for me through all of the late nights, long weekends, tolerated a 60 hour/week work week, and listened to all of my talks, over and over again, even if you didn't understand a word I was saying. You are now closing your business and making a tremendous sacrifice so that I

can pursue my scientific career across the country- thank you for that gift. It is remarkable. I am truly blessed to have you in my life.

ABSTRACT

Tissue regeneration after injury poses a major challenge that requires the fine balance between stimulation and dysregulation of cell proliferation in order to facilitate homeostatic repair. We have shown that fusion between circulating bone marrow-derived cells (BMDCs) and non-hematopoietic cells occurs in response to intestinal epithelial injury as a potential regenerative mechanism. We suggest that fusion also occurs in tumorigenesis based upon the observation of shared microenvironments between injury and tumor models. However, the cellular and environmental requirements for intestinal cell fusion remain unknown. Importantly, the physiologic impact of cell fusion on epithelial homeostasis and tumorigenesis has not been defined. Therefore, to investigate the physiologic relevance of this process in repair and disease, the work in this thesis will test the hypothesis that cell fusion hybrids represent a unique cellular population, retaining characteristics of both parental fusogenic populations. To test this hypothesis, I explored the microenvironmental mediators of cell fusion, identified the fusogenic cell populations within the BMDCs, and investigated and compared the transcriptome profile of cell fusion hybrids with their parental fusogenic cell types. Using both transplantation and parabiosis model systems, I identified two important environmental factors critical for mediating intestinal cell fusion: local inflammation and epithelial proliferation. Significantly, these factors characterize the regenerative and tumorigenic microenvironment. Further, temporal analysis of the cellular dynamics preceding epithelial cell fusion

revealed that GFP-expressing donor cells traffic to the intestine and cluster around hyperproliferative intestinal crypts, forming a pre-fusion complex. Interestingly, these clusters were composed of differentiated macrophages, B and T cells. This result led to a systematic survey of the fusogenic potential of FACS-isolated discrete blood cell populations, where I determined that macrophages are a primary BMDC fusion partner. Finally, to investigate the physiologic potential of intestinal cell fusion hybrids, comparative transcriptome analysis of cell fusion hybrids, unfused epithelia and unfused macrophages revealed that epithelial-like cell fusion hybrids retain a portion of the macrophage transcriptional profile. Taken together, this work provides a significant foundation for understanding the mechanism of cell fusion as well as the overall physiologic impact of cell fusion on intestinal epithelial regeneration and tumorigenesis. Importantly, the implication of inflammation in the cell fusion process coupled with the unique transcriptional potential of cell fusion hybrids suggests a potential role for cell fusion in linking intestinal inflammatory diseases and cancer.

CHAPTER 1

BACKGROUND AND INTRODUCTION

I. The Structure and Function of the Mammalian Intestine

A. Rapid renewal of the intestinal epithelium

B. Functional nutrient uptake reflected in the diversity of the proximal-distal axis

C. Intestinal barrier structure and function: physical boundaries and immune regulation

II. Intestinal regenerative response to injury

A. Cellular signaling pathways control intestinal response to injury

B. Tumorigenesis as a misregulated repair process

III. Implications for stem cell fusion

A. Intestinal stem cell fusion as a regenerative response to injury and implications for disease

B. Cell fusion with myeloid cells as a mechanism to acquire new properties

IV. Cellular fusion: requirements for fusion and implications for cell fate

A. Intrinsic factors that mediate intestinal cell fusion

B. Biological implications of cell fusion

V. Hypothesis and Rationale

The intestinal epithelium is critical to the survival of higher vertebrates in serving multiple functions including both nutrient uptake and as a barrier to the external environment. As such, the primary and secondary structure of the intestine is engineered to reflect its diverse functional capacity. The intestinal epithelial surface is organized as a single cell layer, exploiting secondary and cellular microvilli to optimize the absorptive surface area. Structurally and functionally, the epithelium is delineated into a gradient of proliferative to differentiated cells on the radial, or crypt-villus, axis. The intestinal epithelial stem cell resides in the proliferative crypt, a structural invagination that provides physical protection from environmental assault of the luminal contents. The stem cell and its immediate progeny are responsible for the continual renewal of the intestinal epithelium during homeostasis and are stimulated to proliferate in response to epithelial injury for maintenance of barrier function. Epithelial regeneration after injury is a well-described process, but the underlying molecular mechanisms are not clear. We have shown that cell fusion between the intestinal epithelium and cells of the mesenchyme acts as one mechanism for repair after injury. In addition, fusion event are enhanced in tumors, suggesting that the tumor microenvironment is more permissive for cell fusion. In order to determine if cell fusion plays a significant physiologic role in tumorigenesis, defining the microenvironmental factors involved in cell fusion is essential to guide our understanding of this process. Further, identification of the cellular partners will provide insight into the underlying mechanism mediating cell fusion as well as provide clues to the potential physiologic consequence of cell fusion hybrid

generation in both regenerative and tumorigenic contexts. The overall goal of my research is to investigate the cellular and microenvironmental factors in the context of cell fusion-mediated epithelial regeneration.

I. The Structure and Function of the Mammalian Intestine

The mammalian intestine possesses a diverse structure down its length to optimally serve its primary functions. Nutrient absorption is perhaps the most well-appreciated function attributed to the intestine. This process occurs in various stages down the entire length of the intestine and is mirrored by diverse physical characteristics of the small intestine (duodenum, jejunum, ileum) and the large intestine (colon, rectum). To facilitate its absorptive capacity, the surface area of the small intestine is expansive. In fact, the total epithelial surface area from an adult human intestine is $100m^2$, about the size of a tennis court (Artis 2008). In addition, the continuous layer of epithelium also serves as a barrier to protect the organism from the vast population of indigenous microorganisms residing on the intestinal luminal surface. In this capacity, the tightly joined polarized epithelial cell sheet overlying one of the body's largest reservoirs of immune cells acts as both a physical and immune barrier. Therefore it is clear that tight regulation of the epithelial and mesenchymal cell programs down the length of the intestine are critical to the survival of the organism.

A. Rapid renewal of the intestinal epithelium

The intestine is organized into two anatomically distinct regions: the small and large intestine. Both regions are characterized by a continuous single layer of simple columnar epithelia that undergoes rapid renewal supporting tissue homeostasis. The epithelium is physically organized along the radial axis in a gradient of undifferentiated cells that reside in a proliferative zone, to terminally differentiated cells that reside in a functional zone (Figure 1.1). The proliferative zone is a physically protective invagination called the crypt of Lieberkühn which harbors intestinal stem cells as well as the transient-amplifying (TA) cell population (van der Flier and Clevers 2009). The cells in the proliferative zone give rise to the terminally differentiated cells that reside within the functional zone of the intestine. In the small intestine, the functional zone is comprised of numerous villi or finger-like projections that extend into the intestinal lumen. Characteristically, the villus structures are absent in the large intestine and are replaced by differentiated cells that encircle the opening of the crypt and are called colon cuff cells. Delineation of proliferative and functional regions along the radial axis allows for efficient and effective epithelial self-renewal that is driven by the crypt-based stem cell population.

The intestinal epithelial stem cells are physically located near the base of the proliferative crypt below the TA cells. The stem cells are stimulated to undergo asymmetric cell division regenerating the stem cell while producing a TA or daughter cell. The TA population is largely responsible for expanding the progenitor pool within the crypt and directly gives rise to the differentiated

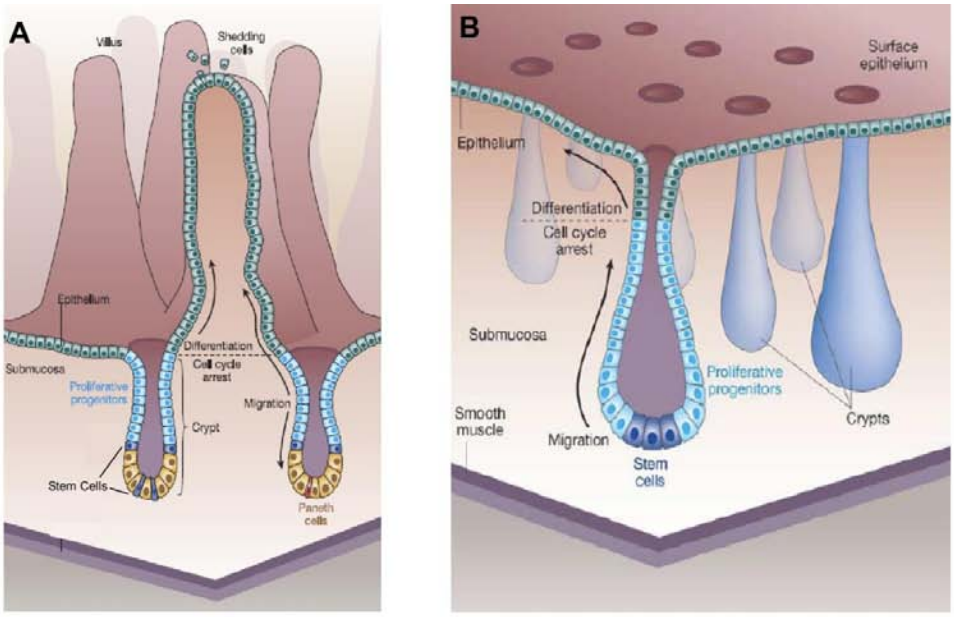

Figure 1.1 Tissue anatomy of the adult small and large intestine. (A) Cartoon of the small intestinal epithelium. Putative stem cells (dark blue) reside immediately above the Paneth cells (yellow) and in the crypt bottom. Proliferating progenitor cells occupy the remainder of the crypt. Differentiated cells (green) populate the villus, and include goblet cells, enterocytes and enteroendocrine cells. (B) Cartoon of the large intestinal epithelium. Putative stem cells (dark blue) reside at the crypt bottom. Proliferating progenitor cells occupy two-thirds of the crypt. Differentiated cells (green) populate the remainder of the crypt and the flat surface epithelium. Reprinted by permission from Macmillan Publishers Ltd: Reya et al., Nature 434, 843–850. © April 2005

epithelial lineages (Barker, van de Wetering et al. 2008). Although the exact number of stem cells within each crypt and the exact identity of the stem cell remain controversial, it is generally believed that the proliferative crypt harbors 5-6 multi-potent stem cells (van der Flier and Clevers 2009). Additionally, the specific location of the intestinal stem cells within the intestinal crypt is debated. Label-retaining studies identified a long-lived progenitor population located at cell position 4 (or "+4") from the base of the small intestinal crypt (Potten, Kovacs et al. 1974) (Figure 1.2A). This +4 stem cell expresses the polycomb protein Bmi1 and is capable of giving rise to all of the differentiated epithelial intestinal lineages within the mouse (Sangiorgi and Capecchi 2008), providing evidence that this cell population is a likely candidate for the intestinal epithelial stem cell (Figure 1.2B). However, a group of crypt-based columnar-shaped cells represent a second population of viable stem cell candidates, located in the base of the crypt and intermixed between differentiated Paneth cells (Bjerknes and Cheng 1999). These cells express Lgr5 (leucine-rich-repeat-containing G-protein-coupled receptor 5) (Barker, van Es et al. 2007) (Figure 1.2C), give rise to all four principal differentiated lineages *in vivo*, and undergo clonal expansion after mutagenesis. Further, these cells have been grown in culture from single cell isolates and shown to generate all four differentiated lineages (Sato, Vries et al. 2009). It is possible that these discrete progenitor populations exist within a hierarchy along the gradient of lineage differentiation. Clearly, the exact relationship between these populations and the differentiated lineages remains to be determined.

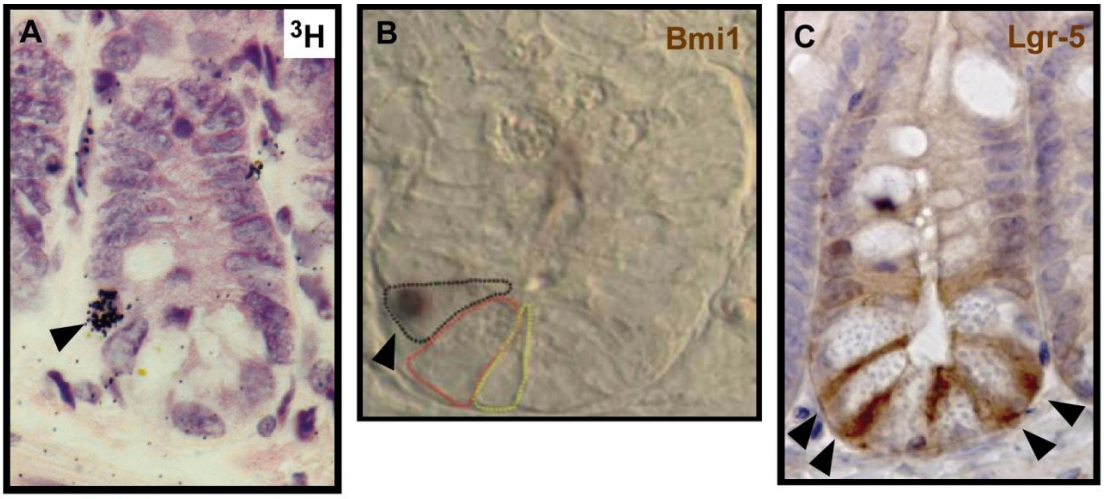

Figure 1.2. Labeling intestinal stem cells. (A) A tissue section from a mouse small intestinal crypt with autoradiographic silver grains overlying a single nucleus in the "+4" stem-cell region, stained with Hematoxylin and Eosin. Black arrowhead indicates the stem cell. Modified and reprinted by permission from Copyright Clearance Center. J. Clin. Invest. 105(11): 1493-1499 © June 2000. (B) Bmi1 expression in a Bmi1Cre$^{ER/+}$;Rosa26$^{LacZ/+}$ mouse. Bmi1 is expressed in a cell (black dashed line, black arrowhead) located above a Paneth cell (red dashed line). Next to the Paneth cell, a crypt base columnar cell is visible(yellow dashed line). Reprinted by permission from Macmillan Publishers Ltd: Sangiorgi et al., Nature 40, 915-920. © June 2008. (C) Lgr5^{+}intestinal stem cells. GFP-staining of an Lgr5 knock-in allele showing that Lgr5 is expressed only in the crypt base columnar cells that are located in between Paneth cells. Modified and reprinted by permission by Annual Reviews: van der Flier et al., Annu. Rev. Physiol. 2009. 71:241–60. © 2009.

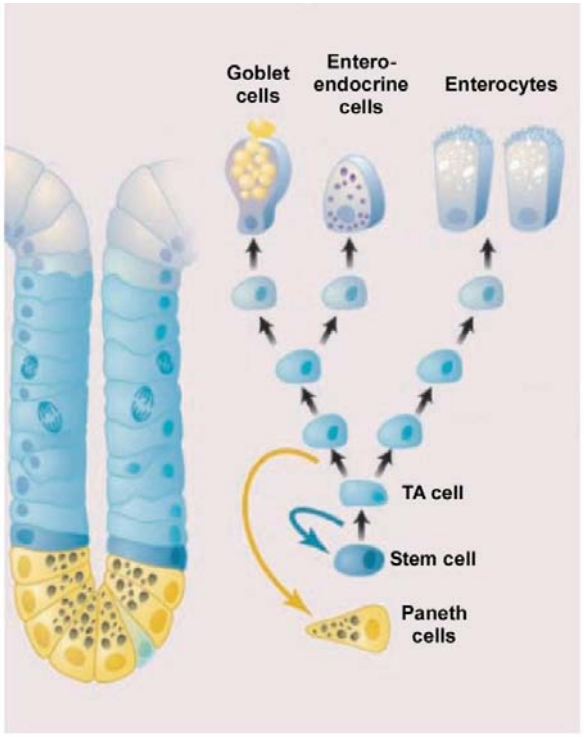

Figure 1.3. The cell lineages of the small intestine. The lineage scheme depicts the stem cell which asymmetrically divides and gives rise to the transit-amplifying cells (TA cells). The TA cells divide into the absorptive and secretory differentiated cell lineages. The right branch constitutes the enterocyte lineage; the left is the secretory lineage, comprised of the Paneth (yellow), Goblet and Enteroendocrine cells. Relative positions along the crypt-villus axis correspond to the schematic graph of the crypt on the left. From Radtke et al., Science 307, 1904 (2005). Reprinted and modified with permission from AAAS.

The intestinal stem cell is multi-potent and provides diversity along the radial axis (cypt-villus or crypt-cuff). Four principal, terminally differentiated epithelial lineages are represented within the small intestine: absorptive enterocytes, hormone-secreting enteroendocrine cells, mucous-secreting goblet cells and immune-regulatory Paneth cells (Figure 1.3). In the small intestinal crypt, immature enterocytes, enteroendocrine cells and goblet cells migrate up onto the villus as they undergo terminal differentiation. These cells continue to migrate up the villus before undergoing apoptosis or are sloughed off into the lumen at the villus tip. In contrast, the Paneth cells undergo a downward migration to the base of the crypt. In the large intestine, the differentiated cells undergo an upward migration onto the crypt “cuff”, a subset of cells that bridge two crypts. It is of note that the colon does not contain Paneth cells (Booth and Potten 2000). The census of differentiated cells present within the epithelial compartment changes down the length of the intestine, and this is directly related to the different functional roles the epithelium serves from the most proximal small intestine to the most distal portion of the large intestine. In both regions, all differentiated cell types cooperate to perform both nutrient absorption and protective barrier functions of the intestine, and thus maintenance of the epithelia in the face of continual self-renewal is critical to the viability of the intestine and host organism.

B. Functional nutrient uptake reflected in the diversity of the proximal-distal axis

Both the small and the large intestine serve unique functions in nutrient absorption. The most proximal region of the small intestine, the duodenum, primarily functions in optimized fluid and nutrient absorption. To facilitate this role, the duodenal villi are elongated and tightly packed for optimal surface area. Nutrient transporters are clustered at the apical surface of the polarized epithelium within this region and are critical for the absorption of metals, vitamins and minerals obtained from the diet (Schuck and Simons 2004). In a gradient fashion down the length of the small intestine, the villi become shorter and less closely spaced and the expression pattern of the nutrient transporters changes as the need for nutrient absorption decreases. For example, metal transporters, including those for iron and copper, are exclusively expressed in the proximal small intestine (Kaplan and Lutsenko 2009; Simpson and McKie 2009). Alternatively, the bile acid transporter is a key transporter restricted to the most distal region of the small intestine and functions to recycle bile acid, a critical component of cholesterol synthesis (Wong, Oelkers et al. 1994). Transition into the large intestine is physically defined by the absence of villi. This structural change reflects the functional shift from a nutrient absorptive capacity to one of salvage by the activity of the indigenous microbiota (Falk, Hooper et al. 1998). The large intestine is also a primary location for fluid absorption, which is accommodated by the increase in surface area in the secondary structure of the colon. In lower vertebrates, the cecum is a large pocket-like structure that adjoins

the ileum of the small intestine to the colon. In humans, the cecum is replaced by the appendix, which joins the ileum to the colon and is largely a rudimentary organ. Functionally, the diverse primary intestinal structure is elegantly coupled with the diverse cellular composition down the length of the intestine to efficiently dictate nutrient absorption.

The vast majority of cells that comprise the intestine are absorptive enterocytes, reflecting its tremendous absorptive capacity. As such, enterocytes are the primary epithelial lineage of the proximal small intestine. A second major epithelial lineage is the mucin-secreting goblet cell. Although these cells are scattered throughout the small intestine, they exist in an inverse gradient down the length, more concentrated in the distal region. Increased secretion of mucins facilitates passage of luminal contents as their aqueous content is decreased. The unstirred mucin bilayer provides a protective coating for the intestinal epithelium, preventing injury from shearing. Functionally consistent, and in contrast to the proximal small intestine that exhibits a high enterocyte to goblet ratio, the large intestine harbors primarily goblet cells. Although the intestine is physically diverse, it coordinately functions to efficiently absorb nutrients without waste.

C. Intestinal barrier structure and function: physical boundaries and immune regulation

The small and large intestine are highly subject to microenvironmental assaults, due to their contact with the luminal contents originating from the

external environment. Guarding against these assaults, the intestinal epithelium provides a substantially protective physical and immunological barrier down its length. The physical barrier is comprised of structurally organized epithelial cells connected by tight junctions, resulting in a cohesive sheet of cells. The immunological barrier consists of blood cells present within the epithelial compartment and is basolaterally juxtaposed to the epithelium, constantly surveying the intestinal environment for invasion of harmful pathogens (Figure 1.4).

The physical barrier, maintained by the epithelial cells, is a first line protection from the environment. The majority of intestinal epithelial cells have actin-rich microvilli that physically impede microbial attachment and invasion, and the intestinal epithelial goblet cells secrete mucins, generating an impermeable protective layer over the apical side of the epithelial cells (Turner 2009). Below this protective layer, the epithelial plasma membranes of the small and large intestine harbor both tight and adherens junctions. The tight junctions are almost entirely impermeable to most hydrophilic material and, therefore, passage of specific nutrients requires transepithelial transport governed by both the size and charge of the molecules and is directly related to the absorptive properties of both the small and large intestine. Specifically, essential cations such as Mg^{2+}, Ca^{2+}, Na^{+} and H^{+} are actively transported or exchanged through this tight barrier, while potentially hazardous materials are excluded, thereby protecting the organism (Turner 2009). The regulation of transepithelial transport is also governed by adherens junctions, another critical component of the physical

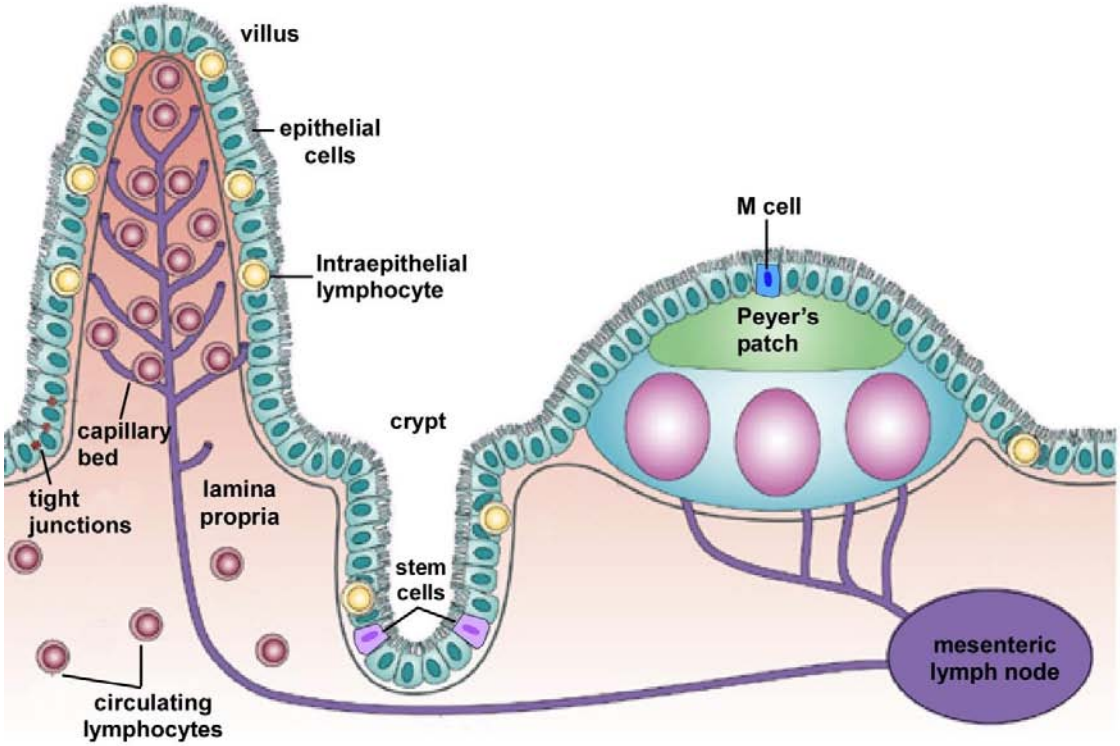

Figure 1.4. Gut-associated lymphatic tissue (GALT) of the small intestine. Lymphocytes and leukocytes circulate throughout the GALT of the small intestine passing in between the local mesenteric lymph nodes (purple), Peyer's patches and capillary bed of the lamina propria. The epithelial cells (green) on both the vilus and crypt harbor tight junctions between them, acting as a barrier between the GALT and the luminal space. Intraepithelial lymphocytes (yellow) are located in the epithelial compartment at the basolateral membrane. The M cell (blue) is located within the Peyer's patch epithelium. Adapted and reprinted by permission from Macmillan Publishers Ltd: Cheroutre et al., Nature Reviews Immunology 4, 290–300. © April 2004

barrier. Adherens junctions are comprised of adhesive proteins that are absolutely required to maintain epithelial integrity via the preservation of cell-to-cell adherence, as loss of adherens junctions results in changes in cellular differentiation and cell death (Hermiston and Gordon 1995). Adherens junctions also facilitate intracellular communication to regulate epithelial polarization (Turner 2009). Both the small and large intestinal epithelium are polarized, harboring functionally distinct apical and basolateral regions. Polarization is important for nutrient absorption, but also for maintenance of appropriate regulation between the luminal and mesenchymal areas of the organ. Loss of cell polarization results in the loss of intestinal differentiation and subsequent cell death, thereby compromising the intestinal barrier (Hermiston and Gordon 1995).

The immune system of the intestine acts as a second line of defense in protecting the organism, as its primary role is to destroy and remove invading microbes and viruses from the body. Indeed, as a primary barrier to the external environment in the face of a vast presence of commensal microbiota, the intestine is one of the largest immunoregulatory organs in the body. Intestinal immunological response is mediated by both the epithelial cells as well as the blood-derived cells organized throughout the intestine termed gut-associated lymphatic tissue (GALT) (Figure 1.4). In the epithelial compartment, microfold cells (M cell; Figure 1.4) are responsible for transporting organisms and particles from the gut lumen to immune cells across the epithelial barrier, and thus are important in stimulating mucosal immunity. Paneth cells of the small intestine secrete antimicrobial peptides, including defensins and cryptidins, which protect

against microbial colonization by forming pores in bacterial cell walls and promoting the rapid apoptosis of the invading bacteria (Porter, Bevins et al. 2002; Wehkamp, Chu et al. 2006). Such a rapid response to bacterial invasion is essential for preserving the total number of bacteria to a level permissive for symbiosis.

Present in a population 10 times greater than the total number of somatic cells in the human body, approximately 10^{14} commensal microbiota reside in the human intestinal lumen and maintain a symbiotic relationship with their hosts (Hooper and Gordon 2001; Backhed, Ley et al. 2005). The moist environment of the intestine provides a hospitable environment wherein commensal bacteria can thrive. In return, the bacteria facilitate digestion and absorption of material that the epithelium is unable to process. Further, they also promote angiogenesis (Hooper, Stappenbeck et al. 2003) and, importantly, compete with harmful pathogens for nutrients and physical space within the microenvironmental niche (Xu and Gordon 2003). Moreover, commensal intestinal microbiota are required for proper development, differentiation and function of immune regulatory blood cells present in the GALT, and mice that lack commensal bacteria from birth cannot properly activate their immune system to respond to foreign pathogens (Gordon 1959; Helgeland, Vaage et al. 1996; Macpherson and Harris 2004).

As scavengers, the intestinal microbiota primarily reside in the distal small intestine and colon. Accordingly, the immune cells within the GALT are organized down the length of the intestine, with larger immune structures clustered distally. Immunologically responsive intraepithelial lymphocytes reside in the epithelial

compartment and are present throughout the length of the small intestine (Guy-Grand, Cerf-Bensussan et al. 1991; Hayday, Theodoridis et al. 2001). Intraepithelial cells are a subpopulation of T cells that function in adaptive immunity to monitor epithelial damage, survey for pathogens and relay information to the other immune-regulatory cells within the GALT (Figure 1.4). As the bacterial census increases down the intestinal length, so does the immunological protective barrier. In the distal small intestine, specialized immunoregulatory aggregates called Peyer's patches are strategically located in the mesenchyme below the epithelium and harbor both lymphocyte and leukocyte populations (Figure 1.4). These cells are responsible for coordinating an immunologic response to the presence of foreign pathogenic antigens as they migrate throughout the intestinal capillary beds in the lamina propria, on the basolateral side of the intestinal epithelium. Intestinal macrophages and dendritic cells extravasate out of capillaries and position themselves in between the junctional complexes of epithelial cells to sample intestinal lumen antigens and trigger an innate immune response to all foreign pathogens, as well as initiate the T and B cell-mediated adaptive response. Critically, these antigen-detecting cells are able to discern between commensal bacteria and foreign pathogens to primarily relegate an immune response to the harmful microbiota.

II. Intestinal regenerative response to injury

Proper and carefully orchestrated regulation of intestinal epithelial self-renewal is essential to the survival of the intestine. In response to epithelial

injury, a number of developmental signaling pathways are stimulated to facilitate epithelial regeneration. These same signaling pathways, when disregulated, have been implicated in intestinal tumorigenesis. This observation highlights the close relationship between accurate epithelial regeneration after injury and disease.

A. Cellular signaling pathways control intestinal response to injury

The Wnt, BMP and Notch cellular signaling pathways are critical for intestinal development, epithelial homeostasis and are also elicited during epithelial regeneration (Scoville, Sato et al. 2008). A prime example is the essential requirement of the Wnt signaling pathway in epithelial proliferation and expansion during development, homeostasis, its stimulation after epithelial injury (Potten 1977; Davies, Dismuke et al. 2008- see Appendix 3), and its dysregulation resulting in hyperproliferation and tumorigenesis (Reya and Clevers 2005). In these contexts, the Wnt signaling pathway regulates the cell cycle and stem and/or progenitor cell division to initiate the cascade of proliferation to differentiation that is essential for epithelial regeneration. Additionally, it is thought that mesenchymal cells are recruited to the site of injury and secrete Wnt stimulatory ligands (Pinto, Gregorieff et al. 2003; Davies, Dismuke et al. 2008- see Appendix 3). A second signaling pathway, the BMP pathway, works in concert with the Wnt pathway to promote intestinal stem cell self-renewal and proliferation of the TA population. Bmpr1a mutant mice develop hyperproliferative intestinal polyps, reminiscent of proliferative epithelial defects

in patients with juvenile polypsis syndrome (He, Zhang et al. 2004). In response to injury, the BMP signaling pathway acts on a downstream component of the Wnt signaling pathway, β-catenin (Crosnier, Stamataki et al. 2006). Activation of the Wnt signaling pathway causes β-catenin to translocate to the nucleus and bind transcriptional activators to promote expression of downstream genes involved in the control of cellular proliferation. A third important pathway regulating intestinal epithelial renewal is the Notch signaling pathway, which directs epithelial lineage commitment of the nascent daughter cells (Crosnier, Stamataki et al. 2006). Mice harboring mutant *Hes1,* a Notch target gene, have an increased number of mucus secreting and enteroendocrine cells at the expense of absorptive enterocytes (Jensen, Pedersen et al. 2000). Consistent with a role for Notch signaling in cell fate decision-making during epithelial renewal, Notch1 null mice have depletion of intestinal secretory lineages and increased proliferation (Fre, Huyghe et al. 2005). Together, coordinate regulation of these essential signaling pathways is critical to proper stem cell self-renewal in intestinal homeostasis and maintenance of epithelial integrity after injury.

B. Tumorigenesis as a misregulated repair process

Signaling cascades essential for intestinal self-renewal are often dysregulated in hereditary and sporadic intestinal cancers. Studies in mice have demonstrated that misregulation of these signaling pathways can lead to intestinal epithelial tumorigenesis (Moser, Pitot et al. 1990; He, Zhang et al. 2004). Specifically, persistent stimulation of the Wnt signaling pathway results in

hyperproliferative epithelia and initiates intestinal cancer formation in both humans and mice (Reya and Clevers 2005). Patients with Familial Adenomatous Polyposis inherit inactivating mutations in the gene *Adenomatous Polyposis Coli* (*APC*), a critical intracellular mediator of the Wnt signaling pathway. These patients acquire numerous intestinal adenomas that can transform to carcinoma (Groden, Thliveris et al. 1991; Joslyn, Carlson et al. 1991; Korinek, Barker et al. 1997; Bienz and Clevers 2000). While the Wnt signaling pathway is the dominant mediator of intestinal tumorigenesis, the BMP and Notch pathways have been implicated as well: mutations in the BMP pathway have been found in juvenile polyposis syndrome, an inherited polyposis syndrome that predisposes humans to colorectal cancer (Hardwick, Kodach et al. 2008); and maintenance of undifferentiated, proliferative cells in adenomas requires the concerted activation of the Notch and Wnt cascade (Crosnier, Stamataki et al. 2006). Due to the role of developmental signaling pathways in regulating proliferation, it is not surprising that mutations within these pathways also control tumorigenesis.

III. Implications for stem cell fusion

Cells derived from the blood compartment have been demonstrated to incorporate into injured tissues and function to enhance tissue regeneration (Ferrari, Cusella-De Angelis et al. 1998; Lagasse, Connors et al. 2000). However, the mechanism by which this process impacts physiologic repair and function is controversial. It was speculated that blood cell progenitors possessed a plasticity that allowed them to “transdifferentiate” down various cell lineages to

participate in repair of the injured tissue. As such, initial transplantation experiments incorporating genetically tagged bone marrow into recipient mice attributed the presence of donor-derived cells in injured tissue as transdifferentiation (Brazelton, Rossi et al. 2000; Jackson, Majka et al. 2001; Krause, Theise et al. 2001; Orlic, Kajstura et al. 2001). These early conclusions were quickly dispelled, when a closer evaluation of the donor-derived cells revealed that they were tetraploid in the brain (Weimann, Johansson et al. 2003) or harbored both donor and recipient markers. Thus, cell fusion emerged as an alternative mechanism by which blood-derived cells may participate in tissue regeneration. Since cellular fusion plays an essential role in many essential biological functions including fertilization, formation of bone and placenta, and the innate immune response (Chen and Olson 2005), it was possible that blood cells also harbored the capacity to fuse with organs of interest in a regenerative response to disease. Supporting this hypothesis, cells from the bone marrow fuse with embryonic stem cells in culture harboring DNA from both the bone marrow and the embryonic stem cell parental cell types (Terada, Hamazaki et al. 2002). Although the physiologic relevance of this observation is still being clarified, it is intriguing to speculate that cell fusion may result in the delivery of undamaged genetic material to cells that have a compromised genome and is, therefore, a critical regenerative response to tissue injury.

A. Intestinal stem cell fusion as a regenerative response to injury and implications for disease

Cell fusion represents an intriguing mechanism by which the intestine undergoes repair after injury. Bone marrow transplantation of donor GFP-expressing cells into a lethally irradiated β-galactosidase-expressing recipient mouse resulted in the detection of donor-marked cells within the intestinal epithelium (Rizvi, Swain et al. 2006). A closer examination of donor-derived cells revealed the expression of both donor and recipient markers, suggesting that cell fusion is the mechanism underlying the incorporation of BMDCs into the intestinal compartment (Figure 1.5). Interestingly, GFP expression was detected in all of the differentiated intestinal epithelial lineages, providing evidence that intestinal epithelial fusogenic partner was a multi-potent stem or progenitor cell (Rizvi, Swain et al. 2006). Corroborating this observation, GFP-expressing epithelial cells persisted for more than 17 months after transplantation, further implicating a long-lived progenitor cell as the epithelial target for fusion. It is known that exposure to gamma-irradiation (γ-IR) results in an apoptotic response within proliferative cells of the crypt (Potten, Owen et al. 1990) and a corresponding stimulation of dormant stem cells to divide in a Wnt-mediated fashion (Davies, Dismuke et al. 2008- see Appendix 3). Therefore, it is possible that BMDCs fuse with intestinal stem or progenitor cells that have actively entered the cell cycle.

Interestingly, intestinal cell fusion hybrids are mononucleated (unpublished observation). This result is in contrast to other systems where cell fusion results in binucleated cells (Wang, Willenbring et al. 2003; Weimann, Johansson et al.

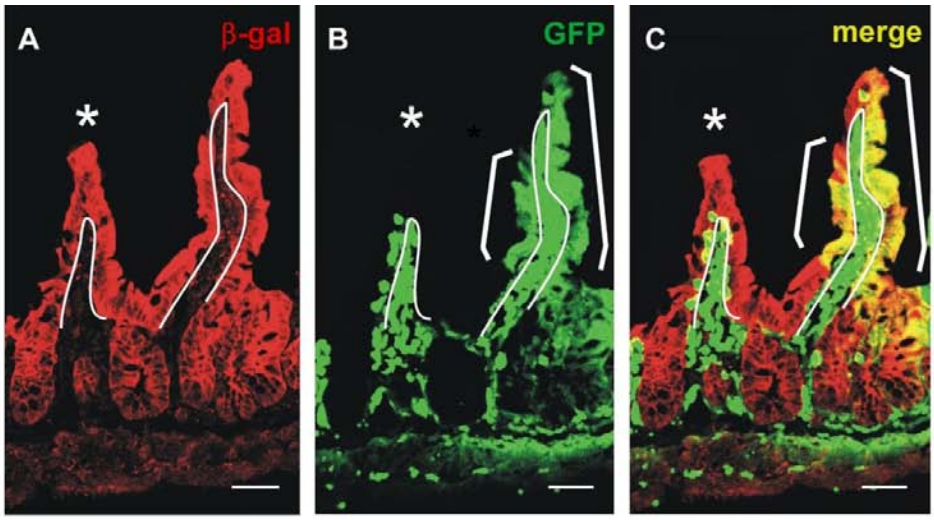

Figure 1.5. Fusion between BMDCs and intestinal epithelium. Intestinal tissue section from a β-gal-expressing recipient transplanted with GFP-positive BMDCs was analyzed for coexpression of β-gal and GFP by confocal microscopy. White line indicates the boundary between the epithelium and lamina propria. White asterisk denotes a villus lacking GFP epithelial expression. (A) β-gal (red) is uniformly expressed in the intestinal epithelium as detected with antibodies to β-gal and cy5-conjugated secondary antibodies. (B) GFP expression (green) on the same tissue section as A detected by direct fluorescence. (C) Merge of β-gal- and GFP-stained tissue showing colocalization of markers for both donor and recipient populations (yellow). Epithelial cells expressing β-gal only appear red, and GFP-positive lamina propria cells are green. Scale bars: 25 μm. Reprinted with permission. Rizvi et al., PNAS vol. 103 no. 16 6321-6325. Copyright 2006 National Academy of Sciences, U.S.A.

2003). One possible explanation for the existence of mononucleated cell fusion products within the intestinal epithelium is that the intestinal environment actively selects for cells that have a normal DNA content. The rationale supporting this intriguing hypothesis is that the progeny of stem cells continue to divide for multiple rounds and must execute this process with high fidelity to avoid the propagation of errors that could impede cytokinesis. One possible mechanism by which a cell fusion hybrid may reduce its DNA content is by reduction division. Indeed, there is precedent for unequal reduction division after fusion in the liver (Duncan, Hickey et al. 2009). Therefore, it is intriguing to speculate that while cell fusion may be a mechanism that facilitates epithelial regeneration after injury, the process of reduction division may contribute to tumorigenesis in the solid organs. Interestingly, we showed that cell fusion occurs in the epithelium of mice prone to colorectal tumors (Rizvi, Swain et al. 2006) and I have data demonstrating that fusion occurs at a higher incidence in these mice compared to wild-type (Figure 1.6). These data collectively suggest that fusion may also play an important role in intestinal tumorigenesis, however this possibility has not been fully investigated.

B. Cell fusion with myeloid cells as a mechanism for acquiring new properties

In many instances where BMDCs fuse with somatic or stem cells, the resulting hybrid cells are aneuploid or polyploid (Alvarez-Dolado, Pardal et al. 2003; Wang, Willenbring et al. 2003; Weimann, Johansson et al. 2003).

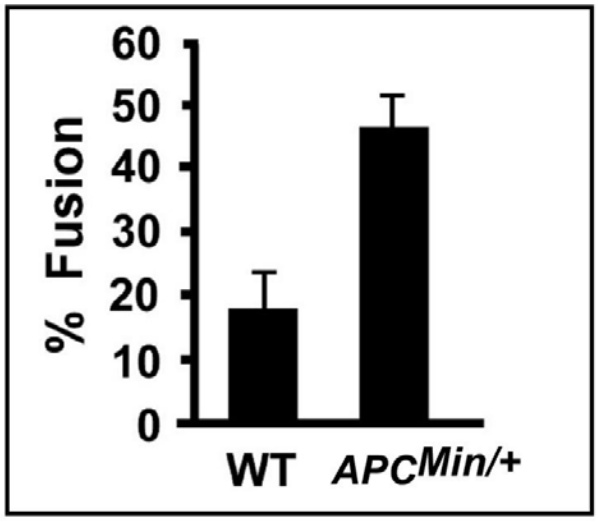

Figure 1.6. Fusion is increased in a tumorigenic setting. Distal small intestines from *ROSA26* (wild-type; WT) and $APC^{Min/+}$ mice transplanted with $1.8x10^6$ GFP^+ WBM were examined for fusion. $APC^{Min/+}$ mice exhibit higher levels of fusion when compared to *ROSA26* mice.

Abnormal chromosomal content is a hallmark of many cancer cells and this loss or gain of chromosomes is directly related to the tumorigenicity of a given population (Duesberg and Li 2003; Vogelstein and Kinzler 2004). In many cases, changes in chromosomal complement affect the cell's ability to properly grow and divide. Further, chromosomal rearrangements may contribute to gain of function mutations allowing cells to obtain characteristics that they did not previously possess.

Supporting this idea, *in vitro* studies from over 30 years ago demonstrated that cancer cells are more fusogenic than non-tumor cells and they acquire more aggressive tumorigenic phenotypes by fusing with BMDCs (Goldenberg 1968; Mekler 1971). Many malignant and metastatic cell types share similar genetic expression profiles with migratory cells from the myeloid blood lineage (Pawelek 2005). In theory, myeloid cells could convey their migratory properties to tumorigenic cells through cell fusion. Interestingly, the macrophage is one such myeloid cell type that is fusogenic in nature, as it self-fuses in the foreign body giant cell response of the innate immune system. Thus, macrophages are prime candidates for fusion with tumor cells, as they already harbor the proper cellular machinery that can facilitate cell fusion. In addition, macrophages are recruited to sites of tumorigenesis and represent a distinct population termed tumor-associated macrophages (Mantovani, Schioppa et al. 2006). It is possible that these cells may exploit their fusogenic capability to fuse with tumor cells and generate tumor-macrophage cell fusion hybrids that have certain phenotypic characteristics of a true macrophage, such as migration. Indeed, malignant

metastatic tumor cells acquire the capacity to migrate to distant sites and evade the immune system. While this epithelial-to-mesenchymal transition (EMT) is only one aspect metastatic behavior, EMT is critical to cancer aggressiveness and yet underlying mechanism for EMT is not clearly defined. Cell fusion with bone marrow-derived macrophages represents an intriguing avenue to promote EMT. Therefore, identifying the blood-derived cells capable of fusing with the intestinal epithelium represents a critical first-step in fully understanding fusion in regeneration and in tumorigenesis.

IV. Cellular fusion: requirements of fusion and implications for cell fate

The physiologic implication of BMDC fusion in tissue regeneration and tumorigenesis remains unclear. However, cell fusion occurs at an appreciable level in the intestine, suggesting this process plays an important role. Insights uncovered by examining the cellular and microenvironmental properties required for cell fusion will provide a basis for understanding how this process is involved in tissue homeostasis. Further, donor-specific genetic markers are maintained within cell fusion hybrids, suggesting that additional donor-specific genes are also retained after fusion. This provides the intriguing possibility that the donor cell transcriptome may effectively influence the phenotype of the cell fusion hybrid and in this capacity, a cell fusion hybrid could have a proliferative or survival advantage during epithelial regeneration or in tumorigenesis. Ultimately, examination of these factors will provide insight into the physiologic relevance of intestinal cellular fusion and has the potential to impact treatment of disease.

A. Intrinsic factors that mediate intestinal cell fusion

The microenvironmental factors that promote cell fusion are largely unexplored. My data demonstrates that BMDC-epithelial fusion occurs at a higher rate in mice harboring intestinal adenomas compared to wild-type mice (Figure 1.6), suggesting that the tumor microenvironment is supportive of cell fusion. It is well-documented that intestinal tumors are characterized by both increased epithelial proliferation and an active inflammatory response (Moser, Pitot et al. 1990; Karin and Greten 2005; Reya and Clevers 2005; Karin 2008) providing a basis for exploring the role of proliferation and inflammation in the cell fusion process.

The extent of cell fusion reported in the continually proliferative intestinal epithelium (Rizvi, Swain et al. 2006) is higher than other in organs that do not self-renew or do so at a much slower rate (Johansson, Youssef et al. 2008; Nygren, Liuba et al. 2008), supporting the idea that a proliferative state may be important for the fusion process. Moreover, data from human bone marrow transplant patients also suggest that donor-derived intestinal epithelia arise from proliferative progenitors (Okamoto, Matsumoto et al. 2006). Examination of donor-derived epithelial cells with the proliferative cell marker Ki67 revealed that a subset reside in the proliferative portion of the intestinal crypt, suggesting that BMDC fusion has occurred with stem- or early progenitor epithelial populations. Currently, the direct requirement for cell proliferation in the fusion mechanism has yet to be investigated and is an aspect of cell fusion I investigate in my thesis work.

Inflammation represents a second factor suggested to be influential from our results of fusion in tumor-bearing mice. Interestingly, BMDC-neural cell fusion is increased chronic systemic inflammation by 10-100 fold over non-inflammatory models (Johansson, Youssef et al. 2008). Data from human intestinal tissues also supports the idea that chronic inflammatory states may increase BMDC fusion in the intestine (Okamoto, Matsumoto et al. 2006). Tissue from a female patient who had undergone a gender mismatched bone marrow transplant and subsequently developed acute graft-versus-host disease was examined for the presence of the donor-derived Y-chromosome in her intestinal epithelia. In comparison to tissue from patients that did not have graft-versus-host disease after transplantation, the chronically inflamed tissue had a 9-fold increase in donor-derived epithelia. Similarly, another female patient that developed a gastric ulcer after bone marrow transplantation harbored 40-50 times as many donor-derived epithelial cells in the regenerating epithelia of the stomach when compared to the surrounding normal epithelia (Okamoto, Matsumoto et al. 2006). While neither of these studies investigated fusion as a mechanism, the data strongly suggests that microenvironmental inflammation may be important for intestinal BMDC incorporation via cell fusion in humans.

Chronic inflammation is detrimental to the intestine in multiple ways. It is characterized by infiltration of both leukocytes and lymphocytes that leads to remodeling of the mucosal and intestinal structures as well as changes within the differentiated epithelial cells themselves (Baumgart and Carding 2007; Xavier and Podolsky 2007). To this end, there is increasing evidence suggesting that

chronic inflammatory status can be a precursor to intestinal cancer as patients with chronic inflammatory conditions have a 15% greater risk for developing colorectal cancer (Bernstein, Blanchard et al. 2001; Eaden, Abrams et al. 2001). Therefore, investigating the contribution of inflammation-mediated cellular fusion in tumor progression is an intriguing possible mechanism for linking inflammation and cancer and is an aspect of cell fusion I investigate in my thesis work.

B. Biological implications of cell fusion

Although cell fusion is a likely mediator of intestinal regeneration after injury, the physiologic impact of cell fusion hybrids is not known. While cell fusion is an intriguing avenue for tissue regeneration and an exciting potential opportunity for gene therapy, it is also possible that cell fusion hybrids are unstable and could promote tumorigenesis. For this reason, it is critical to determine if there are significant transcriptome-wide alterations in the cell fusion hybrids.

The only example of circulating hematopoietic cells fusing with somatic cells for gene therapy is in the case of defective liver hepatocytes. Vassilopoulos and colleagues elegantly employed bone marrow transplantation as a means for introducing a wild-type gene into *Fah*$^{-/-}$ hepatocytes in a mouse model of tyrosinemia type I (Vassilopoulos, Wang et al. 2003). Surprisingly, the clonal expansion of hepatocytes harboring wild-type *Fah* rescued the transplant recipients. In this setting, circulating *Fah*$^{+/+}$ BMDCs fused with the *Fah*$^{-/-}$ hepatocytes, effectively replacing the null allele. In a subsequent study,

Willenbring and colleagues identified the granulocytic macrophage progenitor and differentiated macrophage as the fusogenic cells within the bone marrow that participate in liver cell fusion (Willenbring, Bailey et al. 2004). While macrophages are known to be highly fusogenic cells (Vignery 2005), this was the first *in vivo* evidence that macrophages or their progenitor cells could undergo fusion with somatic cells and facilitate the rescue of a disease phenotype. Determining BMDC that mediates intestinal cell fusion is an important aspect of my thesis work. These investigations are an important first step for elucidating the biological requirements for cell fusion, and will provide direction and guidance to understand the implications of cell fusion on cell fate.

Cellular fusion with myeloid cells leads to migratory, invasive phenotypes in culture, suggesting that the act of fusion results in alterations of the transcriptome (Pawelek 2000). Supporting this idea, genomic analysis performed on *in vitro*-generated cell fusion hybrids (Palermo, Doyonnas et al. 2009) indicated that a donor-specific subset of transcriptional markers was maintained in the cell fusion hybrids. Despite these analyses, it is still unclear how and to what extent fusion hybrids are transcriptionally unique. It is clear that unveiling the distinctions between the cell fusion hybrid transcriptome and that of wild-type epithelium will shed light on the physiologic significance of intestinal cell fusion, both in a regenerative and tumor context. To this end, an important focus of my thesis research is to define transcriptional alterations within the cell fusion hybrid population compared to their parental lineages.

V. Hypothesis and Rationale

Cell fusion between BMDCs and non-hematopoietic cells is a well-established observation in multiple organ systems; however the physiologic consequence of cell fusion is unclear. Identification of factors involved in this process is an essential starting point for dissecting the physiologic impact of cell fusion in regeneration and disease. My research goal is to elucidate the cellular dynamics that support cell fusion-mediated intestinal epithelial regeneration, specifically defining the cellular participants, identifying the environmental factors promoting fusion and investigating the physiologic fate of the cell fusion hybrid.

Hypothesis: Based upon the observations that a tumor microenvironment promotes intestinal epithelial cell fusion, I hypothesize that extrinsic factors, such as microenvironmental inflammation, and intrinsic factors, such as epithelial proliferation, play an essential role in mediating cell fusion in a regenerative context. Additionally, I hypothesize that the key fusogenic bone marrow-derived lineage is the macrophage. Finally, I hypothesize that cell fusion hybrids are transcriptionally unique from either of their parental fusogenic lineages. To test these hypotheses, I have addressed the following experimental aims:

1. Identify the microenvironmental and cellular factors responsible for promoting cell fusion in the intestine.

2. Identify the origin of the BMDC capable of fusing with the intestinal stem cell.

3. Examine the transcriptome of cell fusion hybrids relative to their parental cells.

CHAPTER 2

Inflammation and proliferation act together to mediate intestinal cell fusion

CHAPTER 2

Inflammation and proliferation act together to mediate intestinal cell fusion

Paige S. Davies[1*], Anne E. Powell[2*], John R. Swain[1], and Melissa H. Wong[1,2]

[1]Department of Dermatology, Knight Cancer Institute, Oregon Stem Cell Center; [2]Department of Cell and Developmental Biology; Oregon Health & Science University, Portland, OR 97239, USA.

*Equal contribution.

PLoS ONE. 4(8):e6530.

AEP participated in planning of all experiments within the study, as well as the writing of the manuscript.

ABSTRACT

Cell fusion between circulating bone marrow-derived cells (BMDCs) and non-hematopoietic cells is well documented in various tissues and has recently been suggested to occur in response to injury. Here we illustrate that inflammation within the intestine enhanced the level of BMDC fusion with intestinal progenitors. To identify important microenvironmental factors mediating intestinal epithelial cell fusion, we performed bone marrow transplantation into mouse models of inflammation and stimulated epithelial proliferation. Interestingly, in a non-injury model or in instances where inflammation was suppressed, an appreciable baseline level of fusion persisted. This suggests that additional mediators of cell fusion exist. A rigorous temporal analysis of early post-transplantation cellular dynamics revealed that GFP-expressing donor cells first trafficked to the intestine coincident with a striking increase in epithelial proliferation, advocating for a required fusogenic state of the host partner. Directly supporting this hypothesis, induction of augmented epithelial proliferation resulted in a significant increase in intestinal cell fusion. Here we report that intestinal inflammation and epithelial proliferation act together to promote cell fusion. While the physiologic impact of cell fusion is not yet known, the increased incidence in an inflammatory and proliferative microenvironment suggests a potential role for cell fusion in mediating the progression of intestinal inflammatory diseases and cancer.

INTRODUCTION

Cell fusion between bone marrow-derived cells (BMDCs) and somatic cells has been reported in a number of different organ systems as an intriguing means for tissue regeneration in response to injury (Ferrari, Cusella-De Angelis et al. 1998; Lagasse, Connors et al. 2000; Alvarez-Dolado, Pardal et al. 2003; Camargo, Green et al. 2003; Corbel, Lee et al. 2003; Vassilopoulos, Wang et al. 2003; Weimann, Johansson et al. 2003; Camargo, Finegold et al. 2004; Nygren, Jovinge et al. 2004; Rizvi, Swain et al. 2006). The low incidence described in early studies led critics to suggest that cell fusion was physiologically inconsequential. However, two groups recently published that chronic inflammation can potentiate this process in the brain, muscle, liver and heart (Johansson, Youssef et al. 2008; Nygren, Liuba et al. 2008) suggesting that physiologic mediators can affect cell fusion. We have previously reported that BMDCs fuse with intestinal stem or progenitor cells after γ-IR-induced epithelial injury and that cell fusion is markedly increased in intestinal tumors (Rizvi, Swain et al. 2006). Intestinal tumors are well-characterized by chronic inflammation (Karin 2005; Karin and Greten 2005; Nelson and Ganss 2006; Karin 2008) leading to the possibility that inflammation plays an important role in tumor progression. Notably, patients with chronic intestinal inflammation have a higher incidence for developing colorectal cancer (Bernstein, Blanchard et al. 2001; Eaden, Abrams et al. 2001). This highlights the importance of understanding how the microenvironment impacts cell fusion and if this process contributes to tumorigenesis.

RESULTS AND DISCUSSION

To identify if well-characterized tumor microenvironmental factors mediate intestinal cell fusion, we set out to directly test the hypothesis that cell fusion is enhanced by inflammation. Utilizing the established mouse model of colonic inflammation, the *IL-10*$^{-/-}$ mouse (Kuhn, Lohler et al. 1993; Rennick, Davidson et al. 1995; Berg, Davidson et al. 1996), we compared the incidence of epithelial cell fusion in mice transplanted with green fluorescent protein (GFP)-expressing whole bone marrow (WBM) with those treated with the anti-inflammatory drug, 5-aminosalicylic acid (5-ASA), or to wild-type (WT) transplanted mice (Figure 2.1A). Analyses of peripheral blood after WBM transplantation revealed high levels of donor-blood reconstitution in all analyzed mice (>90% GFP expression, data not shown). Cell fusion between donor BMDCs and the colonic epithelium was identified by co-expression of the donor marker, GFP, and the WT epithelial marker, β-galactosidase (β -gal) by confocal microscopy (Figure 2.1C-E). GFP epithelial expression was detected by immunohistochemical analysis using antibodies to GFP or by direct fluorescence (Figure 2.2A-F). Proper controls were analyzed to confirm that epithelial GFP-expression was not due to artifact (Figure 2.3). GFP-expressing cells residing in the epithelial compartment were confirmed to be predominantly epithelial cells based upon morphology and co-expression of E-cadherin (Figure 2.2G-J). Phenotypically distinct CD45-positive

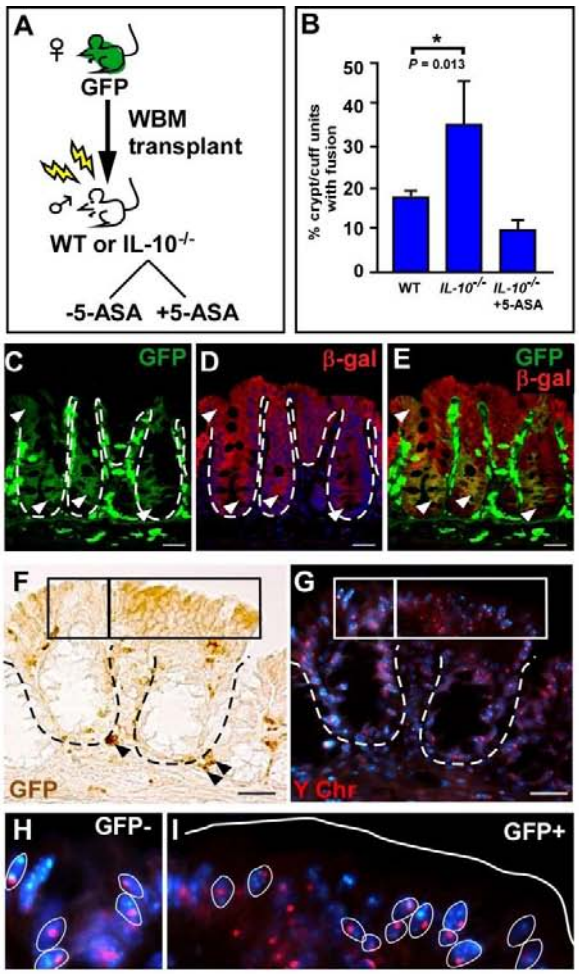

Figure 2.1. Inflammation promotes cell fusion between bone marrow-derived cells (BMDCs) and intestinal epithelium. (A) Schematic representation of experimental design. Whole bone marrow (WBM) from a female GFP-expressing donor mouse was transplanted into lethally irradiated wild-type (WT) or IL-$10^{-/-}$ male mice. A subset of IL-$10^{-/-}$ recipient mice were given the anti-inflammatory drug, 5-ASA. (B) Comparison of cell fusion in colonic epithelium between recipient mice. Cell fusion is quantified as the percentage of crypt/cuff units with at least one GFP-expressing cell. (C-E) Single plane confocal image of a colon cross-section from a ROSA mouse transplanted with GFP WBM. GFP expression (C, green) and β-gal expression (D, red) exist in the same cell (E, yellow) indicating fusion between the donor and recipient cell. Arrowheads denote fused epithelium on the cuff and in the crypts. (F-I) GFP-expressing epithelial cells in transplanted IL-$10^{-/-}$ colons are also fusion products, as determined by co-expression of GFP (F, brown, right box) and the Y chromosome (G, red, right box). (H & I) Higher magnification of GFP-negative and GFP-positive boxed regions from panels F & G. Y chromosome is found in Hoechst stained nuclei (blue, examples circled in white). Solid white line denotes epithelial/luminal border; dashed white lines indicate epithelial/mesenchymal border. Bars = 25μm.

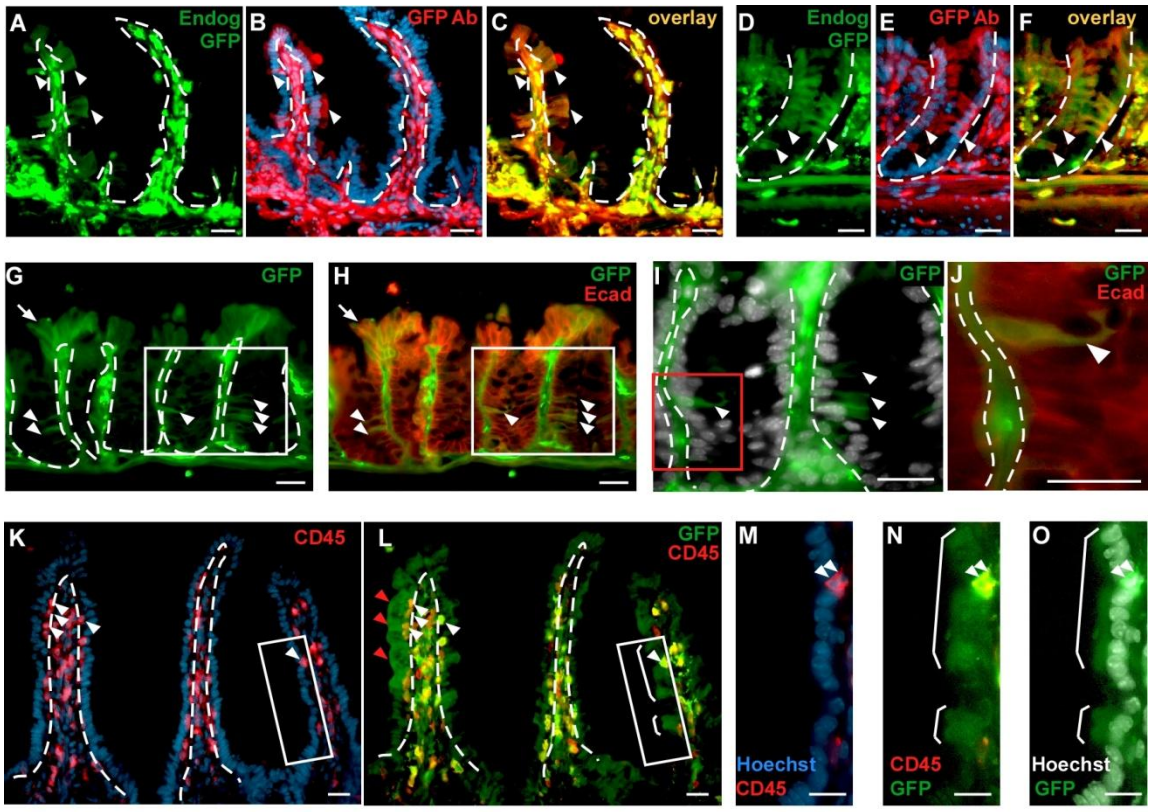
A
Endog GFP
B
GFP Ab
C
overlay
D
Endog GFP
E
GFP Ab
F
overlay
G
GFP
H
GFP Ecad
I
GFP
J
GFP Ecad
K
CD45
L
GFP CD45
M
Hoechst CD45
N
CD45 GFP
O
Hoechst GFP

Figure 2.2.

Figure 2.2. GFP-expressing cell type. Wild-type (WT) mice were transplanted with GFP-expressing whole bone marrow (WBM). (A-F) Five micron DSI (A-C) and colon (D-F) sections were stained with Rabbit anti-GFP antibodies followed by Anti-Rabbit Cy5 secondary antibodies. Images were captured in the FITC channel (A,D; green) to document endogenous GFP fluorescence, followed by capturing the same region in the Cy5 channel (B,E; red) to document the GFP antibody-stained tissue. These images were overlayed (C,F; yellow). Since the FITC and Cy5 channels are spectrally distinct, this demonstrates the Rabbit anti-GFP antibody is accurately representing endogenous GFP expression in the mouse intestinal blood cell compartment and epithelium. Arrowheads indicate examples of GFP-positive epithelium. (G-J) GFP-expressing epithelium (green) can be identified by co-staining with the epithelial cell marker E-cadherin (red; arrowheads mark yellow co-stained cells in the crypt; arrow marks co-stained cells on the cuff). (I) Higher magnification of white boxed region in panels G & H. (J) Further magnification of red boxed region from panel I. GFP-positive laminia propria can be observed next to a GFP-positive epithelial cell co-staining for E-cadherin. (K-O) The GFP-positive epithelium can be distinguished from the GFP-positive blood cells. Five micron DSI sections were co-stained for GFP and CD45. (K) Most CD45-positive cells reside within the lamina propria of the villus core, however, some lie along the base of the epithelial cells (arrowheads), known as intra-epithelial lymphocytes (IELs). (L) GFP-expressing epithelium (red arrowheads) can be distinguished from GFP-expressing blood cells (white arrowheads) in this co-stained image. (M-O) GFP-expressing epithelium can be distinguished from CD45-positive IELs because while the nuclei of the IEL are small and sit at the base of the epithelial layer (arrowheads), the epithelial cells have larger/longer nuclei oriented in a single layer and the cell extends much further towards the lumen. The epithelial cells that are GFP-positive can be appreciated (brackets) when juxtaposed to GFP-negative epithelial regions and are distinct from IELs (arrowheads). The long columnar shape of the GFP-positive epithelial cells is distinct from blood cells residing in the lamina propria or IELs. Dashed white lines indicate epithelial/mesenchymal border. Bars = 25μm.

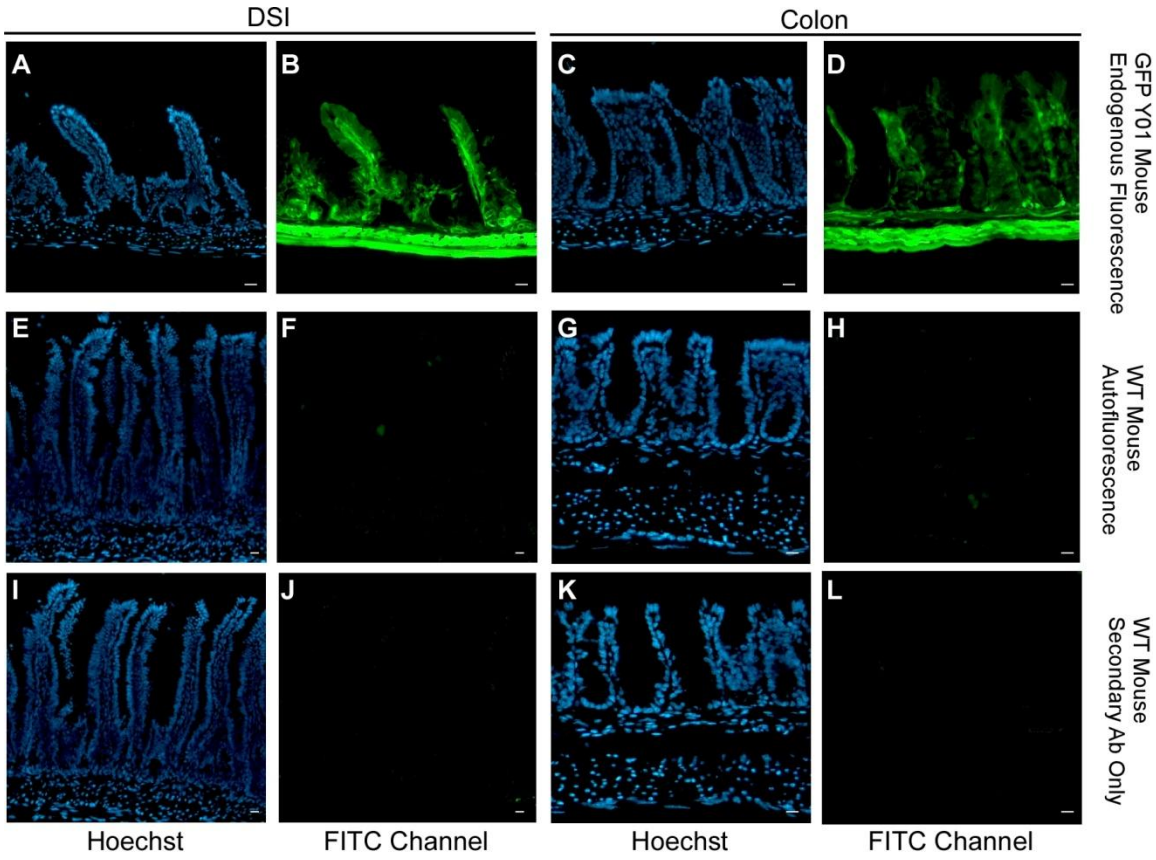

Figure 2.3 Fluorescence background controls. (A-D) Detection of endogenous GFP fluorescence from a Y01 GFP mouse DSI (A-B) and colon (C-D). WT C57B6 mouse DSI (E-F) and colon (G-H) do not exhibit appreciable levels of autofluorescence in the FITC channel. (I-L) There is no detectable signal in the FITC channel from DSI (I-J) or colon (K-L) that has been stained with Anti-Rabbit Alexa 488 secondary antibody alone. Images in panels B & C were captured under the same configuration, but at one-third the exposure time as panels E,G,I,K. Nuclei are stained with Hoechst dye (A,C,E,G,I,K; blue). Bars = 25μm.

cells (intra-epithelial lymphocytes) were also present in this compartment, but were much smaller and did not extend to the apical border (Figure 2.2K-O). Together, these rigorous standards definitively establish that GFP-expressing epithelial cells of both the small and large intestine can be accurately identified.

Cell fusion was analyzed in the chronically inflamed colon from male *IL-10*$^{-/-}$ mice that were transplanted with GFP-expressing WBM from a female donor. Detection of the recipient marker (Y-chromosome) by *in situ* hybridization and the donor marker (GFP) by immunohistochemical analysis provides an additional approach to analyze cell fusion (Figure 2.1F-I). The presence of co-localized Y-chromosome in GFP-expressing cell regions (Figure 2.1I) indicates that cell fusion occured in the presence of chronic inflammation. Controls verifying the specificity of the Y-chromosome probe are presented in Figure 2.4.

We chose to use epithelial GFP-expression as the basis for quantifying cell fusion based upon two criteria. First, cell fusion was initially confirmed in all experimental groups and in all recipient backgrounds used in the studies reported here. This was established using confocal microscopy and immunohistochemical, or histochemical co-detection of donor and recipient markers in the same epithelial cell (Figure 2.1C-I and Figure 2.5A-C). Second, we and others have reported that in all of the mice surveyed for cell fusion, the donor marker predominantly expresses the recipient marker (Alvarez-Dolado, Pardal et al. 2003; Wang, Willenbring et al. 2003; Nygren, Jovinge et al. 2004; Rizvi, Swain et al. 2006; Johansson, Youssef et al. 2008; Nygren, Liuba et al. 2008), or in other words, presence of the donor marker in the intestinal

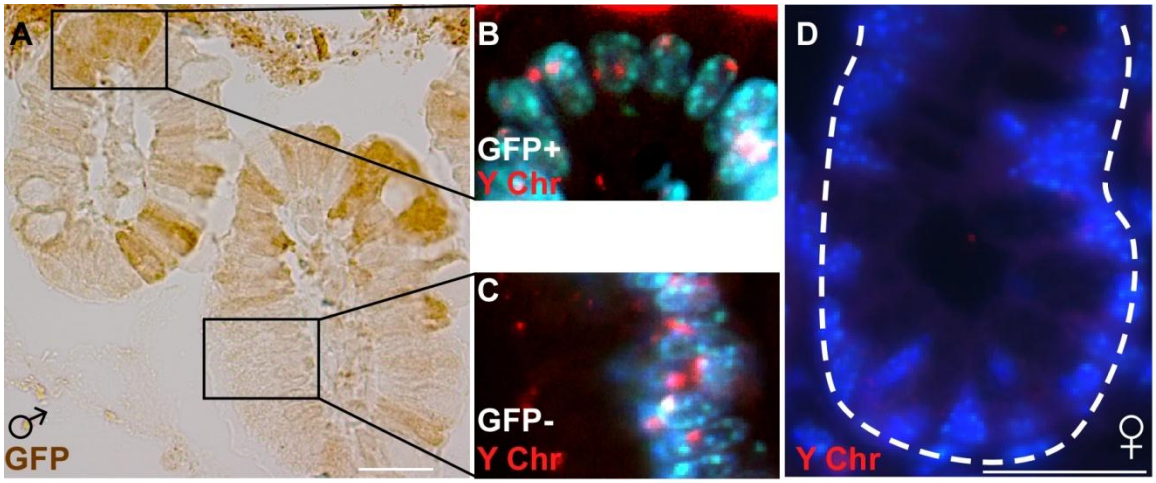

Figure 2.3 FISH controls. (A) Five micron cross-section of distal small intestine from a male GFP mouse was stained for GFP and developed with DAB (brown). Both GFP-positive (upper black box) and GFP-negative (lower black box) regions are identified due to the variegation of the GFP expression in this mouse. Y-chromosome can be detected in the nuclei in both boxed regions as magnified in B & C, demonstrating that the Y-chromosome probe can successfully detect Y-chromosome when the GFP antibody and detection reagents are present. (D) A crypt from a female mouse stained with the Y-chromosome probe demonstrating the lack of staining and the specificity of the probe. Nuclei are stained with Hoechst dye. Bars = 25μm.

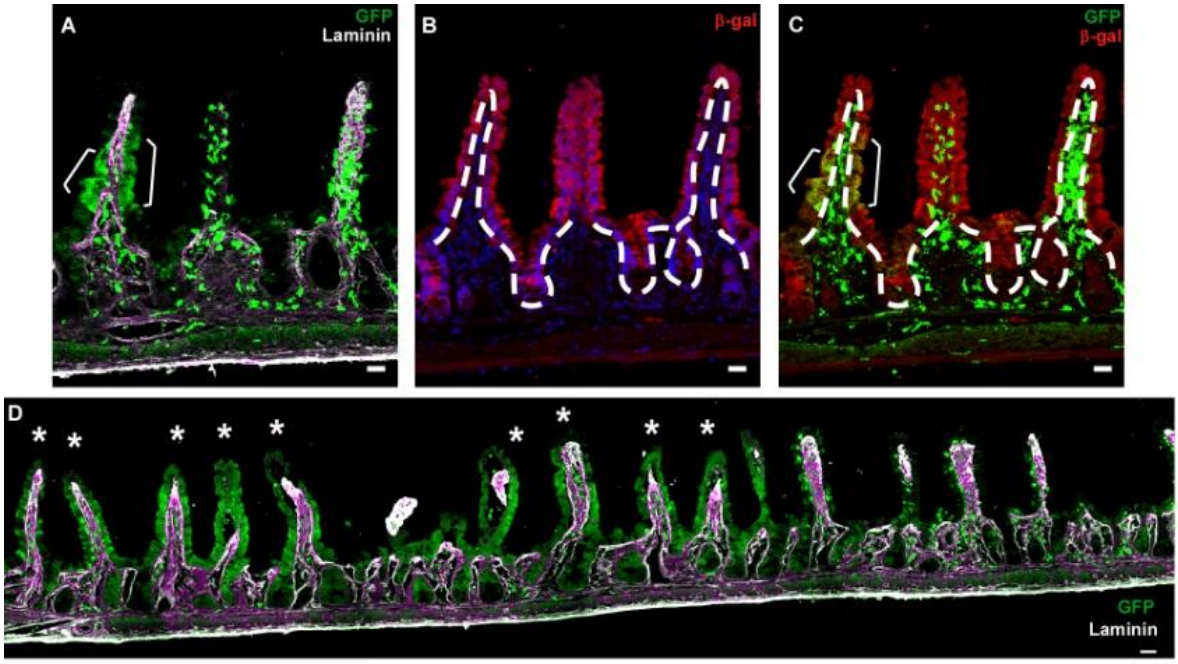

Figure 2.5. Defining Fusion. (A-C) Rosa mice transplanted with GFP-expressing bone marrow were analyzed for fusion in the epithelium by confocal microscopy. Tissue from the distal small intestine were co-stained for GFP (green; donor), β-gal, (red; recipient), laminin (grayscale; laminia propria compartment), and Hoechst (blue; nuclei). Fusion can be detected in the epithelium (brackets) by the co-expression of GFP and β-gal. Dashed white lines indicate epithelial/mesenchymal border and were drawn based on laminin staining from panel A. (D) A broad view of a typical stretch of DSI tissue after transplantation. The GFP-expressing epithelium indicative of fusion is apparent (asterisks). Bars = 25μm.

epithelium does not support transdifferentiation, a change in cell fates from the BMDC to a non-hematopoietic cell type. Based upon these criteria, cell fusion was quantified in each animal by counting the percentage of crypt units (crypt/villus or crypt/cuff in the small intestine or colon, respectively) that contained GFP-expressing epithelial cells in a total of 1500 crypt units.

Interestingly, we observed a dramatically higher amount of epithelial cell fusion in WBM-transplanted WT mice than what we had previously reported (Rizvi, Swain et al. 2006). This observation is the result of optimization of our transplantation protocols for intestinal cell fusion, including the use of a more robust and detectable GFP-expressing transgenic line for donor bone marrow (Osb-Y01) (Nakanishi, Kuroiwa et al. 2002; Anderson, Wu et al. 2005), more effective GFP detection by antibody staining, and establishing stringent quantification methods. We now report that fusion within the intestinal epithelium is detected at a level of 37.3 ± 3.6% in the distal small intestine (DSI; n = 10, Figure 2.5D) and 20.6 ± 2.1% (n = 4) in the colon. The prominent level of cell fusion sets the intestine apart from other systems where only low levels are observed (Ferrari, Cusella-De Angelis et al. 1998; Lagasse, Connors et al. 2000; Alvarez-Dolado, Pardal et al. 2003; Camargo, Green et al. 2003; Corbel, Lee et al. 2003; Vassilopoulos, Wang et al. 2003; Weimann, Johansson et al. 2003; Camargo, Finegold et al. 2004; Nygren, Jovinge et al. 2004), suggesting that there is a physiologically important role for cell fusion in self-renewing tissues.

In assessing the role of inflammation, direct comparison of cell fusion in colons from *IL-10*$^{-/-}$ mice (chronic inflammation) with WT controls revealed a

significant increase (*IL-10*$^{-/-}$: 35.2 ± 9.6%, *n* = 3; WT: 19.04 ± 1.1%, *n* = 9; *P* = 0.013) (Figure 2.1B). To further implicate the presence of local intestinal inflammation in promoting cell fusion, we treated *IL-10*$^{-/-}$ mice with the anti-inflammatory drug, 5-ASA (Azad Khan, Piris et al. 1977), a standard therapy for inflammatory bowel disease in humans. Treatment with 5-ASA resulted in a marked decrease in cell fusion (8.5 ± 2.7%, *n* = 3; Figure 2.1B) compared to untreated *IL-10*$^{-/-}$ mice. This dramatic effect of modulating microenvironmental inflammation on cell fusion is depicted in tissue sections from each of the experimental groups and presented in Figure 2.6. We confirmed by quantitative reverse transcriptase-polymerase chain reaction (qRT-PCR) that *IL-10*$^{-/-}$ intestines had heightened inflammation and that treatment with 5-ASA greatly suppressed the inflammatory response (Dionne, Hiscott et al. 1997; Kokkotou, Moss et al. 2008); (Mchr1, Melanin-concentrating hormone receptor1 and IL-1β, Interleukin-1β, Table 2.1).

It is well-established that γ-IR also induces an inflammatory response in the intestine (Molla and Panes 2007). Given that the transplantation procedure involved γ-IR, we utilized a parabiosis approach to introduce traceable bone marrow without γ-IR. Surgically joined parabiotic mouse pairs were maintained together for 4-6 weeks to establish a shared circulating blood supply (Bunster and Meyer 1933; Wright, Wagers et al. 2001; Abkowitz, Robinson et al. 2003), which was confirmed by flow cytometry (data not shown). After the mice were separated, intestinal inflammation was induced by administration of dextran sodium sulfate (DSS), a well-documented protocol for eliciting inflammation in the

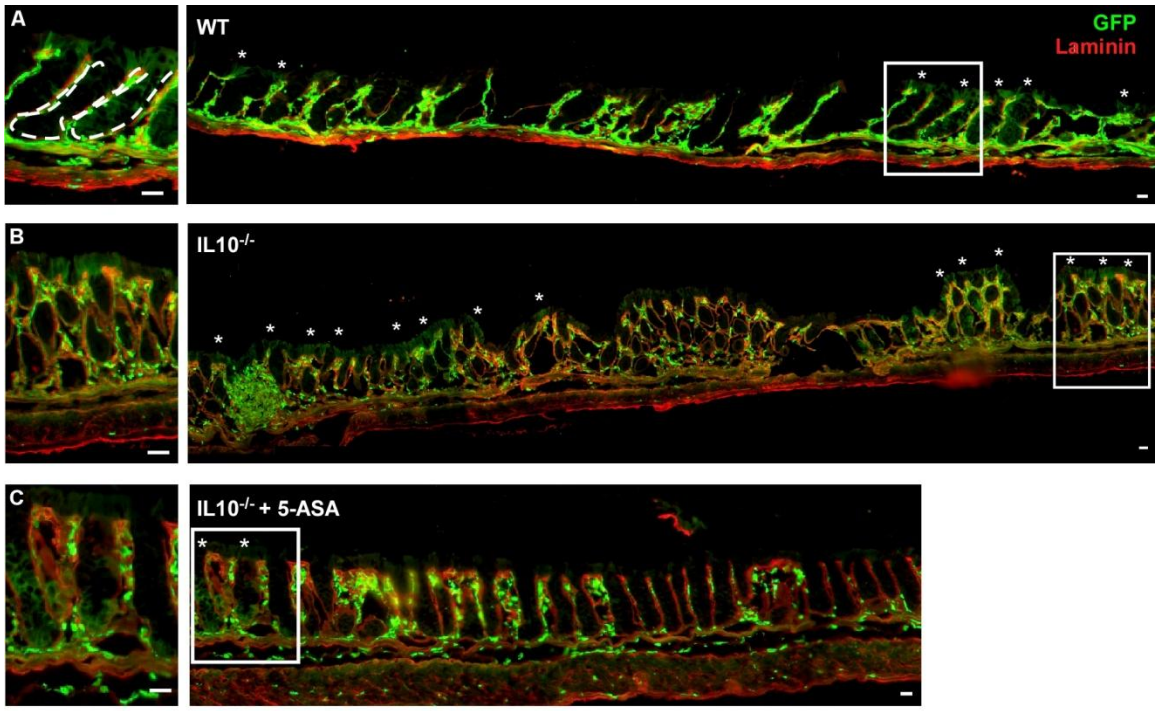

Figure 2.6. Amounts of fusion can be modulated. (A) Wild-type (WT) mice were transplanted with GFP-expressing whole bone marrow (WBM). An example of a stretch of tissue from the colon stained with antibodies against GFP and laminin demonstrated an appreciable amount of GFP-positive fused epithelium (asterisks). (B) When IL-$10^{-/-}$ mice were transplanted with GFP-expressing WBM, the amount of GFP-positive epithelial fusion that could be quantified increased compared to WT (asterisks), but was decreased again when the anti-inflammatory 5-ASA was given (C). Left-hand panels are higher magnifications of boxed regions from the larger stretches of tissue on the right, demonstrating GFP-positive epithelium on the colonic cuffs and in the crypts. Dashed white lines indicate epithelial/mesenchymal border. Bars = 25μm.

		Fold-Change	
cDNA	**Relative to**	**IL-1β**	**Mchr1**
IL10$^{-/-}$ Colonic Epithelium	WT Colonic Epithelium	6.7	N.D.
IL10$^{-/-}$ Colonic Epithelium + 5-ASA	IL10$^{-/-}$ Colonic Epithelium	-303	-3.7
IL10$^{-/-}$ Colonic Mesenchyme + 5-ASA	IL10$^{-/-}$ Colonic Mesenchyme	-24	N/A[a]
Induced AhCre^{+};Apc$^{-/-}$ Intestinal Epithelium	WT Mock Induced Intestinal Epithelium	-1.01	-1.09

[a] not expressed in mesenchyme; N.D., Not Determined

Table 2.1. Inflammatory Status. qRT-PCR was carried out for Interleukin-1β (IL-1β) and Melanin-concentrating hormone receptor 1 (Mchr1) on various experimental samples to determine changes in inflammatory status. These genes have been demonstrated to increase in an intestinal inflammatory setting in both human and mouse samples. mRNA was isolated from either whole intestine, mesenchyme, or epithelium and cDNA transcribed. Each sample was normalized to Gapdh and compared to its appropriate baseline control. The *IL-10$^{-/-}$* samples exhibited decreases when treated with anti-inflammatory drugs, while the *AhCre^{+};Apc$^{-/-}$* proliferative model samples showed no change in inflammatory status when compared to mock-injected controls.

mouse intestine and colon (Jurjus, Khoury et al. 2004) (Figure 2.7A). The DSS phenotype can be appreciated on both gross morphologic and cellular levels (WT compared to DSS-treated, Figure 2.8). Again, cell fusion was apparent in the DSS-induced colons of these animals by co-detection of donor and recipient markers using confocal microscopy (β-gal and GFP; Figure 2.7B-D). Distinct epithelial regions expressing both GFP and β-gal were readily detectible in both the crypt cuff (Figure 2.7B,C; arrowheads) and in the colonic crypt (Figure 2.7B,D; arrowheads). Quantification of cell fusion revealed a statistically significant increase in the DSS-treated parabiotic partners compared to untreated controls (Figure 2.7E; WT: 5.8 ± 3.4%, *n* = 5; DSS-treated: 19.6 ± 2.6%, *n* = 4; *P* = 0.017*)*. These data, along with our observations in the WBM-transplanted mice strongly implicate inflammation as a key mediator for pathologically-induced cell fusion in the intestine.

In support of a physiologic role for intestinal epithelial cell fusion, an appreciable baseline level of cell fusion was observed in non-DSS treated parabiotic pairs in both the colon (-DSS, 5.8 ± 3.4%, *n* = 5) and DSI (-DSS, 15.0 ± 3.2%, *n* = 5) (Figure 2.7E). Even though parabiosis surgery is well-accepted as a "non-damage" model, there is considerable post-surgery stress to the animal resulting in weight loss, and it is possible that intestinal injury occurs during or immediately after the surgical procedure. To rule out the possibility of surgically-induced inflammation that could potentially create an artificial baseline level of cell fusion within the intestinal epithelium, we repeated the parabiotic experiment

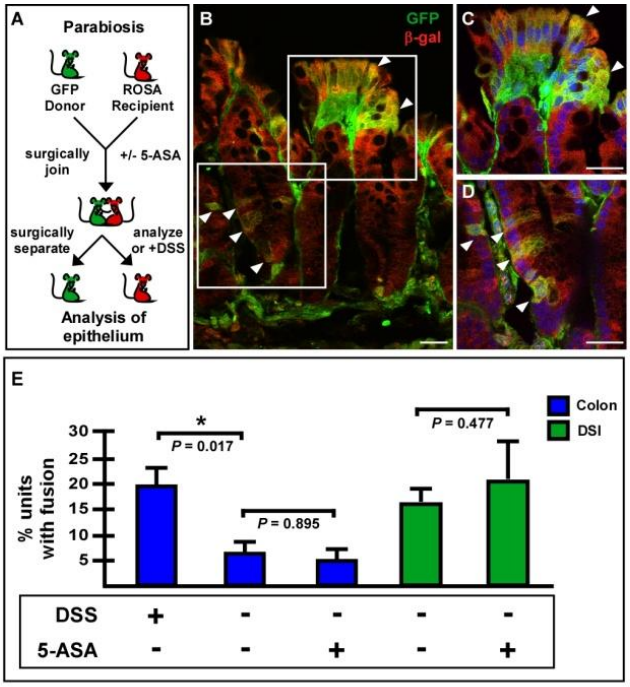

Figure 2.7. Intestinal cell fusion persists at low levels in a non-damage model system. (A) Schematic representation of parabiosis experimental design. GFP and ROSA mice were surgically joined. (B-E) Extensive cell fusion was observed in colons from DSS-treated animals. (B) Single plane confocal microscopy images of GFP (green) and ß-galactosidase (red) detected by antibodies demonstrate fusion by co-localization in yellow. Arrowheads denote fused cells. (C & D) depict higher magnifications of the boxed regions in panel B. Nuclei were visualized with the Hoechst dye (blue). Bars = 25μm. (E) Cell fusion in DSS-treated animals was significantly increased over non-treated animals (P = 0.017). When the animals were given 5-ASA during parabiosis to inhibit inflammation, there was no difference in fusion levels in colon (blue bars; P = 0.895) or DSI (green bars; P = 0.477), however, a baseline level of fusion existed in both tissues.

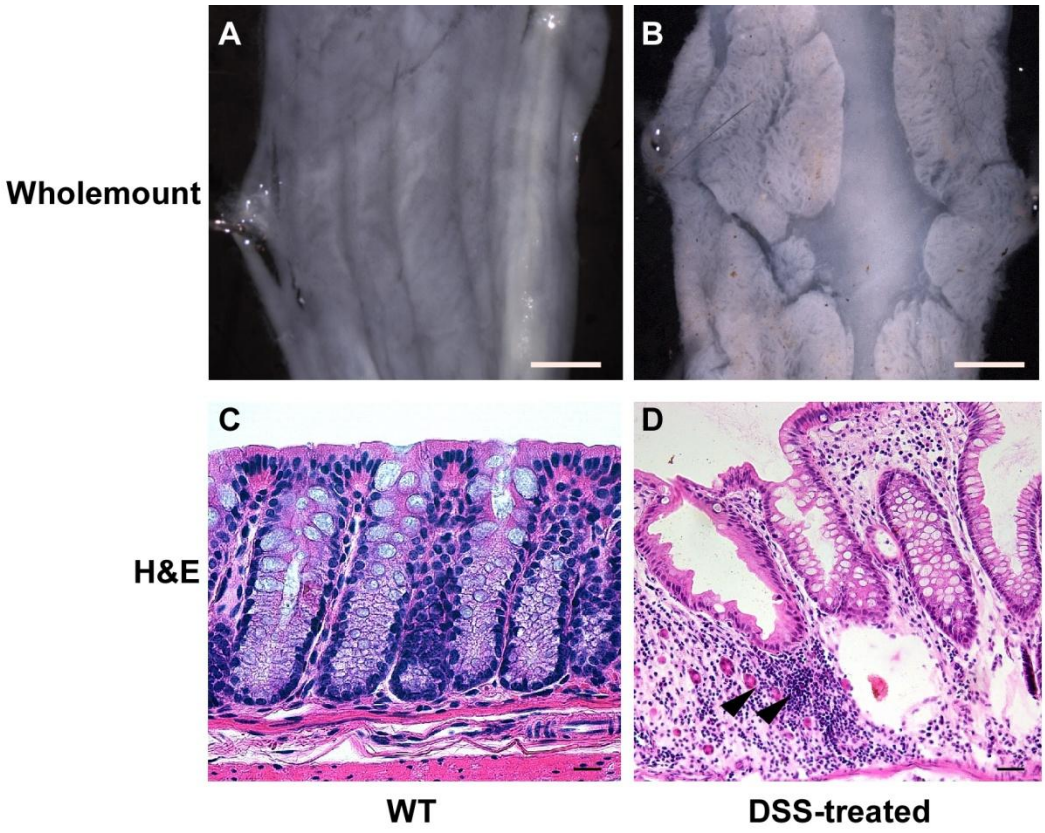

Figure 2.8. Dextran Sodium Sulfate (DSS) Model of colonic inflammation. After separation, a subset of parabiotic mice were administered dextran sodium sulfate (DSS), to induce inflammation. Wholemount colon from a DSS-treated mouse (B) has major inflammatory changes compared to a wild type mouse (A). This is further appreciated by H&E, where the DSS-treated animal has extensive immune infiltrate (D, arrowheads) compared to the WT colon cross-section (C). Bars in A & B = 1.5mm. Bars in C & D = 25μm.

by joining GFP and ROSA mice along with oral administration of an anti-inflammatory drug cocktail during and after the surgery (Figure 2.7A). In these animals, the baseline level of cell fusion persisted and was unchanged relative to the untreated animals in both the colon (5-ASA treated: 5.3 ± 2.0%, n = 5, P = 0.895) and DSI (5-ASA treated: 21.3 ± 7.8%, n = 5, P = 0.477) (Figure 2.7E). Further, we confirmed by qRT-PCR that animals receiving an anti-inflammatory drug regimen had minimal epithelial inflammation (Table 2.1). This is in agreement with the data presented in Figure 2.1B, which showed *IL-10*$^{-/-}$ mice treated with 5-ASA after transplantation also displayed appreciable levels of cell fusion. Together, these observations highlight the existence of an endogenous baseline level of epithelial cell fusion in the intestine, suggesting that the nature of rapidly self-renewing epithelium may sensitize or prime it for fusion with circulating BMDCs under certain microenvironmental conditions. These findings strongly suggest that additional factors are important for the fusion process in the intestine.

Currently, reports in other organ systems show that baseline levels of cell fusion are relatively non-detectable (Johansson, Youssef et al. 2008; Nygren, Liuba et al. 2008; Nern, Wolff et al. 2009). Important differences between these other organ systems and the intestine is that the intestinal epithelium is a rapidly renewing, highly proliferative tissue that dynamically responds to its microenvironment. An additional distinction between the intestine and the other somatic organs lies in the host fusogenic cell. We have previously reported that

BMDC fusion occurs with a stem or progenitor population in the intestine (Rizvi, Swain et al. 2006), whereas in other tissues fusion takes place with differentiated cells (Alvarez-Dolado, Pardal et al. 2003; Wang, Willenbring et al. 2003; Nygren, Jovinge et al. 2004; Nygren, Liuba et al. 2008). These differences along with the respective disparity in homeostatic cell fusion levels suggest that host-cell proliferative status may be a factor in the fusion process. It is well established that γ-IR elicits intestinal microenvironmental inflammation (Molla and Panes 2007), and that the epithelium undergoes massive apoptosis that peaks within the first 24h post-irradiation (Potten 1990) accompanied by a proliferative response (Potten, Owen et al. 1990). Further, we have previously shown that γ-IR also stimulates the Wnt signaling pathway, a critical regulator of intestinal epithelial proliferation (Davies, Dismuke et al. 2008). Taken along with our observation that fusion is increased in a tumor setting (Rizvi, Swain et al. 2006), these elements implicate cell death or proliferation signals as possible additional factors that promote cell fusion.

To gain additional insights from the pre-fusion intestinal microenvironment, we detailed the temporal events surrounding the generation of cell fusion hybrids. The dynamic trafficking of GFP-expressing BMDCs to the intestine was defined at various early time points post-transplantation. Since our initial observations implicated progenitor cells as the host fusion partner (Rizvi, Swain et al. 2006), we focused our analyses on the stem cell niche. At 1 day post-transplant, the first detectable GFP-positive BMDCs were present scattered around the crypt region in the intestinal mesenchymal compartment (Figure 2.9A, B; arrowheads). By 4

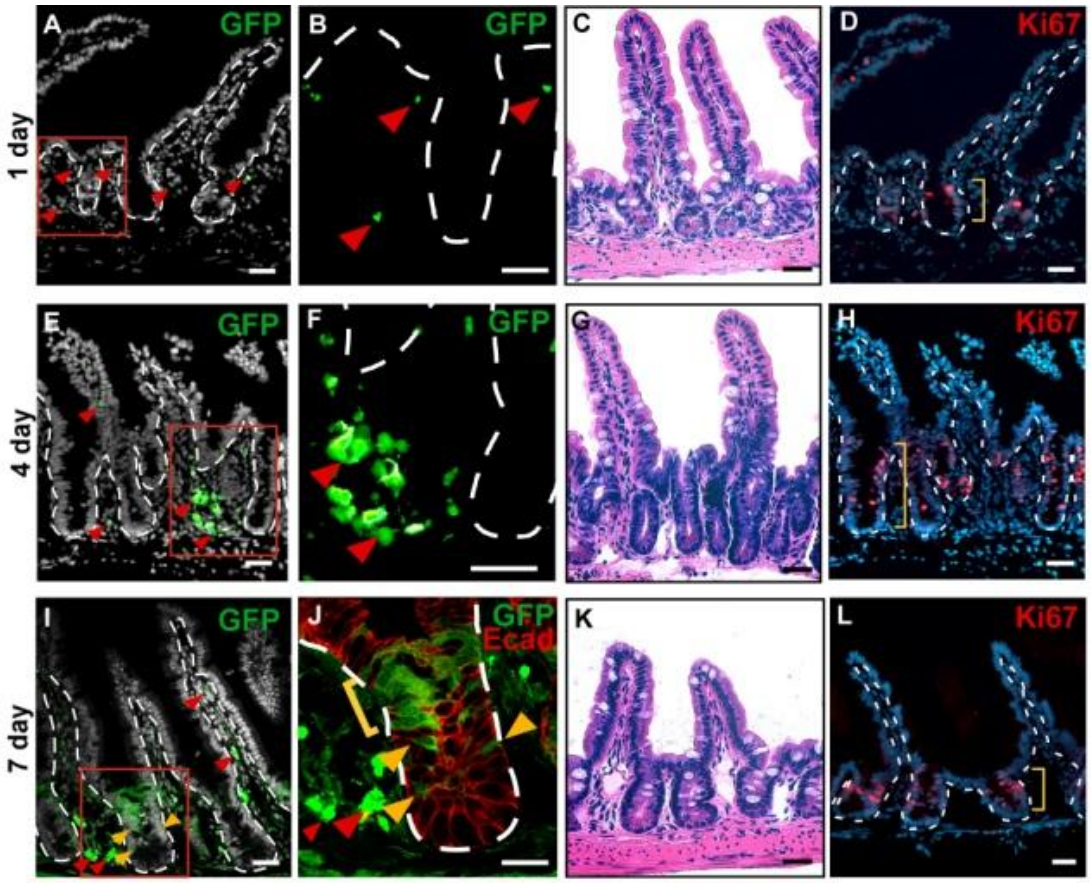

Figure 2.9. Increased epithelial proliferation occurred after gamma-irradiation. Wild-type (WT) mice were transplanted with GFP-expressing whole bone marrow (WBM). The distal small intestine was analyzed at 24h increments for 1 week. (A-B) At 1 day post-transplantation, few GFP-positive cells (green) were located in the mesenchyme (arrowheads) and none were found in the epithelium. (C-D) H&E and Ki67 detection (red) with Hoechst dye (blue) indicated normal morphology at one day post-transplant. (E-F) At 4 days post-transplant, more GFP-positive cells were found surrounding the crypt (arrowheads), while none were detected in the epithelium. (G-H) H&E and Ki67 staining (red) revealed a dramatic increase in proliferation of the crypts. (I-J) By 7 days post-transplant, single plane confocal microscopy depicts the presence of GFP-positive cells in the mesenchyme surrounding the crypt as well as in the villi core (red arrowheads). GFP-positive epithelium was observed in the stem cell (yellow arrowheads) and transient-amplifying (yellow bracket) zones of crypts. Epithelial cells are marked with antibodies against E-cadherin (red). (K-L) H&E and Ki67 staining depicted morphology close to normal by 7 days post-transplant. Dashed white lines indicate epithelial/mesenchymal border. Red boxes in (A,E,I) are displayed in higher magnification in (B,F,J). Yellow brackets denote the depth of the Ki67-positive cells in (C,G,K). The nuclear dye Hoechst is depicted in grayscale in (A,E,I) and in blues in (D,H,L). D & H are the same tissue sections as A & E, respectively. Bars = 25μm.

days post-transplant, an appreciable level of GFP-expressing BMDCs populated the intestine, but GFP-expressing epithelium was not yet observed (Figure 2.9E, F; arrowheads). Cell fusion in the epithelial compartment (Figure 2.9J; yellow brackets and arrowheads) was routinely detected 7 days post-transplant and was accompanied by high levels of GFP-expressing cells in the mesenchyme (Figure 2.9I,J; red arrowheads). The arrival of GFP-expressing BMDCs into the intestine coincided with a striking increase in proliferation of the intestinal epithelium, appreciated both histologically by Hematoxylin and Eosin (H&E) staining and by Ki67 antibody staining (Figure 2.9C,D,G,H,K,L; yellow brackets). Intriguingly, the dramatic proliferative epithelial response coincident with clustering of GFP-expressing BMDCs in the stem cell niche suggested that intestinal cell fusion may also be governed by the proliferative status of the recipient cell.

The homeostatic, or baseline, levels of cell fusion observed in both transplanted mice with suppressed inflammation and parabiotic mice may be due to the intrinsic proliferative nature of the intestinal crypt. Approximately 60% of crypt cells are actively engaged in the cell cycle (Kovacs and Potten 1973; Potten, Owen et al. 1990) supporting rapid self-renewal of the epithelium. We and others (Potten, Owen et al. 1990) have shown that this proliferative zone is expanded in response to γ-IR (Figure 2.9G,H). However, in other tissues where cell fusion occurs after γ-IR, it is reported that the host fusion partner is a differentiated cell type that is not known to be actively cycling (Alvarez-Dolado, Pardal et al. 2003; Wang, Willenbring et al. 2003; Johansson, Youssef et al. 2008). Despite this, notexin-induced injury in skeletal muscle, where BMDC

fusion has been described, results in a transient increase in cell numbers (Sacco, Doyonnas et al. 2008), suggesting that these differentiated cells might be capable of entering the cell cycle. Based upon this observation and our data in the intestine, we hypothesized that host cell proliferative status is important in driving cell fusion. Therefore, to determine if entry into the cell cycle might also be stimulated in a subset of other organs after γ-IR, we surveyed for cycling cells in the liver and skeletal muscle using antibodies to Ki67. A visible increase of Ki67-positive cells was observed (Figure 2.10), further supporting the idea that cell cycle status of the host cell within these organs may also mediate cell fusion.

Therefore, to directly implicate epithelial proliferative status as a contributing host factor in promoting cell fusion, we utilized a mouse model in which we could temporally manipulate epithelial proliferation in the intestine. The previously described intestinal-specific, inducible *AhCre* mouse (Ireland, Kemp et al. 2004) harboring floxed *Apc* alleles (Shibata, Toyama et al. 1997), results in a dramatic induction of intestinal epithelial proliferation upon Cre activation (Sansom, Reed et al. 2004). We showed by H&E that an increase in immune infiltrate was not readily apparent during the timeframe in which epithelial proliferation was stimulated (compare Figure 2.11B,C). Further, qRT-PCR showed that there was not an increase in inflammation in these mice (Table 2.1). To evaluate cell fusion in this proliferative model, we transplanted $AhCre^{+};Apc^{fl/fl}$ mice on day 0, induced epithelial proliferation on day 2, then analyzed cell fusion in the intestine on day 7 (Figure 2.11A). Dramatically, a significant increase in epithelial cell fusion within the crypt and villus, compared to mock-injected

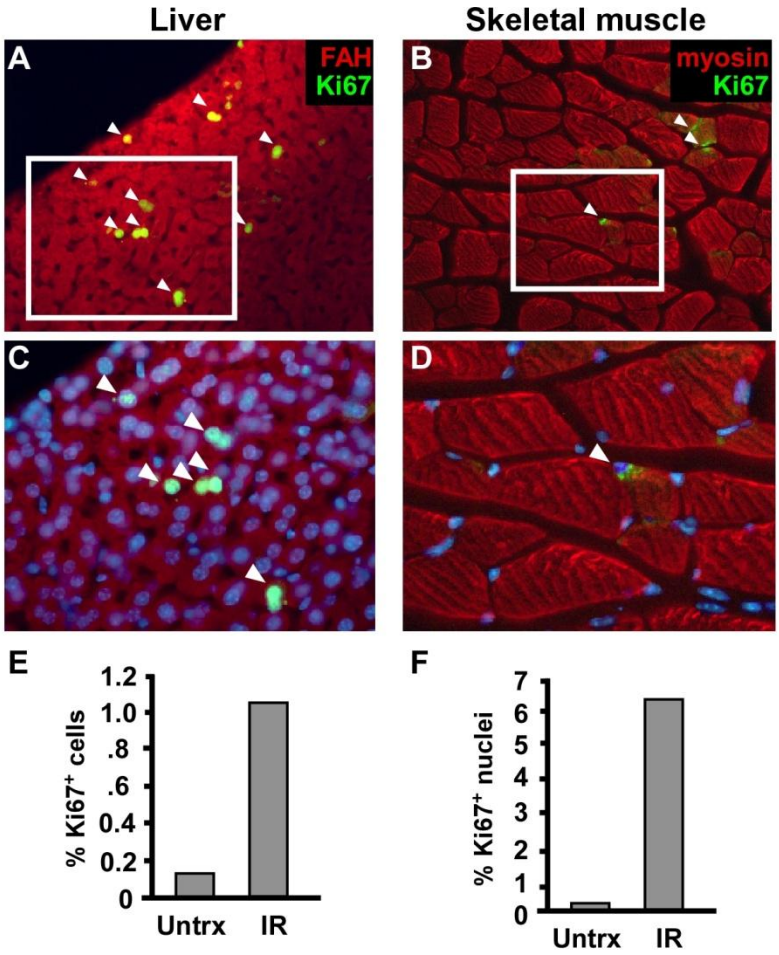

Figure 2.10. Liver hepatocytes and skeletal muscle have a proliferative response to lethal irradiation. To examine proliferation in the liver and skeletal muscle after irradiation-induced injury, wild type (WT) mice were administered a single lethal dose of whole-body γ-IR (9Gy). Liver and skeletal muscle (quadricep, tibialis anterior and soleus muscles) were isolated 7 days post-irradiation. (A-D) Liver and skeletal muscle sections from lethally irradiated mice were stained with the proliferative marker Ki67 (green), either FAH (liver; red) or myosin (muscle; red) and Hoechst dye (blue). White arrowheads indicate Ki67-positive nuclei. Boxed regions in A & B are magnified in C & D. (G,H) Quantification of percentage Ki67-positive nuclei revealed that lethally irradiated mice harbored a marked proliferative response in the liver and skeletal muscle when compared to unirradiated control animals.

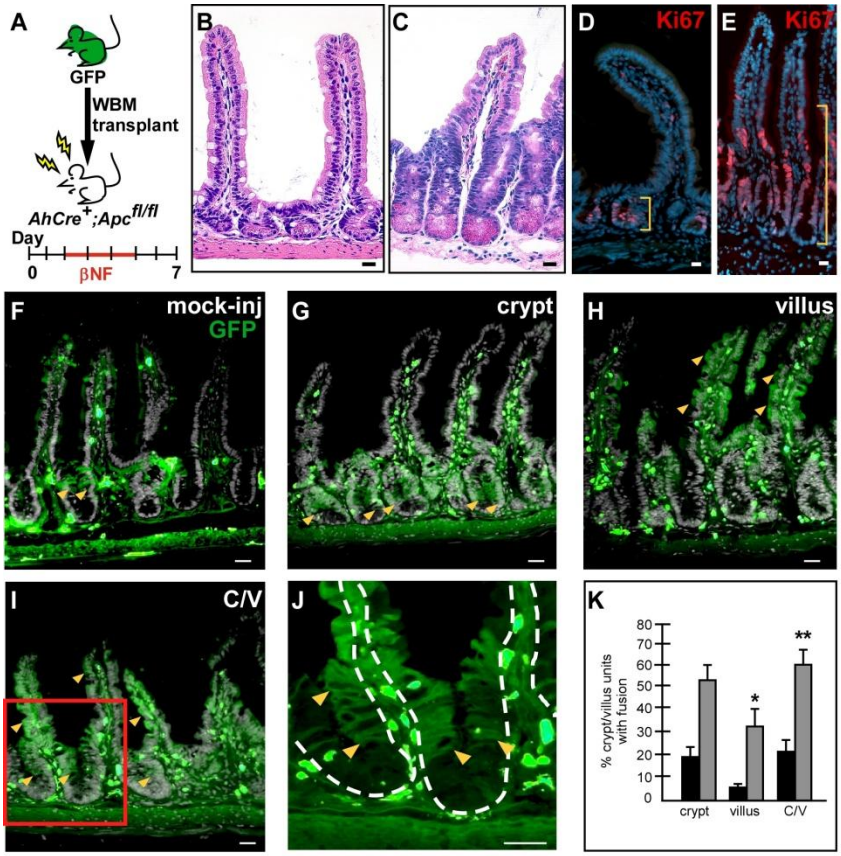
A
GFP
WBM
transplant
AhCre+;Apcfl/fl
Day
0
βNF
7
B
C
D
Ki67
E
Ki67
F
mock-inj
GFP
G
crypt
H
villus
I
C/V
J
K
% crypt/villus units with fusion
80
70
60
50
40
30
20
10
0
*
**
crypt
villus
C/V

Figure 2.11

Figure 2.11. Increased epithelial proliferation correlates with increased cell fusion. (A) Schematic representation of experimental design. AhCre^{+};Apc$^{fl/fl}$ mice were transplanted with GFP-expressing whole bone marrow (WBM) on day 0. Two days later, Cre recombinase was induced by β-naphthoflavone (β-NF) administration for 4 consecutive days (days 2-5). Mice were sacrificed on day 7 and the distal small intestine analyzed for fusion (B-E). The intestinal-specific deletion of Apc resulted in an extensive hyperproliferation of crypt cells compared to wild-type (WT) mice, as seen by H&E stain (C vs. B) and Ki67 staining (red, indicated by yellow brackets; E vs. D). (F-K) Detection of GFP-expressing cells (green; yellow arrowheads mark examples) denoting cell fusion was increased in the AhCre^{+};Apc$^{-/-}$ mice compared to mock-injected WT mice. Three patterns of cell fusion were observed: (G) crypt-only, (H) villus-only, (I) both crypt and villus regions in one crypt/villus unit. Panel (J) is a higher magnification of the red box in panel (I) demonstrating that the Paneth cell region at the base of the crypt remained GFP-negative. Solid white lines denote epithelial/luminal border; dashed white lines indicate epithelial/mesenchymal border. Bars = 25μm. (K) A significant increase in fusion was observed in villus only ($P = 0.011$) and crypt/villus ($P = 0.009$) AhCre^{+};Apc$^{-/-}$ mice (gray bars) compared to mock-injected WT mice (black bars).

controls, was observed (Figure 2.11F-K). Cell fusion in crypt/villus units displayed three distinct patterns: fusion restricted to the crypts, fusion on the villus only, and fusion in both crypt and villus epithelium (Figure 2.11G-J). Differences in each of these three patterns were significant when compared to mock-injected control intestines (crypt: $P = 0.056$; villus: $P = 0.011$; crypt/villus: $P = 0.009$; mock injected $n = 5$, *AhCre*$^{+}$;*Apc*$^{-/-}$ $n = 7$). Because the induction of proliferation occurs over a window of 4 days, the differences in the crypt, villus or crypt/villus fusion expression patterns likely represented different kinetics of cell fusion and subsequent expansion of progeny. For example, it is possible that fusion in the crypt epithelium represents an initial fusion event in a proliferative cell that occurred only a short time before analysis (perhaps on day 5-6). Likewise, GFP-expressing epithelia in both the crypt and villus might represent an early fusion event in a crypt-based progenitor cell, perhaps on day 2. Notably, crypt-based differentiated Paneth cells which have a >20 day turnover (Cheng, Merzel et al. 1969), remain unmarked and are not descendents from the cell fusion event (Figure 2.11J).

Importantly, detection of cell fusion only on the villus where proliferative cells do not normally reside, strongly implicated the proliferative status of the host cell as a critical component of cell fusion. Noticeably, each crypt/villus unit had extensive GFP-expressing cells which could argue for a more rapid expansion of progeny from the original fusion event. However, the fact that there were significantly more total crypt/villus units harboring at least one GFP-expressing cell indicated there were also more initial cell fusion events ($P = 0.009$). Our

assay cannot distinguish between whether the host fusion target is a progenitor or if it is a cell actively engaged in the cell cycle. Regardless, our data indicates that the host cell must be receptive or primed for the fusion process. Importantly, these observations suggest that proliferative capacity of the host cell contributes to promote cell fusion in the intestinal epithelium.

Perhaps the most pressing question relating to *in vivo* cell fusion is if the generated cell fusion hybrids have a physiologic impact on normal organ function. Although it is apparent that these intestinal cell fusion hybrids retain an overt epithelial phenotype, it is unclear if the BMDC transcriptome is modified. To explore the possibility that cell fusion results in nuclear reprogramming of the donor genome, we transplanted WBM from mice harboring a *Villin-Cre* transgene (Madison, Dunbar et al. 2002) into recipient mice homozygous for the floxed *Apc* allele (Shibata, Toyama et al. 1997)(Figure 2.12A). Villin is an epithelial-specific promoter and Cre recombinase is not expressed in any of the blood lineages under this context (Madison, Dunbar et al. 2002). Therefore, functional Cre recombination of the *Apc* allele would only occur if Cre recombinase were activated, such as in the event of cell fusion between the BMDC (*Villin-Cre*) and the epithelial cell. The intestines from transplanted mice possessed hyperproliferative epithelial regions in both the distal small intestine and colon appreciated by wholemount analysis (Figure 2.12B,D) and morphologically by H&E (Figure 2.12C,E). The polyp-like region in the distal small intestine was reminiscent of Min mouse polyps (Moser, Pitot et al. 1990) where the *Apc* allele is mutated. To confirm the phenotype was due to Cre mediated recombination of

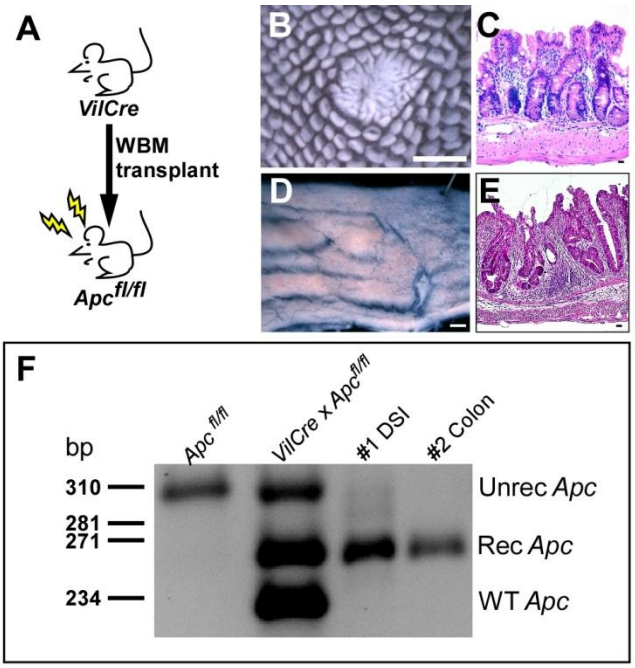

Figure 2.12. Bone-marrow/epithelial cell fusion causes genetic reprogramming. (A) Schematic diagram of transplantation scheme. Whole bone marrow (WBM) from mice expressing Cre recombinase driven by the intestinal epithelial-specific Villin promoter (VilCre) was transplanted into recipient mice that were homozygous for floxed Apc. Resulting intestinal phenotypes were observed in transplanted mouse intestine by wholemount analysis as polyps (B) in the distal small intestine (DSI) and as thickened unorganized epithelia (D) in the colon. H&E staining confirmed the phenotypic morphology (C,E). Bars in B & D = 1mm, bars in C & E = 25μm. (F) To confirm that the phenotype was the result of recombination at the Apc allele, PCR analysis of epithelium from recipient mice using primers that specifically detect the recombined Apc allele was performed. The 258bp band was present in the transplanted DSI and colon samples, indicating cell fusion by activation of Cre-recombinase.

the *Apc* allele, we isolated DNA from intestinal tissue sections and performed PCR with primers specific to the recombined floxed *Apc* allele. In both the DSI and the colon, a 258bp amplicon was identified, confirming that Cre recombinase had been activated within the tissue. This observation not only strongly supports the occurrence of cell fusion, but it importantly illustrated that these cell fusion hybrids can reprogram BMDC gene expression by activating an epithelial-specific promoter. While this functional evidence supports the implication that cell fusion can create a genetically distinct hybrid cell, the extent of reprogramming of the genome remains an intriguing and important future focus of investigation.

It is clear, from our studies presented here and previous reports (Wang, Willenbring et al. 2003; Rizvi, Swain et al. 2006; Johansson, Youssef et al. 2008; Nygren, Liuba et al. 2008) that cell fusion between BMDCs and non-hematopoietic tissues presents an important physiologic occurrence. Here, we report considerable baseline levels of cell fusion in the intestine under homeostatic conditions, greater than that reported in other organ systems (Alvarez-Dolado, Pardal et al. 2003; Wang, Willenbring et al. 2003; Johansson, Youssef et al. 2008). Further, we demonstrate that intestinal cell fusion with BMDCs is mediated by both inflammation and cellular proliferation. A possible physiologic role for intestinal cell fusion may be to facilitate rapid regeneration of the epithelial barrier after injury. Because the intestinal epithelium is the largest surface barrier to the external environment, barrier maintenance is critical for the organism's survival. If cell fusion participates in this rapid response, the intestine

is certainly poised to solicit fusion with both its intrinsic immune capacity and functional proliferation. While previous reports dismiss the importance of cell fusion or tie its potential to therapeutic gene replacement strategies, our data implicates cell fusion in a role to potentially impact inflammatory disease pathogenesis, including inflammatory bowel disease and cancer. Only by understanding the long-term fate of the epithelial cell fusion hybrid will we uncover its physiologic potential in both homeostasis and disease.

METHODS

Mice. Mice were housed in a specific pathogen-free environment under strictly controlled light cycle conditions, fed a standard rodent Lab Chow (#5001 PMI Nutrition International), and provided water *ad libitum*. All procedures were approved and performed in accordance with the Oregon Health and Science University animal ethics committee: the Oregon Health & Science University Institutional Animal Care and Use Committee. There are no human subjects involved in this study.The C57Bl/6, 129/Sv or ROSA (Soriano 1999) (WT), *IL-10*$^{-/-}$ (Kuhn, Lohler et al. 1993; Berg, Davidson et al. 1996) and *Villin-Cre* (Madison, Dunbar et al. 2002) mice were obtained from The Jackson Laboratory. *AhCre* mice (Ireland, Kemp et al. 2004) were kindly provided by Dr. Douglas Winton (University of Cambridge). Osb-Y01 (GFP) (Nakanishi, Kuroiwa et al. 2002; Anderson, Wu et al. 2005) and *Apc*^{580S} mice (designated as *Apc*$^{fl/fl}$ in the unrecombined state and *Apc*$^{-/-}$ after recombination) (Shibata, Toyama et al. 1997) were bred in-house.

Bone Marrow Transplantation. Whole bone marrow (WBM) transplantation was carried out as we have previously described with some modifications (Rizvi, Swain et al. 2006). Briefly, 6-week-old recipient male WT, *IL-10*$^{-/-}$, *Apc*$^{fl/fl}$, or *AhCre*$^{+}$;*Apc*$^{fl/fl}$ mice received whole-body γ-IR (12 Gy: in two 6 Gy doses, 4 hours apart). BMDCs were harvested from 5- to 12-week-old donor GFP (Nakanishi, Kuroiwa et al. 2002; Anderson, Wu et al. 2005) or *Villin-Cre* (Madison, Dunbar et al. 2002) mice using standard procedures (Battaile, Bateman et al. 1999), filtered to obtain a single-cell suspension and resuspended in Hank's balanced salt solution supplemented with 3% fetal bovine serum and 10mM HEPES . A total of 1 x 10^7 WBM cells were then injected retro-orbitally into recipient mice. To confirm hematopoietic engraftment, peripheral blood leukocytes were isolated from recipient mice as previously reported (Bailey, Willenbring et al. 2006) and analyzed using a Becton Dickinson FACSCalibur.

Parabiosis. Parabiosis surgery was performed between GFP and ROSA mice (*n* = 5 pair for WT, *n* = 5 pair for 5-ASA, *n* = 4 pair for DSS treatments) as described previously (Bailey, Willenbring et al. 2006). Briefly, pairs of 6- to 12-week age- and weight-matched mice were surgically joined from the elbow to knee. Each parabiotic partner was given recombinant human granulocyte colony-stimulating factor (250 μg/kg subcutaneously; Amgen) for 4 days starting at day 17 post-surgery (Abkowitz, Robinson et al. 2003). Mice were separated approximately 7 weeks after surgery and intestinal tissue analyzed.

Manipulation of intestinal inflammation. To suppress inflammation in *IL-10*$^{-/-}$ mice, 5-aminosalicylic acid (5-ASA) was administered in the drinking water at the time of WBM transplantation (500ppm 5-ASA/5mM Sodium Phosphate; Sigma). Mice were analyzed 3-7 months later. For parabiosis studies, animals were administered 5-ASA 1 week prior to surgery and continually until surgical separation. Meloxicam (a Cox-2 inhibitor; Boehringer Ingelheim) was concurrently administered for 4 days post-surgery. To induce inflammation in parabiotic mice, dextran sodium sulfate (DSS; TdB Consultancy AB) was given in drinking water (2.5% DSS in 5% sucrose) (Jurjus, Khoury et al. 2004) 1 week after separation followed by regular water for 1 week, at which point the animals were sacrificed and analyzed.

Intestinal proliferative model. To examine enhanced proliferation in the mouse intestine, we crossed *Apc*$^{fl/fl}$ (Shibata, Toyama et al. 1997) mice to the AhCre intestinal-specific inducible mouse line (Ireland, Kemp et al. 2004). *AhCre*$^{+}$*; Apc*$^{fl/fl}$ progeny were induced by intraperitoneal injection of β-naphthoflavone (β-NF; Sigma) dissolved in corn oil (80mg/kg) for four days (Sansom, Reed et al. 2004) and analyzed 2 days later. For transplantation studies, β-NF injections were initiated two days post-transplant.

Intestinal analysis of transplanted and parabiotic mice. Cell fusion was confirmed by co-localization of GFP expression developed for brightfield and Y-chromosome fluorescence *in situ* hybridization, or for fluorescent detection by

confocal microscopy with co-staining of antibodies for □-gal (1:500, Immunology Consultants Laboratory, Inc.) and GFP as reported previously (Rizvi, Swain et al. 2006) (*n* = 18).

Mice were analyzed at varying times post-transplantation (*IL-10*$^{-/-}$ studies: 3 and 7 months post-transplant, *n* = 7; proliferation studies: *n* = 13; WT transplants: 1-11 months for colon, *n* = 9, 3-11 months for DSI, *n* = 10; genetic recombination studies: 2-5 months, *n* = 11). Analysis of parabiotic pairs took place at time of separation (4-9 weeks; *n* = 10) or 3 weeks after separation for DSS studies (*n* = 4). Small intestine and colon was isolated *en bloc,* processed for wholemount imaging and subsequent frozen block preparation and sectioned as previously described (Wong, Rubinfeld et al. 1998). Tissue sections (5 μm) were analyzed for GFP-expressing cells by using polyclonal antibodies to GFP (1:500; Molecular Probes) and fluorescent secondary antibodies (1:500, Alexa 488, Molecular Probes; 1:500, Cy3 and 1:250, Cy5, Jackson Immuno Research) or for brightfield detection by using biotin–avidin secondary antibodies and visualization with 3-3′-diaminobenzidine (DAB) according to the manufacturer's guidelines (Vector Laboratories). For controls, tissues were stained with anti-CD45 (1:500; eBioscience), anti-E-cadherin (1:1000; Zymed), and anti-laminin (1:1000; Chemicon) followed by detection with appropriate fluorescent secondary antibodies. In some cases, tissue sections were also labeled with antibodies to the proliferation marker Ki67 (1:500; Abcam). Nuclei were counterstained with Hoechst (33258; Sigma; 0.1 μg/ml). For H&E images, paraffin sections were prepared as previously described (Wong, Rubinfeld et al. 1998). Sections were

examined with a Leica DMR microscope and digital images were captured with a DC500 digital camera and IM50 Image Manager Software (Leica Microsystems) or confocal images were acquired using an IX81 Inverted Microscope equipped with Fluoview FV1000-Spinning Disc Confocal (Olympus) scan head and FV10 ASW 1.7 software (Olympus). Cy3 images were captured as grayscale and digitally converted to red images with Adobe Photoshop CS2 (Adobe Systems Inc.). In some instances, Hoechst or laminin images were converted to grayscale.

To examine the temporal dynamics of peripheral blood infiltration and fusion in the intestine, WBM-transplanted WT mice were analyzed 1-7 days post-transplantation (*n* = 2-6 for each time point). GFP and Ki67 expression was surveyed in the DSI by co-staining with antibodies as described above. H&E images were captured from paraffin tissues prepared from γ-IR treated mice at the same time points.

Analysis for recombination of the *Apc* allele. DNA was isolated from 10μm thick paraffin tissue sections from *Apc*$^{fl/fl}$ mice that had received WBM from a *Villin-Cre* donor. PCR for the recombined *Apc* allele was performed as previously reported (Shibata, Toyama et al. 1997). The resulting bands mark various *Apc* status: Unrecombined = 314bp, Recombined = 258bp, Wildtype = 226bp. Controls were run with the following primers [P3, P4, P5 from (Shibata, Toyama et al. 1997)]: 5'GTTCTGTATCATGGAAAGATAGGTGGTC3'; 5'CACTCAAAACGCTTTTGA GGGTTGATTC3'; 5'GAGTACGGGGTCTCTGTCTCAGTGAA3'. Touchdown from 65 ºC to 55ºC,

followed by 14 cycles at 55ºC. Experimental samples were run with a nested PCR as follows: 1st PCR reaction: F-5'TAACCTGTTCTGCAGTATGTTATCATTC3' R-5'GAGCACCCAGTACGCTTCTAGAG3'. Touchdown from 65ºC to 52ºC, followed by 9 cycles at 52ºC; extension time of 4 minutes. 2nd PCR reaction (P3 and P5 primers from (Shibata, Toyama et al. 1997) : F-5'GTTCTGTATCATGGAAAGATAGGTGGTC3' R-5'GAGTACGGGGTCTC TGTCTCAGTGAA3'. Touchdown from 65ºC to 55ºC followed by 14 cycles at 55ºC.

Analysis of liver and skeletal muscle. WT mice were exposed to a single dose of whole-body γ-IR (9Gy) (Johansson, Youssef et al. 2008) and sacrificed 1-7 days later. Liver and skeletal muscle (quadicep, tibialis anterior and soleus muscles) were isolated and fixed in 4% paraformaldehyde and prepared as a frozen block. Tissue sections (10μm) were co-stained for the proliferation marker Ki67 as described above, along with cell-type specific antibodies. Skeletal muscle was pretreated to eliminate auto-fluorescence by incubating tissue in sodium tetraborohydrate (10mg/ml; Sigma), followed by subsequent staining for myosin heavy chain (Anti-myosin MY-32; 1:750; Sigma) using a mouse-on-mouse detection kit (M.O.M.; Vector Labs) followed by secondary detection with Anti-Biotin Cy5 Streptavidin (1:200; Jackson ImmunoResearch). Liver sections were initially stained with Ki67, imaged, and sequentially stained using rabbit anti-FAH (1:10,000; a kind gift from Markus Grompe (Azuma, Paulk et al. 2007))

followed by Cy5 secondary detection. Nuclei were counterstained with Hoechst dye. Digital images were captured as described above. Ki67-positive cells were quantified from 7 distinct 20x fields of view containing approximately 3500 hepatocytes or for skeletal muscle, 4 distinct 40x fields of view containing approximately 500 nuclei.

Inflammation assay. Quantitative reverse transcriptase polymerase chain reaction (qRT-PCR) was used to measure changes in the mRNA levels of Interleukin-1β (IL-1β) and Melanin-concentrating hormone receptor 1 (Kokkotou, Moss et al. 2008) (Mchr1) in isolated epithelial and mesenchymal cell populations from transplanted mice. Epithelial cell populations were isolated using a modified Weiser preparation (Weiser 1973; Weiser 1973) as we previously described (Davies, Dismuke et al. 2008). Following epithelial cell isolation, mesenchymal cells were isolated by scraping the remaining tissue on a tissue sieve (Bellco Glass, Inc.) to dislodge the mesenchymal population. Total RNA was purified from each cell population and cDNA was synthesized as we have previously described (Wong, Saam et al. 2000). qRT-PCR was performed using a SYBR Green-based assay and a 7900 HT Sequence Detector according to established protocols (Wong, Saam et al. 2000; Hooper, Wong et al. 2001; Davies, Dismuke et al. 2008). Each cDNA sample was analyzed in triplicate, along with triplicate samples of the endogenous reference gene, Glyceraldehyde-3-phosphate dehydrogenase (Gapdh). Primers used are listed as follows:

Gapdh: F- 5'AAATATGACAACTCACTCAAGATTGTCA3', R-5'CCCTTCCACAATGCCAAAGT3';

Mchr1: F-5'GGTAATGGTGTCTGGCACTTTG3', R-5' GCCATAGCAGTCAGGATGTAGGT3'; IL-1β: F-5'CGTGCTGTCGGACCCATATG3', R-5'GCCCAAGGCCACAGGTATTTT3'.

Statistics. Cell fusion was quantified by reporting the total number of crypt/villus (DSI) or crypt/cuff (colon) units harboring at least one or more GFP-positive cell(s). A unit is defined as one villus and its adjacent crypt (DSI) or a single colonic crypt and its adjacent epithelial cuff (colon). For each animal, tissue sections at least 125μm apart were quantified and at least 1500 units were examined. This quantification standard reports the percentage of units containing at least one fusion event. We do not quantitate on a per cell basis because this would overestimate the extent of cell fusion due to proliferative expansion of the initial fusion event. Statistical significance between experimental populations was determined using a Student's two-tailed, paired *t*-test or unpaired *t*-test as determined appropriate for each experimental scenario. *P* values <0.05 were considered statistically significant. Statistical analysis was performed using GraphPad Prism for Windows (GraphPad Software). All data are presented as the mean ± s.e.m.

CHAPTER 3

Macrophage-stem cell fusion results in reprogrammed intestinal epithelium

CHAPTER 3

Macrophage-stem cell fusion results in reprogrammed intestinal epithelium

Anne E. Powell[2], Eric C. Anderson[3] Paige S. Davies[1], Soren Impey[1,2] and Melissa H. Wong[1,2§]

[1]Department of Dermatology, Oregon Cancer Center, Oregon Stem Cell Center; [2]Department of Cell and Developmental Biology; [3]Department of Internal Medicine, Division of Hematology and Medical Oncology; Oregon Health & Science University, Portland, OR 97239, USA.

Submitted to *Science*, April 2010.

AEP participated in the planning of all experiments within the study as well as the writing of the manuscript.

ABSTRACT

Acquisition of the necessary molecular machinery for transformation into metastatic disease represents the most deadly phase of tumorigenesis. Although it is clear that epithelial-mesenchymal interactions play an important role in this process, the underlying mechanism is poorly understood. Interestingly, we have shown that mesenchymal cells can fuse with intestinal epithelia in a tumor microenvironment. This raises the intriguing possibility that generation of cell fusion hybrids between tumor and mesenchymal cells at critical stages of tumorigenesis may impact tumor behavior. Here we identify a blood-derived mesenchymal cell fusion partner, the macrophage, a cell that possesses the ability to migrate and navigate the vascular system. Further, we show that intestinal epithelial cell fusion hybrids express a unique transcriptome distinguishing them from their two parental lineages, macrophages and intestinal epithelium. These data implicate cell fusion as a mechanism for tumor heterogeneity and support a novel potential role in metastatic conversion.

INTRODUCTION

Metastasis is the most deadly aspect of cancer progression; however, it is the least well understood. The underlying mechanism by which cancer cells acquire the ability to escape the primary tumor site, migrate to a distant location and re-establish aggressive tumorigenesis is not known. Clearly, it is a multi-faceted process involving both changes in the tumor epithelia as well as influences from the surrounding tumor microenvironment. It has long been

speculated that fusion between mesenchymal cells and tumor cells can lead to phenotypic diversity and plays an important role in tumorigenesis (Duelli and Lazebnik 2003; Pawelek 2005). Mounting evidence suggests that cellular fusion may result in aneuploidy or other genetic alterations that could initiate tumorigenesis (Holland and Cleveland 2009). Interestingly, tumor suppressor genes were first identified in cell fusion assays where their loss resulted in a cancer phenotype (Harris, Miller et al. 1969). Notably, the concept that oncogene activation or tumor suppressor loss may select for cells with a greater propensity for malignant conversion has been illustrated both *in vitro* and *in vivo* (Klein and Klein 1984). We have previously shown that circulating bone marrow-derived cells (BMDCs) readily fuse with the intestinal epithelium upon tissue injury (Rizvi, Swain et al. 2006; Davies, Powell et al. 2009). Important factors that are stimulated during injury and regeneration, specifically inflammation and epithelial hyperproliferation, are mediators of intestinal cell fusion (Davies, Powell et al. 2009). Intriguingly, these two factors are also key components of the tumor microenvironment, suggesting that cell fusion may be enhanced in tumors.

Importantly, while cell fusion between blood leukocytes and tumor cells has been shown to occur both *in vitro* and *in vivo* (Rupani, Handerson et al. 2004; Willenbring, Bailey et al. 2004), the physiologic consequence of cell fusion on tumorigenesis remains unknown. It has been proposed that cell fusion may impart migratory blood cell properties to tumor cells as a potential contribution to drive metastatic disease (Pawelek 2005; Pawelek and Chakraborty 2008), however no definitive *in vivo* evidence for this process exists. While it is clear that

implicating cell fusion in cancer progression could revolutionize how we currently understand the biology of metastatic disease, it is a formidable undertaking. First, definitive proof that fusion occurs *in vivo* between circulating cells and tumor cells must be demonstrated. Second, it must be determined whether cell fusion hybrids exist as a transient population or are integrated into the surrounding cell population, as this is critical for establishing their long-term impact. Next, acquired genetic alterations exhibited within cell fusion hybrids would strongly support a unique role for this distinct cell population. Finally, the physiologic impact of cell fusion on tumor progression must be demonstrated. While not all of these criteria will be easily performed, incremental steps toward understanding this process may lead to a novel mechanism for acquisition of metastatic potential and open a new avenue for preventing this deadly transition. The studies presented here provide the initial steps toward building a basis for implicating cell fusion in tumorigenesis.

RESULTS AND DISCUSSION

Tumor epithelia fuse with circulating bone marrow-derived cells *in vivo*

The observation that both inflammation and epithelial proliferation, two characteristics of a tumor microenviroment (Coussens and Werb 2002), are strong mediators of cell fusion (Davies, Powell et al. 2009) supports the notion that cell fusion occurs as part of the natural process of tumorigenesis. To determine that this is indeed the case, we established that cell fusion occurs between the intestinal tumor epithelium and genetically marked circulating

BMDCs in a non-injury experimental system, parabiotic mice (Figure 3.1). Using parabiosis, the surgical joining of two mice, to introduce green fluorescent protein (GFP)-expressing circulating blood (Nakanishi, Kuroiwa et al. 2002; Anderson, Wu et al. 2005) into a tumor-bearing *Apc*$^{Min/+}$;ROSA26 mouse (Moser, Pitot et al. 1990; Soriano 1999) (Figure. 3.1A), resulting tumors harbored epithelium that co-expressed the "donor" marker (GFP) and the "recipient" marker (β-galactosidase; β-gal), as determined by confocal microscopy (n=4; Figure 3.1B-C). We have previously documented the occurrence of cell fusion between BMDCs and the intestinal epithelium using a dual marker system (GFP/β-gal or GFP/Y-chromosome) (Rizvi, Swain et al. 2006; Davies, Powell et al. 2009) as well as by a genetic approach using Cre/lox to mark cell fusion hybrids (Davies, Powell et al. 2009). In addition, we show here that endogenous GFP expression can be recognized by immunohistochemistry as well as antibodies to GFP with high fidelity (Figure. 3.2A-C) and that cell fusion in the epithelial compartment is not mistaken as intraepithelial lymphocytes or as tissue auto-fluorescence (Figure 3.2D-L, Figure 3.3). Therefore, the detection of tumor epithelia co-expressing GFP and β-gal in parabiotic mice strongly supports that cell fusion occurs in the context of tumorigenesis. Tumor cells are known to be highly fusogenic; this is especially evident in cell culture systems (Pawelek 2005). However, the physiologic relevance of tumor cell fusion is currently not clearly defined. Important advancements in elucidating a physiologic impact of cell fusion in tumorigenesis require an initial understanding of the basic mechanism by which cell fusion occurs. Therefore, identification of the cell fusion partners represents

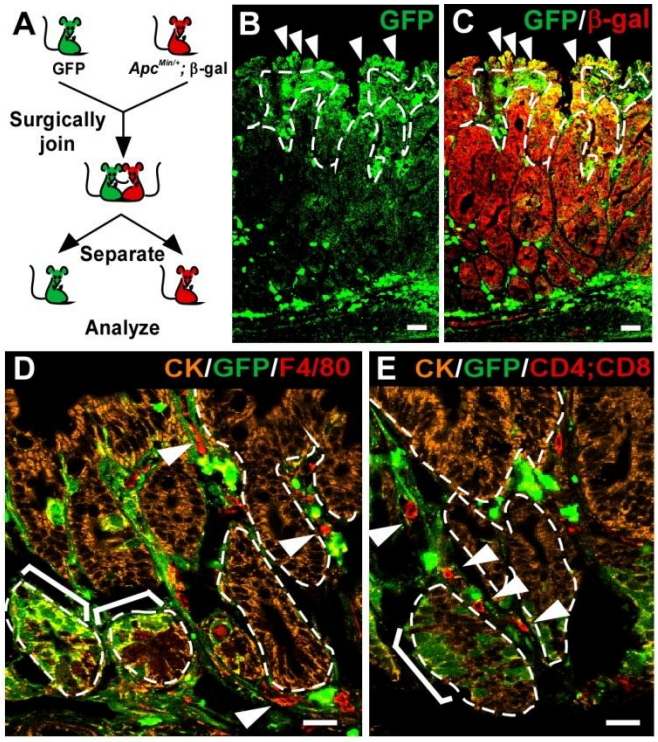

Figure 3.1. Intestinal cell fusion in tumorigenesis. (A) Parabiosis experimental design. GFP and $Apc^{Min/+}$;ROSA26 mice were surgically joined. (B-C) Cell fusion was observed in small intestinal polyps. Single plane confocal microscopy images of GFP (green) and ß-galactosidase (red) detected by antibodies demonstrate fusion by co-localization in yellow (C). Arrowheads denote examples of fused cells. (D-E) Lymphocytes and leukocytes are present within small intestinal polyps that have undergone fusion. Single plane confocal microscopy depicts fusion-derived (brackets) and unfused epithelia detected with antibodies to GFP (green) and cytokeratin (marking the epithelial compartment, orange). Arrowheads indicate F4/80+ macrophages (red) (D) or CD4+ or CD8+ T cells (red) (E) in the tumor mesenchyme. Dashed white lines indicate epithelial/mesenchymal border. Bars = 25μm.

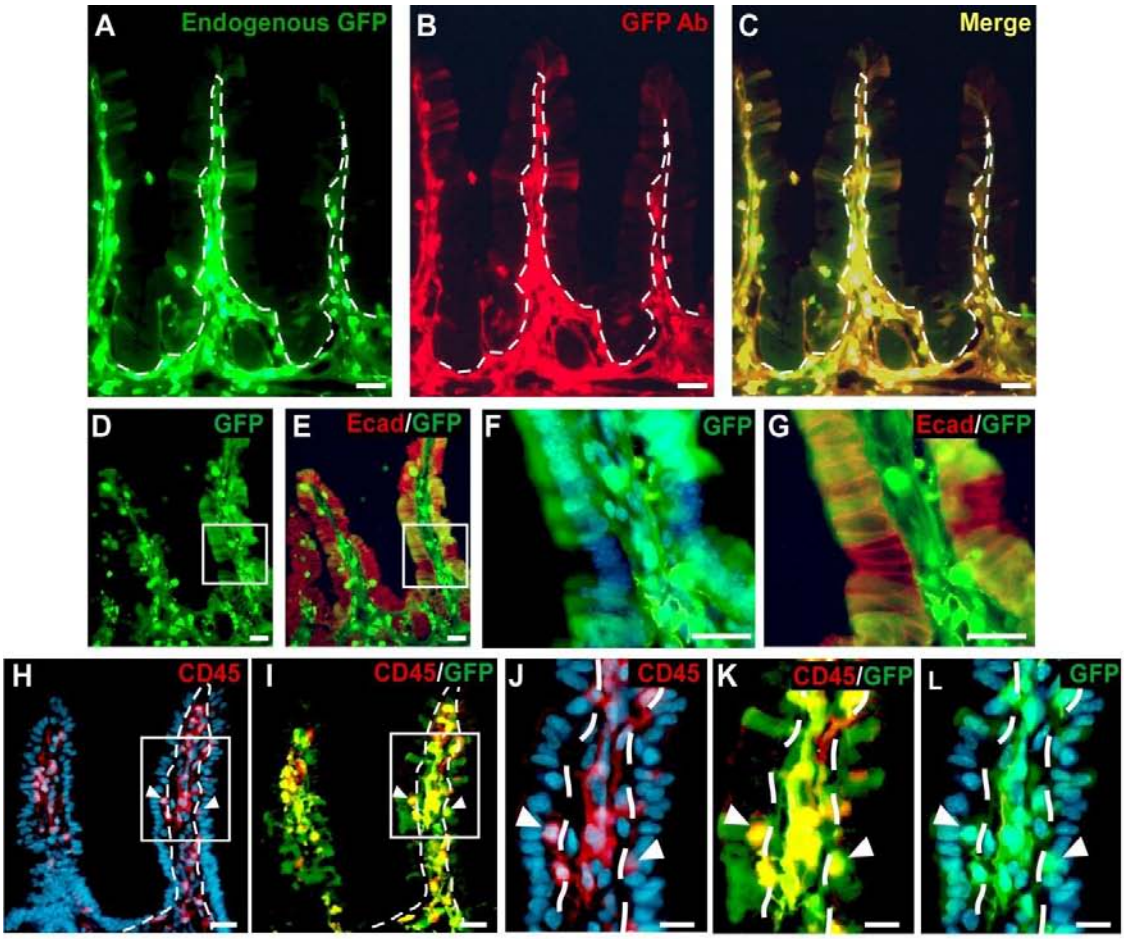

Figure 3.2. Detection of GFP expressing cells. Intestinal tissue sections from GFP-expressing whole bone marrow transplanted mice. (A-C) Endogenous GFP detectable expression (A; green) is recapitulated by GFP expression detected with anti-GFP antibodies and detection with cy5-conjugated secondary antibodies (B; red) as determined by complete overlay visualized in (C; yellow). (D-G) GFP-expressing epithelium (D,F; green) expresses the epithelial cell marker E-cadherin identified by antibody staining (E,G; Ecad; red). f-g, Higher magnification of boxed region in panels D and E. (H-I) GFP-expressing epithelium does not express the blood marker, CD45 (red). (H) The majority of CD45-positive cells (red) reside within the lamina propria of the intestinal villus. Intraepithelial lymphocytes (IELs, arrowheads) are blood cells that reside in the epithelial compartment.(I) GFP-expressing epithelium (green) is distinguished from GFP-expressing blood cells (yellow) in this GFP and CD45 co-stained tissue section.(J-L) Higher magnification of white boxed regions in H-I. Dashed white lines indicate epithelial/mesenchymal border. Some sections stained with Hoechst, blue. Bars = 25μm.

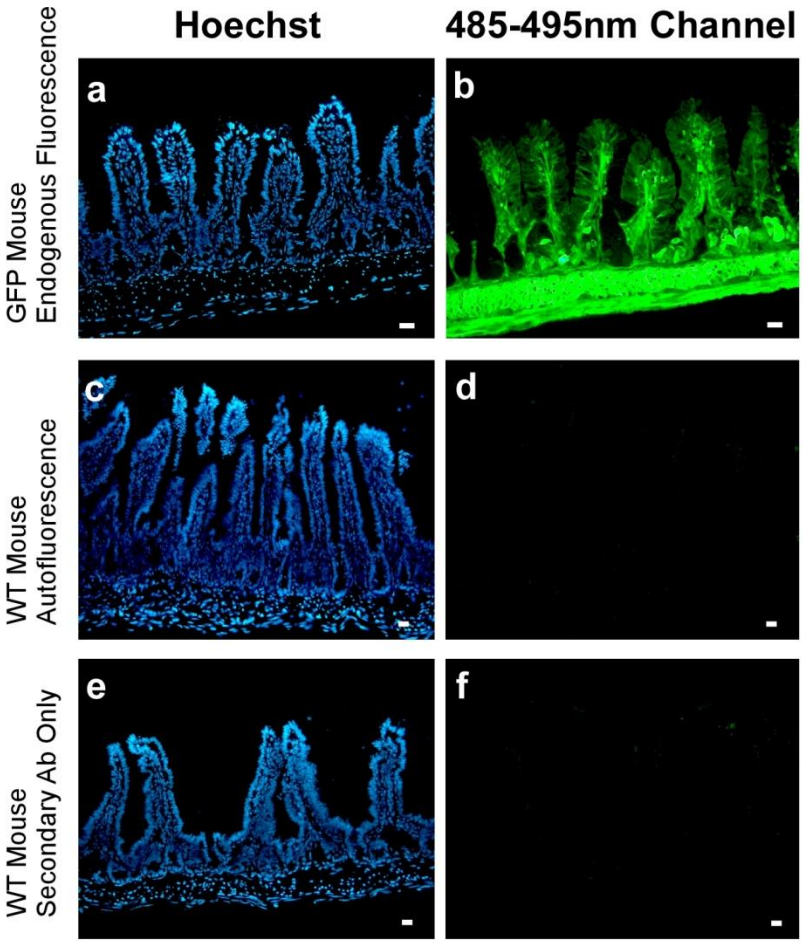

Figure 3.3. GFP antibody immunohistochemistry controls. (A-B) Endogenous GFP fluorescence (green) in the small intestine of a transgenic GFP-expressing mouse. (C-D) Tissue autofluorescence using a GFP-detectable filter (485-495 nm) is not observed in the small intestine of a wild-type mouse. (E-F) Secondary antibody staining controls (anti-rabbit Alexa-488) do not demonstrate a fluorescent signal. Image in panel B was captured under the same conditions, but at one-third the exposure time as panels D and F. Nuclei are stained with Hoechst dye (A, C, E; blue). Bars = 25μm.

an important first step. Our previous work, examining cell fusion in the intestinal epithelium, revealed that the intestinal stem cell is capable of fusion (Rizvi, Swain et al. 2006); however the BMDC fusion partner has not been identified. Therefore, to examine potential candidate cells within the tumor microenvironment, we stained intestinal adenomas from the parabiotic mice with antibodies to macrophages, T and B cells (Figure 3.1D,E). All three blood-derived populations were present within the mesenchyme of the tumor microenvironment, suggesting that these populations may be poised for epithelial cell fusion.

The macrophage lineage robustly fuses with the intestinal epithelium

It is possible that a number of mesenchymal cells are capable of cell fusion, as several BMDC lineages have previously been described to undergo this process (Willenbring, Bailey et al. 2004; Johansson, Youssef et al. 2008; Nygren, Liuba et al. 2008). Therefore, to determine which BMDC lineages contribute to intestinal cell fusion, we systematically surveyed the fusogenic capacity of GFP-expressing blood lineages isolated by Fluorescence-Activated Cell Sorting (FACS) in a mouse bone marrow transplantation system (Figure 3.4a). We have previously utilized gamma-irradiation and bone marrow transplantation to effectively promote cell fusion with the intestinal epithelium (Rizvi, Swain et al. 2006) as a model of epithelial regeneration after injury, akin to the microenvironment of epithelial tumors. Using this model system, we transplanted common myeloid and common lymphocyte progenitors (CMP and

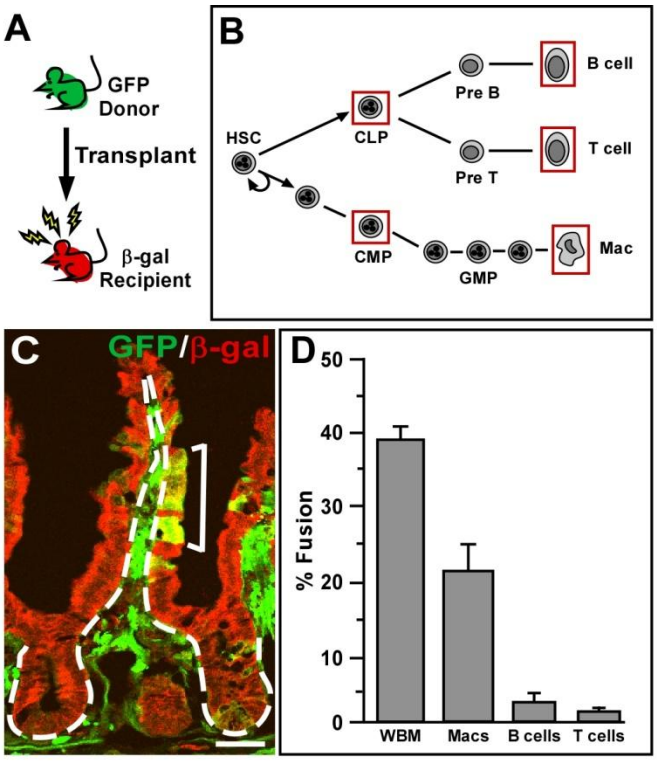

Figure 3.4. Macrophages are primarily responsible for fusion with injured intestinal epithelium. (A) Schematic representation of experimental design. Whole bone marrow or FACS-isolated blood populations were transplanted from GFP-expressing mice into lethally irradiated wild-type ROSA26 mice. (B) Hematopoietic cell lineages. Red boxes indicate the isolated cell populations used for transplantation. (C) Macrophage fusion with the intestinal epithelium in a ROSA26 mouse transplanted with $2x10^5$ GFP-positive sorted macrophages. Single plane confocal microscopy image of GFP (green) and β-galactosidase (red) detected by antibodies demonstrates fusion by co-localization in yellow (bracket). (D) Fusion was observed with all transplanted lineages, however macrophage fusion was significantly more robust than in the B and T cell transplanted animals. Dashed white lines indicate epithelial/mesenchymal border. $P<0.01$. Bars = 25 μm.

CLP, respectively), as well as differentiated macrophages, B and T cells (Figure 3.4B) isolated by FACS using standard cell surface antigens (Coffman 1982; Zwadlo, Brocker et al. 1985; Godfrey, Kennedy et al. 1994; Kondo, Weissman et al. 1997; Akashi, Traver et al. 2000) (Figure 3.5). We then evaluated their ability to fuse with the intestinal epithelium using a quantification scheme that accounts for fusion at the intestinal stem cell level (Figure 3.6). Interestingly, all five isolated populations displayed the ability to fuse with the intestinal epithelium to varying degrees. Fusion between CMPs (n=4) or CLPs (n=2) and the epithelium was detected, but was extremely rare. To further restrict possible candidates, mice were transplanted with $Rag1^{-/-}$;GFP whole bone marrow (WBM) that is genetically devoid of mature B and T cells (Mombaerts, Iacomini et al. 1992). Interestingly, robust epithelial cell fusion was observed (n=4; Figure 3.7), suggesting that mature B and T cells were not required for cell fusion and that immature B or T cells and/or the myeloid lineage effectively contributed to cell fusion. When FACS-isolated macrophages, B and T cells were independently transplanted into our fusion model, all lineages were observed to participate in cell fusion (Figure 3.4D). However, very low levels of epithelial cell fusion were detected in B and T cell transplanted mice (n=4 each). Not surprisingly, the characteristically fusogenic macrophage (Chen, Grote et al. 2007) displayed the most robust cell fusion (n=14), resulting in fusion that resembled that in whole bone marrow transplanted intestines (Figure 3.4C-D). Because the macrophage population is functionally diverse, we wondered if activated macrophages possessed different fusogenic capabilities compared to those isolated from WBM

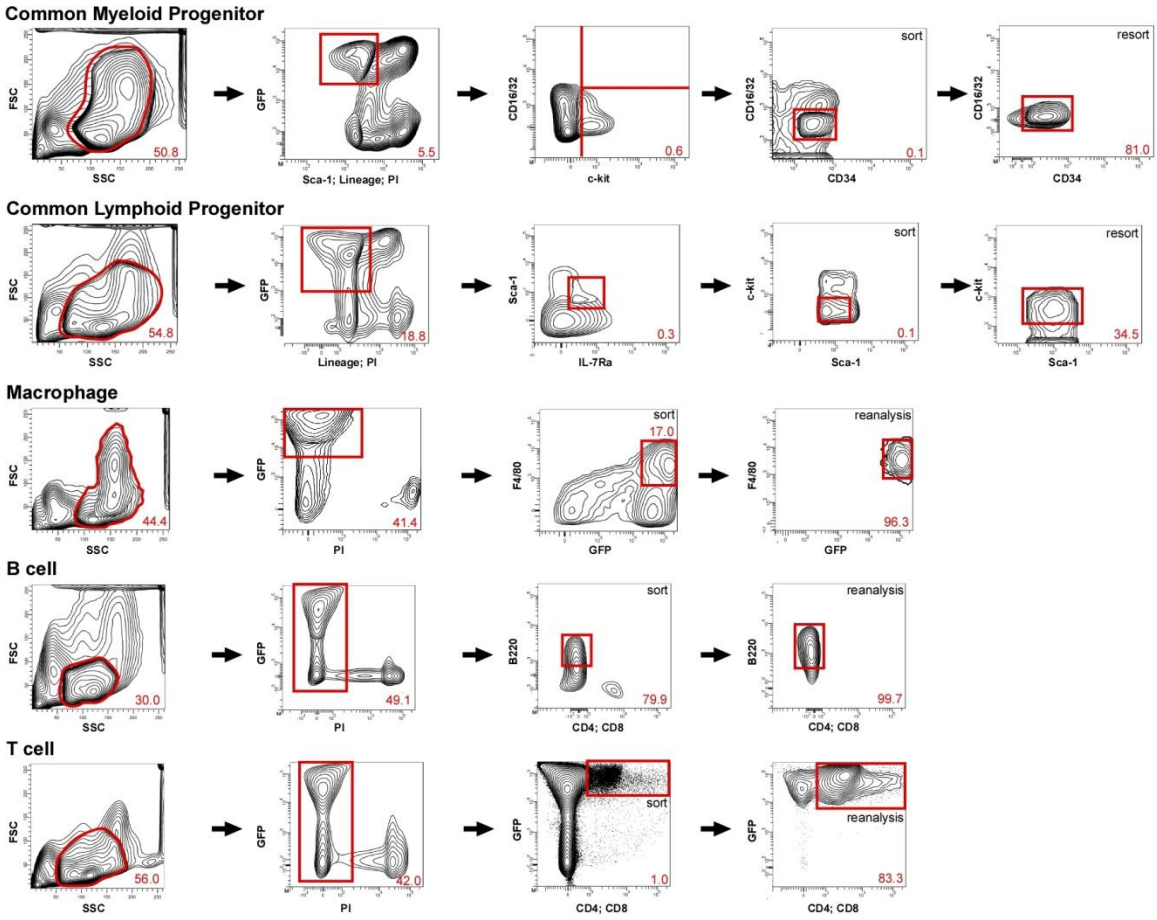

Figure 3.5 FACS isolation of whole bone marrow or peripheral blood cell populations. Cell sorting gates for the isolation of Common Myeloid Progenitors, Common Lymphoid Progenitors, Macrophages, B cells and T cells. All cells were initially gated using forward scatter and side scatter (FSC and SSC). Desired populations were then isolated based on their GFP and lineage or stem cell antigen expression using fluorescent-conjugated antibodies. For all populations shown, progressive sorting gates proceed from left to right (indicated in red). Percentages of the total population within a given gating parameter are indicated. Isolated populations were re-sorted to ensure purity. Antibody staining conditions and target cell antigen expression patterns are provided in Table 3.1. Dead cells were excluded with propidium iodide (PI) staining.

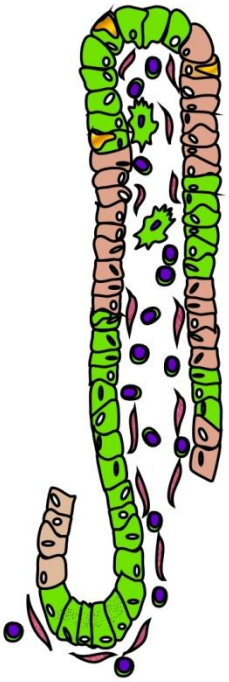

one crypt/villus (C/V) unit

$$\left(\frac{\text{C/V units with GFP}^{+}\text{ epithelial cells}}{\text{1500 C/V units}}\right) \times 100 = \%\ \text{fusion}$$

Figure 3.6. Quantifying cell fusion. Cell fusion was reported as the percentage of crypt/villus (C/V) units that harbored at least one or more GFP-positive cell(s). A C/V unit is defined as one villus and an adjacent crypt. For each experiment, cell fusion was quantified from intestinal tissue sections that were cut at least 125μm apart. A minimum of 1500 C/V units were examined and at least n=3 mice/experiment.

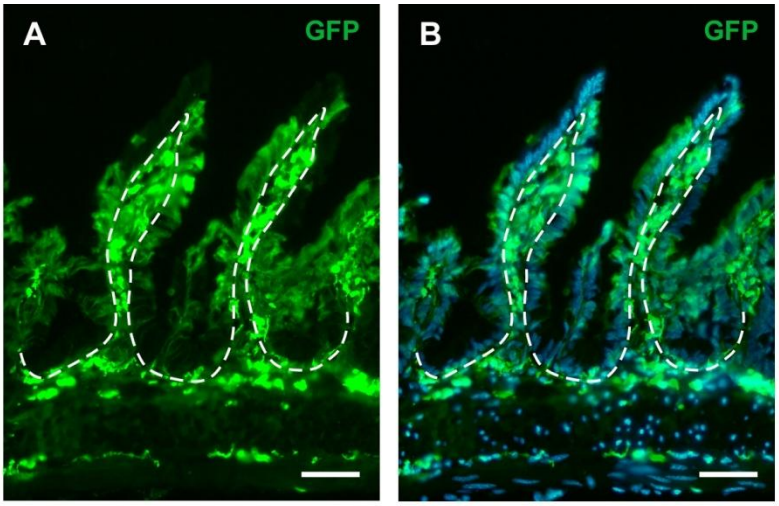

Figure 3.7. Rag1$^{-/-}$; GFP whole bone marrow cells fuse with intestinal epithelium. Intestinal tissue sections from Rag1$^{-/-}$;GFP-expressing whole bone marrow transplanted mice. (A-B) GFP-expressing epithelial cells (green) were detected with antibodies to GFP, indicating that bone marrow devoid of mature B and T cells can support epithelial cell fusion. Nuclei are stained with Hoechst dye (B; blue). Dashed white lines indicate epithelial/mesenchymal border. Bars = 25μm.

and peripheral blood or from those grown in culture. Interestingly, we found no difference in levels of cell fusion between these macrophage populations. Although this might suggest that the type of macrophage is not important in cell fusion, it is likely that once transplanted into the recipient mouse, different macrophage populations are appropriately activated to fuse with the intestinal epithelium.

Macrophages are known to be actively recruited to the site of injury (Pull, Doherty et al. 2005), and in this context may be stimulated to fuse with the injured epithelium. Our previous work established that GFP-expressing BMDCs transit to the intestine after irradiation injury, just prior to detection of epithelial fusion (Davies, Powell et al. 2009). This suggests that specific pre-fusion mesenchymal actions must occur to facilitate events leading to fusion, including crossing of the basement membrane into the epithelial compartment. A detailed time course examining the arrival of GFP-expressing transplanted BMDCs into the intestine revealed a clustering of cells around the intestinal stem cell niche, forming a pre-fusion cluster, 4 days post-transplantation (Figure 3.8). Confocal microscopy (Figure 3.9A-G) and 3-dimensional reconstruction of individual intestinal crypts from 50μm thick tissue sections revealed that these BMDCs are juxtaposed the basement membrane adjacent to the epithelial compartment (Movie). Interestingly all three lineages, macrophages, B and T cells, were present in these donor-marked crypt cell clusters (Figure 3.9H-I; Figure 3.10). Further, a detailed evaluation of pre-fusion clusters by confocal serial slices through an intact crypt revealed rare instances where GFP-expressing

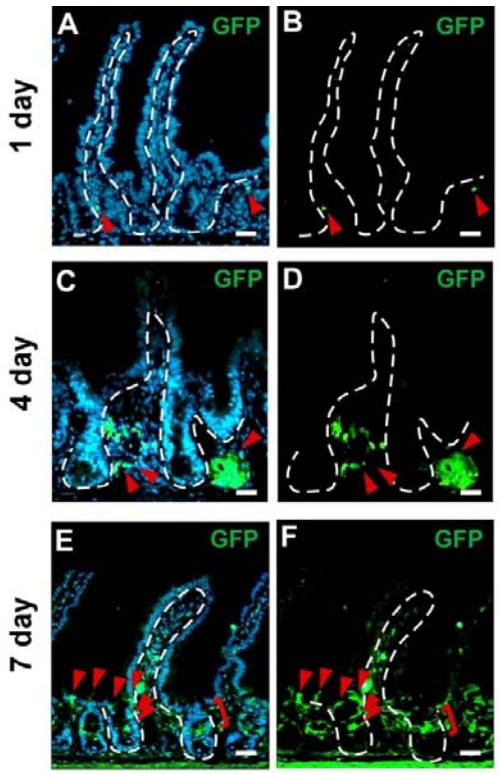

Figure 3.8. Epithelial cell fusion is detected 7 days after transplantation. Wild-type mice were transplanted with GFP-expressing whole bone marrow (WBM). The DSI was analyzed at 24h increments for 1 week. (A-B) At 1 day post-transplantation, few GFP-positive cells (green) were located in the mesenchyme (arrowheads) and none were found in the epithelium. (C-D) At 4 days post-transplantation, GFP-positive cells cluster near crypts (arrowheads), while none were detected in the epithelium. (E-F) By 7 days post-transplantation, GFP-positive epithelium was observed in the crypts (arrowheads and brackets). Nuclei are stained with Hoechst dye (A, C, E; blue). Dashed white lines indicate epithelial/mesenchymal border. Bars = 25μm.

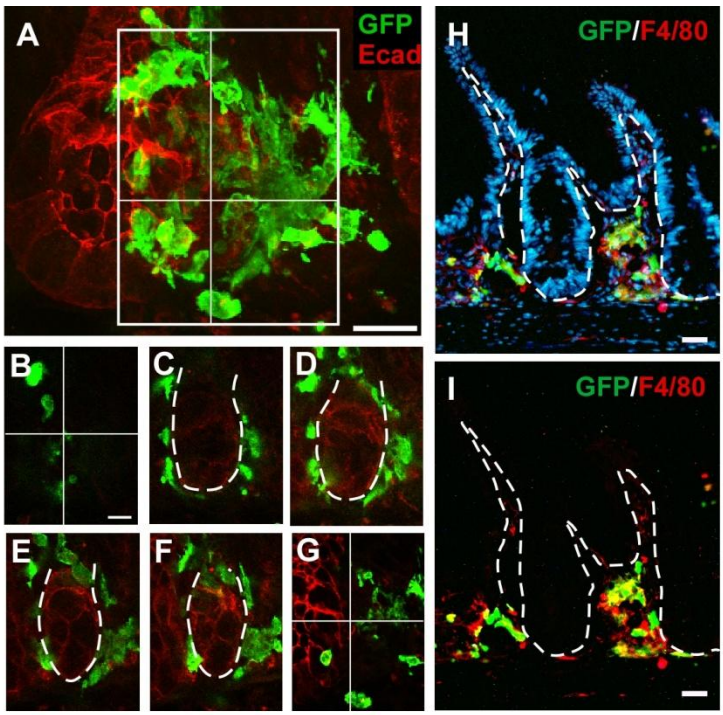

Figure 3.9. Pre-fusion clusters of BMDCs contain macrophages. (A) 50µm tissue section and 3-dimensional crypt reconstruction of a confocal z-stack image illustrating GFP-positive BMDCs (green) surrounding the crypt/stem cell niche. Epithelial cells are marked with E-cadherin (red). (B-G) Sequential sections through z-stack shown in (A). (H-I) Pre-fusion cell clusters contain F4/80-positive macrophages (red) consisting of both donor-derived (yellow) and non-donor-derived cells. Nuclei are stained with Hoechst (H; blue). Dashed white lines indicate epithelial/mesenchymal border. Bars = 25 µm.

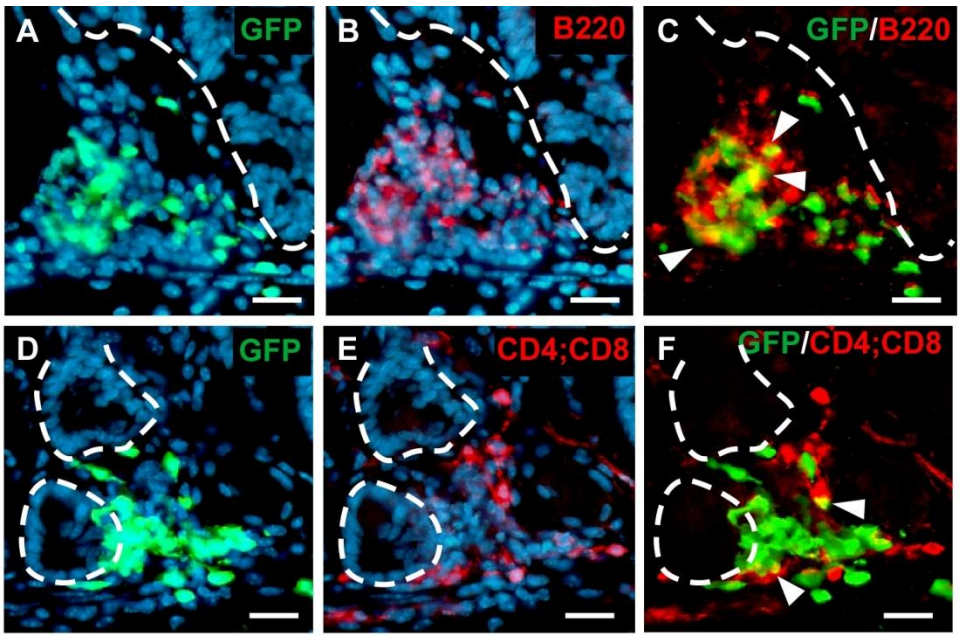

Figure 3.10. B and T cells are present within GFP-expressing blood cell clusters 4 days after transplantation. (A-C) Intestinal tissue sections from GFP-whole bone marrow transplanted mice, four days post-transplant co-stained with antibodies to GFP (A, green) and B220, a B cell marker (B, red). Donor-derived, GFP-expressing cell clusters contain B cells, apparent in merged image (C; yellow cells, white arrowheads). (D-F) Likewise, donor-derived GFP-expressing cell clusters (D; green) also contain T cells (E, red) when double-stained with antibodies to the T cell markers CD4 and CD8. Arrowheads in the merged image (F) indicate donor-derived T cells (yellow). Nuclei are stained with Hoechst dye (blue). Dashed white lines indicate epithelial/mesenchymal border. Bars = 25μm.

macrophages were straddling or crossing the laminin-marked basement membrane, protruding into the epithelial space 4 days after transplantation (Figure 3.11A-I). In these confocal panels, macrophages expressing GFP in the cytoplasm were identified by cell-surface F4/80 expression on both sides of the laminin-marked boundary in both the upper crypt and the lower stem cell region. While intraepithelial lymphocytes are located on the epithelial side of the basement membrane, it is rare to observe a macrophage exhibiting this behavior. It is possible that our data represents a snapshot of a macrophage in the process of antigen sampling, in which they have been described to cross the basement membrane and protrude between epithelial cells (Duerkop, Vaishnava et al. 2009). However, active transit into the epithelial compartment is a likely prerequisite for fusion with the epithelial cell, and therefore our data demonstrate the capacity for the macrophage to position itself in the proper location. While our focus on the macrophage does not exclude the possibility that B and T cells can also fuse, our limited-lineage transplantation analysis suggested that epithelial cell fusion involving these lymphocytes is significantly less frequent than with macrophages. Regardless, capturing the act of pre-fusion macrophages invading the epithelial compartment provides compelling evidence that it is a primary partner for cell fusion with the intestinal epithelium.

Cell fusion hybrids retain macrophage-specific gene expression

Identification of *in vivo* intestinal epithelial cell fusion partners provides important insight into the physiologic behavior of the resulting cell fusion hybrids.

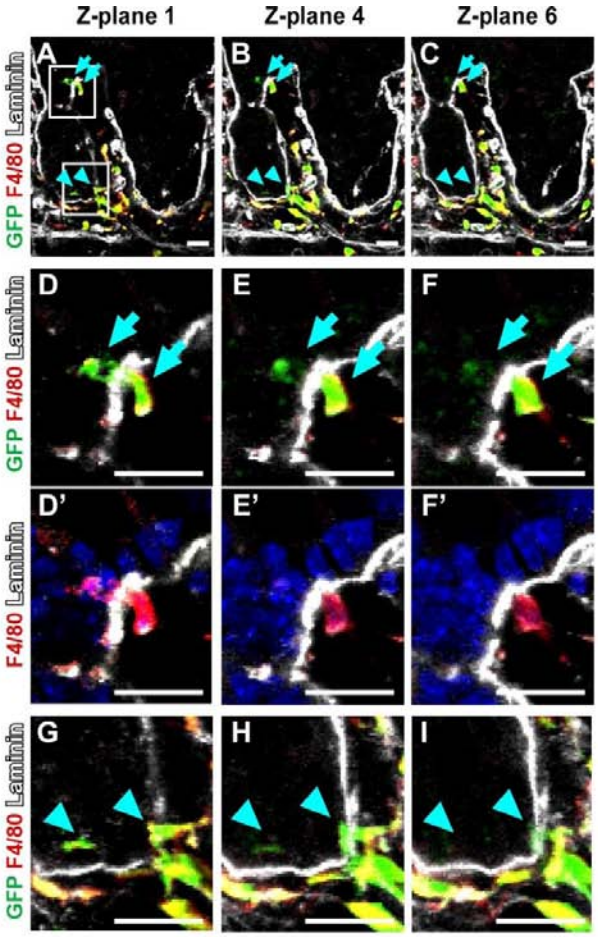

Figure 3.11. Macrophages cross the basement membrane early after transplantation. Confocal image Z-planes (0.5 μm) from a 50μm Z-stack of the small intestine from a 4-day post-GFP transplanted GFP mouse. (A-C) GFP-positive (green) cells stained with antibodies to the macrophage marker F4/80 (red) and laminin (white) to mark the epithelial-mesenchyme boundary. Arrows and arrowheads represent macrophages that are crossing or have crossed into the epithelial space from the mesenchyme. (D-F), (D'-F') Magnified view of upper boxed region from panels (A-C). A GFP-positive cell (green) lies in both the mesenchymal and epithelial region and is identified as a macrophage (red). (G-H) Magnified view of lower boxed region from panels (A-C) depicting two more GFP-positive cells in the epithelial space that are co-stained with F4/80 (yellow). Bars = 25 μm.

We initially characterized intestinal cell fusion hybrids to primarily posses epithelial phenotypes based upon their physiologic location, their epithelial expression pattern, and the loss of expression of the pan-lymphocytic donor marker CD45 (Rizvi, Swain et al. 2006). Interestingly, these cell fusion hybrids retain the transgenic donor marker, GFP, suggesting that these cells may exhibit donor transcriptome expression. To further explore this possibility, newly generated cell fusion hybrids were assayed for expression of the macrophage-specific gene, F4/80. This membrane glycoprotein was co-expressed in GFP-expressing cell fusion hybrids within the intestinal crypt (Figure 3.12A-B). Interestingly, although F4/80 is a cell surface protein in macrophages, it appeared to be localized to the cytoplasm in the epithelial cells. This reveals a potential inability of the epithelial-like cell fusion hybrid to traffic this protein to the proper macrophage location. However, by 4 weeks post-transplantation, cell fusion hybrids have lost the ability to express the F4/80 protein, but retained mRNA expression, as detected by quantitative reverse transcriptase-PCR (qRT-PCR) in FACS-isolated GFP-positive cell fusion hybrids (Figure 3.12C; Figure 3.13). Although cell fusion hybrids expressed a similar amount of the epithelial-specific transcript, E-cadherin, when compared to the adjacent GFP-negative wild-type epithelium, a significantly higher level of the F4/80 transcript was detected (n=3). It is possible that a dynamic regulation of macrophage-specific genes occurs within the cell fusion hybrids, such that macrophage-specific gene expression is temporally modulated. Importantly, the cell fusion hybrid retains the ability to express the F4/80 transcript even 4 weeks after fusion, suggesting that

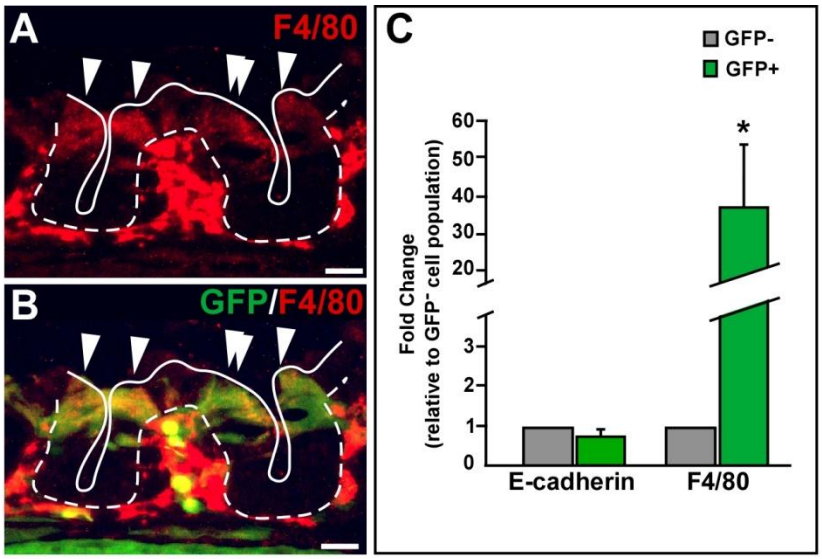

Figure 3.12. Epithelial cell fusion hybrids express macrophage-specific markers. (A) The macrophage-specific protein F4/80 (red) is detectable in both the mesenchyme and epithelial compartment 7 days post-transplantation. (B) F4/80^{+} epithelium also expresses GFP (green) suggesting they are fusion products of donor-derived cells (yellow). Arrowheads indicate examples of fusion hybrid cells. (C) qRT-PCR analysis of isolated GFP^{+} epithelia (fusion hybrids) 4 weeks after transplantation revealed a significant expression of the macrophage marker F4/80, when compared to the adjacent GFP^{-} epithelia; whereas the epithelial specific marker E-cadherin was expressed at a similar level. $P<0.01$. Bars = 25 μm.

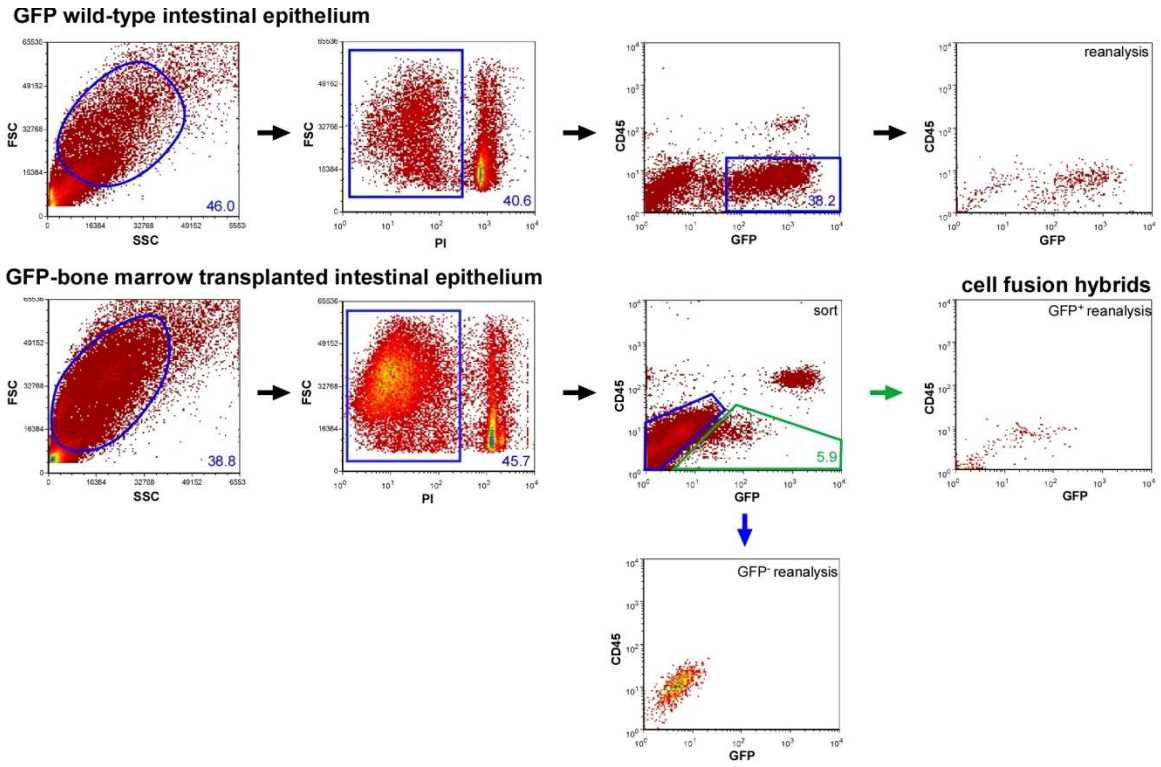

Figure 13.13. FACS isolation of intestinal epithelium. Sorting gates for both the isolation of GFP-expressing wild-type epithelium and cell fusion hybrids (GFP-expressing epithelium from transplanted mice). All cells were gated using forward scatter and side scatter (FSC and SSC). Desired populations were isolated based on GFP expression and lack of the blood cell antigen, CD45. For all populations shown, progressive sorting gates proceed from left to right and gates are boxed. Numbers within the sort plots represent percentages of the total population within a given parameter. For transplanted mice, both GFP-positive (cell fusion hybrids) and GFP-negative epithelial populations were isolated. Antibody staining conditions and target cell antigen expression patterns are provided in Table 3.1. Dead cells were excluded based on propidium iodide (PI) staining.

long term reprogramming at the stem or progenitor level has occurred. Intriguingly, novel gene expression within this population of cells may have significant impact on cellular physiology and subsequent behavior.

Acquired gene expression is an important step in tumor progression. Therefore, we set out to determine if the macrophage transcriptome is preserved in cell fusion hybrid cells. To do this, we used the unbiased and comprehensive RNA-Seq approach (Wang, Gerstein et al. 2009), a genome analysis approach that has been validated and confirmed by microarray (Tang, Barbacioru et al. 2009). Using RNA-Seq, we compared the transcriptome profiles of three FACS-isolated populations: unfused intestinal epithelial cells (from n=3 animals), unfused macrophages (from n=3 animals) and epithelial-macrophage cell fusion hybrids (from n=4 animals) (Figure 3.14). Rigorous isolation procedures were followed to ensure purity of FACS-isolated populations (Figure 3.15, Figure 3.16).

Comparative transcriptome analysis revealed that of ~20,000 transcripts analyzed, 20.8%, were differentially-regulated between at least two populations at significant levels ($p<0.01$). Of these differentially regulated transcripts, 32.8% were similarly regulated between cell fusion hybrids and wild-type intestinal epithelium (Figure 3.14A), and intriguingly, 4.0% of differentially-regulated transcripts were shared between cell fusion hybrids and blood-derived macrophages (Figure 3.14B). The most compelling finding from this analysis was that 3.4% of the differentially-regulated transcripts were uniquely expressed in the cell fusion hybrids, relative to either parental lineage (Figure 3.14C). Expression of this set of genes provides strong evidence that cell fusion hybrids

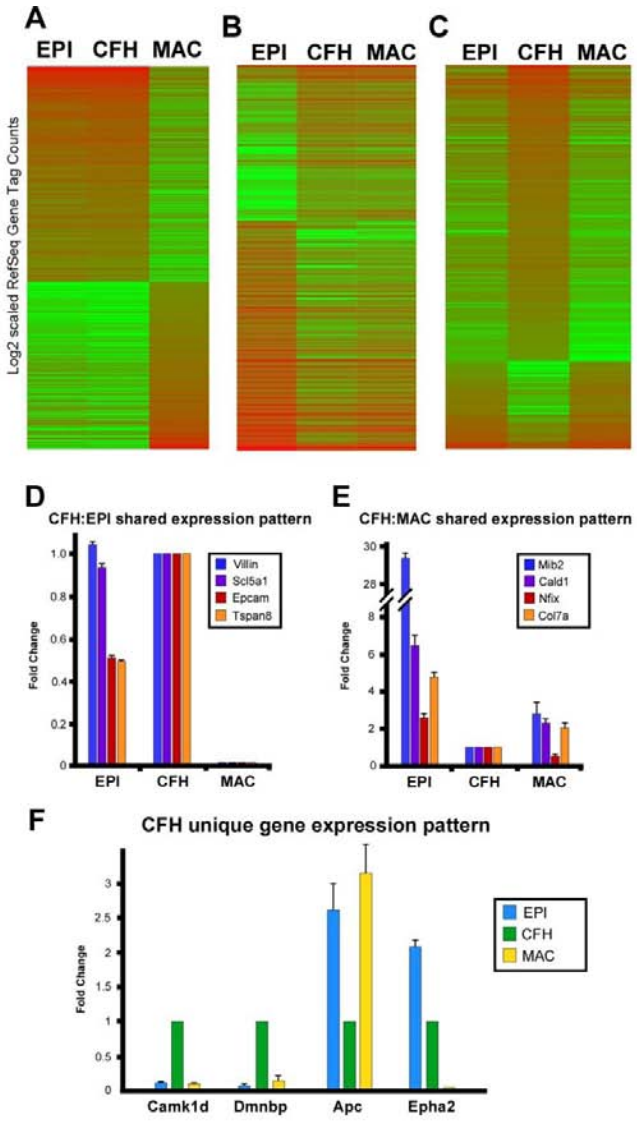

Figure 3.14. Cell fusion hybrid epithelia express a unique transcriptome. (A-C) Heat maps illustrating subsets of cell fusion hybrid (CFH) Ref-Seq genes identified by RNA-Seq that harbor shared or unique transcriptional profiles with wild-type epithelium (Epi) and macrophages (Mac). (D-E) Transcript expression from (A-C) confirmed by qRT-PCR. Three categories were confirmed: genes shared by CFH and Epi (D), genes shared by CFH and Mac (E) and genes unique to CFH (F). Data is represented as fold change of triplicate samples +/- S.E. normalized to an internal reference gene and relative to expression in the CFH population.

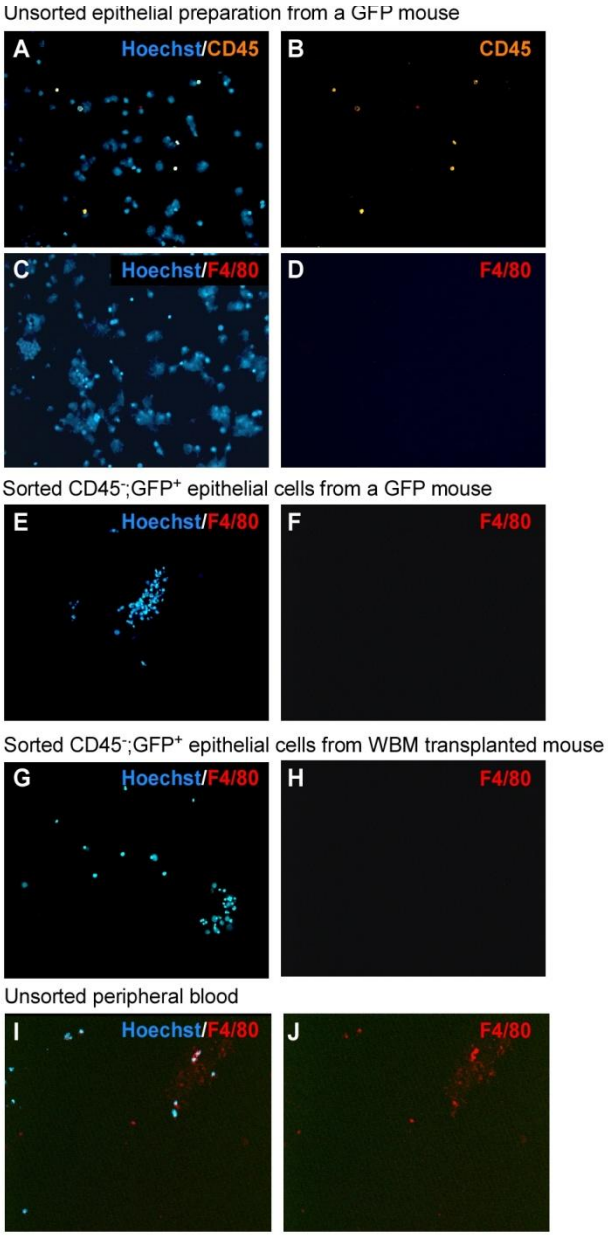

Figure 3.15. Isolated cell fusion hybrid epithelium lacks detectable macrophage contamination. (A-D) Unsorted small intestinal epithelial cells isolated from a GFP mouse, cytospun and subsequently stained with antibodies to the pan-blood cell antigen CD45 (A-B) or with antibodies to the pan-macrophage marker F4/80 (C-D) had some blood cell contamination but were devoid of macrophages. (E-F) GFP-positive; CD45-negative FACS sorted epithelial cells isolated from a GFP mouse, cytospun and stained with antibodies to the pan-macrophage marker F4/80 were devoid of macrophages. (G-H) GFP-positive; CD45-negative FACS sorted epithelial cells (cell fusion hybrids) isolated from a GFP-whole bone marrow transplanted mouse. Cells cytospun and stained with antibodies to the pan-macrophage marker F4/80 were devoid of macrophages. (I-J) Unsorted peripheral blood contains macrophages detected with antibodies

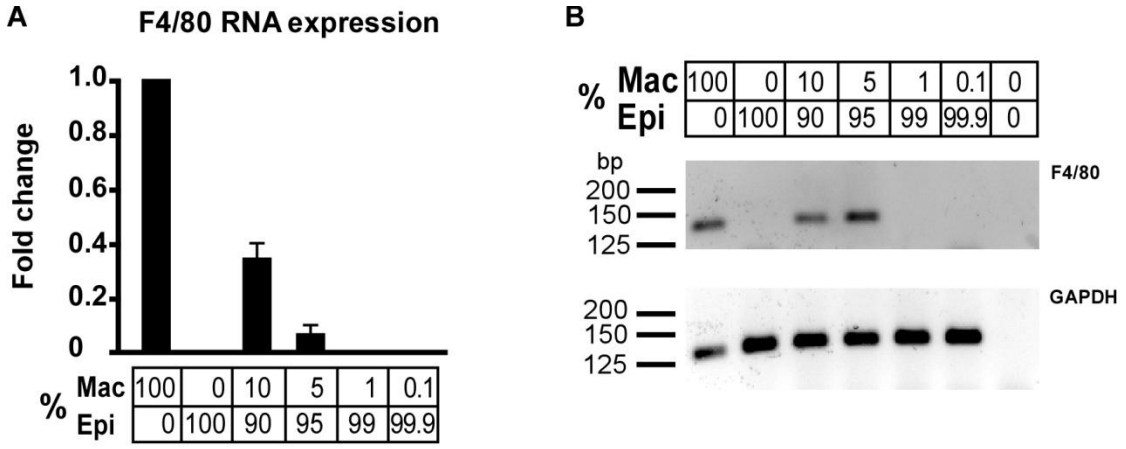

Figure 3.16. Possible macrophage contamination within the epithelial preparation cannot account for macrophage transcript expression. (A) Quantitative RT-PCR (qRT-PCR) detection of the robustly expressed macrophage gene, F4/80, in mixed ratios of macrophage:epithelial cDNA. Expression levels normalized to the reference gene Gapdh and reported as a fold change relative to a pure population of macrophages. Error bars, s.e. (n=3). (B) qRT-PCR products resolved on a 2% agarose gel. Amplicons for F4/80 (147 bp) and Gapdh (130 bp) are detectable.

do in fact represent a unique population; specifically, genes that displayed elevated expression within the cell fusion hybrid population but were suppressed in both the epithelial and macrophage population suggest that some transcripts were activated in response to cell fusion. It is possible that expression of these genes could act as a surrogate marker for identifying cell fusion hybrids. To further validate the distinct transcriptome profiles, qRT-PCR was employed (Figure 3.14D-E). Confirmation of the deep sequencing results established that cell fusion hybrids retained transcriptome characteristics from both parental lineages. Similarity with the epithelial transcriptome was not surprising based upon the epithelial appearance and localization of the cell fusion hybrid population (Rizvi, Swain et al. 2006). However, retention of macrophage-like and identification of unique gene expression profiles in hybrid cells provide the exciting possibility that these newly generated cells have distinct physiologic potential to participate in tissue regeneration or disease progression.

Our data builds upon the demonstration that *in vitro* cell fusion can lead to transcriptional changes (Chakraborty, Pawelek et al. 2001; Palermo, Doyonnas et al. 2009) by presenting a comprehensive, *in vivo* transcriptional analysis of cell fusion hybrids. The intriguing finding that products of cell fusion are genetic hybrids of their parental populations provides mechanistic evidence for how tumor cells may acquire genetic heterogeneity. Additionally, our data illustrating cell fusion between tumor epithelium and macrophage populations provide an exciting explanation for how tumor cells gain the physical macrophage-attributed properties involved in tumor metastasis such as extravasation, migration and

immune evasion. While the concept of fusion between tumor cells and blood cells as a mechanism for tumor progression was first proposed in 1911(Pawelek 2005), the physical evidence for *in vivo* cell fusion driving tumorigenesis is newly emerging. Perhaps the best evidence for cell fusion in cancer comes from cell culture studies where donor gene expression can be detected in cancer cell fusion hybrids (Chakraborty, Pawelek et al. 2001; Rupani, Handerson et al. 2004). *In vivo* examples of cell fusion in cancer have been observed in melanoma with acquisition of a myeloid-associated enzymatic activity and in renal cancer where detection of a donor Y-chromosome was detected in a female patient with renal carcinoma after bone marrow transplantation (Yilmaz, Lazova et al. 2005). However, presence of a donor-marker does not fully demonstrate the breadth of phenotypic alterations where cell fusion can lead. Importantly, our data demonstrating that *in vivo*-generated cell fusion hybrids can acquire macrophage transcriptional properties provides a critical piece of evidence supporting the impact of cell fusion on tumor progression. Although the mechanism for cell fusion requires further investigation, it is clear that its physiologic relevance in tumorigenesis is the acquisition of novel transcriptional expression. Further, cell fusion, akin to Darwin's theory of evolution, may allow for cells that have acquired favorable genetic changes to survive and adapt to the tumor microenvironment. This exciting possibility not only presents a potential paradigm shift in how we perceive metastatic spread, but opens new possibilities for inhibiting tumor-associated cell fusion as an additional preventative or therapeutic means.

METHODS

Mice. Mice were housed in a specific pathogen-free environment under strictly controlled light cycle conditions, fed a standard rodent Lab Chow (#5001 PMI Nutrition International), and provided water *ad libitum*. All procedures were performed in accordance to the OHSU Animal Care and Use Committee. The C57Bl/6, ROSA26 (Soriano 1999), $Rag1^{-/-}$ (Mombaerts, Iacomini et al. 1992), and $Apc^{Min/+}$(Moser, Pitot et al. 1990) mice were obtained from The Jackson Laboratory. OsbYO1 (GFP)(Nakanishi, Kuroiwa et al. 2002) mice were bred in-house.

Bone Marrow Transplantation. Bone marrow transplantation was conducted as previously described (Rizvi, Swain et al. 2006) with approximately $5x10^6$ GFP-expressing whole bone marrow cells or $8x10^4$ to $3x10^5$ lineage-limited populations supplemented with $2x10^5$ unlabeled carrier whole bone marrow. Briefly, 6-week-old recipient male WT, $Apc^{Min/+}$, ROSA26, or ROSA26/$Apc^{Min/+}$ mice received whole-body γ-IR (12 Gy: in two 6 Gy doses, 4 hours apart). WBM was harvested from 5- to 12-week-old donor GFP-expressing mice using standard procedures (Rizvi, Swain et al. 2006), filtered to obtain a single-cell suspension and resuspended in modified Hank's balanced salt solution (HBSS). WBM cells or a subset of FACS-isolated bone marrow cells were then injected into the retro-orbital sinus of recipient mice. To confirm hematopoietic engraftment or to check for contamination in FACS-isolated populations, peripheral blood leukocytes were isolated from recipient mice 2 weeks after

transplantation as previously reported (Willenbring, Bailey et al. 2004) and analyzed using a Becton Dickinson FACSCalibur.

Parabiosis. Parabiosis surgery was performed between GFP and ROSA26/*Apc*$^{Min/+}$ mice (n = 8 pair) as described previously (Davies, Powell et al. 2009). Briefly, pairs of 6- to 12-week age-, gender and weight-matched mice were surgically joined from the elbow to knee. Mice were separated approximately 7 weeks after surgery and intestinal tissue analyzed.

Intestinal analysis of transplanted and parabiotic mice. Cell fusion was identified using immunohistochemical analysis and co-localization of GFP and β-galactosidase expression antibodies for β-galactosidase (1:500, Immunology Consultants Laboratory, Inc.) and GFP (1:500; Molecular Probes) followed by fluorescent secondary antibodies (1:500, Alexa488, Molecular Probes; 1:250, cy5, Jackson Immuno Research) and confocal microscopy, as we have reported previously (Rizvi, Swain et al. 2006; Davies, Powell et al. 2009). Mice were analyzed at 4 or 8 weeks post-transplantation for all studies, with the exception of the early timecourse analysis, where the mice were analyzed every 24 hours post-transplantation for 7 days. Analysis of parabiotic pairs took place at time of separation (4-9 weeks; n = 4). Small intestine and colon was dissected *en bloc,* processed for wholemount imaging and subsequent frozen block preparation and sectioned as previously described (Wong, Rubinfeld et al. 1998). Tissue sections (5 μm or 50 μm) were analyzed for GFP-expressing cells as described above.

Blood cell antigens were detected with antibodies to CD45 (1:500; BD Pharmingen), B220 (1:500; BD Pharmingen) CD4 & CD8 (1:500; BD Pharmingen), F4/80 (1:500; eBioscience). Epithelial cells were detected with anti-E-cadherin antibodies (1:1000; Zymed), and the basement membrane detected with anti-laminin antibodies(1:1000; Chemicon). Nuclei were counterstained with Hoechst (33258; Sigma; 0.1μg/ml). Sections were examined with a Leica DMR microscope, digital images were captured with a DC500 digital camera and IM50 Image Manager Software (Leica Microsystems) or confocal images were acquired using an IX81 Inverted Microscope equipped with Fluoview FV1000-Spinning Disc Confocal (Olympus) scan head and FV10 ASW 1.7 software (Olympus). Standards for cell fusion quantification are described in Figure 3.6.

Statistics. Cell fusion was quantified by reporting the total number of crypt/villus units harboring at least one or more GFP-positive cell(s). A unit was defined as one villus and its adjacent crypt. For each animal, tissue sections at least 125μm apart were quantified and at least 1500 units were examined. This quantification standard reports the percentage of crypt/villus units containing fusion events. We do not quantify on a per cell basis because this would overestimate the extent of cell fusion due to proliferative expansion of the initial fusion event. Statistical significance between experimental populations was determined using a Student's two-tailed, unpaired *t*-test as determined appropriate for each experimental scenario. *P* values <0.01 were considered statistically significant. Statistical

analysis was performed using GraphPad Prism for Windows (GraphPad Software). All data are presented as the mean ± s.e.m.

Epithelial FACS. Epithelium was isolated for FACS and subsequent gene expression analysis. The intestinal epithelium was isolated using a modified Weiser preparation (Davies, Dismuke et al. 2008). Cells were then incubated in Type III Collagenase (30min; 15units/ml; Sigma), dispase (30min; 0.3units/ml; Invitrogen), then filtered through a 12x75mm filter (BD Falcon) to obtain a single-cell suspension. Cells were then stained with anti-CD45-APC (1:100; BD Pharmingen) for 30 minutes at 4ºC. Cells were washed twice in HBSS and resuspended in HBSS supplemented with 1% Bovine Serum Albumin and 5mg/ml propidium iodide (PI). GFP^+; $CD45^-$; PI^- epithelial cells were isolated from the GFP^+;$CD45^+$;PI^- intra-epithelial lymphocytes with an InFlux flow cytometer (Cytopeia) using a 150 µm nozzle. Cells adhering to each other (i.e., doublets) were eliminated on the basis of pulse width. The purity of sorted populations was determined at the end of each sorting experiment and only highly purified populations (>99% pure) were used for subsequent assays. Cell purity was also determined by cytospinning an aliquot of the sorted population onto slides for examination by immunohistochemistry for lineage marker expression.

Bone marrow FACS. Blood cell progenitors were isolated by FACS for subsequent limited-lineage transplantation. Bone marrow from GFP mice was isolated as described (Rizvi, Swain et al. 2006), then stained with the appropriate

combination of antibodies against cell-surface antigens depending on the desired populations. For separate macrophage, B cell, and T cell isolation followed by transplantation, whole bone marrow cells were first combined from whole bone marrow or peripheral blood before FACS isolation. Peripheral blood was obtained by retro-orbital bleeding of GFP mice and subsequent sedimentation and red blood cell lysis. Common myeloid progenitors (CMPs), common lymphocyte progenitors (CLPs), B cell, T cell and macrophages were isolated using FACS staining markers and concentrations are listed in Table 3.1 and a Becton Dickinson FACSVantage with a 70µm nozzle. All antibody staining was performed for 30 minutes at 4ºC. Cells were washed twice in HBSS and resuspended in HBSS supplemented with 3% Fetal Bovine Serum (FBS) and 5mg/ml PI. Cell populations were isolated on the Becton Dickinson FACSVantage with DiVa (Digital Vantage) option, using a 70µm nozzle. Cell doublets were eliminated on the basis of pulse width. The purity of sorted populations was determined as above, and only highly purified populations (>99% pure) were used for subsequent assays. Separate pure populations were subsequently transplanted into lethally irradiated mice as described above. All limited-lineage transplanted mice were also given 2-5x10^5 recipient-matched carrier WBM to promote survival. In some cases, macrophages were isolated and snap frozen for further qRT-PCR analysis.

Quantitative reverse transcriptase polymerase chain reaction (qRT-PCR). qRT-PCR was used to measure changes in the mRNA levels of specific genes in

CLP **$GFP^+;Lin^-;IL\text{-}7Ra^+;Sca\text{-}1^{lo};c\text{-}kit^{lo};PI^-$**

Antibody	Company	Catalog number	Concentration
IL7-Ra-Alexa647	Biolegend	121109	1:50
B220-PE	BD Pharmingen	553090	1:100
CD3-PE	BD Pharmingen	553064	1:100
CD4-PE	BD Pharmingen	553653	1:100
CD8-PE	BD Pharmingen	553033	1:100
Mac-1-PE	BD Pharmingen	553311	1:100
Gr-1-PE	BD Pharmingen	553128	1:100
Ter119-PE	BD Pharmingen	553673	1:100
Sca-1-PE-Cy7	Biolegend	122513	1:50
c-kit-APC-Alexa750	eBioscience	27-1171-82	1:100

CMP **$GFP^+;Lin^-;IL\text{-}7Ra^-;Sca\text{-}1^-;c\text{-}kit^+;CD34^+;CD16/32^{lo};PI^-$**

Antibody	Company	Catalog number	Concentration
IL7-Ra-PE	eBioscience	12-1271-81	1:50
B220-PE	BD Pharmingen	553090	1:100
CD3-PE	BD Pharmingen	553064	1:100
CD4-PE	BD Pharmingen	553653	1:100
CD8-PE	BD Pharmingen	553033	1:100
IgM-PE	eBioscience	12-5890-81	1:100
Gr-1-PE	BD Pharmingen	553128	1:100
CD19-PE	BD Pharmingen	557399	1:100
Ter119-PE	BD Pharmingen	553673	1:100
Sca-1-PE	BD Pharmingen	553336	1:50
c-kit-APC-Alexa750	eBioscience	27-1171-82	1:100
CD34-Biotin	BD Pharmingen	553334	1:100
Streptavidin-PE-Cy7	eBioscience	25-4317-82	1:100
CD16/32-APC	eBioscience	17-0161-81	1:100

B cells **$GFP^+;B220^+;PI^-$**

Antibody	Company	Catalog number	Concentration
B220-APC	BD Pharmingen	553092	1:100

T cells **$GFP^+;CD4^+;CD8^+;PI^-$**

Antibody	Company	Catalog number	Concentration
CD4-APC	BD Pharmingen	553051	1:100
CD8-APC	BD Pharmingen	553035	1:100

Macrophages **$GFP^+;F4/80^+;PI^-$**

Antibody	Company	Catalog number	Concentration
F4/80-APC	eBiosience	17-4801-82	1:100

GFP+ epithelium **$GFP^+;CD45^-;PI^-$**

Antibody	Company	Catalog number	Concentration
CD45-APC	BD Pharmingen	559864	1:100

Table 3.1. List of antibodies used to isolate various cell populations via Fluorescence Activated Cell Sorting (FACS.)

isolated epithelium or macrophages from GFP or transplanted mice. Total RNA was prepared from sorted cells using RNeasy Mini kit (Qiagen). RNA quality was assessed using Agilent's PicoChip on the 2100 Bioanalyzer. Amplified cDNA was prepared from 20 nanograms of each RNA sample following the NuGEN Ovation RNA Amplification System v2 protocol. qRT-PCR was performed using a SYBR Green-based assay and a 7900 HT Sequence Detector according to established protocols (Davies, Dismuke et al. 2008). Each cDNA sample was analyzed in triplicate, along with triplicate samples of the endogenous reference gene, Glyceraldehyde-3-phosphate dehydrogenase (Gapdh). All primers used are listed in Table 3.2.

RNA-Seq and Bioinformatic Analyses. Intestinal epithelium was isolated from GFP-expressing mice (n=3) and WBM transplanted mice (n=4), as well as macrophages from GFP-expressing mice (n=3) by FACS sorting, as described above. Total RNA (0.1-1μg) was isolated using the RNeasy Mini kit (Qiagen) according to the manufacturer's instructions. Poly(A) RNA was purified using oligotex-dT30 latex beads (Qiagen). First-strand cDNA synthesis was conducted using Superscript III and Oligo dT-20 according to the manufacturer's instructions (Invitrogen). Second strand synthesis was generated according to standard methods, followed by double stranded cDNA fragmentation (100-700 bp) with 65 watt pulse on a Misonix sonicator. cDNA was polished with the DNA terminator repair kit (Lucigen) and a single A base was added with Klenow exo-(3' to 5' exo minus) prior to ligation of genomic DNA adapters (Illumina Solexa Genomic 1G)

Gene name	Accession #	→	Reverse Primer (5' → 3')
Apc	NM_007462	TAGGAAGAGCAGCGCAGACA	AGACCCGGATGGCGTTAG
Cald1	NM_145575	ATGCTTTCAGCCCCAGCCGT	TTCGTTCTCCGTCTCCCCGC
Camk1d	NM_177343	GGCTTCTCGCAGGGTGGCTT	CCGGAGTGCGGTTCACCTGT
Col7a	NM_007738	CAGAGCAGCTGCGTCGCTTG	AAGGCCCTGTTTGCGGCTCT
Dnmbp	NM_028029	TCCATCGGGGAGACCTGGTGA	TCGGCTCCGAGAGGAGAGGC
E-cadherin	NM_009864	GTCAACACCTACAACGCTGCC	GTTGTGCTCAAGCCTTCGC
Epcam	NM_008532	ACCGCCGGAGTCCGAAGAAC	CGCCTCTTGAAGCGCAGTCT
Epha2	NM_010139	GGACCGAAGCACCACCTCCC	GGCATCCCCCTTCTTGCGGT
F4/80	NM_010130	ATGAGTGCACCCAAGATCCATT	TCCATATCCTTGGGAGCCTTCT
GAPDH	NM_008084	GTCAACACCTACAACGCTGCC	GTTGTGCTCAAGCCTTCGC
Mib2	NM_145124	TCGGGGCATGCGTTGGAAGT	TCAGCGTAACCGGGCGTGAG
Nfix	NM_001081982	ACCAAGCGCCCCAAGTCCAT	CAGGGCCTGCATCCACGTCA
Slc5a1	NM_019810	ACCCATGTCCAGCACACGCA	CCCAGGCTTCAGTCCCTGCC
Tspan8	NM_146010	AGCTGCAGGCACACGGATCT	ACAGCTGCTCACACCTGCCA
Villin	NM_009509	TCAGGCCTCGGCAAAACCCA	ATGCGCCACACCTGCACTTC

Table 3.2 List of genes and their respective primers used in quantitative reverse transciptase polymerase chain reaction (qRT-PCR).

Forward Primer (5' 3')

at 22°C. Amplification of the library using 10 cycles of limited PCR using Phusion HF DNA polymerase (NEB) and genomic PCR primer (Illumina; Solexa Genomic primers 1.1 and 2.2) was conducted.

Double stranded cDNA libraries were sequenced on a Solexa G1 Genome Analyzer and image analysis and base-calling were conducted with the standard Illumina Analysis Pipeline 1.0 (Firescrest-Bustard). 36 bp sequence tags were mapped to the mouse genome (NCBI Build 37) by calling the Eland algorithm (Illumina Analysis pipeline Gerald module) with Perl scripts. A C^{++} program was used to count the number of uniquely mapped reads within exons of Ref-Seq genes (UCSC Genome Browser mm9 annotation). All statistical analyses were performed in the R statistical programming environment. RNA-Seq tag counts in Ref-Seq genes were mean-scaled and pair wise comparisons were performed using the $\chi 2$ statistic. The Storey Q-test was used to correct for multiple comparisons (Storey 2002). Differentially regulated RefSeq genes with a $p<0.01$ were considered significant. Relational comparisons between data sets called an R annotation script and SQL data base queries.

To identify transcripts that were differentially regulated between at least two cell populations, RefSeq genes with a $p<0.01$ from comparisons between each pair of cell populations were compiled and represented 19,696 transcripts. Within this differentially regulated population of RefSeq genes, we identified genes in which cell fusion hybrids a) shared gene expression profiles with wild-type epithelium, b) shared gene expression profiles with macrophages, or c) expressed unique gene expression profiles. For category a) we selected genes

that were differentially regulated between macrophages and cell fusion hybrid epithelium ($p<0.01$) but not between cell fusion hybrid epithelium and wild-type epithelium comparisons ($p>0.05$). For category b) we selected genes that were differentially regulated between cell fusion hybrid epithelium and macrophages ($p<0.01$) but not between wild-type epithelium and macrophages ($p>0.05$). For category c) differentially regulated genes between wild-type epithelium and cell fusion hybrid epithelium ($p<0.01$) and wild-type epithelium and macrophages ($p<0.01$). Heatmaps for each of these categories were generated in the R programming environment and depict mean- and log-scaled total RefSeq gene tag counts mapped to an 8 bit color scale.

CHAPTER 4

CONCLUSIONS AND FUTURE DIRECTIONS

Conclusions

The intestine plays critical roles both in acting as a barrier to environmental assault as well as in facilitating efficient nutrient absorption. To effectively support these essential functions, the cellular dynamics of the intestinal epithelium are tightly regulated. An intact and functional epithelium is essential for survival, thus efficient cellular regeneration during homeostasis and in the face of injury is critical. It is known that infectious invasion, ischemia and exposure to irradiation can damage the intestinal epithelium, leading to cell death within the stem cell niche. In these injury contexts, inflammatory cells from the mesenchyme home to the intestine and participate in the regenerative process in multiple ways, including engulfing and purging dead cells and pathogens, secreting cytokines to promote wound healing, and stimulating cellular proliferation and differentiation. We have previously shown that in the context of gamma-irradiation damage to the epithelium, inflammatory cells derived from the bone marrow fuse with the intestinal epithelium. While this process presumably participates in tissue repair, it is largely unknown what factors promote this process and whether cell fusion with the intestinal stem cell has long-term genetic consequences in the epithelium. In this dissertation, I have addressed the dynamic relationship between the intestinal epithelium and the inflammatory

cells in the context of cell fusion, in response to intestinal damage, and in disease using mouse model systems. The experimental results obtained from my studies have led me to the following conclusions:

An inflammatory and hyperproliferative epithelial microenvironment promotes intestinal cell fusion.

We identified intestinal inflammation as a critical mediator of cell fusion in both injury (γ-IR and bone marrow transplantation) and non-injury (parabiosis) contexts. Using both chemical and genetic inductions of microenvironmental inflammation, we established that increased intestinal inflammation resulted in enhanced cell fusion. These findings have a significant impact on the cell fusion field. First, an inflammatory microenvironment is a key factor involved in tumorigenesis. Our findings provide intriguing evidence that cell fusion may be an important factor in tumor progression. Importantly, our results implicate inflammation as a key cell fusion mediator and are consistent with the observation that cell fusion is increased in skeletal muscle, heart and brain in the context of tissue inflammation (Nygren, Jovinge et al. 2004; Johansson, Youssef et al. 2008). The second novel aspect of this research is a high level of fusion observed in both transplant and parabiosis systems, which is significantly greater than fusion described in any other organ system (Alvarez-Dolado, Pardal et al. 2003; Wang, Willenbring et al. 2003; Johansson, Youssef et al. 2008). These significant outcomes suggest an important role for cell fusion specific to intestinal epithelial homeostasis, such that it is increased in response to tissue injury and

may promote tissue regeneration.

A detailed time course analysis of intestinal and mesenchymal changes immediately after irradiation and bone marrow transplantation revealed the trafficking of BMDCs to the intestinal stem cell niche as early as 24 hours after transplantation and preceding epithelial cell fusion 7 days after transplantation. In our temporal analysis, we observed that the crypt epithelium is hyperproliferative 4 days after exposure to gamma-irradiation, consistent with previous reports (Potten 1990). Interestingly, we determined that this hyperproliferation was attenuated by 7 days after transplant and correlated with apparent cell fusion in the epithelial compartment. Based upon this observation, we used the $AhCre^{+}/Apc^{fl/fl}$ inducible genetic mouse model to show that cellular proliferative status mediates cell fusion. In addition, we demonstrate that cellular proliferation occurs in response to gamma irradiation in both the liver and skeletal muscle, two organs where cell fusion has been extensively described (Corbel, Lee et al. 2003; Wang, Willenbring et al. 2003; Willenbring, Bailey et al. 2004; Nygren, Liuba et al. 2008). Significantly, this is the first demonstration that recipient cell requirements are important in promoting cell fusion in any model system. The idea that cellular proliferation or a proliferative state of the “recipient” epithelial cell promotes cell fusion is consistent with the notion that cell fusion occurs with the intestinal stem or early progenitor cell that is activated to divide in response to injury. It is also consistent with the idea that cellular fusion is an important process in normal intestinal homeostasis, as the epithelial compartment undergoes constant cellular turn over. Therefore, fusion with the intestinal stem

cell is ongoing, as we demonstrate in our parabiosis model, but is increased in contexts where epithelial proliferation is heightened, such as tumorigenesis.

Analysis of the temporal dynamics of cellular fusion reveals a prefusion cluster of BMDCs around the stem cell niche.

Congruent with the idea that hyperproliferation is critical for cell fusion, in our detailed time course analysis we found that GFP-marked BMDCs cluster around the base of the stem cell niche 4 days after γ-IR exposure and subsequent transplantation. This represents the same time point in which the intestinal crypts are deepened due to hyperproliferation and immediately prior to the observation of cell fusion in the epithelial compartments. Confocal microscopy illustrated that these cells cluster and invade the epithelial compartment. This analysis is the first demonstration of the cellular dynamics preceding epithelial cell fusion and extends our previous work demonstrating that cellular fusion occurs at the level of the intestinal stem or progenitor cell (Rizvi, Swain et al. 2006). Our time course analysis suggests that BMDCs are actively recruited to the stem cell niche after injury and is consistent with the Wnt signaling-mediated intestinal epithelial regenerative response after lethal irradiation (Davies, Dismuke et al. 2008- see Appendix 3). Together these data suggest that blood cells may play a role in both the promotion of cellular proliferation via modulation of the Wnt signaling pathway within the intestinal stem cell niche, as well as actively participating in cell fusion. This novel observation is an exciting advance in the field, as pre-fusion cell clustering has

not been described in any organ system where fusion has been observed. Significantly, these findings establish the importance of blood-derived cells as actively engaged in the fusion mechanism, revealing that they appropriately physically position themselves in the mesenchyme in a manner to promote cell fusion. In addition, I have demonstrated that 4 days after transplantation represents a critical time point for cell fusion that can now be further investigated to visualize specific interactions between macrophages and intestinal epithelia during cell fusion *in vivo*. Significantly, our studies provide a physical framework to further examine the mechanics of cellular fusion in response to tissue injury.

The macrophage is a primary mediator of the intestinal cell fusions process.

Interestingly, in depth examination of the pre-fusion clusters at the base of small intestinal crypts 4 days after irradiation and transplantation revealed that they contained macrophages, B and T cells. Using limited-lineage analysis and transplantation of irradiated mice, I identified the macrophage as a cell type that contributes to cell fusion at a level similar to that observed after whole bone marrow transplantation. In some instances, we observed evidence of the macrophages crossing the basement membrane into the epithelial compartment, presumably in preparation for a fusion event, suggesting that macrophages were a potential important mediator of cell fusion. This is the first description of the blood-derived population responsible for cell fusion in the intestine and significantly, contributes to further understanding the mechanism for cell fusion in

both *in vitro* and *in vivo* model systems. The macrophage, a known fusogenic cell type, can now potentially be targeted to either promote or inhibit intestinal cell fusion, allowing for a deeper understanding of the physiological impact that cell fusion has in epithelial regeneration or in tumorigenesis. My important distinction implicating the macrophage as a primary mediator of cell fusion is consistent with the fusogenic blood population that has been described in the liver (Willenbring, Bailey et al. 2004). Further, my results support the idea that macrophages may use their endogenous fusogenic cellular machinery (Vignery 2005; Vignery 2005; Helming and Gordon 2009) to fuse with damaged cells in response to an injury or tumorigenic environment.

Reprogramming of the transcriptome occurs in epithelial cell fusion hybrids.

Using immunohistochemistry, qRT-PCR, and whole transcriptome sequencing, I established that cell fusion hybrids retain the gene expression patterns of donor-derived macrophages. While we know that intestinal cell fusion hybrids express the GFP-donor marker (Rizvi, Swain et al. 2006), results from my detailed gene profile analysis provides the first demonstration that intestinal cell fusion hybrids represent a truly unique population possessing a transcriptional profile distinct from wild-type intestinal epithelium with an unexpected striking overlap with the macrophage gene profile. My discovery that intestinal cell fusion hybrids maintain genetic hallmarks of the donor cell population is consistent with genomic analyses of *in vitro*-generated cell fusion

hybrids (Palermo, Doyonnas et al. 2009). While this investigation was an intriguing demonstration of the potential consequences of cell fusion on nuclear reprogramming, it was limited to the *in vitro* model system and subsequent evaluation with only a limited number of candidate gene markers.

My work provides the first whole-genome sequence analysis attributed to transcriptional outcomes of *in vivo* cell fusion. This significant finding establishes the extent to which the intestinal epithelial cell fusion hybrid is transcriptionally modified and demonstrates the power of cell fusion in altering genetic regulation. The exciting concept that transcriptional changes can be attributed to cell fusion in tissue regeneration and tumorigenesis (Willenbring, Bailey et al. 2004; Pawelek 2005; Duncan, Hickey et al. 2009; Palermo, Doyonnas et al. 2009) is strongly supported by the data presented in this dissertation. Findings from genome-wide investigations provide intriguing insight into the potential impact of cell fusion in tissue remodeling and the possible ramifications cell fusion can exemplify in the promotion of tumorigenesis.

Future Directions

Although cell fusion has been well-studied in the intestine, as well as in other organ systems (Wang, Willenbring et al. 2003; Nygren, Jovinge et al. 2004; Johansson, Youssef et al. 2008; Nygren, Liuba et al. 2008), many important biologic questions, especially those addressing the physiologic importance of cell fusion remain. First, the mechanism by which blood cells fuse to epithelium during tissue regeneration or tumorigenesis is unclear. Second, it is unknown

why the proliferative nature of the intestinal epithelium modulates cell fusion. It is currently undetermined if the proliferative status of the epithelial cell is of key importance for the mechanism of fusion, or if a more stem-like state is the necessary component to promote cell fusion. The latter idea has been demonstrated for many mesenchymal- and embryonic stem cell model systems (Terada, Hamazaki et al. 2002; Spees, Olson et al. 2003; Yu, Vodyanik et al. 2006), as well as in a cancer setting (Pawelek 2005; Vignery 2005). Finally, despite the evidence that cell fusion occurs in both tissue regeneration (Wang, Willenbring et al. 2003; Nygren, Liuba et al. 2008) and tumorigenesis (Chakraborty, de Freitas Sousa et al. 2001; Chakraborty, Pawelek et al. 2001; Chakraborty, Lazova et al. 2004; Rizvi, Swain et al. 2006), the long-term implications of cell fusion on the epithelium have not been elucidated.

The mechanism for cell fusion in the intestine is unknown.

While my studies implicate the bone-marrow derived macrophage as a primary cellular fusion partner with the intestinal stem cell, it is evident that blood lymphocytes can also participate in cell fusion. It is unclear if certain environmental factors promote macrophage fusion over B or T cell fusion. Although it is possible that both epithelial and mesencyhmal signals control the recruitment and subsequent fusion of blood cells in the epithelial stem cell niche, these signals have yet to be identified and may vary depending on context. Different microenvironments may promote cell fusion with macrophages over

lymphocytes or vice versa, however the factors controlling this level of regulation remain to be investigated.

The exact molecular mechanism for cell fusion between blood cells and the intestinal epithelium remains undefined. While mechanisms for general membrane fusion have been extensively described (Martens and McMahon 2008), it is unknown if the cell fusion process I have described harnesses any components of this cellular machinery for cell fusion between blood and epithelial cells after injury. Based on my data identifying the macrophage as a primary mediator of intestinal cell fusion, it is possible that the innate cellular fusion machinery used by the macrophage for generation of foreign body giant cells or osteoclasts (Vignery 2005) is also utilized in the intestinal cellular fusion mechanism. The inherent fusion capability possessed by macrophages has been well-described, and it is possible that one of these innate mechanisms is exploited for use during intestinal cell fusion. Two intriguing possibilities include the utilization of one of the macrophage fusion receptors, SIRPα or DC-STAMP. In macrophage fusion, the "donor" SIRPα binds an opposing cell surface receptor CD47 on the "recipient" cell to trigger cell fusion (Vignery 2005). It is not known if intestinal epithelial cells express CD47 within 7 days after irradiation, but this remains one intriguing avenue of investigation for macrophage-intestinal stem cell fusion. In addition to SIRPα, macrophages also express a cell surface protein DC-STAMP, to accomplish cell fusion. The expression of DC-STAMP precedes macrophage cell fusion, is required for the formation of foreign body giant cells in mice (Vignery 2005) and represents an appealing protein with potential for an

important role in intestinal cell fusion. While the “recipient” receptor ligand for DC-STAMP is unknown, it will be critical to investigate whether macrophages found in pre-fusion clusters express DC-STAMP.

In addition to examining the early time points after transplantation for known cell fusion receptors, *in vitro* models of intestinal cellular fusion with macrophages could be established to understand which combination of receptors and ligands are required for epithelial intestinal cell fusion. It will be especially critical to monitor fusion from an epithelial cell vantage point. It has been demonstrated that macrophages use CD36 recognition of phosphotidylserine on a fusion target cell as a mechanism for engaging in cell-cell fusion (Helming, Winter et al. 2009) and interestingly, intestinal epithelial cells expose phosphotidylserine on their cell surface as part of the apoptotic response to whole body ionizing irradiation (Tyurina, Tyurin et al. 2008). It is unknown if macrophages use this as a mechanism for fusion with the intestinal epithelium, but it represents an intriguing possibility. Currently there are no known fusion mediators in many of the somatic cells that undergo cellular fusion after transplantation, including the intestinal epithelium. Thus *in vitro* examination of fusion would set the framework for determining the mechanism that promotes cell fusion *in vivo.*

The role of a stem-like or proliferative state in intestinal cell fusion is undefined.

Although my studies have demonstrated that a stem-like or proliferative state promotes cell fusion, it is unknown how this specific epithelial cell status optimally supports cell fusion and if this state is truly required for cell fusion in the intestine to take place. While our studies (Rizvi, Swain et al. 2006) indicate that intestinal cell fusion occurs at the level of the stem cell, it will be important to investigate the requirement for a stem-like state in the fusion process. Using newly established methods for isolating and culturing intestinal differentiated and progenitor epithelia (Sato, Vries et al. 2009), studies could be conducted with "donor" macrophages and "recipient" epithelia grown in co-culture to further elucidate if cellular fusion is truly restricted to stem or progenitor populations, or if fusion within the intestinal epithelium is on-going with other differentiated populations.

The intestine is intrinsically proliferative and our non-injury parabiotic studies indicate that fusion may be an important process in maintaining intestinal homeostasis. My studies also demonstrate that cellular proliferation results in enhanced cell fusion and that fusion occurs at a higher rate in mice predisposed to the early stages of colorectal cancer (Figure 1.6). It may be that the hyperproliferative status of these cells contributes to the increased amount of cell fusion observed. Despite this evidence supporting the importance of proliferation in cell fusion in the intestine, it is currently unknown if epithelial proliferation is absolutely required. To investigate this distinction, an inducible genetic approach

for depleting intestinal proliferation coupled with bone marrow transplantation could be examined. Completely eliminating all intestinal proliferation leads to embryonic lethality (Korinek, Barker et al. 1998). However, the AhCre^{+};Myc$^{fl/fl}$ mouse harbors a floxed copy of the cell cycle regulator, *c-Myc*, which can be inducibly knocked-out specifically in the intestinal epithelium. Deletion of *c-Myc* in this model system occurs in a mosaic pattern, such that many crypts retain cells with wild-type levels of the protein (Muncan, Sansom et al. 2006) and therefore, the health of the mouse is maintained during the experiment. These mice could be transplanted to evaluate the amount of fusion that occurs in the absence of proliferation. This study would be designed to determine whether the recipient cell must possess stem cell characteristics or if it merely needs to be actively engaged in the cell cycle. It remains critical to determine if the proliferative state of the intestine is an essential component for fusion and ultimately if fusion is increased above homeostatic levels during tissue regeneration after injury and/or potentially exploited in tumorigenesis.

The long-term implications of cell fusion are unknown.

Although my studies demonstrate that genome-wide transcriptional changes occur within cell fusion hybrids, the long-term implications of these transcriptional changes are unclear. A full genome analysis of the RNA-Seq data will reveal potential phenotypic differences between cell fusion hybrids and wild-type epithelium that have previously been unappreciated (Rizvi, Swain et al. 2006). Specifically, the identification of alterations in important cellular signaling

pathways that may have phenotypic changes in the cell fusion hybrid epithelium are intriguing, as they will provide insight into how these unique cells impact overall epithelial function.

Of priority, it will be important to examine the transcriptional data for macrophage-specific genes that are imperative for macrophage motility. Macrophage fusion has been shown to impart motile characteristics on static cells in culture (Rachkovsky, Sodi et al. 1998; Sodi, Chakraborty et al. 1998; Chakraborty, de Freitas Sousa et al. 2001; Chakraborty, Pawelek et al. 2001), and fusion with this population is one intriguing avenue to generate cells that have acquired the ability to leave their endogenous niche and establish residence at distant sites, as in cancer metastasis. It is currently unknown if macrophage-epithelial cell fusion is a critical mediator in metastasis, but the data presented here suggests macrophage-like characteristics can be acquired and maintained after macrophage cell fusion.

One potential physiologic impact of cell fusion on tumorigenesis is the possibility that macrophages fuse with a cancer stem or proliferative progenitor cell imparting macrophage characteristics to this “cancer stem cell” population. It is believed that cancer stem cells have unique properties distinct from endogenous tissue stem cells and surrounding cancer cells (Visvader and Lindeman 2008). This unique quality may allow them to recapitulate the original cancer, as well as cancers in metastatic niches. It is possible that cell fusion may lead to treatment-resistant cancer cells, or that it could be an underlying mechanism for metastatic disease.

In addition to these studies, an indepth genome-wide transcriptional survey of the cell fusion hybrid epithelium immediately after fusion will provide insight into the complexity of merging two genomes. An analytical transcriptome survey immediately after fusion, compared with 4 weeks after transplantation will provide insight into which gene expression signatures are maintained and which are not essential. Further, comparing cell fusion hybrids at these time points between wild type and tumor cells may provide the foundation for their participation in tumor progression. Since cellular fusion is important in tissue regeneration after injury and has also been implicated in tumorigenesis, it is critical to more fully understand how the process of merging a macrophage and stem cell genome may directly impact the long-term status of the intestinal epithelium.

In conclusion, my studies have contributed to the understanding of how cellular fusion impacts epithelia in both tissue regeneration and tumorigenesis. I have identified microenvironmental and cellular factors that mediate intestinal cell fusion, as well as defined the macrophage as a primary mediator of cell fusion after transplantation. Significantly, I show that cellular fusion causes genome-wide transcriptional changes that may impact intestinal epithelial function over the life of the organism. A summary of this work, as well as experimental future directions to extend my findings are presented in Figure 4.1. Together, the studies provide novel insight into the importance of intestinal cell fusion: its essential role in intestinal regeneration after injury and its potential impact on intestinal tumorigenesis.

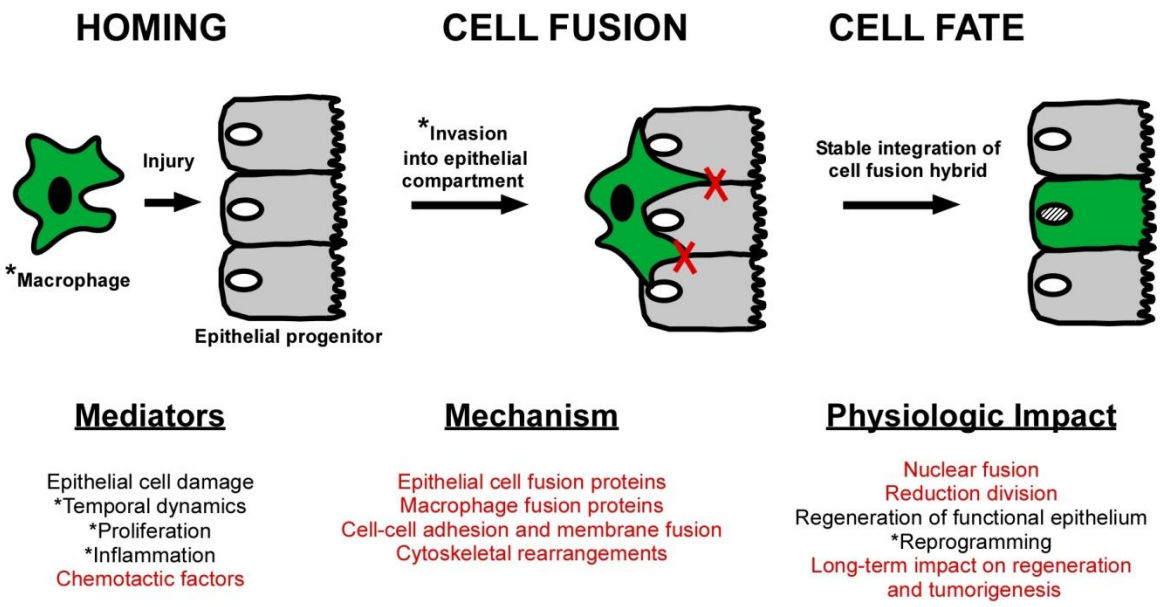

Figure 4.1. Macrophage fusion with intestinal epithelial progenitors. After epithelial injury, macrophages home to the intestine, invade into the epithelial compartment and undergo fusion with intestinal epithelial progenitor cells. This results in the generation of genetically-distinct cell fusion hybrid epithelium. The aspects of this process that have been experimentally defined by our laboratory or others are shown in black, while the unknown factors involved in this multi-step process are noted in red. Factors in black indicated with an asterisk (*) are experimentally defined in this dissertation.

APPENDIX 1

Characterization of the intestinal cancer stem cell marker, CD166/ALCAM, in the human and mouse gastrointestinal tract

Trevor G. Levin[1], Anne E. Powell[1], Adria D. Dismuke[2], Paige S. Davies[3], Eric C. Anderson[4], John R. Swain[3], Christine Glynn[3] and Melissa H. Wong[3]

[1]Department of Cell and Developmental Biology, [2]Department of Molecular and Medical Genetics, [3]Department of Dermatology, Knight Cancer Center, Oregon Stem Cell Center, [4]Department of Internal Medicine, Division of Hematology and Medical Oncology, Oregon Health & Science University, Portland, OR.

Under review, *Gastroenterology*, January 2010

AEP contributed to planning of all experiments, immunofluorescence and sorting of cells in Figure A1.2 and Figure A1.3 and editing of the manuscript.

Abstract

Background & Aims: CD166 or ALCAM, a colorectal cancer stem cell marker, represents an emerging indicator for aggressive cancer and therefore is a potentially exciting therapeutic target. Although cell surface expression of CD166 has been correlated with a shortened patient survival, little is known about the molecule's function and expression pattern in normal intestinal epithelia. **Methods:** In this study, we characterized the CD166 protein expression pattern in normal and diseased, human and mouse intestinal tissue using immunohistochemical and flow cytometry. **Results:** Our data showed that the CD166 expression pattern was expressed on the epithelial cell surface in the stem cell niche down the intestinal length and was conserved across species. In the small intestine, CD166 was observed on both crypt-based Paneth cells and intervening crypt-based columnar cells, putative stem cells. Further, a subset of CD166-positive crypt-based columnar cells co-expressed stem cell markers Lgr5 or Musashi-1. Examination of CD166 expression within human tumors identified both cytoplasmic and cell surface staining patterns. Interestingly, CD166-positive cells were also detected in mouse benign adenomas, as well as rare double-positive CD166 and CD44 or ESA cells. **Conclusions:** Significantly, our studies illustrate a robust expression pattern for CD166 within the endogenous intestinal stem cell niche. We show that CD166-positive cells are evident in multiple stages of intestinal carcinoma, including benign tumors and metastatic disease. Our findings provide the foundation for investigating the function of CD166 within the

stem cell niche and, more importantly, have implications on targeting CD166 for disease therapy.

Keywords: cancer stem cell; intestinal carcinoma; CD166/ALCAM; Paneth cells

Colorectal cancer (CRC) is the third most prevalent cancer in the United States, with nearly 150,000 new cases diagnosed each year. Despite efforts to improve early detection and treatment, over one-third of patients die annually from this disease.(2008) The focus on cancer initiation and progression has dominated the effort to better understand disease pathology and guide therapeutic approaches. As such, the cancer stem cell (CSC) theory, which suggests that cancer is driven by cells harboring stem cell-like qualities, offers one explanation for why many current therapeutic approaches ultimately result in relapse of disease. In this model, some CSCs or cancer-initiating cells may be quiescent and, thus, evade eradication by standard cytotoxic therapies designed to target proliferating cells. These surviving cells can then proceed to support tumor growth and may hold the potential to initiate recurrent or metastatic disease.(Pardal, Clarke et al. 2003; Cho and Clarke 2008; Dylla, Beviglia et al. 2008) The reinvigoration of the CSC theory(Nowell 1976; Weiss 2000; Vermeulen, Sprick et al. 2008) has led to identification, isolation and characterization of subsets of intestinal cancer cells that can recapitulate tumorigenesis when transplanted into immune-deficient mice(Al-Hajj, Wicha et al. 2003; Dalerba, Dylla et al. 2007; Li, Heidt et al. 2007; O'Brien, Pollett et al. 2007; Hong, Gupta et al. 2008). While some cell surface molecules, such as CD133

and CD44, have been shown to mark CSCs in multiple organs, additional number of markers have shown promising CSC expression in intestinal cancer including DCAMKL-1, ESA and CD166.(Dalerba, Dylla et al. 2007; O'Brien, Pollett et al. 2007; May, Riehl et al. 2008)

CD166 or Activated Leukocyte Cell Adhesion Molecule (ALCAM) expression is pathologically correlated with aggressive disease in a variety of cancers including melanoma, prostate, breast, ovarian, esophageal, and bladder cancers.(van Kempen, van den Oord et al. 2000; Kristiansen, Pilarsky et al. 2003; Tomita, van Bokhovenâ€ et al. 2003; Verma, Shukla et al. 2005; Burkhardt, Mayordomo et al. 2006; Klein, Wu et al. 2007; Mezzanzanica, Fabbi et al. 2008) In human CRC, aberrant cell surface CD166 expression is strongly correlated with a 15 month shortened patient survival.(Weichert, Knosel et al. 2004) Subsequent isolation of CD166/CD44 or CD166/ESA double-positive cells from human CRCs cells can recapitulate tumorigenesis when injected at low numbers into immune-deficient mice(Dalerba, Dylla et al. 2007), a hallmark of a CSC population. Although these findings suggest that CD166 may have a role in the progression of CRC, little is known about its endogenous function and cellular localization within the intestine.

In other organ systems, CD166 has a myriad of functions. This conserved cell adhesion protein participates in physiologic processes including leukocyte intravasation across the blood brain barrier, monocyte migration across endothelial junctions, angiogenesis, capillary formation, protection against apoptosis in breast cancer cells, and T-cell activation by both antigen presenting

and tumor cells.(Ohneda, Ohneda et al. 2001; Hassan, Barclay et al. 2004; Ikeda and Quertermous 2004; Jezierska, Matysiak et al. 2006; Kato, Tanaka et al. 2006; Masedunskas, King et al. 2006; Cayrol, Wosik et al. 2008) Further, CD166 has been described as a ligand that binds to CD6 on thymic epithelium (Kanki, Chang et al. 1994; Bowen, Patel et al. 1995; Patel, Wee et al. 1995), acting in homophilic adhesion complexes between epithelial cells(Degen, van Kempen et al. 1998), and as a cell surface marker for both a subset of hematopoietic progenitor cells(Corbel, Cormier et al. 1992; Uchida, Yang et al. 1997) and multipotent mesenchymal stem cells.(Bruder, Ricalton et al. 1998; Arai, Ohneda et al. 2002) Based upon the intriguing CD166 expression pattern in multiple stem cell populations, this molecule has a potential role in maintaining a stem cell status in both normal and disease states. However, the potential overlap between CD166 normal and tumorigenic physiologic function have not been defined. Further, based upon its multiple roles in tumor-related processes, CD166 could play an important role in tumor pathology.

Correlation of the CD166 expression pattern with aggressive disease has led to efforts for targeting this molecule as a cancer therapeutic. Treatment of cancer cells with a CD166-internalizing antibody conjugated to chemotherapy filled lipid vesicles was shown to effectively target and kill CD166-expressing ovarian cancer cells and prostate cancer cells *in vitro* (Piazza, Cha et al. 2005; Roth, Drummond et al. 2007). While early results from these types of targeted cancer therapies appear promising, it necessitates an even more careful understanding of the endogenous expression pattern and function of CD166. In

the current study, we analyzed CD166 expression in normal human and mouse intestine. We identified enriched cell surface CD166 expression in the colon and small intestine (SI) crypt base. Interestingly in the SI, CD166 marked both the differentiated Paneth cell population and the intervening crypt-based columnar cells. We also confirmed observations for both elevated cell surface and cytoplasmic CD166 expression in human CRC samples. (Weichert, Knosel et al. 2004) Notably, both normal and tumor CD166 expression patterns were conserved in mice, highlighting the value of using the mouse as a model for studying CD166 regulation in cancer. Further, we show that a subset of CD166-expressing cells residing in the stem cell niche co-express other putative stem cell markers, including Musashi-1 (Msi-1) and Lgr5.(Potten, Booth et al. 2003; Barker, van Es et al. 2007; Sato, Vries et al. 2009) We propose that CD166 marks both progenitor and differentiated cell subpopulations within the normal intestinal stem cell niche, and that a possible function for CD166 is to maintain the epithelial microenvironment of the stem cell niche. Therefore, targeting this cell surface antigen in cancer therapy requires careful consideration of potential effects on normal tissues.

Material and Methods

Mice

Mice were housed in a specific pathogen-free environment under strictly controlled light cycle conditions, fed a standard rodent Lab Chow (#5001 PMI Nutrition International), and provided water *ad libitum*. All procedures were

performed in accordance to the OHSU Animal Care and Use Committee. The C57Bl/6 and $Apc^{Min/+}$ mice(Moser, Pitot et al. 1990) were purchased from The Jackson Laboratory (Bar Harbor, ME).

Immunohistochemical and histochemical analyses of intestinal tissue

Adult (>6 weeks) and embryonic [(E) 14.5, 15.5, 16.5, 17.5, 18.5] mouse intestines were dissected and prepared for paraffin and frozen tissue analyses as we have previously described.(Wong, Rubinfeld et al. 1998) Human small intestine (SI) and colonic tissue was fixed in 10% buffered formalin prior to embedding in paraffin or OCT. Human tissues were acquired from the Knight Cancer Institute Histopathology Shared Resource. Tissue sections were cut to a 5 μm thickness, then stained with antibodies to CD166 (15ug/ml; R&D Systems), Msi-1 (1:100; Chemicon International), Lgr5 (1:100, GeneTex), Ki67 (1:250; Abcam), seratonin (1:500; Incstar), E-cadherin (1:1000; Decma), or the lectin UEA-1 (1:1000; Sigma). For paraffin embedded tissues, antigen retrieval was performed for a subset of antibodies. Briefly, slides were incubated in 10mM citrate buffer, pH=6 or in 10mM Tris, 1mM EDTA, pH=9 for 20 minutes at 100˚C. Antigens were visualized using either species-specific secondary antibodies [Indocarbocyanine3 (Cy3), Indocarbocyanine5 (Cy5), Fluorescein isothiocyanate (FITC)] (1:500; Jackson ImmunoResearch), or brightfield diaminobenzidine (DAB) detection (Vectastain ABC kit; Vector, Burlingame, CA) and Methyl green counter staining (Vector, Burlingame, CA). Nuclear counterstaining with Hoechst dye (33258; Sigma; St. Louis, MO; 0.1 μg/ml) was performed for fluorescent

analyses. For detection of CD166-positive Paneth cells, human SI tissue sections were first incubated with antibodies to CD166, visualized with secondary antibodies conjugated to Cy3, and images were captured using a Leica DMR fluorescent microscope (Leica Microsystems, Bannockburn, IL). The tissue was then re-stained with Lendrum's Phloxine Tartrazine according to standard procedures(Luna 1968), images recaptured and superimposed using Canvas X software (ACD).

Analyses of isolated intestinal epithelial cells

The differentiated and undifferentiated epithelial cells of the mouse SI and colon were independently isolated using a modified Weiser preparation(Davies, Dismuke et al. 2008), stained with antibodies to CD166, and sorted using a Cytopeia Influx to collect $CD166^+$ SI villus or colonic cuff epithelia (differentiated cells) and $CD166^+$ SI and colonic crypt epithelia (undifferentiated cells). Briefly, intestines were cut longitudinally, rinsed with modified Hanks Buffered Saline Solution (HBSS without Ca^{2+} and Mg^{2+}), incubated in HBSS supplemented with EDTA (for SI differentiated cells: 1 mM EDTA, for colonic differentiated cells: 10mM EDTA) for two rounds at 4°C, 15 min. This was followed by two additional incubations for isolation of the undifferentiated fractions (for SI undifferentiated cells: 5mM EDTA, for colonic undifferentiated cells: 15mM EDTA). Cells were resuspended in modified HBSS and gently filtered through a 0.45μm filter. Cells were then incubated on ice for 20 min with a combination of antibodies against CD45 conjugated to Allophycocyanin (APC; 1:100; BD Pharmingen), CD166

(1:100; R&D Systems) and Lgr5 (1:100) on ice for 20 min, followed by incubation with secondary antibodies conjugated to FITC for CD166 (1:500; Jackson Immunoresearch) or PE for Lgr5 (1:500; Molecular Probes). Cells were resuspended in modified HBSS/ 5μg/ml propidium iodide/1% bovine serum albumin and sorted using a Cytopeia Influx (150 μm nozzle, 4.5 psi) and Spigot software. FACS data was analyzed using FCS Express Version 3 Research Edition (DeNovo Software). $CD166^+$, $CD45^-$, PI^- cells (10^5) were collected and spun onto glass slides using a Shandon Cytospin 4 (Thermo Electron) and subsequently analyzed for expression of Paneth cell markers or expression of Lgr5 as described in the previous section.

Results

CD166 protein expression is enhanced in the base of the human and mouse small intestinal and colonic crypt epithelium

CD166 expression has been documented in human CRC(Weichert, Knosel et al. 2004), but extensive evaluation of its expression pattern in normal tissue has not been performed. A previous study localizes CD166 to the cytoplasm of colonic epithelial cells within the crypt base.(Weichert, Knosel et al. 2004) To confirm this finding and extend our knowledge of CD166 expression in the human intestinal tract, we stained normal human SI and colonic tissue sections with antibodies to CD166. Consistent with its function in immune cells, CD166-expressing cells were detected within the intestinal mesenchyme (Figure A1.1A, arrows). In the epithelial compartment, detection with both fluorescent

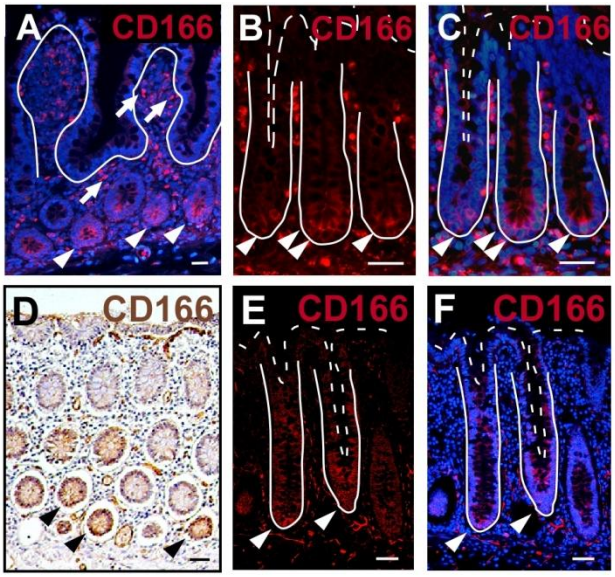

Figure A1.1. CD166 expression pattern in the human small intestine and colon. (A-C) Human small intestine stained with antibodies to CD166 (red) and counterstained with Hoechst (blue). (A) CD166-positive cells are located both in the mesenchymal (arrows) and epithelial compartments (arrowheads). (B-C) Enlarged view of small intestinal crypts. (D-F) Human colon stained with antibodies to CD166, visualized with DAB (brown) in (D) and with fluorescence (red) and Hoechst counterstain (blue) in (E, F). Arrowheads designate epithelial expression. Solid lines demark epithelial-mesenchymal boundary and dashed lines mark the apical epithelial surface. Bar = 25 μm.

and brightfield immunohistochemistry revealed enriched expression of CD166 protein in cells at the base of the crypts in both the SI (Figure A1.1A-C, arrowheads) and colon (Figure A1.1D-F, arrowheads). CD166 expression appeared strongest on the cell surface, and existed in a pronounced gradient that had an increased intensity towards the base of the crypt.

Next, to validate the mouse as a viable model organism for future studies examining the role of CD166 in normal intestinal physiology and tumorigenesis, we characterized CD166 expression patterns in the mouse SI. Because the mouse intestinal tissue is easily dissected, oriented and manipulated, it allowed for a more in-depth analysis of CD166 intestinal epithelial expression. Interestingly, crypt-based expression did not vary down the length of the SI, as has been reported for other putative stem cell markers such as Bmi1.(Sangiorgi and Capecchi 2008) Further, CD166 expression recapitulated the human expression pattern, as CD166 was detected on the epithelial plasma membrane with an increasing expression gradient toward the small intestinal and colonic crypt base or stem cell niche (Figure A1.2A-E). Because the protein expression was more readily detectable and robust in the mouse, a greater resolution of the distinct expression domain in the small intestinal crypt was apparent. CD166 expression appeared to be predominantly on the cell surface of a subset of crypt-base cells (Figure A1.2B). Lower levels of cell surface CD166 were also apparent on the small intestinal villus when sectioned on a tangential plane (Figure.A1.2C, arrowheads).

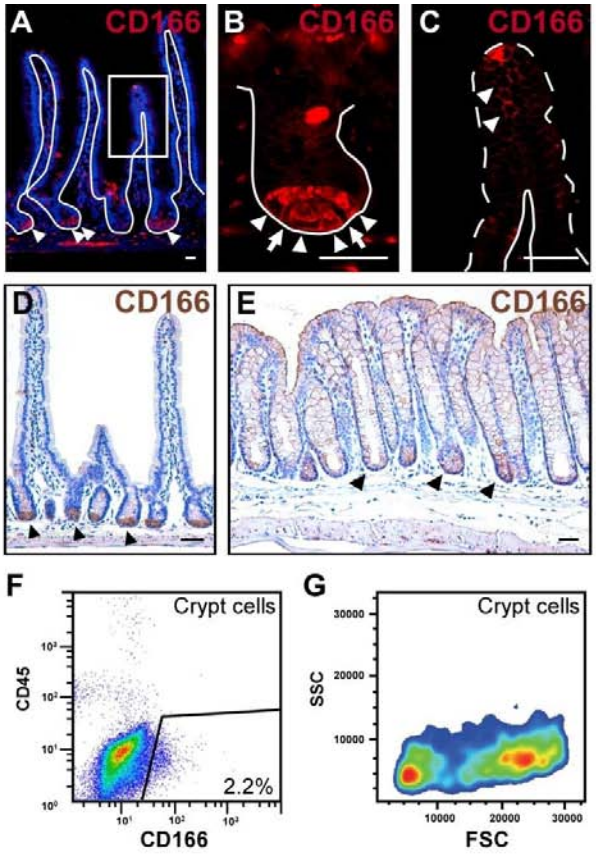

Figure A1.2. CD166 expression pattern in the mouse small intestine and colon. (A-C) Mouse small intestine (SI) stained with antibodies to CD166 (red) and counterstained with Hoechst (blue). Arrowheads mark CD166-expressing cells (A). Boxed region marks a tangential section through a villus, magnified in (C). (B) Higher magnification of CD166 expression in the SI crypt. Arrowheads mark differentiated Paneth cells, arrows mark intervening crypt-base columnar cells. Solid lines denote the epithelial-mesenchymal boundary and dashed line marks the apical epithelial surface. (D, E) Mouse SI and colon stained with antibodies to CD166 (brown), demonstrating enhanced expression in the crypt base of both organs (black arrowheads). Bar = 25 μm. (F) Flow cytometry analysis of isolated crypt epithelial cells stained with CD166 antibodies. (F') Forward and side scatter of $CD166^{hi}$ crypt epithelial cells display two distinct populations of cells.

To confirm cell surface expression on epithelial cells, we isolated the intestinal epithelium using a method that disrupts cell adhesion complexes(Davies, Dismuke et al. 2008), then performed FACS analyses to isolate CD166-positive epithelium. Enriched populations of differentiated, villus epithelium and undifferentiated crypt-based epithelium were isolated (Figure A1.2F, and Figure A1.3). A $CD166^{lo}$ population was characteristic of the positive villus epithelium (Figure A1.3), while crypt epithelium contained both $CD166^{lo}$ (5.9%) and $CD166^{hi}$ populations (2.2%). Reanalysis of the $CD166^{hi}$ crypt cell population revealed two distinct populations (Figure A1.2F'), and recapitulated the observed presence of two CD166-expressing cell populations in the crypt based on morphology (Figure A1.2B). Paneth cells (Figure A1.2B, arrowheads), as well as intervening crypt-based columnar cells (Fig. A1.2B, arrows) express cell surface CD166, likely functioning in homophilic adhesion. In the Paneth cell population, both granules and the junctional cell membranes stained positive for CD166 (Figure A1.2B, arrowheads). Paneth cells contain granules that are known to non-specifically cross-react with antibodies, yielding potentially false-positive results. Therefore, FACS was performed to more accurately collect and examine CD166-positive cells. The resulting cells remained fully intact and allowed for effective isolation of a population based only upon cell surface expression (Figure A1.4A). To confirm our immunohistochemical observations, we subsequently stained FACS-isolated CD166-expressing cells with markers for Paneth cells (Figure A1.4A, A'). Phloxine Tartrazine, an established Paneth cell histochemical stain, identified a subset of CD166-positive sorted cells (Figure

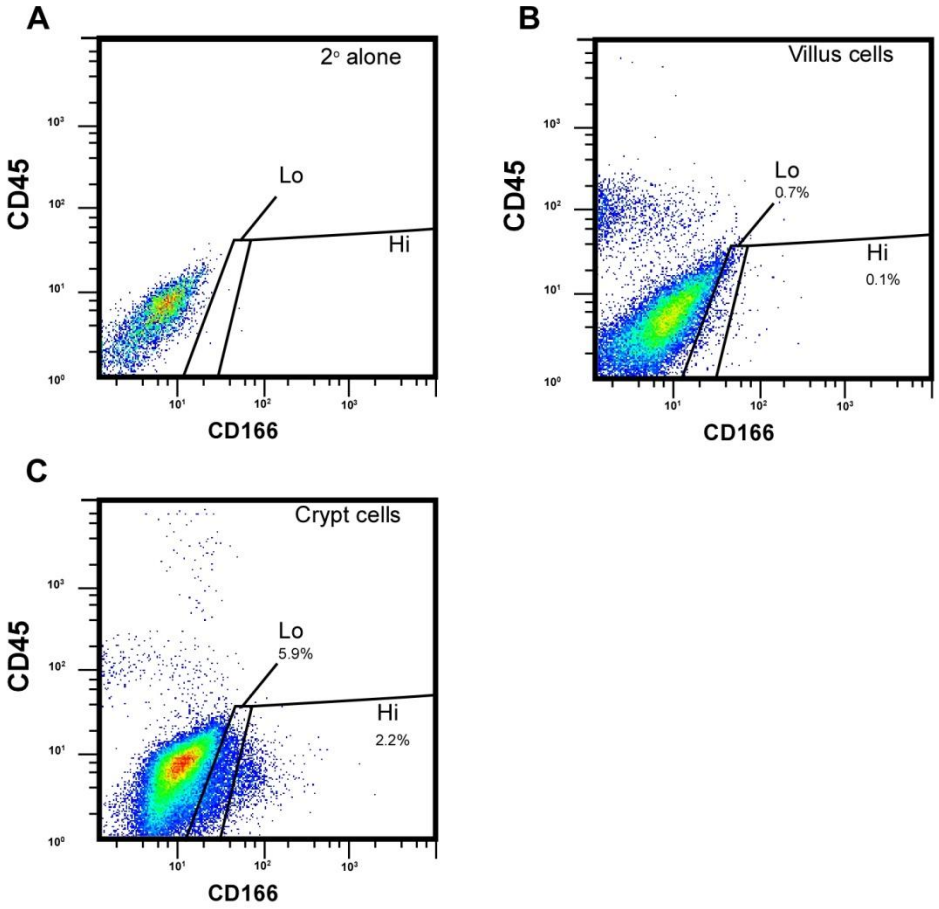

Figure A1.3. FACS analysis of CD166-expressing cells in the mouse intestine. (A) Isolated intestinal cells stained with secondary antibody only. (B) Isolated intestinal villus epithelial cells stained with antibodies to CD45 and CD166. (C) Isolated intestinal crypt epithelial cells stained with antibodies to CD45 and CD166. Gates designating the $CD166^{lo}$ and $CD166^{hi}$ populations are shown.

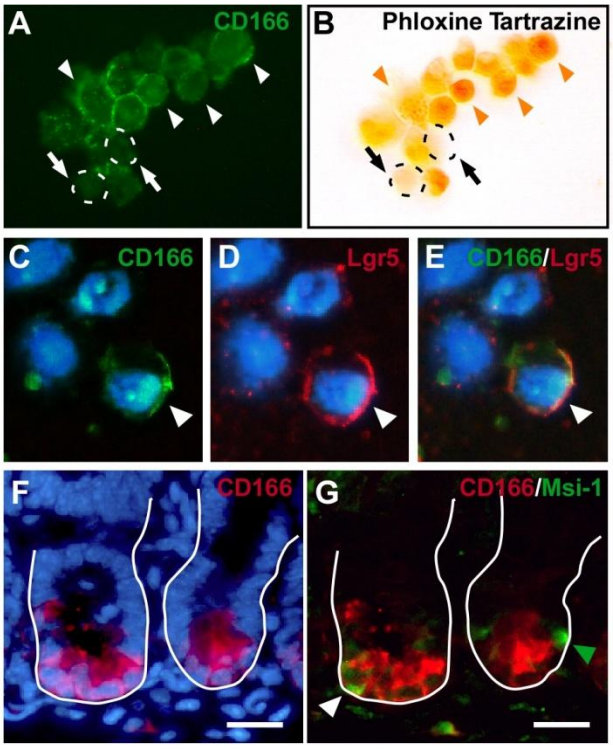

Figure A1.4. CD166 is expressed in crypt-based Paneth cells. (A-A') Isolated CD166-positive mouse crypt cells (magenta) cytospun onto a slide, co-stained with Phloxine Tartrazine that label the intracellular granules (A'; orange). White arrowheads designate CD166-positive cells, orange arrowheads designate CD166-positive, Phloxine Tartrazine positive cells. Arrows and dashed circles designate CD166-positive, Phloxine Tartrazine-negative cells. (B-B'') Isolated CD166-positive cells (magenta) co-stained with antibodies to Lgr5, a putative stem cell marker (green). Arrowhead designates a double-labeled cell. (C-C') Mouse intestinal tissue co-stained with antibodies to CD166 (magenta) and the putative stem cell marker, Musashi-1 (Msi-1, green). Nuclei stained with Hoechst (blue). White arrowhead designates co-expressing cell; green arrowhead designates a Msi-1-positive, CD166-negative cell. White lines mark epithelial-mesenchymal boundary. Bar = 25 μm.

A1.4A, A'; arrowheads). CD166-expressing cells were also positive for UEA-1, an additional Paneth and goblet cell marker (not shown). Interestingly, there was a population of CD166-positive cells that did not co-stain for UEA-1 or Phloxine Tartrazine (Figure A1.4A, A'; arrows). The human expression pattern was consistent with the mouse pattern in the SI as determined by sequential staining of human tissue with antibodies to CD166 and the histochemical stain, Phloxine Tartrazine (Figure A1.5, arrowheads).

Given that only a subset of FACS-isolated CD166-expressing cells represented Paneth cells, we sought to characterize the CD166-positive crypt-base columnar cells. To determine if these cells co-expressed additional putative stem cell markers, we performed FACS analysis on Lgr5 and CD166 double-labeled small intestinal crypt cells. Lgr5-positive cells represented a small fraction of CD166-positive crypt-based cells. This rare population of double-labeled cells was also apparent by IHC on CD166-isolated cells (Figure A1.4B-B"; arrowheads). A second putative stem cell marker, Msi-1(Potten, Booth et al. 2003), also shared overlapping expression with a subset of CD166-expressing cells (Figure A1.4C-C', white arrowhead), but also identified CD166-negative cells (green arrowhead). Further, a subset of CD166-expressing crypt-based cells also co-expressed markers for enteroendocrine cells (5-HT) and enterocytes (E-cadherin) (Figure A1.6).

Interestingly, in contrast to the adult intestine, analysis of the developing mouse intestine revealed that CD166 expression was ubiquitously expressed in the epithelium at embryonic day (E)14.5 (Figure A1.7A). However, at the onset of

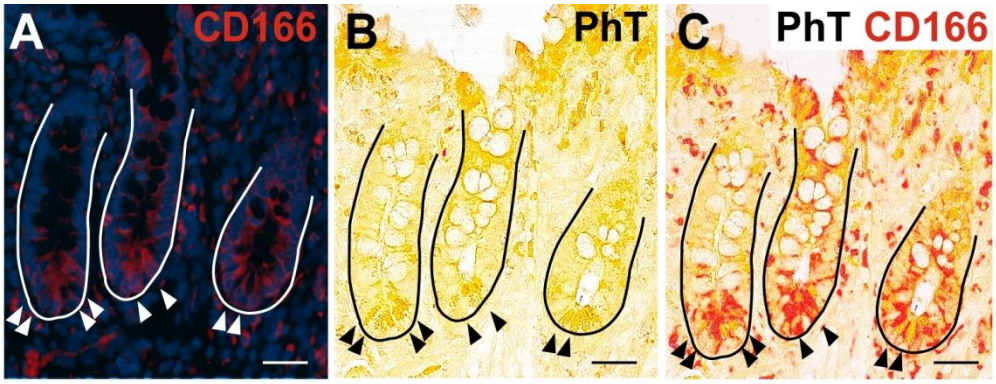

Figure A1.5. Paneth cells express CD166 in the human intestine. (A) CD166-expressing crypt-base cells (red, arrowheads) exist in the human small intestine. The intestine is counterstained with the nuclear dye Hoechst (blue). (B) The same section is stained with the histochemical stain Phloxine Tartrazine, identifying Paneth cells (yellow stain, black arrowheads). (C) Digital overlay of images from A and B indicate that these stains identify the same cell population (arrowheads). Bar = 25 μm.

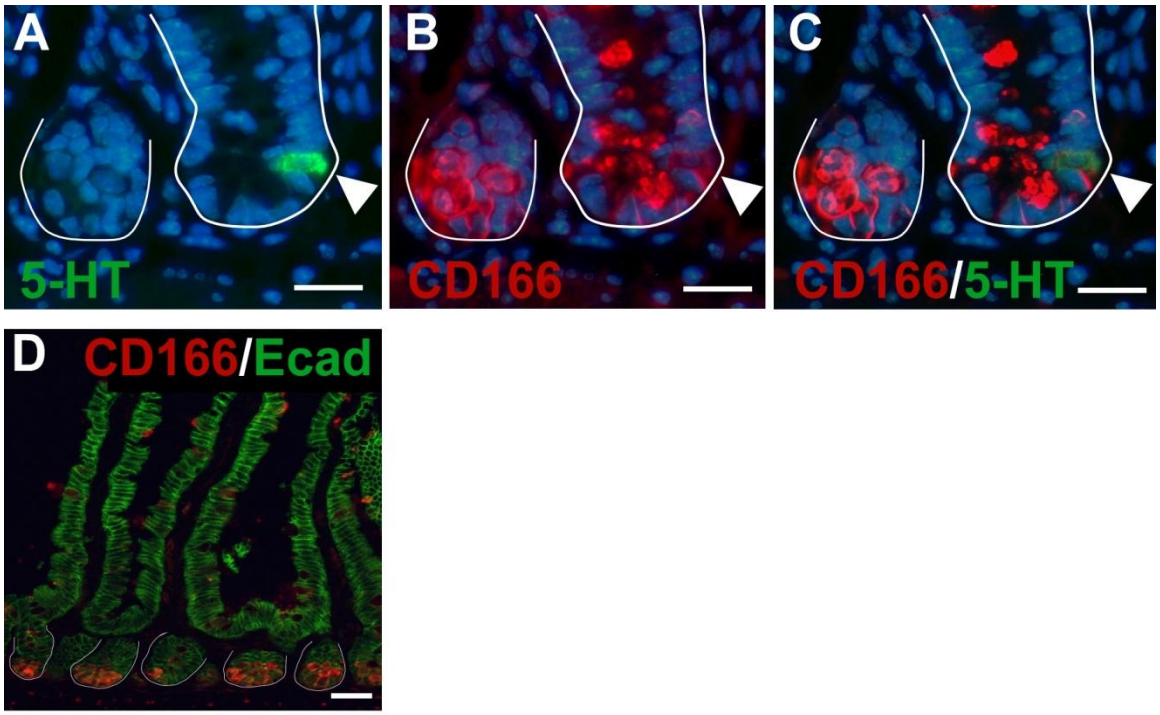

Figure A1.6. Differentiated cells also express CD166. (A-C) Some differentiated enteroendocrine cells, marked by expression of serotonin (5-HT, green) also express CD166 (red). A double-positive cell is marked by the arrowhead. (D) Differentiated enterocytes, identified with E-cadherin (Ecad) co-express CD166 (red). Bar = 25 μm.

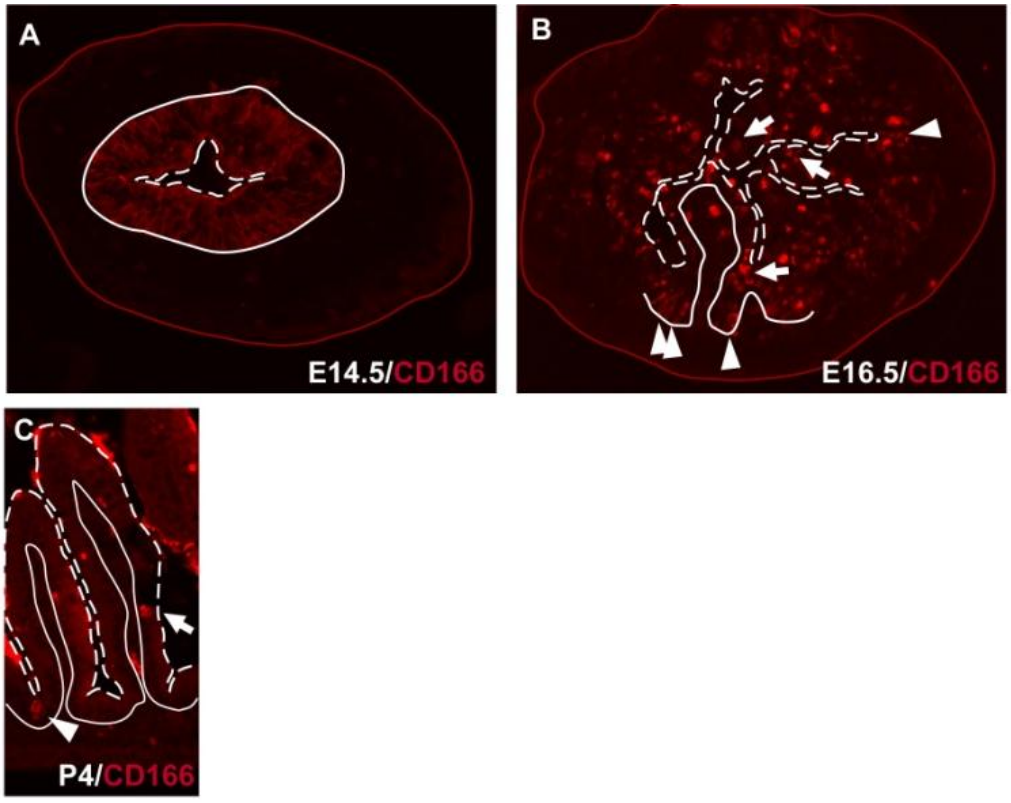

Figure A1.7. CD166 expression in the developing mouse intestine. (A) CD166 is ubiquitously expressed in the epithelium at embryonic day (E) 14.5. (B) At the onset of villus formation, E16.5, CD166 expression is localized to both the villus (arrow) and intervillus region (arrowheads). (C) By post-natal (P) day 4, CD166 expression was detected in the intervillus region (arrowhead) and sporadically on the villus (arrow). Solid red line marks the outside of the intestinal tube. Dashed line marks the intestinal lumen. Solid white line designates the epithelial mesenchymal boundary.

villus formation, E16.5, CD166 expression became localized to both the villus (arrows) and intervillus region (arrowheads; Figure A1.7B), and by post-natal (P) development, expression was localized in the intervillus region (P4; arrowhead; Figure A1.7C).

CD166 is highly expressed in human colon adenocarcinoma and liver metastases

To further characterize the expression patterns of CD166 during intestinal tumorigenesis, we stained human adenocarcinoma and liver metastases with antibodies to CD166. We identified both cell surface (arrowheads) and cytoplasmic (arrows) expression in primary tumors and metastases (Figure A1.8). Human tumors were decidedly heterogeneous in their CD166 expression. While some tumor samples exhibited only cell surface or cytoplasmic expression (Figure A1.8B, C), others exhibited both cell surface and cytoplasmic expression (Figure A1.8A). CD166-positive cells generally appeared within clustered regions of epithelium. Interestingly, for one matched primary tumor and liver metastasis, the expression pattern was identical (data not shown).

Tumors in a mouse model for intestinal tumorigenesis, the $Apc^{Min/+}$ mouse(Moser, Pitot et al. 1990), displayed a strikingly similar CD166 expression pattern compared to human colorectal tumors (Figure A1.9A, B). Both predominant cell surface staining and diffuse cytoplasmic expression was detected. Interestingly, only a subset of the CD166-expressing tumor cells was actively in the cell cycle, as determined by co-expression of the proliferative

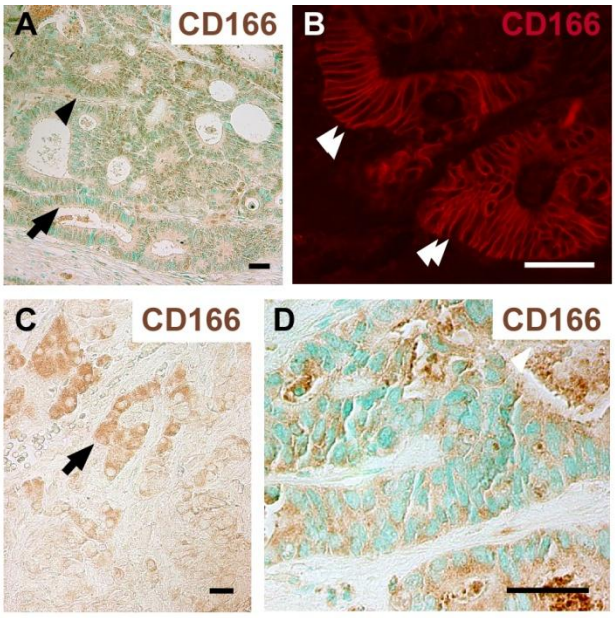

Figure A1.8. CD166 expression in human colorectal cancer. (A-C) Human primary colorectal adenomas stained with antibodies to CD166 for (A, C) brightfield detection (brown) with Methyl Green counterstain or (B) fluorescent detection (red). CD166 is expressed in both the cytoplasm (arrows) and on the cell surface (arrowheads) and (D) is also apparent in human liver metastatic colorectal cancer lesions. Bar = 25 μm.

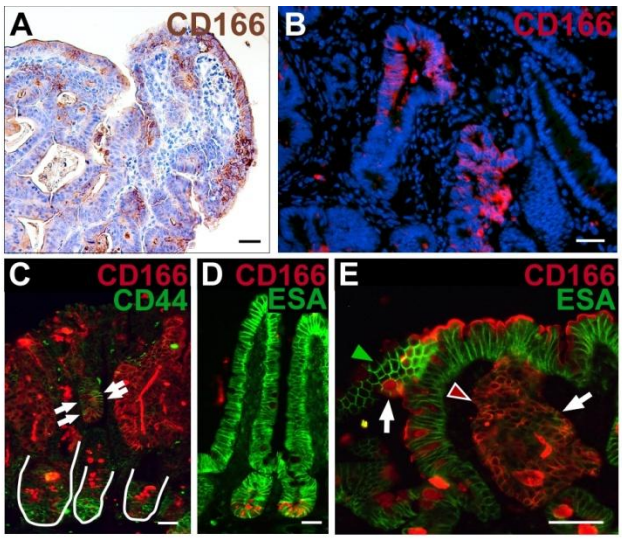

Figure A1.9. Rare double-positive CD166/CD44 or CD166/ESA cells reside in benign mouse intestinal tumors. (A-E) Benign mouse intestinal tumors stained with antibodies to CD166 (brown or magenta) in ApcMin/+ mouse intestine. (C) Double-positive CD166 (magenta) and CD44 (green) are present in the adenoma (arrows). White lines designate the rudimentary crypts at the base of the adenoma. (D-E) Double-stained CD166 (magenta) and ESA (green). (D) ESA stains ubiquitously in normal crypts, but (E) stains only a subset of tumor cells. A rare population of double-stained cells is designated with arrows. Arrowheads mark mutually exclusive expressing regions. Bar = 25 μm.

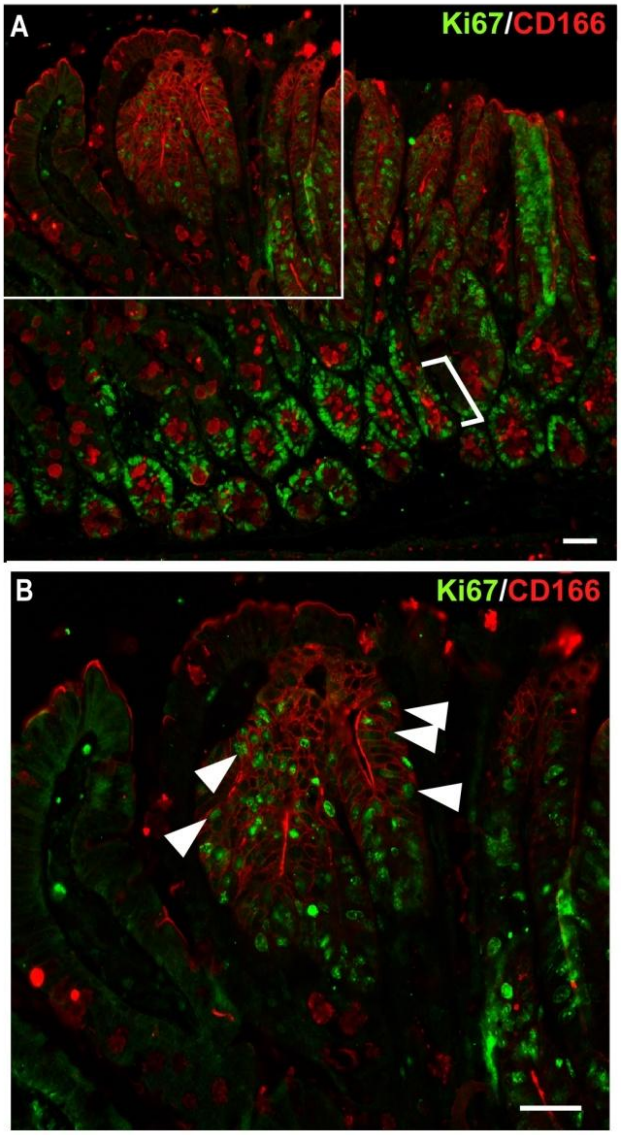

Figure A1.10. A subset of CD166-expressing mouse tumor cells are proliferating. (A) Ki67-positive cells (green) are scattered throughout the mouse intestinal tumor and clustered in the base of the crypt structures marking the transient-amplifying cells (white bracket). The boxed region in (A) is magnified in (B). A subset of CD166-expressing cells (red) also express Ki67 (green), and are marked by arrowheads. Bar = 25 μm.

marker Ki67 (Figure A1.10). This might reflect the possibility that at any one time, only a subset of CSCs were actively cycling. Supporting this notion, in crypt-like regions of the $Apc^{Min/+}$ mouse intestine, Ki67 generally marked the transient-amplifying cell population (Figure A1.10A, bracket), but also marked a rare subset of CD166 crypt-base columnar epithelial cells.

To further characterize the expression domain of CD166 in the normal intestine and in intestinal tumors, we performed double staining with CD166 and either CD44 or ESA on $Apc^{Min/+}$ mouse intestinal sections. CD44 and ESA were previously used in combination with CD166 to identify and isolate a CSC population in human CRC(Dalerba, Dylla et al. 2007). We found that CD44 was undetectable in the normal intestine (not shown); while in nearby adenomas, CD44 expression was primarily restricted to aberrant crypts within the tumor structure (Figure A1.9C). Interestingly, CD166 expression was generally lost in the aberrant crypt structures and, therefore, CD166 and CD44 were primarily expressed in mutually exclusive cell populations. However, there was a small subset of dual-expressing cells (Figure A1.9C, arrows). In contrast, ESA was expressed on all epithelial cells in the normal intestine (Figure A1.9D), and its expression was lost on large clusters of tumor cells (Figure A1.9E). As with CD44, CD166 and ESA were generally expressed in mutually exclusive cell populations (Figure A1.9E, arrowheads), although a small subset of cells expressed both antigens (Figure A1.9E, arrows).

Discussion

Our findings suggest that CD166 is an important molecule in the stem cell niche of both the human and mouse intestine. We show that CD166 was expressed at low levels in the differentiated cell population of the SI and colon and at high levels within the stem cell niche at the base of the crypt. In the SI, CD166 was distinctly present on both a putative stem cell population, comprised of the crypt-based columnar epithelial cells, and the differentiated Paneth cell population. In light of its previously described role in cell adhesion and its capacity to form homodimers across adjacent cell membranes, it is intriguing to postulate that CD166 may have an important function in anchoring the stem cell within the intestinal stem cell niche, or in instructing stem cell behavior. In support of this, a precedence exists for the participation of adhesion molecules to establish cell polarity and asymmetric stem cell division.(Picco, Hudson et al. 2007)

The intestinal stem cell marker Lgr5(Haegebarth and Clevers 2009) was co-expressed in a subset of CD166-expressing crypt cells. In contrast, the putative stem cell marker Msi-1 was often expressed in a single crypt cell surrounded by CD166-positive cells. Interestingly, Msi-1 was also expressed in crypt cells at the +6 position where they were not surrounded by CD166-positive cells. While the current understanding of the relationship between these potential discrete intestinal progenitor populations is lacking, it is clear that development of a multi-marker stem cell signature will be required to gain a deeper understanding for the implication of CD166-expressing cells in disease.

CD166 may possess multiple functions within the intestinal epithelium. This is suggested by its multi-faceted expression pattern in subsets of fully differentiated Paneth and enteroendocrine cells juxtaposed to its expression in a putative stem population. Interestingly, we also observed this type of expression pattern displayed for other putative intestinal stem cell markers including Dcamkl-1(May, Riehl et al. 2008) and Msi-1. Future exploration of CD166 differential function and regulation in intestinal epithelium will contribute to a better understanding of whether its dysregulation contributes to disease progression in intestinal cancer.

Consistent CD166 expression in both human and mouse tumors demonstrates that the mouse provides a viable model for studying the function and expression of CD166 in tumorigenesis. Interestingly, CD166 was highly expressed in early adenoma formation in the $Apc^{Min/+}$ mouse. Further, we confirmed that CD166 expression was retained within human CRC and metastatic disease, and that both a cell surface and cytoplasmic expression pattern was apparent. These findings, in particular an alteration in cellular localization of CD166, support a potential functional role for this molecule in tumorigenesis. Our analyses extend these initial findings and show that the observed expression patterns are also retained in metastatic lesions.

CD166 expression relative to other CSC and proliferative markers in the $Apc^{Min/+}$ mouse recapitulated previous findings(Dalerba, Dylla et al. 2007) that cells positive for both CD166, CD44 and ESA constitute a small subpopulation of total tumor mass. By analyzing the expression pattern of these markers in the

$Apc^{Min/+}$ mouse, a model of pre-neoplastic intestinal cancer, our findings suggest that mere co-expression of these markers may not be sufficient to promote invasive tumorigenesis. Alternatively, it is possible that the presence of cells with these markers suggest that these benign tumors have the potential for metastatic advance. Analysis of CD166 expression in $Apc^{Min/+}$ polyps found that crypt-like structures near the muscularis tend to be low or lack expression of CD166 although they are high in CD44 and Ki67 expression. While the significance of this observation is not known, it is possible that loss of CD166 cell surface expression is a precursor for tumor progression.

Our data are the first to describe and compare the normal expression pattern of CD166 in human and mouse intestine and to characterize its expression in both Lgr5-positive crypt cells and Paneth cells. This characterization of expression suggests that the mouse is a valid model for understanding CD166 function and its role in tumorigenesis. Before CD166 can be therapeutically targeted in cancer, we must first better understand its normal function.

Conclusions

Cell surface antigen expression of CD166 was recently identified as an important marker on human intestinal CSCs.(Dalerba, Dylla et al. 2007) Along with this observation and its history in cancer progression as a marker for aggressive disease(Weichert, Knosel et al. 2004), it represents an intriguing molecule for therapeutic targeting in the treatment of intestinal cancer. For

effective targeting of any cell surface antigen, its endogenous expression pattern must first be elucidated. Here, we report a broad range of CD166 expression patterns in the human and mouse intestine. We show that CD166 is expressed on a number of intestinal cells, including putative stem cells and differentiated crypt-based cells. This discovery provides important implications for future targeting of CD166 in disease therapy and, significantly, provides insight into the potential functional role of this critical molecule.

APPENDIX 2

Lessons from development: A role for asymmetric stem cell division in cancer

Anne E. Powell[1], Chia-Yi Shung[2^], Katherine W. Saylor[3^], Karin A. Müllendorff[3^], Joseph B. Weiss[4], and Melissa H. Wong[1,5]

[1]Department of Cell and Developmental Biology, [2]Shriners Hospital for Children Research Division, [3]The Vollum Institute, [4]Department of Cardiology, [5]Department of Dermatology, Knight Cancer Center, Oregon Stem Cell Center, Oregon Health and Science University, Portland, OR

[^]These authors contributed equally.

***Stem Cell Research*, 2010; 4(1):3-9.**

AEP wrote the manuscript.

Abstract

Asymmetric stem cell division has emerged as a major regulatory mechanism for physiologic control of stem cell numbers. Reinvigoration of the cancer stem cell theory suggests that tumorigenesis may be regulated by maintaining the balance between asymmetric and symmetric cell division. Therefore, mutations affecting this balance could result in aberrant expansion of stem cells. Although a number of molecules have been implicated in regulation of asymmetric stem cell division, here, we highlight known tumor suppressors with established roles in this process. While a subset of these tumor suppressors were originally defined in developmental contexts, recent investigations reveal they are also lost or mutated in human cancers. Mutations in tumor suppressors involved in asymmetric stem cell division provide mechanisms by which cancer stem cells can hyperproliferate and offer an intriguing new focus for understanding cancer biology. Our discussion of this emerging research area derives insight from a frontier area of basic science and links these discoveries to human tumorigenesis. This highlights an important new focus for understanding the mechanism underlying expansion of cancer stem cells in driving tumorigenesis.

Introduction

The ability of stem cells to undergo asymmetric cell division as a way to self-renew is a tightly regulated process that occurs during development, tissue

maintenance, regeneration, and may be disrupted in hyperproliferative disease states such as cancer. Asymmetric cell division is typically restricted to stem cell populations where a need exists to preserve both a progenitor and a simultaneously generated differentiated progeny. This process is nicely exemplified in self-renewing tissues such as the epithelial layer of the human skin and intestine. Both organs possess stem cell pools that derive differentiated epithelia needed to maintain the function of the organ. The stem cell employs asymmetric division to maintain an appropriate census of daughter cells (or transient amplifying cells) and terminally differentiated cells. In the intestine, transient amplifying cells are characterized by their ability to amplify the epithelial population and likely undergo symmetric cell division to generate terminally differentiated cell populations. In these self-renewing tissues, a critical balance between asymmetric and symmetric cell division is required to maintain tissue homeostasis. Asymmetric stem cell division is vital for this maintenance thus it is likely that tumors will develop if it is not properly regulated (Figure A2.1A) (Morrison and Kimble 2006). This dysregulation is consistent with the notion that expansion of a subpopulation of cancer cells harboring stem cell-like properties (cancer stem cells) may be the basis for propagating tumorigenesis. Though still controversial, there is growing acceptance that tumors may be dictated by this stem cell hierarchy, knowledge of how mutations in molecules that influence asymmetric stem cell division will provide insight into tumorigenesis. Mechanisms of asymmetric stem cell division have primarily been elucidated in invertebrate

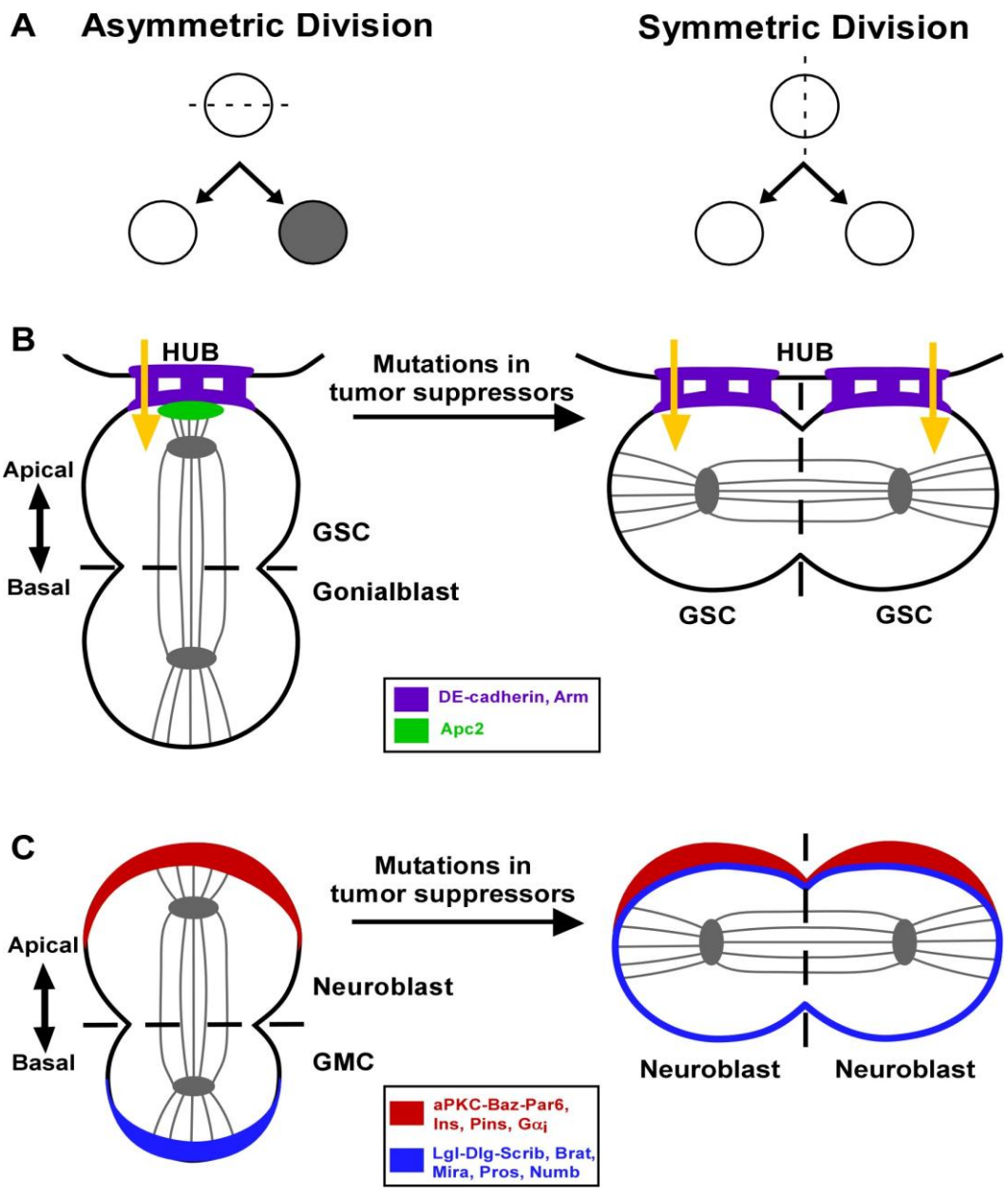
A
Asymmetric Division
Symmetric Division
B
HUB
Mutations in
tumor suppressors
HUB
Apical
Basal
GSC
Gonialblast
GSC
GSC
DE-cadherin, Arm
Apc2
C
Mutations in
tumor suppressors
Apical
Basal
Neuroblast
GMC
Neuroblast
Neuroblast
aPKC-Baz-Par6,
Ins, Pins, Gαi
Lgl-Dlg-Scrib, Brat,
Mira, Pros, Numb

Figure A2.1

Figure A2.1. Model illustrating how mutations in factors regulating asymmetric stem cell division in Drosophila neuroblast and germline cells result in uncontrolled expansion of stem cells. (A) Stem cells can undergo asymmetric division giving rise to both a stem cell (white) and a differentiated cell (gray), or symmetric division that produces two stem cells. (B) In the Drosophila germline stem cells (GSC) asymmetric cell division requires Adenomatous polyposis coli-2 (Apc2; green oval) and its partners DE-cadherin and Armadillo (Arm)/ß-catenin (purple) at the HUB cell interface to support proper mitotic spindle orientation, as well as additional microenvironmental extrinsic cues (yellow arrows). This yields one GSC and one Gonialblast. However, mutations in tumor suppressors results in symmetric cell division that yields two GSCs and consequent hyperproliferation of the stem cell pool. (C) Asymmetric division of the Drosophila neuroblast requires correct localization of the apical complex (red crescent): atypical Protein Kinase C-Bazooka-Par6, Inscuteable, Partner of Inscuteable, and Gai (aPKC-Baz-Par6, Ins, Pins and Gai) and basal restriction of Lethal giant larvae-Discs large-Scribble, Brain tumor, Miranda, Prospero, Numb (Lgl-Dlg-Scrib, Brat, Mira, Pros, Numb; blue crescent). Normal asymmetric neuroblast division results in self-renewal of the stem cell and production of a differentiated ganglion mother cell (GMC). Mutations in tumor suppressors cause mislocalization of the basal proteins and thus generate two neuroblasts resulting in uncontrolled stem cell proliferation.

systems and encompass a number of molecules highly conserved in vertebrates (Morrison and Kimble 2006; Yu, Kuo et al. 2006; Doe 2008; Knoblich 2008).

A subset of proteins important for regulating asymmetric stem cell division are known tumor suppressors expressed in both invertebrate and vertebrate systems. Many of these tumor suppressors in *Drosophila melanogaster* have a role in tumor formation, and many of these genes have human homologues. Whether the function of these tumor suppressors in asymmetric stem cell division significantly contributes to cancer progression in vertebrate systems is not yet fully established, however based upon evolutionary conservation, it is intriguing to speculate that they may play an important role in human cancers.

Our intention is to review the role of four specific tumor suppressors involved in asymmetric stem cell division and discuss potential roles for their function in human cancer. Importantly, the lessons learned from the consequences of misregulating asymmetric stem cell division in developmental systems can inform the emerging research focus on the mechanism underlying cancer stem cell expansion as it relates to tumor progression.

Much of what is known about the molecular mechanism underlying asymmetric cell division is based on examination of developmental systems in *Drosophila*. Through elegant studies of the *Drosophila* neuroblast and germline cells, we know that the polarity and spindle orientation of the stem cell—the major determinants of asymmetric stem cell division—are governed by factors that are both intrinsic and extrinsic (Bilder 2004; Yu, Kuo et al. 2006; Doe 2008;

Knoblich 2008). For example, in the fly neural stem cells or “neuroblasts,” segregation of intracellular proteins to the apical or basolateral region of the cell determines whether a stem cell asymmetrically divides, giving rise to both a stem cell and a differentiated daughter cell, or if it symmetrically divides to produce two stem cells (Bowman, Neumuller et al. 2006; Lee, Robinson et al. 2006). In contrast, *Drosophila* germline cells rely on extrinsic factors within the stem cell niche to define the orientation of the mitotic spindle, which is critical for proper cell division (Yamashita, Jones et al. 2003; Yamashita, Mahowald et al. 2007). In addition, proper cell division of the self-renewing, polarized mouse intestinal epithelium is regulated but the positioning of the mitotic spindle (Fleming, Zajac et al. 2007). From these two model systems, it is clear that both the orientation of the spindle and segregation of polarity components ultimately determine whether a stem cell will asymmetrically or symmetrically divide.

While it is yet unclear if these two well-defined examples of asymmetric stem cell division directly apply to division of human stem cells or to a putative cancer stem cell population, they offer a testable model to shape our investigation of the link between mammalian cancer and stem cell biology. Moreover, emerging evidence from the fly and mouse suggests that mutations in particular tumor suppressors that govern asymmetric stem cell division disrupt the normal ratio of stem cells to differentiated cells and contribute to unregulated proliferation of tumors. The following tumor suppressors - Adenomatous polyposis coli (Apc), Lethal giant larvae (Lgl), Brain tumor (Brat) and p63 - display a novel and intriguing link between invertebrates and vertebrates and the

regulation of asymmetric stem cell division in both tissue stem cells and tumorigenesis.

Adenomatous polyposis coli: a novel role in stem cell mitotic spindle orientation

APC is a human tumor suppressor with a well-documented role in the Wnt signaling pathway, primarily governing proliferative division of stem cells (Morin, Vogelstein et al. 1996; Rubinfeld, Albert et al. 1997). In this capacity mutations in APC result in upregulated cellular proliferation and tumor formation. Not surprisingly, this gene is mutated or suppressed in a number of cancers, including hepatoblastoma (Oda, Imai et al. 1996), medulloblastoma (Huang, Mahler-Araujo et al. 2000), adult T-cell leukemia (Yang, Takeuchi et al. 2005) and most notably in colorectal cancer where nearly all forms harbor mutations in APC (Su, Steinbach et al. 2000). The dominant association between APC and the Wnt signaling pathway overshadows the multiple functions of the APC protein (reviewed in (Hanson and Miller 2005)). The human APC gene encodes a large multi-domain protein that can interact with a number of partner proteins (Hanson and Miller 2005). As such, APC has been demonstrated to interact with microtubules, suggesting a role in cell migration (Hanson and Miller 2005; Dikovskaya, Schiffmann et al. 2007; Kroboth, Newton et al. 2007). Additionally, it has been shown to be involved in regulating mitotic spindle assembly and chromosome segregation (Kaplan, Burds et al. 2001). Further, APC has also been described to participate in regulation of cell cycle progression and apoptosis (Baeg, Matsumine et al. 1995; Dikovskaya, Schiffmann et al. 2007).

Although each of these roles attributed to APC have potential importance in tumor progression, its role in asymmetric stem cell division most intriguingly suggests an important function in modulating expansion of cancer stem cells. Recently, Apc was discovered to be a component of the centrosome complex of *Drosophila* germline cells. Here it functions in establishing asymmetric stem cell division, distinct from its role in Wnt signaling. In this capacity, mutations in APC could effectively expand early cancer cells or a putative cancer stem cell pool.

In the male *Drosophila* germline, Apc2 anchors the mother centrosome of the germline stem cell so that it is adjacent to the hub cell. The hub cell provides extrinsic, supportive cues to the stem cell that orient the mitotic spindle. The contact surface between the hub cell and the germline stem cell is also marked by concentrated levels of proteins known to interact with Apc2 (Figure A2.1B). This interaction localizes Apc2 to the interface between the hub germline stem cell, fixing the mother centrosome at one pole of the stem cell and allowing the daughter centrosome to migrate to the opposite side of the germline stem cell (Figure A2.1B). This movement allows the correct orientation of the mitotic spindle (Penman, Leung et al. 2005; Yamashita, Mahowald et al. 2007). In *Drosophila,* deletion of both *Apc* genes results in mis-orientation of centrosomes and the mitotic spindle, and consequently disrupts asymmetric stem cell division. At the tissue level, the phenotypic consequence is hyperproliferation of germline stem cells at the expense of differentiated cells (Yamashita, Jones et al. 2003).

To date, the most well investigated role of *APC* has been its function as a tumor suppressor. However, these new findings in *Drosophila* reveal a novel role

for *Apc* in asymmetric stem cell division, which may intensify its role in tumor progression. It is easy to speculate that APC in humans may also be essential for spindle orientation and proper asymmetric division of tissue stem cells. In this scenario, mutations in *APC* would also lead to increased numbers of cancer stem cells. Investigation of APC's role in the regulation of asymmetric stem cell division represents an important future focus of human cancer biology.

Lethal giant larvae: regulating stem cell polarity and differentiation

Normal asymmetric neuroblast division results in self-renewal of the stem cell and production of a differentiated ganglion mother cell (GMC; Figure A2.1C). The correct positioning of both apical and basal protein complexes is critical for proper asymmetric cell division. Mutations in tumor suppressors cause mislocalization of these basal proteins, generating two neuroblasts that result in uncontrolled stem cell proliferation (Figure A2.1C). Three *Drosophila* tumor suppressor genes, *lethal giant larvae* (*lgl*), *discs-large* (*dlg*) and *scribble* (*scrib*), act in a common pathway in the mitotic neuroblast to establish the asymmetrically localized cortical basal complex and ultimately influence asymmetric stem cell division. Specifically, Lgl interacts with the apical complex shown in Figure A2.1C – atypical protein kinase C-Bazooka-Par6, Inscuteable, Partner of Inscuteable, and Gα_i (aPKC, Ins, Pins and Gα_i). In addition, it restricts the localization of active basal complex molecules (Betschinger, Mechtler et al. 2003; Wirtz-Peitz, Nishimura et al. 2008) and this is illustrated in mutants for Lgl that possess abnormal targeting of the basal complex proteins Miranda,

Prospero and Numb (Mira, Pros, Numb) (Figure A2.1C; (Betschinger, Mechtler et al. 2003; Lee, Robinson et al. 2006)).

Proper location and function of Lgl is critical to the prevention of tumor formation. Lgl mutants do not asymmetrically divide but instead produce two stem cells at the expense of neuronal populations. This ultimately leads to expansion of the stem cell population and subsequent formation of brain tumors (Lee, Robinson et al. 2006). Supporting this role in tumor suppression and the regulation of proper asymmetric cell division, loss of mouse Lgl1 results in disrupted asymmetric cell division and a brain tumor phenotype (Klezovitch, Fernandez et al. 2004). Tumor initiation and cancer progression in humans may, in part, be driven by misregulation of Lgl homologues. Strikingly, a human homologue of *lgl*, *HUGL-1*, is lost in many solid tumors and is strongly correlated with advanced stages of malignant melanoma, colorectal cancer and endometrial cancer (Schimanski, Schmitz et al. 2005; Kuphal, Wallner et al. 2006; Tsuruga, Nakagawa et al. 2007). In addition, recent work examining *HUGL-1* in human hepatocellular carcinoma reveals that the mRNA is frequently mutated by aberrant splicing. This renders the protein inactive and functions as an important mediator of hepatocellular carcinoma progression (Lu, Feng et al. 2009).

HUGL-1 is highly structurally and functionally conserved, as observed by the ability of *HUGL-1* to rescue *Drosophila lgl* mutants (Grifoni, Garoia et al. 2004). Both HUGL-1 and another Lgl human homologue, HUGL-2, directly interact with the human aPKC-Par6 protein complex (Yasumi, Sakisaka et al. 2005) (Figure A2.1C), behaving just as Lgl does in *Drosophila*. Further, inhibition

of this binding induces disorganization of the mitotic spindle during normal mitosis and results in aberrant cell division (Yasumi, Sakisaka et al. 2005). Even further evidence from the examination of the behavior of *Drosophila* polarity proteins in human ovarian cancer epithelium reveals that Lgl function is conserved (Grifoni, Garoia et al. 2007) between flies and humans. This suggests that both HUGL-1 and HUGL-2 play active roles in establishing polarity and spindle orientation for asymmetric cell division of human epithelial stem cells and, when mutated, may result in tumor initiation and/or expansion of cancer stem cells. This intriguing possibility has yet to be directly investigated.

Brat: a critical protein for balancing stem cell self-renewal and proliferation

The *Drosophila* larval neuroblast tumor suppressor with emerging relevance to human cancer is the newest member of the basal complex, “Brain tumor” (*brat*, Figure A2.1C). Brat, like Prospero, Miranda, and Numb, is asymmetrically localized during neuroblast cell division to the basal cortex (Figure A2.1C). Brat removal results in extensive proliferation of larval neuroblasts at the expense of differentiated neurons and generates tumors (Betschinger, Mechtler et al. 2006; Lee, Wilkinson et al. 2006). Further investigation revealed that Brat mutants exhibit and uncontrolled expansion of transient amplifying cells, resulting from a failure to progress through the cell cycle (Bowman, Rolland et al. 2008).

The structure of Brat contains clues about its role in asymmetric stem cell division and control of tissue proliferation. Brat contains an NHL domain, an

evolutionarily conserved motif found in proteins that post-transcriptionally regulate gene expression via mRNA binding and inhibition of translation. Indeed, in *Drosophila*, Brat is thought to be a post-transcriptional inhibitor of Myc (Sonoda and Wharton 2001). Myc transcriptionally regulates a variety of cell cycle and cell growth genes to support proliferation as opposed to differentiation. Interestingly, dMyc translation is de-repressed in cells without Brat. Studies in the mouse neocortex support this finding where TRIM32, a Brat homologue, is asymmetrically localized in one of the two daughter cells and becomes upregulated during neuronal differentiation (Schwamborn, Berezikov et al. 2009). TRIM32 has dual roles as both a tumor suppressor functioning to degrade cMyc, and in asymmetric cell division where it is asymmetrically located and activates certain microRNAs important for stem cell self-renewal (Schwamborn, Berezikov et al. 2009). Although a role for TRIM32 in asymmetric stem cell division in human cancers has not been described, its overexpression in human head and neck squamous cell carcinoma samples highlights its activity as an E3 ubiquitin ligase (Horn, Albor et al. 2004; Albor and Kulesz-Martin 2007; Boulay, Stiefel et al. 2009; Locke, Tinsley et al. 2009), and it has been suggested to potentially be a cause of cancer. This analysis is complicated by functional redundancy in the mouse and human systems, as both species also express TRIM2 and TRIM3, which are also human Brat homologues. To this end, loss of heterozygosity of the tumor suppressor TRIM3 has recently been implicated human malignant gliomas (Boulay, Stiefel et al. 2009), where it is intriguing to speculate that it may have a role in asymmetric cell division and formation of a potential cancer stem

cell population. Clearly, additional studies are required to establish a role for the Brat family homologues in asymmetric stem cell division in humans. However, the intriguing evidence from mouse and fly suggests that Brat is certainly multi-functional. Importantly, like the APC tumor suppressor, Brat is most well-known for an early-described function in tumorigenesis that overshadows a potentially important role in asymmetric stem cell division specifically contributing to cancer stem cell expansion.

p63: a novel role in stem cell spindle orientation and proliferation

While numerous studies have examined asymmetric cell division in invertebrates, recent reports have uncovered a role for this process in mammalian systems. For example, *p63*, a closely related member of the *p53* tumor suppressor family, is highly expressed in asymmetrically dividing stratified epithelial cells that are susceptible to cancer (Yang, Schweitzer et al. 1999). *p63* has been implicated and is now classically described as a master switch regulator of epithelial stem cell commitment, maintenance, and differentiation (Koster, Kim et al. 2004).

In both mouse and human, full length *p63* is spliced into multiple isoforms and all of the resulting protein products have distinct, complex roles described in both oncogenesis and tumor suppression depending on the tissue and/or tumor-specific context for which they are examined (Westfall and Pietenpol 2004; Deyoung and Ellisen 2007). For example, ΔNp63α is upregulated in breast, gastric, cholangiocarcinoma, and chronic myeloid leukemia, but not in leukemia,

where the *TAp63* isoform is overexpressed. In addition, molecular interactions between the isoforms, which limit the activity of one another have also been described further complicating analyses of these proteins (Deyoung and Ellisen 2007).

Interestingly, the *p63* transcription factor was recently implicated in mitotic spindle orientation during asymmetric epidermal stem cell division, one of the first studies to examine *in vivo* asymmetric stem cell division in a mammalian system (Lechler and Fuchs 2005). Accordingly, its role in establishing spindle orientation may be related to the proliferative potential of dividing cells, a critical mediator in cancer progression. Stratified epithelial cells undergo symmetric and asymmetric divisions during normal development. Under these conditions, the mitotic spindle orients perpendicular to the basement membrane and mammalian homologues of the apical complex localize to the apical cortex prior to cell division. In contrast, in a *p63* null mouse mutant, the spindle is parallel in orientation and the complex is mislocalized (Lechler and Fuchs 2005), resulting in the disruption of tissue organization.

In general, misregulation of any of the *p63* isoforms is implicated in human tumor formation, however a definitive and consistent correlation between expression of the *p63* isoforms and either cancer initiation or progression remains controversial (Westfall and Pietenpol 2004; Deyoung and Ellisen 2007). Many human cancers harbor an overexpression of one or more isoforms of *p63*, supporting an oncogenic role in tumorigenesis. In addition, some studies indicate that overexpression of *p63* can cause an epithelial-to-mesenchymal

transition, leading to an upregulation of genes involved in cell migration and invasion during metastasis (Koster, Lu et al. 2006). Interestingly and conversely, human bladder and urothelial cancers exhibit loss of *p63*, supporting a tumor suppressive role (Park, Lee et al. 2000; Koga, Kawakami et al. 2003). In either situation and in light of the mouse and fly data, it is possible that either over- or underexpression of *p63* may contribute to aberrant spindle orientation in the stem cell population. Clearly, the existence of multiple *p63* isoforms complicates our appreciation of its role in asymmetric stem cell division, although the extensive descriptions of the function of p63 in epithelial stem cell biology combined with the recent spindle orientation studies in the mouse (Lechler and Fuchs 2005) provides an undeniable basis for further examination of the role of p63 in spindle orientation as it results in asymmetric stem cell division.

Conclusion

In any self-renewing tissue, maintaining a balance between stem cells and their differentiated progeny depends upon tightly regulated asymmetric stem cell division (Morrison and Kimble 2006). Recent investigations in invertebrate and vertebrate systems have established that successful asymmetric cell division is dependent on asymmetrically localized proteins and mitotic spindle orientation. Proper execution of these two cellular programs functions in cell fate determination to control whether a cell assumes either a stem or differentiated identity. When mutations occur in genes involved either directly or downstream of the intrinsic or extrinsic cues governing these mechanisms, the resulting

asymmetric cell division is abnormal and leads to uncontrolled amplification of stem cell populations.

The tumor suppressor proteins described in this review represent just four examples of molecules that regulate developmental or adult homeostatic asymmetric cell division, but we highlight the critical need for further investigations regarding the relevance of these tumor suppressors in disrupting asymmetric stem cell division in human cancer. Indeed, a precedent for such translational research is ongoing in work addressing *Drosophila* cell polarity determinants and proliferation control, and their implications on mammalian cancer progression (Bilder 2004; Grifoni, Garoia et al. 2004; Caussinus and Gonzalez 2005; Gonzalez 2007; Grifoni, Garoia et al. 2007; Hawkins and Russell 2008). Studies emerging from this nascent field may implicate a critical and novel role for these proteins in early tumor initiation and asymmetric stem cell division of a putative cancer stem cell population.

Direct links between tumorigenesis and asymmetric stem cell division do exist in mutants of the well-documented mammalian tumor suppressor APC, the p53 family member, p63, and the *Drosophila* polarity protein, Lgl (summarized in Table A2.1). Mutations in these tumor suppressors are associated with advanced tumor progression, metastasis and poor patient prognosis, yet their function in aberrant asymmetric stem cell division in cancer has not been fully explored despite the amount of overwhelming evidence derived from lessons in developmental biology. The findings we present here likely represent but a few

Roles for tumor suppressors in asymmetric stem cell division and cancer

	Fly	Mouse	Human
Apc	ACD linked to tumor formation	ACD; Tumor formation	Tumor formation
Lgl	ACD linked to tumor formation	ACD linked to tumor formation	ACD linked to tumor formation
Brat	ACD linked to tumor formation	Tumor formation	ACD; Tumor formation
p63	*ND*	ACD linked to tumor formation	Tumor formation

Table A2.1. A summary of the investigations of mutations in APC, Lgl, Brat and p63* from fly, mouse and human cancers and their potential link to asymmetric stem cell division (ACD). ACD linked to tumor formation = the protein has defined role in asymmetric stem cell division that has been linked experimentally to tumor formation. ACD; Tumor formation = the protein has defined role in asymmetric stem cell division as well as tumor formation, but these functions have not been experimentally linked. Tumor formation = the protein has defined role in tumor formation, but a link to ACD has not yet been described. *The full length p63 isoform is referred to here. ND = not determined, as a full length, p63 homologue has not been identified in Drosophila. This table encompasses the investigations cited in this review.

examples of how clues from developmental biology can illuminate key insights into cancer cell biology; specifically, the study of aberrant asymmetric stem cell division of human tissue stem cells and the expansion of a cancer stem cell pool in tumorigenesis. Clearly defining a role for the underlying mechanism driving aberrant expansion of a cancer stem cell pool provides further justification for targeting the cancer stem cell as an important therapeutic approach for treatment of disease.

APPENDIX 3

Wnt-reporter expression pattern in the mouse intestine during homeostasis

Paige S. Davies[1], Adria D. Dismuke[2], Anne E. Powell[3], Kevin H. Carroll[1] and Melissa H. Wong[1]

[1]Department of Dermatology, Oregon Cancer Center, Oregon Stem Cell Center; [2]Department of Molecular and Medical Genetics; [3]Department of Cell and Developmental Biology; Oregon Health & Science University, Portland, OR.

***BMC Gastroenterology*, 8: 57 (2008).**

AEP performed immunohistochemical analyses and participated in editing of the manuscript.

Abstract

Background: The canonical Wnt signaling pathway is a known regulator of cell proliferation during development and maintenance of the intestinal epithelium. Perturbations in this pathway lead to aberrant epithelial proliferation and intestinal cancer. In the mature intestine, proliferation is confined to the relatively quiescent stem cells and the rapidly cycling transient-amplifying cells in the intestinal crypts. Although the Wnt signal is believed to regulate all proliferating intestinal cells, surprisingly, this has not been thoroughly demonstrated. This important determination has implications on intestinal function, especially during epithelial expansion and regeneration, and warrants an extensive characterization of Wnt-activated cells. Methods: To identify intestinal epithelial cells that actively receive a Wnt signal, we analyzed intestinal Wnt-reporter expression patterns in two different mouse lines using immunohistochemistry, enzymatic activity, *in situ* hybridization and qRT-PCR, then corroborated results with reporter-independent analyses. Wnt-receiving cells were further characterized for co-expression of proliferation markers, putative stem cell markers and cellular differentiation markers using an immunohistochemical approach. Finally, to demonstrate that Wnt-reporter mice have utility in detecting perturbations in intestinal Wnt signaling, the reporter response to gamma-irradiation was examined.

Results: Wnt-activated cells were primarily restricted to the base of the small intestinal and colonic crypts, and were highest in numbers in the proximal small intestine, decreasing in frequency in a gradient toward the large intestine. Interestingly, the majority of the Wnt-reporter-expressing cells did not overlap with the transient-amplifying cell population. Further, while Wnt-activated cells expressed the putative stem cell marker Musashi-1, they did not co-express DCAMKL-1 or cell differentiation markers. Finally, gamma-irradiation stimulated an increase in Wnt-activated intestinal crypt cells.

Conclusions: We show, for the first time, detailed characterization of the intestine from Wnt-reporter mice. Further, our data show that the majority of Wnt-receiving cells reside in the stem cell niche of the crypt base and do not extend into the proliferative transient-amplifying cell population. We also show that the Wnt-reporter mice can be used to detect changes in intestinal epithelial Wnt signaling upon physiologic injury. Our findings have an important impact on understanding the regulation of the intestinal stem cell hierarchy during homeostasis and in disease states.

Introduction

It is well established that the canonical Wnt signaling pathway plays a critical role in regulating intestinal proliferation at the level of the stem cell(Kinzler and Vogelstein 1996; Korinek, Barker et al. 1998; Bienz and Clevers 2000; Booth and Potten 2000; Pinto, Gregorieff et al. 2003; Kuhnert, Davis et al. 2004) and has been inferred to regulate proliferation of all intestinal crypt-based cells including the bulk of proliferative cells, the transient-amplifying-cell (TA-cell) population(Kinzler and Vogelstein 1996; Korinek, Barker et al. 1998; Bienz and Clevers 2000; Booth and Potten 2000; Pinto, Gregorieff et al. 2003; Kuhnert, Davis et al. 2004; Van der Flier, Sabates-Bellver et al. 2007). Surprisingly, the proliferative influence of the Wnt signal on discrete cell populations within the crypt has not been previously characterized. Confounding issues for making these distinctions is that manipulation of Wnt signaling in the stem cell population will invariably affect the downstream TA-cell population, complicating interpretation. Further, there is precedence for a Wnt signal acting as a global regulator of proliferation in development prior to the establishment of the stem cell hierarchy(Korinek, Barker et al. 1998). However, there is also evidence that proliferative control of crypt-based cells may be more multi-faceted than originally thought. Most interestingly, the TA-cell population does not express the recently identified Wnt-target stem cell marker, Lgr5(Barker, van Es et al. 2007), nor does it harbor nuclear β-catenin staining, a hallmark of activated Wnt signaling(Batlle, Henderson et al. 2002; van de Wetering, Sancho et al. 2002). In addition, Wnt signaling has been shown to differentially regulate stem cell and TA-cell

populations in other epithelial systems such as the skin(DasGupta and Fuchs 1999; Blanpain, Horsley et al. 2007), suggesting that a more complex regulation of proliferation may exist. Therefore, determining the influential distinction of the Wnt signal within the different proliferative intestinal cell populations is important for understanding epithelial homeostasis, regeneration after injury, and cellular dynamics during proliferative diseases.

Epithelial proliferation is confined to the intestinal crypts. The proliferative capacity of the intestine is defined by approximately 4-6 active stem cells and a second rapidly proliferating crypt population made up of the TA-cells that is situated adjacent to the stem cells. Multiple signaling cascades, including the Wnt, Notch, and Sonic Hedgehog pathways(Radtke, Clevers et al. 2006), converge within the crypt niche to regulate the gradient of proliferation-to-differentiation. The canonical Wnt signaling pathway is well established as an important regulator of intestinal epithelial proliferation(Korinek, Barker et al. 1998) and homeostasis(Korinek, Barker et al. 1998; Lickert, Kispert et al. 2001; Gregorieff and Clevers 2005; Muncan, Sansom et al. 2006). During mouse intestinal development, ablation of the downstream transcription factor, Tcf4 links loss of Wnt signaling with a loss of epithelial proliferation(Korinek, Barker et al. 1998). In the adult mouse, a proliferative role for this pathway is recapitulated when the Wnt inhibitor Dickkopf-1 is over-expressed, leading to collapse of the crypt structure(Kuhnert, Davis et al. 2004), and most notably in disease, where mutations in this pathway result in epithelial hyperproliferation leading to colorectal cancer(Kinzler and Vogelstein 1996).

The canonical Wnt signal is conveyed through the binding of a soluble ligand to cell surface co-receptors, Frizzled and Lrp5/6(Logan and Nusse 2004), then propagated by inhibiting the degradation of β-catenin, which stimulates the transcription of target genes(Molenaar, van de Wetering et al. 1996; Gordon and Nusse 2006, Molenaar, 1996 #39). The Wnt target gene Lgr5 is a putative stem cell marker based upon its crypt mRNA localization and a functional knock-in reporter experiment(Barker, van Es et al. 2007). Interestingly, Lgr5 is expressed only in epithelial columnar cells, but not higher up in the crypt within the TA-cell population. This suggests that Wnt signals may influence discrete cell populations rather than act as a global proliferative regulator within the crypt. Therefore, it is possible that proliferation of stem cells and the TA-cell population are differentially controlled.

In other systems, such as the hematopoietic system, the Wnt signal also provides proliferative cues to progenitor cells(Staal and Clevers 2005). Self-renewal of both the hematopoietic stem cells and their TA-cell populations are thought to be regulated by the Wnt pathway. Conversely, in epithelial systems such as the skin, stem and TA-cell populations appear to be differentially activated by Wnt signals(DasGupta and Fuchs 1999; Blanpain, Horsley et al. 2007). In the intestine, however, definitive stem cell markers have been slow to be established. The absence of these markers and the inability to accurately distinguish stem and progenitor populations within the intestinal crypt presents an obstacle for determining if Wnt acts as a global regulator of cell proliferation. One approach to establishing the role of Wnt signaling on the discrete intestinal crypt

cell populations is to characterize cells within the crypt that are Wnt-activated. Here, we validate for the first time, the Wnt-reporter mouse as a useful resource for evaluation of Wnt-activation within the intestine. Further, we establish that during intestinal homeostasis, activation of the Wnt pathway occurred primarily in an intestinal progenitor cell and not in the actively cycling TA-cell population. Our data validates the Wnt-reporter mouse as a functional tool for detecting changes in Wnt signaling within the intestinal epithelium. We show that the canonical Wnt pathway is stimulated in response to gamma-irradiation-induced apoptosis both by an increased expression of the Wnt-reporter as well as Wnt ligands and the *c-Myc* target gene. The characterization of Wnt signaling within the intestine provides an important foundation for understanding the regulation of the intestinal stem cell hierarchy during homeostasis and in disease states.

Materials and Methods

Mice

Mice were housed in a specific pathogen-free environment under strictly controlled light cycle conditions, fed a standard rodent Lab Chow (#5001 PMI Nutrition International, Brentwood, MO), and provided water ad libitum. All procedures were performed in accordance to the OHSU Animal Care and Use Committee. The Wnt-reporter TOPGAL(DasGupta and Fuchs 1999), C57Bl/6, and Apc^{MIN-}(Moser, Pitot et al. 1990) mice were obtained from The Jackson Laboratory (Bar Harbor, ME) and the BAT-Gal Wnt-reporter mice were a kind gift from Dr. Stefano Piccolo(Maretto, Cordenonsi et al. 2003).

Analyses of Wnt-responsive intestinal cells

Immunohistochemical analyses. Wnt signaling activity was characterized in adult TOPGAL, BAT-Gal, and C57Bl/6 mouse intestines. The entire length of the intestine was prepared for frozen or paraffin sectioning and the methods used for single and multi-label immunohistochemical staining are previously described(Wong, Rubinfeld et al. 1998). The following antisera were used: anti-β-galactosidase (β-gal; Immunology Consultants Laboratory, Inc.; Newberg, OR; 1:500 dilution), anti-Musashi-1 (#14H-1; a gift from Dr. H. Okano, Keio University, Tokyo; 1:500), UEA-1 (Sigma; St. Louis, MO; 1:500), anti-cryptidin (a kind gift from Andy Oulette, University of California - Irvine; 1:25) and anti-5-HT (Serotonin; Incstar; Stillwater, MN; 1:500). Primary antibodies were detected with species appropriate secondary antibodies conjugated to Cy3, FITC (Jackson ImmunoResearch; West Grove, PA) or Alexa-488 (Molecular Probes; Eugene, OR). Tissues were counterstained with Hoechst (33258; Sigma; St. Louis, MO; 0.1 μg/ml). Paraffin embedded tissue sections were stained with antibodies for β-catenin (Transduction Labs; Lexington, KY; 1:500 dilution) to detect nuclear localization. Staining was performed as described previously(Sansom, Meniel et al. 2007). Biotinylated secondary antibodies and Diaminobenzidine (DAB) were employed for visualization. Images were captured on a DMR microscope and DC500 digital camera with IM50 Image Manager Software (Leica Microsystems; Bannockburn, IL). Cy3 images were captured as grayscale and digitally converted to red images.

Quantification of β-gal-positive cells. To establish the percentage of β-gal-positive crypts and villi down the length of the intestine, tissue sections from mice stained with antibodies to β-gal as described above were quantified. At least 1500 crypts or villi were screened from n = 2-5 mice and reported as a percentages. For a more detailed analysis of the location of β-gal-positive cells within the crypt, the proximal small intestinal crypts were divided into equal thirds. β-gal-positive cells for each region (upper, middle and lower third) were tallied and compared to the total number of β-gal-positive crypt cells (>1500 crypts; n = 2 mice). To determine the percentage of dual-labeled β-gal-expressing Paneth cells, tissue sections were co-stained with UEA-1 and β-gal antibodies as described above. A total of >1500 crypts/mouse were screened (n = 3 mice).

β-gal enzymatic activity. Five μm frozen sections were washed in phosphate buffered saline and prepared for 5-bromo-4-chloro-3-inodyl β-D-galactoside (X-gal) detection followed by nuclear-fast red counterstain modified from previously described protocols(Wong, Hermiston et al. 1996).

Assessment of proliferative status. To detect proliferating cells, 5 μm frozen tissue sections were stained with antibodies against Ki67 (Abcam #ab15580; Cambridge, MA; 1:250) and appropriate fluorescent-conjugated secondary antibodies. Alternatively, mice were injected with 5-bromo-2'deoxyuridine/5-fluoro-2'deoxyuridine (BrdU/FrdU, 120/12 mg/kg body weight; Sigma; St. Louis, MO) 48h prior to sacrifice. Tissue sections were co-stained sequentially with antibodies to BrdU and β-gal. For BrdU staining a modified protocol from the Abcam Resources website was used (www.abcam.com).

Briefly, tissues were washed in phosphate buffered saline and incubated in blocking buffer (1% BSA, 0.3% Triton X-100, 1mM $CaCl_2$) prior to staining with antibodies to BrdU(Wong, Rubinfeld et al. 1998) (a gift from Dr. Jeffrey Gordon, Washington University School of Medicine, St. Louis, MO; 1:1000) and detected with fluorescent secondary antibodies. The tissue was imaged after each step and the acquired images overlayed using Canvas software (ACD Systems; Miami, FL). To quantify β-gal and BrdU expression, >1000 crypts per animal (n = 3) were scored for crypts containing co-labeled cells.

Wnt signaling response to intestinal damage

Irradiation-induced epithelial damage. TOPGAL and C57Bl/6 mice were exposed to 12Gy and sacrificed at 1, 12, 24, 48, and 72h post-irradiation. Intestinal tissue was harvested and processed as described above and stained with Hematoxylin & Eosin (H&E) or with antibodies for β-gal or β-catenin. The number of β-gal-positive crypts were counted and compared to the total number of crypts in each tissue section (≥1300 crypts counted/time point). Intestinal samples from at least three mice per time point were analyzed (n = 19 mice total). Further, for untreated and 24h post-irradiation time points, the number of β-gal-positive cells per crypt (1, 2 or >2) was also tallied and normalized to the total number of crypts (>1500 crypts counted/time point; n = 2 mice each). The number of cells co-stained with antibodies for Ki67 and β-gal were also determined for both non-irradiated (n = 2) and 24h-post-irradiated intestines (n = 2; ≥2000 crypts/animal). Average values were represented ± standard deviation.

Statistical significance was determined by unpaired *t*-tests assuming equal variances using Microsoft Excel. *p* values < 0.05 were considered significant.

mRNA expression

In situ hybridization. To validate the gene expression pattern of *lacZ*, RNA *in situ* hybridization was performed as previously described(Murtaugh, Chyung et al. 1999) using digoxigenin-labeled LacZ riboprobes (1µg/µl), alkaline-phosphatase-conjugated anti-digoxigenin antibody and BM Purple substrate (Roche; Indianapolis, IN).

Quantitative analysis of mRNA expression from isolated intestinal cell populations. β-gal mRNA has a shorter half-life than the protein(Bachmair, Finley et al. 1986; Selinger, Saxena et al. 2003) and can provide a more precise detection of Wnt-activated cells. A modified Weiser preparation(Weiser 1973; Weiser 1973) was used to isolate crypt and villus epithelium from adult Wnt-reporter mouse small intestine. Differentiated epithelial cells were removed in 1mM EDTA and 1mM DTT, where crypt epithelium was isolated in 1 mM EDTA and 5 mM DTT. Total RNA was purified from the isolated villus and crypt cell populations and cDNA was synthesized as we have previously described(Wong, Saam et al. 2000). Quantitative RT-PCR was performed using a SYBR Green-based assay, primers to β-gal and a 7900HT Sequence Detector according to established protocols(Wong, Saam et al. 2000; Hooper, Wong et al. 2001). Each cDNA sample was analyzed in triplicate, along with triplicate samples of the endogenous reference gene, Glyceraldehyde-3-phosphate dehydrogenase. Each

assay for *lacZ* expression was performed at least three independent times on n = 3 mice. The fold-change was determined using established methods(Wong, Saam et al. 2000; Hooper, Wong et al. 2001) and reported relative to levels in crypts.

To demonstrate intestinal Wnt-responsiveness in the TOPGAL model, mice were irradiated as described above and sacrificed 24h later. Crypt epithelial cells were isolated from the small intestine as described above and evaluated by qRT-PCR for gene expression of three Wnt ligands (*Wnt3*, *Wnt6*, *Wnt9b*), a secreted Wnt inhibitor (*sFrp2*), and a Wnt target gene (*c-Myc*) (n = 2 non-irradiated, n = 3 irradiated). For Wnt9b, only distal small intestinal crypt epithelium was surveyed, due to its restricted expression to this region(Gregorieff, Pinto et al. 2005). Primer sequences are presented in Table A3.1.

Table A3.1 Primer sequences for qRT-PCR

Gene	Forward Sequence	Reverse Sequence
lacZ	5'-GATCTTCCTGAGGCCGATACTG-3'	5'-GGCGGATTGACCGTAA TGG-3'
gapdh	5'-TGGCAAAGTGGA GATTGTTGCC-3'	5'-AAGATGGTGATGGGCTTCCCG-3'
wnt3	5'-CAAGCACAACAATGAAGCAGGC-3'	5'-TCGGGACTCACGGTGTTTCTC-3'
wnt6	5'-TGCCCGAGGCGCAAGACTG-3'	5'-ATTGCAAACACGAAAGCTGTCTCTC-3'
wnt9b	5'-AAGTACAGCACCAAGTTCCTCAGC-3'	5'-GAACAGCACAGGAGCCTGACAC-3'
sfrp2	5'-AGGTCCTTTGATGCTGACTGTAAA-3'	5'-TCGGCTTCACCTTTTTGCA-3'
c-myc	5'-AGCTTCGAAACTCTGGTGCATAA-3'	5'-GGCTTTGGCATGCATTTTAATT-3'

Results

Activation of Wnt signaling in single cells within the intestinal crypt.

To identify the intestinal epithelial cell population that actively receives a Wnt signal, we surveyed the entire length of the intestine from two independently established Wnt-reporter mouse lines, TOPGAL and BAT-Gal(DasGupta and Fuchs 1999; Maretto, Cordenonsi et al. 2003), in addition to C57Bl/6 mice. TOPGAL and BAT-Gal transgenic mice express the reporter, β-galactosidase (β-gal), in response to reception and processing of an endogenous canonical Wnt signal, marking cells activated by the signaling cascade(DasGupta and Fuchs 1999; Maretto, Cordenonsi et al. 2003). Both mouse reporter lines displayed a similar pattern (Figure A3.1A,B), therefore TOPGAL mouse intestines are depicted unless otherwise noted. In the Wnt-reporter mouse intestine, we found strong β-gal expression in epithelial cells within the crypt base (Figure A3.1A,B,D). Typically, positive crypts within the proximal small intestine (PSI) contained only one or two β-gal-positive cells (Figure A3.1A,B), although some crypts were uniformly populated with β-gal-positive cells that extended into the TA-cell region (Figure A3.1C) and onto the adjacent villi. The reporter protein expression pattern was confirmed by detecting β-gal expression by enzymatic activity using the substrate, X-gal (Figure A3.1E). Interestingly, while single cells within the crypt base were detected, no crypts with the broader expression pattern, nor villus epithelial expression were observed. We corroborated our findings in the Wnt-reporter mice with identification of crypt cells harboring nuclear β-catenin in wild-type mice, a hallmark of Wnt activation (Figure A3.1F).

The nuclear β-catenin staining pattern recapitulated the Wnt-reporter protein expression pattern (Figure A3.1A,B,D). Because of the discrepancy between the β-gal protein expression on the villus detected by antibodies (Figure A3.1C and A3.2D) and the crypt-based expression of β-gal enzymatic activity (Figure A3.1E), we analyzed reporter RNA expression. Both *in situ* hybridization (Figure A3.1G&H) and qRT-PCR for the *lac*Z gene in isolated crypt or villus epithelial populations (Figure A3.1I) demonstrated that Wnt-activated cells were restricted to the crypt base. An indepth examination of the crypt localization of β-gal-positive cells revealed that the majority resided in the base of the crypt (79.6%), the stem cell niche and the location of differentiated Paneth cells, while fewer β-gal-positive cells were located in the middle third (17.4%) or the upper third of the crypt (3.0%; Figure A3.1J).

Interestingly, a gradient of Wnt-activated, β-gal-positive cells existed in the intestine, with 15.2% of crypts containing a Wnt-activated cell in the PSI compared to 0.8% of colonic crypts (Figure A3.1K). Additionally, villi with β-gal-positive epithelium were also detected in a decreasing gradient down the length of the small intestine (Figure A3.1L). This pattern of Wnt-activated cells parallels the decreasing gradient in cell turnover and proliferation rates that exist down the length of the small intestine and colon(Lipkin 1985).

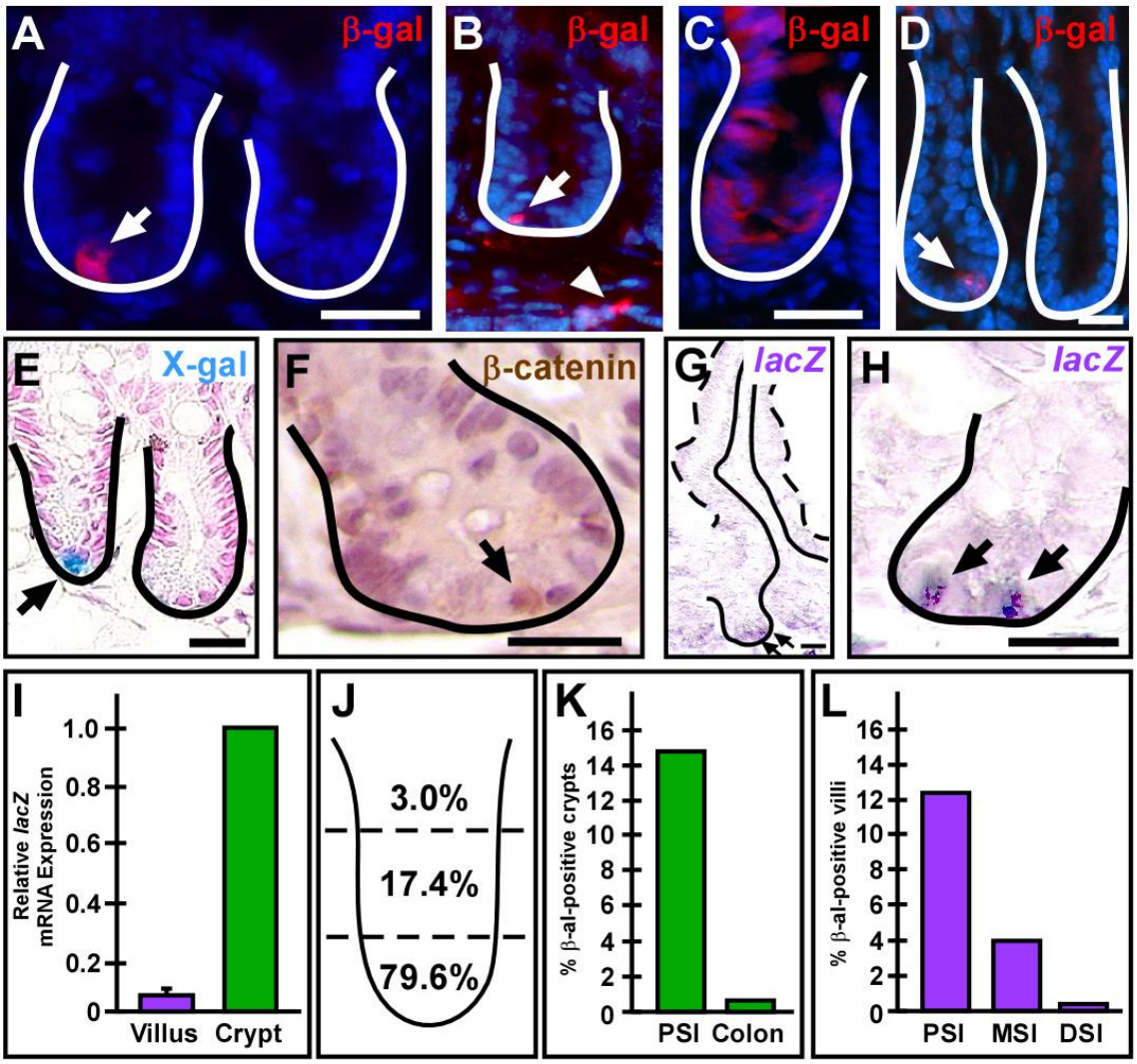
A
β-gal
B
β-gal
C
β-gal
D
β-gal
E
X-gal
F
β-catenin
G
lacZ
H
lacZ
I
Relative lacZ mRNA Expression
1.0
0.8
0.6
0.4
0.2
0
Villus
Crypt
J
3.0%
17.4%
79.6%
K
% β-al-positive crypts
16
14
12
10
8
6
4
2
0
PSI
Colon
L
% β-al-positive villi
16
14
12
10
8
6
4
2
0
PSI
MSI
DSI

Figure A3.1

Figure A3.1 Adult mouse expression pattern of Wnt-receiving epithelial cells. (A,C,D) Cryopreserved adult TOPGAL mouse proximal small intestinal (PSI) or colonic and (B) BAT-Gal mouse PSI tissue sections were stained with antibodies against β-galactosidase (β-gal, red) and counterstained with Hoechst dye (blue). (A&B) The majority of crypts in the PSI contained only one Wnt-activated cell or was devoid of positive cells (arrow). There were occasional mesenchymal cells positive for β-gal (arrowhead) in BAT-Gal intestines (B). (C) Occasionally, β-gal-expressing cells were detected throughout the crypt epithelium and on adjacent villi. (D) Colonic crypts contained only rare single β-gal positive cells near the crypt base. (E) Wnt-receiving cells detected by enzymatic activity, X-gal staining (blue, arrow). (F) Adult wild-type mouse PSI was stained with antibodies against β-catenin (brown; arrow) to detect nuclear expression and counterstained with Hematoxylin. (G-I) Analyses of reporter RNA expression pattern and localization was determined by *in situ* hybridization (G,H; purple, arrow) and are consistent with the expression pattern in (A). (I) qRT-PCR for *lacZ* gene expression in isolated crypt or villus epithelial cells from TOPGAL PSI demonstrated expression in the crypts. (J) The crypt localization of β-gal-positive cells was highest in the lower third and decreased in numbers in the middle and upper third. (K) Crypts with Wnt-receiving cells in TOPGAL intestinal sections were higher in the PSI (15.2%) and decreased down the length of the intestine to 0.8% in the colon. (L) The number of β-gal-positive villi also reflected a decreasing gradient with the highest numbers in the PSI (1A3.3%), less in the the middle small intestine (MSI; 4.0%) and the least in the distal small intestine (DSI; 0.2%). Solid white or black line demarks the epithelial-mesenchymal boundary. Dashed line outlines the apical epithelial border. Bar = 25 μm.

Wnt-receiving cells express cell proliferation markers but are not located in the TA-cell region.

The majority of β-gal-positive cells reside in the base of the intestinal crypt, suggesting that Wnt signaling may influence proliferation in the progenitor population and not the TA-cell population. To distinguish if the Wnt signal conveys a restricted rather than global proliferative response within the intestinal crypt, intestines from Wnt-reporter mice were co-stained with antibodies to β-gal and the proliferation marker Ki67, which designates cells undergoing late G1, S, G2 or M phases of the cell cycle. Ki67-positive cells were located in the middle portion of the crypts and extended toward the lower third, consistent with the location of both the TA-cell population and crypt progenitor cells. Analysis was restricted to crypts containing one or two β-gal positive cells. In most of these crypts, the majority of the Ki67 staining did not co-localize with β-gal-positive cells (Figure A3.2A-C, arrow). Occasionally, β-gal-expressing crypt cells were also Ki67-positive (7.1%), potentially indicating that this Wnt-activated cell was actively dividing (Figure A3.2A-C, arrowhead).

To determine if the Wnt-activated cells were label-retaining cells, we performed BrdU label-retaining assays by injecting BrdU into TOPGAL mice 48h prior to analysis. This timeframe is sufficient for BrdU-labeled epithelial cells to give rise to BrdU-positive descendents that have migrated up the villus (Figure A3.2D, lagging edge BrdU-cell marked by green arrow). At this analytical time point, the BrdU-labeled progeny have migrated away from the BrdU-label-retaining stem cell in the crypt (Figure A3.2D-G, white asterisk), as apparent by

the intervening BrdU-negative cells (Figure A3.2D&E). The β-gal-positive villus epithelial cells overlap with the BrdU-positive villus cells (Figure A3.2D, red bracket) suggesting that they might be derived from the dual BrdU-positive, β-gal positive cell in the crypt. Approximately 7.5% of crypts contained cells with co-localized β-gal and BrdU (Figure A3.2F&G and Figure A3.3), suggesting that a subset of β-gal-positive cells were also crypt label-retaining cells.

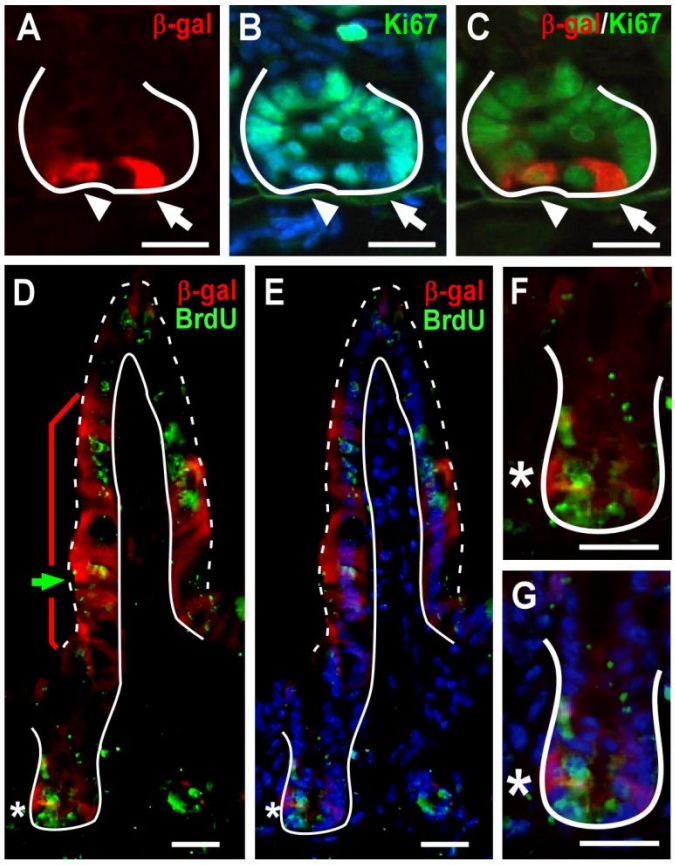

Figure A3.2 Wnt-activated cells represent progenitor cells within the intestinal crypt. (A-C) Cryopreserved intestinal tissue sections from TOPGAL adult mice co-stained with antibodies to β-gal (red) and Ki67 (green) then counter-stained with Hoechst (blue). Arrow indicates a cell with β-gal staining and arrowhead designates a cell co-staining for both markers. (D-G) Co-localization of BrdU (green) and β-gal (red) expression in crypt and villus epithelial cells from adult TOPGAL mice injected with BrdU 2 days prior to sacrifice. Green arrow denotes β-gal-positive cells at the lagging edge of migrating BrdU-positive cells up the villus. Red bracket indicates β-gal-positive villus epithelium. White asterisk marks β-gal and BrdU double-positive crypt cells. (F&G) Higher magnification of crypt regions in D&E. Solid white line demarks the epithelial-mesenchymal boundary. Dashed white line outlines the apical epithelial border. Counter-stained with Hoechst dye (blue). Bar = 25 μm.

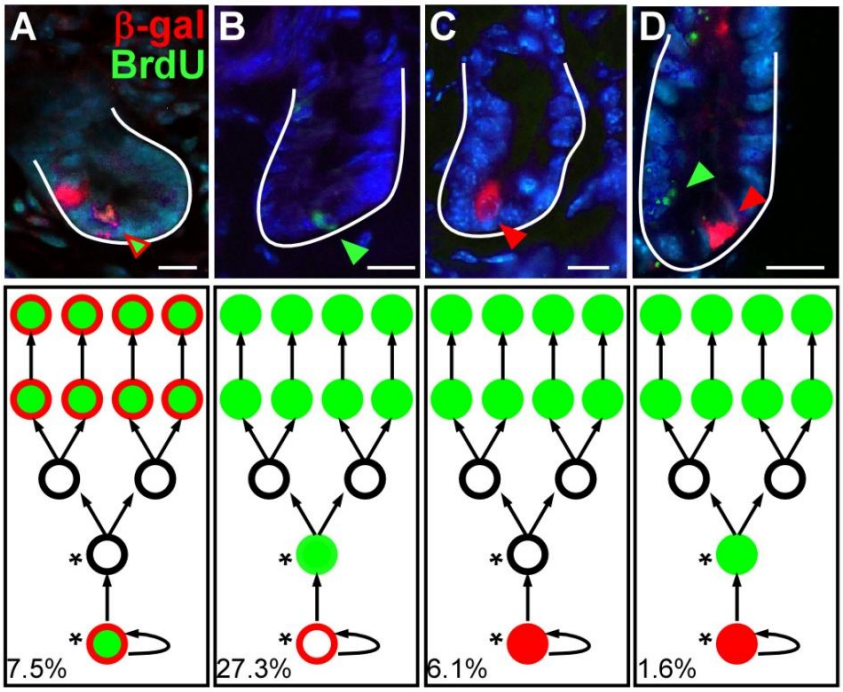

Figure A3.3. β-gal and BrdU co-staining scenarios. Wnt-reporter mouse intestines were injected with BrdU 2 days prior to analyses to assess the proliferative status of the β-gal positive crypt-based cells. (A) Approximately 7.5% of crypts contained a cell that was dual-labeled for β-gal and BrdU, reflecting cells that have been retained within the crypt (label-retaining cells) and that were Wnt-activated. (B) Approximately 27.3% of crypts contained a single BrdU-positive cell, possibly representing a "stem cell" that is not designated by the Wnt signaling pathway. This would be in line with the recently identified Bmi-1 positive stem cell. (C) 6.1% of crypts contained a single positive β-gal cell. This cell likely represents a cell that is activated by the Wnt signal after the effective BrdU labeling half-life in the animal. Finally, (D) a small percentage of crypts, 1.6%, contained a β-gal-positive cell and a BrdU-positive cell distinct from one another, likely representing a combination of the described scenarios. These scenarios are schematized in cartoon form beneath the corresponding fluorescent image that describes our perception of what each scenario may represent. In classical stem cell hierarchy, the lowest circle represents a progenitor cell residing near the base of the crypt and upper circles represent the progeny. Solid green circles represent BrdU-positive cells, solid red circles represent an activated Wnt cell, open red circles represent a cell that may have been Wnt-activated prior to BrdU labeling. These many different scenarios reflect the complex nature of the role of Wnt signaling on the stem cell hierarchy within the intestinal crypt.

To determine if Wnt-receiving crypt cells might share expression with stem or early progenitor cells, Wnt-reporter mouse intestines were stained with antibodies for a putative intestinal epithelial stem cell marker, Musashi-1 (Msi-1)(Kayahara, Sawada et al. 2003; Potten, Booth et al. 2003; He, Zhang et al. 2004). Although Msi-1 and β-gal co-localized (Figure A3.4A&B), the Msi-1 antibody displayed a broader staining pattern within the crypt, also encompassing the TA-cell population. DCAMKL-1 is an alternative putative stem cell marker(May, Riehl et al. 2008), however Wnt-activated cells did not co-express DCAMKL-1 (Figure A3.4C-E).

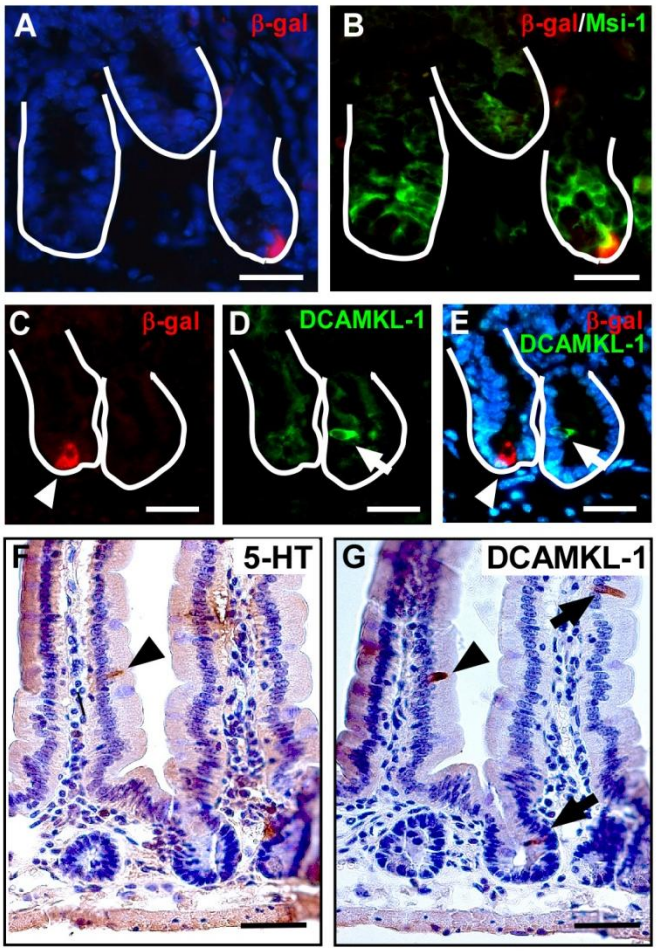

Figure A3.4. Characterization of putative stem cell markers in Wnt-activated cells. (A&B) The putative stem cell marker, Musashi-1 (Msi-1; green) had broad expression within the crypt and co-localized with crypt β-gal-expressing cells (red). (C-E) β-gal-positive cells (red) do not co-localize with another putative stem cell marker, DCAMKL1 (green). Solid white line marks the epithelial-mesenchymal boundary of the intestinal crypt. (F&G) DCAMKL-1 is expressed in a subset of enteroendocrine cells. Serial sections of mouse PSI were stained for serotonin (5-HT, an enteroendocrine marker; F) or DCAMKL-1 (G), a proposed intestinal stem cell marker. Arrowheads mark a single cell that co-labeled with both antibodies. Arrows mark DCAMKL-1-positive cells that do not express serotonin. Bar = 25 μm.

Progenitor cell populations are not the only residents within the intestinal crypt. In the small intestine, differentiated Paneth cells reside at the crypt base, and differentiating goblet and enteroendocrine cells are also scattered within the crypt. Interestingly, a recent study implicated Wnt signaling in Paneth cell differentiation(van Es, Jay et al. 2005). To determine if Ki67-negative/β-gal-positive cells were differentiated cells that resided at the crypt base(Cheng 1974), we stained Wnt-reporter mouse intestines with antibodies raised against epithelial differentiation markers. Co-localization of β-gal and the lectin, UEA-1, a dual goblet and Paneth cell marker, revealed that approximately 40.7% of the β-gal-positive cells possessed overlapping Paneth cell expression (Figure A3.5A-C; arrowhead), while 59.3% were distinct from Paneth cells (Figure A3.5A-C; arrow). Further, dual-labeling with antibodies to β-gal and cryptidin, a Paneth cell-specific marker, revealed similar findings (Figure 5D-F). It is possible that Wnt-activated, differentiated Paneth cells that retain β-gal protein are progeny from a Wnt-activated stem cell in a similar fashion as the β-gal-positive villus epithelial cells. Additionally, β-gal-positive cells were distinct from enteroendocrine cells when tissue sections were co-stained for the serotonin marker 5-HT (Figure A3.5G-I), and distinct from crypt-based goblet cells (data not shown).

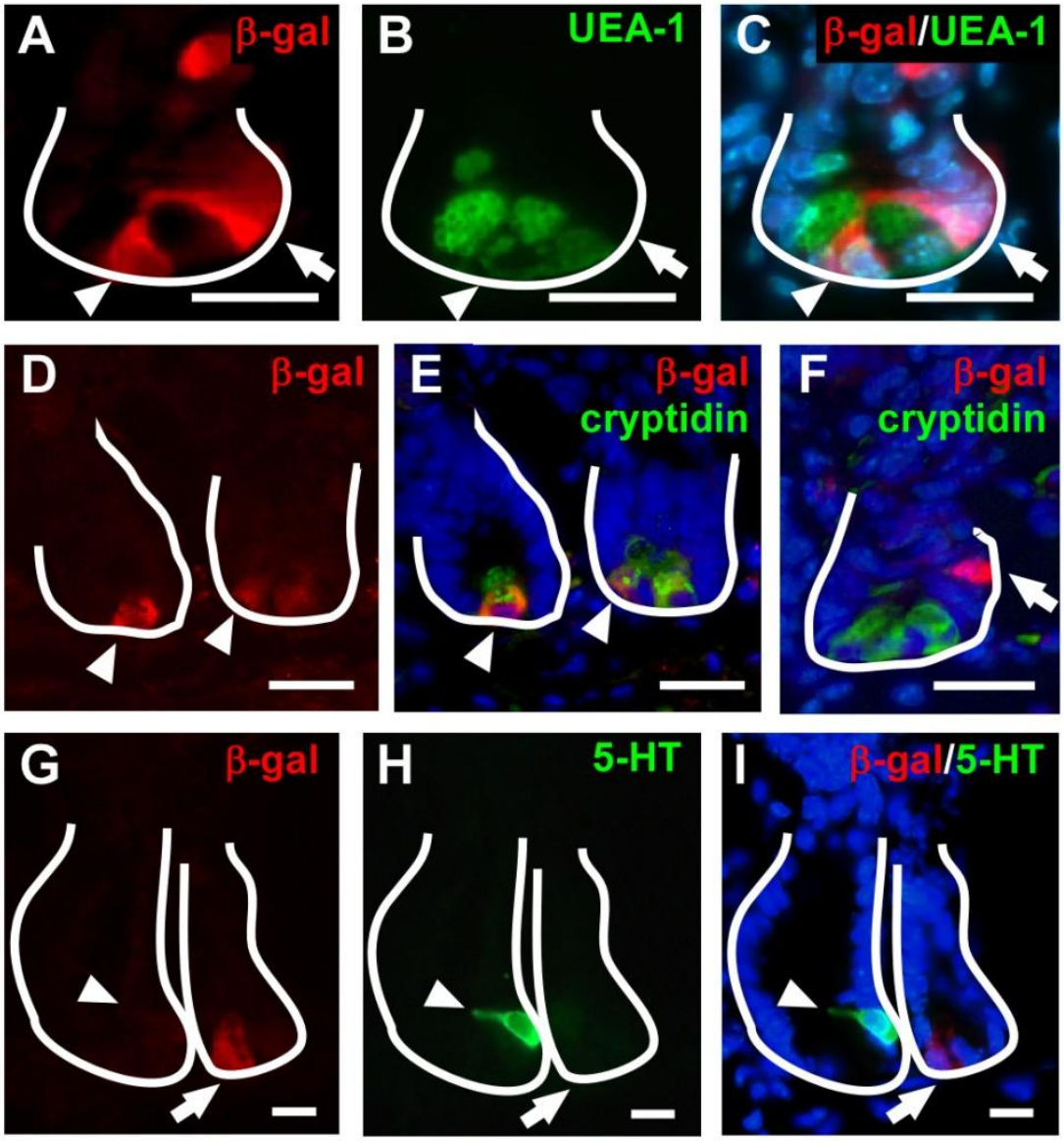

Figure A3.5 Characterization of epithelial differentiation markers in Wnt-activated cells. **(**A-C) Co-incubation of antibodies to β-gal (red) and UEA-1 (green), a lectin to mark Paneth and goblet cells, identifies distinct Wnt-activated cells (arrow) and overlapping expression (arrowhead). (D-F) Similar results are observed for the Paneth-cell-specific marker, cryptidin (green) when co-stained with β-gal (red). (G-I) Co-localization is not observed with dual staining of β-gal (red) and the enteroendocrine marker serotonin (5-HT; green). Solid white line marks the epithelial-mesenchymal boundary of the intestinal crypt. Bar = 25 μm.

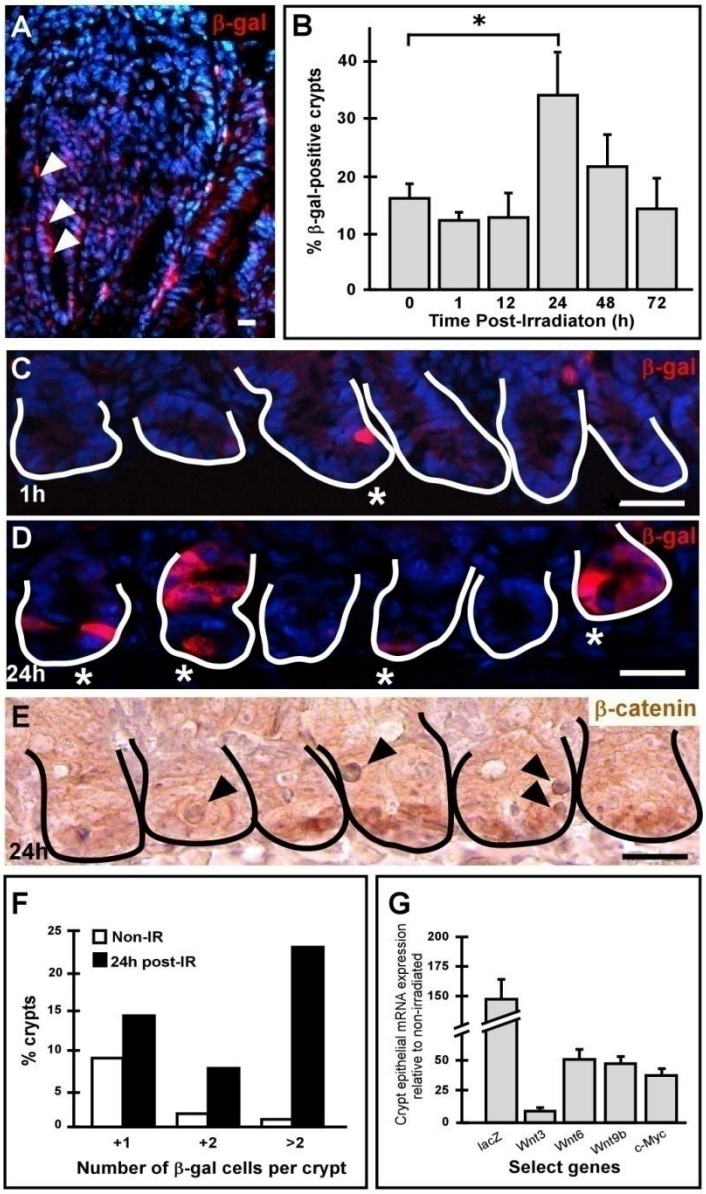
A
β-gal
B
*
% β-gal-positive crypts
40
30
20
10
0
0
1
12
24
48
72
Time Post-Irradiaton (h)
C
β-gal
1h
*
D
β-gal
24h
*
*
*
*
E
β-catenin
24h
F
Non-IR
24h post-IR
% crypts
25
20
15
10
5
0
+1
+2
>2
Number of β-gal cells per crypt
G
Crypt epithelial mRNA expression relative to non-irradiated
200
175
150
50
25
0
lacZ
Wnt3
Wnt6
Wnt9b
c-Myc
Select genes

Figure A3.6 Wnt activity increases after γ-irradiation. (A) An increased number of Wnt-activated cells are detected in an intestinal adenoma from a progeny of a BAT-Gal and Apc^{MIN} mouse mating. β-gal-positive cells are in red (arrows). Wnt signaling is stimulated in response to gamma-irradiation-induced injury. (B) Intestinal tissue sections from lethally irradiated TOPGAL mice harvested at various timepoints were stained with antibodies to β-gal (red) and quantified. At 24 h post-irradiation, the number of crypts harboring Wnt-receiving cells significantly increased (p = 0.004; asterisk) relative to non-irradiated controls. (C&D) Comparison of representative intestinal tissue sections from lethally irradiated TOPGAL mice stained with antibodies to β-gal (red) and counterstained with Hoechst dye (blue) at 1 h post-irradiation (C) and 24 h post-irradiation (D). (E) Wild type mice, 24 h post-irradiation, were examined with antibodies to β-catenin (brown) and counterstained with Hematoxylin (purple). Solid line marks the epithelial-mesenchymal boundary of the intestinal crypts. At 1 h post-irradiation, the number of β-gal-expressing cells was similar to the 0h control, but increased in 24 h post-irradiated tissues. Asterisks denote β-gal or nuclear β-catenin positive crypts; black arrowheads denote apoptotic cells. Bar = 25 μm. (F) The number of β-gal-positive cells per crypt was scored in both non-irradiated (Non-IR) and 24 h post-irradiated (post-IR) intestines. The percentage of crypts with 1, 2 or greater than 2 β-gal-positive cells are shown. (G) qRT-PCR performed on mRNA from small intestinal crypt fractions of TOPGAL mice 24 h post-irradiation revealed an increase in the *lacZ* reporter gene compared to non-irradiated samples. In addition, three Wnt ligands known to be expressed in the intestinal epithelium (*Wnt3*, *Wnt6*, and *Wnt9b*) and a Wnt target gene (*c-Myc*) increased in response to the irradiation stimulus.

Wnt-reporter mouse intestine responded to physiologic increase in Wnt signaling.

In some intestinal diseases, such as colorectal cancer, the Wnt signaling pathway is aberrantly stimulated in epithelial cells resulting in uncontrolled hyperproliferation. This establishes a role for Wnt signaling in epithelial proliferation and highlights the importance of the Wnt signal in maintaining epithelial homeostasis. It has previously been shown, and we demonstrate here, that BAT-Gal reporter mice display an increase in Wnt signaling readout when crossed to tumor-forming Apc^{MIN} mice that overstimulate the Wnt pathway(Maretto, Cordenonsi et al. 2003) (Figure A3.6A). To investigate if the Wnt-reporter mice are useful tools for increased Wnt signaling readout during tissue repair after injury, we examined the reporter response to intestinal gamma-irradiation exposure, which is known to stimulate an epithelial proliferative response.

Exposure to gamma-irradiation elicits massive crypt cell apoptosis, coincident with proliferative changes that peak within the first 24 hours (Potten 1990). To determine if activation of Wnt signaling is important in a regenerative response and if it can be monitored in a Wnt-reporter mouse, we subjected TOPGAL mice to 12Gy of gamma-irradiation. Intestinal tissues were processed and analyzed 1, 12, 24, 48, and 72h after irradiation (Figure A3.6B). At 1h post-irradiation, the intestinal epithelium appeared relatively normal. Wnt-responsive cells, as detected by protein levels, were still present in low numbers in the crypts of the PSI (Figure A3.6B&C). However, by 24h post-irradiation, near the peak of

the apoptotic response, a significant increase in the number of crypts with Wnt-receiving cells was detected (p = 0.004, Figure A3.6B,D,E). Additionally, we observed more Wnt-receiving cells per crypt (Figure A3.6D-F) compared to non-irradiated controls (Figure A3.1A) or to the 1h post-irradiation time point (Figure A3.6C). The most striking increase was represented by β-gal-positive crypts harboring greater than two Wnt-activated cells (Figure A3.6F). The Wnt response returned to non-irradiated, homeostatic levels by 72h (Figure A3.6B).

Interestingly, the increase in Wnt-receiving cells paralleled an increase in β-gal/Ki67 double-positive cells (data not shown). While the majority of Ki67-positive cells remained β-gal-negative, dual β-gal and Ki67-positive cells increased approximately 3-fold (from 7.1% to 23.1%). This double-positive population may represent an actively dividing stem cell or immediate progeny from a newly divided progenitor cell.

To correlate increased Wnt responsiveness to gamma-irradiation, the mRNA expression levels of the three endogenous epithelial Wnt ligands were determined(Gregorieff, Pinto et al. 2005). Crypt epithelium from 24h post-irradiation and non-irradiated TOPGAL intestines was isolated and characterized for changes in Wnt ligand expression (Figure A3.6G). Reporter *lacZ* mRNA expression was elevated in response to gamma-irradiation exposure by ~148-fold in the crypt epithelium. Consistent with this observation, increased expression of the Wnt target gene *c-Myc* was observed (34-fold). Additionally, the canonical Wnt ligands *Wnt3*, *Wnt6*, and *Wnt9b* were also elevated by 10-, 51- and 50-fold respectively. Further, the mRNA expression of the secreted frizzled

protein 2 (*sFrp2*), a Wnt inhibitor, decreased from levels higher than the Wnt ligands at steady state, to undetectable levels in response to gamma-irradiation (data not shown). This data suggests that induced injury to the epithelium results in detectable changes in Wnt signaling that can be appreciated in the Wnt-reporter mouse.

Discussion

While it is well established that Wnt signaling controls intestinal epithelial proliferation and homeostasis, the distinction between the role of Wnt as a direct regulator of both the crypt-based stem cell and TA-cell populations has not been firmly established(Kinzler and Vogelstein 1996; Korinek, Barker et al. 1998; Bienz and Clevers 2000; Pinto, Gregorieff et al. 2003; Kuhnert, Davis et al. 2004). Further, aberrant Wnt signaling has been described as a proliferative stimulus in intestinal disease states such as colorectal cancer(Kinzler and Vogelstein 1996) but a role for the pathway in epithelial regeneration after injury has not been defined. Here we examined the pattern of Wnt-activated cells in the normal mouse intestine during homeostasis and after irradiation-induced injury. Further, we characterize intestinal expression of the Wnt-reporter mouse and show that it is a useful tool in both monitoring Wnt signaling during homeostasis and in response to an epithelial-induced injury.

In both TOPGAL and BAT-Gal mouse intestines, Wnt-activated cells, as identified by Wnt-reporter expression, were primarily confined to the epithelial compartment. In the small intestine, two crypt-based patterns were observed. The majority of small intestinal crypts harbored one or two β-gal-positive cells

detected by both protein and RNA localization. In a minority of crypts the entire crypt population was positive for β-gal protein expression that extended onto the adjacent villus. Additionally β-gal-positive cells were observed on villi that were associated with crypts containing single β-gal-positive cells. However, villus protein expression was not recapitulated with RNA expression profiling using *in situ* hybridization for *lacZ* on tissue sections or by qRT-PCR for *lacZ* expression in isolated crypt and villus epithelial cell populations. Together this suggests that Wnt-reporter expression on the villus was a manifestation of the long half-life of the β-gal protein(Bachmair, Finley et al. 1986). The unique ability to track both protein and RNA expression in the Wnt-reporter mouse provides the power to analyze both lineage tracing (protein) and an identification of the Wnt-activated cell (RNA) within the same model system.

To corroborate that the Wnt-reporter provided a consistent Wnt-activated cell readout, antibody staining to detect cells harboring nuclear localized β-catenin was performed. Consistent with the frequency of β-gal-positive cells, a similar percentage of PSI crypts harbored one or two cells near the crypt base that stained positive for nuclear β-catenin. These data suggest that only a small number of cells within certain crypts were actively receiving a Wnt signal.

Interestingly, but consistent with the observed decreasing gradient of epithelial cell turnover rates down the length of the intestine, a greater number of Wnt-activated cells were observed in the PSI (15.2% of crypts harbored at least one β-gal-positive cell) as compared to the colon (0.8%). Similarly, Bmi1-positive putative stem cells also display a gradient down the length of the intestine, with

greater numbers in the PSI and nearly undetectable levels in the distal small intestine(Sangiorgi and Capecchi 2008).

While it is widely accepted that Wnt signaling influences proliferation in all crypts, the number of Wnt-activiated cells detected in Wnt-reporter mouse intestines was lower than expected. There are several possibilities to explain this discrepancy. It is possible that the Wnt morphogen acts in a gradient highest in the base of the crypt and highest in the PSI with decreasing concentration down the length of the intestine. In this scenario, it is possible that only the highest levels of Wnt-activated cells are detected in the Wnt-reporter mice. Dilution of the protein as cells divide and migrate up the villus is therefore only detected in intestinal regions with the highest levels of Wnt activation. Presence of β-gal-positive villus cells may therefore identify regions of the intestine with robust Wnt signaling.

Some reports suggest a higher level of nuclear localized β-catenin in the crypt base than we show here(Batlle, Henderson et al. 2002; van de Wetering, Sancho et al. 2002). Although believed to be a gold standard, comparing nuclear β-catenin with Wnt-activated cells could be misleading. Some cancer cells display high levels of nuclear β-catenin in the absence of Wnt activity (Kiely, O'Donovan et al. 2007). The mechanism for this in cancer is unclear, although there are known inhibitors of nuclear localized β-catenin that inhibit Wnt activation by binding to β-catenin within the nucleus, including Apc, Chibby and Duplin (Sakamoto, Kishida et al. 2000; Takemaru, Yamaguchi et al. 2003; Sierra, Yoshida et al. 2006).

Despite the decreasing gradient of detectable Wnt signal down the length of the intestine, there remains an important physiologic role of Wnt signaling in colonic homeostasis. It was recently reported that the Wnt target gene and putative stem cell marker, Lgr5, is located in base of both small intestinal and colonic crypts (Barker, van Es et al. 2007). An alternative explanation for the proximal to distal gradient of detectable Wnt-activated cells could be that Wnt signaling in the colonic epithelium is regulated differently than in the small intestine. There are differences in expression of the Tcf/Lef-1 family members between the two regions(Korinek, Barker et al. 1998) and therefore it is likely that other regulatory factors may convey differences in colonic Wnt activity. Due to these caveats in tracking Wnt-activated cells using other approaches, Wnt-reporter mice offer a powerful and direct approach for identifying Wnt-activated cells.

Wnt-receiving intestinal cells represent a progenitor population.

The rarity of single β-gal-positive and nuclear β-catenin-positive cells in the base of the crypt suggests that these Wnt-receiving cells may be a progenitor cell population. Therefore, to further characterize the proliferative status of the β-gal-positive cells, we surveyed intestinal sections with antibodies to Ki67 and β-gal. The majority of Ki67-positive cells were located mid-crypt in the TA-cell region and were negative for β-gal, thus not Wnt-activated. This suggests that Wnt signaling is not a general proliferative stimulant. Supportive of this observation, cells containing nuclear β-catenin were also not located within the

proliferative TA-cell population, consistent with previous data from both the small intestine or colon(Batlle, Henderson et al. 2002; van de Wetering, Sancho et al. 2002). Further, TA-cells have been shown to lack expression of a previously described Wnt-target gene, Lgr5, that marks a columnar crypt-based proposed stem cell(Barker, van Es et al. 2007). This suggests that a second pathway may regulate proliferation of the TA-cell population. Recent evidence shows that the polycomb protein Bmi1, regulated in a Wnt-independent fashion, marks a putative intestinal stem cell population residing at “cell position +4” within the crypt(Sangiorgi and Capecchi 2008). Bmi1-expressing cells display a unique pattern from Lgr5-positive cells in the intestinal crypt(Barker, van Es et al. 2007). These markers identify a population of “stem cells” with different kinetics, suggesting a more complex regulation of the intestinal stem cell hierarchy(Batlle 2008).

We observed that a portion of Ki67-positive cells were also β-gal positive. This represented 7.1% of all crypt-based β-gal positive cells and may possibly represent the stem cell or an early progenitor. We examined co-expression of β-gal with a putative stem cell marker, Msi-1. Even though the majority of β-gal-positive cells co-stained with this putative stem cell marker, Msi-1 displayed a broader pattern of expression that extended into the TA-cell region. While it is controversial whether or not Msi-1 is a true stem cell marker in the intestine, it may be expressed in a gradient including stem cells and their immediate descendents(Potten, Booth et al. 2003, Kayahara, 2003 #44; Topol, Jiang et al. 2003). Despite this, co-localization of β-gal and Msi-1 supports the idea that Wnt-

activated cells could represent progenitor cells. Interestingly, DCAMKL-1, a second putative stem cell marker(May, Riehl et al. 2008), did not co-localize with β-gal positive cells. It is likely that DCAMKL-1 marks a lineage progenitor for enteroendocrine cells, as it is also expressed on the villus epithelium in a similar pattern with serotonin, an enteroendocrine cell marker (Figure 4F&G). Additionally, the putative stem cell marker, Lgr5, is reported to have an mRNA expression pattern encompassing a greater number of crypt cells and more total crypts(Barker, van Es et al. 2007) than the profile of Wnt-activated cells we show here. The overt discrepancy in staining patterns of the putative stem cell markers highlights the current dearth of tools available for pinpointing the intestinal stem cell in vivo.

We also observed a population of Ki67-negative, β-gal-positive cells. These cells might represent quiescent stem cells or the differentiated progeny of a Wnt-activated progenitor cell. Therefore, we performed double staining with β-gal and select antibodies for differentiated cell lineages. β-gal-positive cells did not express differentiation markers for goblet or enteroendocrine cells. Although a majority of the Paneth cells did not express β-gal (98.7%), a small subset was β-gal-positive. The presence of these double positive cells support the previously reported role for Wnt signaling in retaining Paneth cells to the crypt base(van Es, Jay et al. 2005). Alternatively, these β-gal-positive Paneth cells could be recent descendents of an activated progenitor, as we show for differentiated epithelial cells (Figures A3.1C and A3.2D&E), highlighting the usefulness of protein detection for lineage tracing in this model system. Despite the role of Wnt

signaling within the differentiated Paneth cell population, the majority of crypt-based β-gal-positive cells did not express differentiated cell markers (59.3%). Therefore, it is likely that these Wnt-activated cells represent a progenitor pool.

There is an emerging view of a more complex intestinal stem cell hierarchy with multiple pools of progenitor populations. In the absence of an intestinal reconstitution assay to validate Wnt-dependent and Wnt-independent putative stem cell pools, we cannot functionally determine the relationship of Wnt-activated cells within the hierarchy. It is likely that β-gal and nuclear β-catenin expression may be present in only a subset of stem cells. Additionally, quiescent stem cells might not express β-gal, nuclear β-catenin, Lgr5 or Bmi1. Despite these caveats, our data suggested a limited number of Wnt-activated cells within intestinal crypts and is consistent with a role for a Wnt signal in a progenitor pool.

Wnt-reporter response to gamma-irradiation-induced injury.

To determine if a Wnt signal was elicited in response to epithelial injury, we examined intestinal Wnt activation after gamma-irradiation. Upon exposure to gamma-irradiation, analyses of Wnt-reporter mice revealed an appreciable increase in both the number of crypts harboring Wnt-activated cells, as well as an increase in the total number of Wnt-activated cells per crypt. This observation was verified at the RNA level, demonstrating that irradiation-induced injury elicited an intestinal Wnt response. To confirm this increase in intestinal Wnt signaling, we surveyed for expression of a number of Wnt pathway genes in

isolated epithelial crypt cells using qRT-PCR. An increase in *lacZ* was accompanied by increases in the three canonical Wnt ligands reported to be expressed in the crypt epithelium (*Wnt3*, *Wnt6*, *Wnt9b*) and the downstream target *c-Myc*. Further, a decrease in the secreted Wnt inhibitor (*sFrp2*) was observed. This demonstrated that physiological intestinal damage can be appreciated using a Wnt-reporter mouse.

Conclusions

Our data provide a carefully detailed analysis of endogenous Wnt signaling in the intestine of Wnt-reporter mice and corroborates reporter expression with nuclear β-catenin staining. Wnt-activated cells are predominantly located in the base of the crypt where a progenitor population and differentiated Paneth cells reside. This expression pattern is consistent with reported roles for Wnt signaling in maintaining a stem cell pool and in Paneth cell differentiation.

We demonstrate that the Wnt-reporter mouse can be used for *in vivo* analyses of both lineage tracing by detection of protein expression using immunohistochemistry and identification of Wnt-activated cell populations by reporter RNA expression. Importantly, our studies validate the use of the Wnt-reporter mouse (TOPGAL and BAT-Gal) for detection of *in vivo* manipulation of Wnt signaling in response to intestinal epithelial injury.

References

(2008). Cancer Facts & Figures 2008. Atlanta, American Cancer Society.

Abkowitz, J. L., A. E. Robinson, et al. (2003). "Mobilization of hematopoietic stem cells during homeostasis and after cytokine exposure." *Blood* **102**(4): 1249-53.

Akashi, K., D. Traver, et al. (2000). "A clonogenic common myeloid progenitor that gives rise to all myeloid lineages." *Nature* **404**(6774): 193-7.

Albor, A. and M. Kulesz-Martin (2007). "Novel initiation genes in squamous cell carcinomagenesis: a role for substrate-specific ubiquitylation in the control of cell survival." *Mol Carcinog* **46**(8): 585-90.

Al-Hajj, M., M. S. Wicha, et al. (2003). "Prospective identification of tumorigenic breast cancer cells." *Proc Natl Acad Sci U S A* **100**(7): 3983-8.

Alvarez-Dolado, M., R. Pardal, et al. (2003). "Fusion of bone-marrow-derived cells with Purkinje neurons, cardiomyocytes and hepatocytes." *Nature* **425**(6961): 968-73.

Anderson, D. A., Y. Wu, et al. (2005). "Donor marker infidelity in transgenic hematopoietic stem cells." *Stem Cells* **23**(5): 638-43.

Arai, F., O. Ohneda, et al. (2002). "Mesenchymal stem cells in perichondrium express activated leukocyte cell adhesion molecule and participate in bone marrow formation." *J Exp Med* **195**(12): 1549-63.

Artis, D. (2008). "Epithelial-cell recognition of commensal bacteria and maintenance of immune homeostasis in the gut." *Nat Rev Immunol* **8**(6): 411-20.

Azad Khan, A. K., J. Piris, et al. (1977). "An experiment to determine the active therapeutic moiety of sulphasalazine." *Lancet* **2**(8044): 892-5.

Azuma, H., N. Paulk, et al. (2007). "Robust expansion of human hepatocytes in Fah-/-/Rag2-/-/Il2rg-/- mice." *Nat Biotechnol* **25**(8): 903-10.

Bachmair, A., D. Finley, et al. (1986). "In vivo half-life of a protein is a function of its amino-terminal residue." *Science* **234**(4773): 179-86.

Backhed, F., R. E. Ley, et al. (2005). "Host-bacterial mutualism in the human intestine." *Science* **307**(5717): 1915-20.

Baeg, G. H., A. Matsumine, et al. (1995). "The tumour suppressor gene product APC blocks cell cycle progression from G0/G1 to S phase." *Embo J* **14**(22): 5618-25.

Bailey, A. S., H. Willenbring, et al. (2006). "Myeloid lineage progenitors give rise to vascular endothelium." *Proc Natl Acad Sci U S A* **103**(35): 13156-61.

Barker, N., J. H. van Es, et al. (2007). "Identification of stem cells in small intestine and colon by marker gene Lgr5." *Nature* **449**(7165): 1003-7.

Barker, N., M. van de Wetering, et al. (2008). "The intestinal stem cell." *Genes Dev* **22**(14): 1856-64.

Batlle, E., J. T. Henderson, et al. (2002). "Beta-catenin and TCF mediate cell positioning in the intestinal epithelium by controlling the expression of EphB/ephrinB." *Cell* **111**(2): 251-63.

Batlle, E. (2008). "A new identity for the elusive intestinal stem cell." *Nat Genet* **40**(7): 818-9.

Battaile, K. P., R. L. Bateman, et al. (1999). "In vivo selection of wild-type hematopoietic stem cells in a murine model of Fanconi anemia." *Blood* **94**(6): 2151-8.

Baumgart, D. C. and S. R. Carding (2007). "Inflammatory bowel disease: cause and immunobiology." *Lancet* **369**(9573): 1627-40.

Berg, D. J., N. Davidson, et al. (1996). "Enterocolitis and colon cancer in interleukin-10-deficient mice are associated with aberrant cytokine production and CD4(+) TH1-like responses." *J Clin Invest* **98**(4): 1010-20.

Bernstein, C. N., J. F. Blanchard, et al. (2001). "Cancer risk in patients with inflammatory bowel disease: a population-based study." *Cancer* **91**(4): 854-62.

Betschinger, J., K. Mechtler, et al. (2003). "The Par complex directs asymmetric cell division by phosphorylating the cytoskeletal protein Lgl." *Nature* **422**(6929): 326-30.

Betschinger, J., K. Mechtler, et al. (2006). "Asymmetric segregation of the tumor suppressor brat regulates self-renewal in Drosophila neural stem cells." *Cell* **124**(6): 1241-53.

Bienz, M. and H. Clevers (2000). "Linking colorectal cancer to Wnt signaling." *Cell* **103**(2): 311-20.

Bilder, D. (2004). "Epithelial polarity and proliferation control: links from the Drosophila neoplastic tumor suppressors." *Genes Dev* **18**(16): 1909-25.

Bjerknes, M. and H. Cheng (1999). "Clonal analysis of mouse intestinal epithelial progenitors." *Gastroenterology* **116**(1): 7-14.

Blanpain, C., V. Horsley, et al. (2007). "Epithelial stem cells: turning over new leaves." *Cell* **128**(3): 445-58.

Booth, C. and C. S. Potten (2000). "Gut instincts: thoughts on intestinal epithelial stem cells." *J Clin Invest* **105**(11): 1493-9.

Boulay, J. L., U. Stiefel, et al. (2009). "Loss of heterozygosity of TRIM3 in malignant gliomas." *BMC Cancer* **9**: 71.

Bowen, M. A., D. D. Patel, et al. (1995). "Cloning, mapping, and characterization of activated leukocyte-cell adhesion molecule (ALCAM), a CD6 ligand." *J Exp Med* **181**(6): 2213-20.

Bowman, S. K., R. A. Neumuller, et al. (2006). "The Drosophila NuMA Homolog Mud regulates spindle orientation in asymmetric cell division." *Dev Cell* **10**(6): 731-42.

Bowman, S. K., V. Rolland, et al. (2008). "The tumor suppressors Brat and Numb regulate transit-amplifying neuroblast lineages in Drosophila." *Dev Cell* **14**(4): 535-46.

Brazelton, T. R., F. M. Rossi, et al. (2000). "From marrow to brain: expression of neuronal phenotypes in adult mice." *Science* **290**(5497): 1775-9.

Bruder, S. P., N. S. Ricalton, et al. (1998). "Mesenchymal stem cell surface antigen SB-10 corresponds to activated leukocyte cell adhesion molecule and is involved in osteogenic differentiation." *J Bone Miner Res* **13**(4): 655-63.

Bunster, E. and R. K. Meyer (1933). "An improved method of parabiosis." *Anat. Rec.* **57**: 339-343.

Burkhardt, M., E. Mayordomo, et al. (2006). "Cytoplasmic overexpression of ALCAM is prognostic of disease progression in breast cancer." *J Clin Pathol* **59**(4): 403-9.

Cakraborty, A. K., J. Pawelek, et al. (2001). "Fusion hybrids with macrophage and melanoma cells up-regulate N-acetylglucosaminyltransferase V, beta1-6 branching, and metastasis." *Cell Growth Differ* **12**(12): 623-30.

Camargo, F. D., M. Finegold, et al. (2004). "Hematopoietic myelomonocytic cells are the major source of hepatocyte fusion partners." *J Clin Invest* **113**(9): 1266-70.

Camargo, F. D., R. Green, et al. (2003). "Single hematopoietic stem cells generate skeletal muscle through myeloid intermediates." *Nat Med* **9**(12): 1520-7.

Caussinus, E. and C. Gonzalez (2005). "Induction of tumor growth by altered stem-cell asymmetric division in Drosophila melanogaster." *Nat Genet* **37**(10): 1125-9.

Cayrol, R., K. Wosik, et al. (2008). "Activated leukocyte cell adhesion molecule promotes leukocyte trafficking into the central nervous system." *Nat Immunol* **9**(2): 137-45.

Chakraborty, A., R. Lazova, et al. (2004). "Donor DNA in a renal cell carcinoma metastasis from a bone marrow transplant recipient." *Bone Marrow Transplant* **34**(2): 183-6.

Chakraborty, A. K., J. de Freitas Sousa, et al. (2001). "Human monocyte x mouse melanoma fusion hybrids express human gene." *Gene* **275**(1): 103-6.

Chen, E. H., E. Grote, et al. (2007). "Cell-cell fusion." *FEBS Lett* **581**(11): 2181-93.

Chen, E. H. and E. N. Olson (2005). "Unveiling the mechanisms of cell-cell fusion." *Science* **308**(5720): 369-73.

Cheng, H., J. Merzel, et al. (1969). "Renewal of Paneth cells in the small intestine of the mouse." *Am J Anat* **126**(4): 507-25.

Cheng, H. (1974). "Origin, differentiation and renewal of the four main epithelial cell types in the mouse small intestine. IV. Paneth cells." *Am J Anat* **141**(4): 521-35.

Cheroutre, H. and L. Madakamutil (2004). "Acquired and natural memory T cells join forces at the mucosal front line." *Nat Rev Immunol* **4**(4): 290-300.

Cho, R. W. and M. F. Clarke (2008). "Recent advances in cancer stem cells." *Curr Opin Genet Dev* **18**(1): 48-53.

Coffman, R. L. (1982). "Surface antigen expression and immunoglobulin gene rearrangement during mouse pre-B cell development." *Immunol Rev* **69**: 5-23.

Corbel, C., F. Cormier, et al. (1992). "BEN, a novel surface molecule of the immunoglobulin superfamily on avian hemopoietic progenitor cells shared with neural cells." *Exp Cell Res* **203**(1): 91-9.

Corbel, S. Y., A. Lee, et al. (2003). "Contribution of hematopoietic stem cells to skeletal muscle." *Nat Med* **9**(12): 1528-32.

Coussens, L. M. and Z. Werb (2002). "Inflammation and cancer." *Nature* **420**(6917): 860-7.

Crosnier, C., D. Stamataki, et al. (2006). "Organizing cell renewal in the intestine: stem cells, signals and combinatorial control." *Nat Rev Genet* **7**(5): 349-59.

Dalerba, P., S. J. Dylla, et al. (2007). "Phenotypic characterization of human colorectal cancer stem cells." *Proc Natl Acad Sci U S A* **104**(24): 10158-63.

DasGupta, R. and E. Fuchs (1999). "Multiple roles for activated LEF/TCF transcription complexes during hair follicle development and differentiation." *Development* **126**(20): 4557-68.

Davies, P. S., A. D. Dismuke, et al. (2008). "Wnt-reporter expression pattern in the mouse intestine during homeostasis." *BMC Gastroenterol* **8**: 57.

Davies, P. S., A. E. Powell, et al. (2009). "Inflammation and proliferation act together to mediate intestinal cell fusion." *PLoS One* **4**(8): e6530.

Degen, W. G., L. C. van Kempen, et al. (1998). "MEMD, a new cell adhesion molecule in metastasizing human melanoma cell lines, is identical to ALCAM (activated leukocyte cell adhesion molecule)." *Am J Pathol* **152**(3): 805-13.

Deyoung, M. P. and L. W. Ellisen (2007). "p63 and p73 in human cancer: defining the network." *Oncogene* **26**(36): 5169-83.

Dikovskaya, D., D. Schiffmann, et al. (2007). "Loss of APC induces polyploidy as a result of a combination of defects in mitosis and apoptosis." *J Cell Biol* **176**(2): 183-95.

Dionne, S., J. Hiscott, et al. (1997). "Quantitative PCR analysis of TNF-alpha and IL-1 beta mRNA levels in pediatric IBD mucosal biopsies." *Dig Dis Sci* **42**(7): 1557-66.

Doe, C. Q. (2008). "Neural stem cells: balancing self-renewal with differentiation." *Development* **135**(9): 1575-87.

Duelli, D. and Y. Lazebnik (2003). "Cell fusion: a hidden enemy?" *Cancer Cell* **3**(5): 445-8.

Duerkop, B. A., S. Vaishnava, et al. (2009). "Immune responses to the microbiota at the intestinal mucosal surface." *Immunity* **31**(3): 368-76.

Duesberg, P. and R. Li (2003). "Multistep carcinogenesis: a chain reaction of aneuploidizations." *Cell Cycle* **2**(3): 202-10.

Duncan, A. W., R. D. Hickey, et al. (2009). "Ploidy reductions in murine fusion-derived hepatocytes." *PLoS Genet* **5**(2): e1000385.

Dylla, S. J., L. Beviglia, et al. (2008). "Colorectal cancer stem cells are enriched in xenogeneic tumors following chemotherapy." *PLoS ONE* **3**(6): e2428.

Eaden, J. A., K. R. Abrams, et al. (2001). "The risk of colorectal cancer in ulcerative colitis: a meta-analysis." *Gut* **48**(4): 526-35.

Falk, P. G., L. V. Hooper, et al. (1998). "Creating and maintaining the gastrointestinal ecosystem: what we know and need to know from gnotobiology." *Microbiol Mol Biol Rev* **62**(4): 1157-70.

Ferrari, G., G. Cusella-De Angelis, et al. (1998). "Muscle regeneration by bone marrow-derived myogenic progenitors." *Science* **279**(5356): 1528-30.

Fleming, E. S., M. Zajac, et al. (2007). "Planar spindle orientation and asymmetric cytokinesis in the mouse small intestine." *J Histochem Cytochem* **55**(11): 1173-80.

Fre, S., M. Huyghe, et al. (2005). "Notch signals control the fate of immature progenitor cells in the intestine." *Nature* **435**(7044): 964-8.

Godfrey, D. I., J. Kennedy, et al. (1994). "Onset of TCR-beta gene rearrangement and role of TCR-beta expression during CD3-CD4-CD8- thymocyte differentiation." *J Immunol* **152**(10): 4783-92.

Goldenberg, D. M. (1968). "[On the progression of malignity: a hypothesis]." *Klin Wochenschr* **46**(16): 898-9.

Gonzalez, C. (2007). "Spindle orientation, asymmetric division and tumour suppression in Drosophila stem cells." *Nat Rev Genet* **8**(6): 462-72.

Gordon, H. A. (1959). "Morphological and physiological characterization of germfree life." *Ann N Y Acad Sci* **78**: 208-20.

Gordon, M. D. and R. Nusse (2006). "Wnt signaling: multiple pathways, multiple receptors, and multiple transcription factors." *J Biol Chem* **281**(32): 22429-33.

Gregorieff, A. and H. Clevers (2005). "Wnt signaling in the intestinal epithelium: from endoderm to cancer." *Genes Dev* **19**(8): 877-90.

Gregorieff, A., D. Pinto, et al. (2005). "Expression pattern of Wnt signaling components in the adult intestine." *Gastroenterology* **129**(2): 626-38.

Grifoni, D., F. Garoia, et al. (2004). "The human protein Hugl-1 substitutes for Drosophila lethal giant larvae tumour suppressor function in vivo." *Oncogene* **23**(53): 8688-94.

Grifoni, D., F. Garoia, et al. (2007). "aPKCzeta cortical loading is associated with Lgl cytoplasmic release and tumor growth in Drosophila and human epithelia." *Oncogene* **26**(40): 5960-5.

Groden, J., A. Thliveris, et al. (1991). "Identification and characterization of the familial adenomatous polyposis coli gene." *Cell* **66**(3): 589-600.

Guy-Grand, D., N. Cerf-Bensussan, et al. (1991). "Two gut intraepithelial CD8+ lymphocyte populations with different T cell receptors: a role for the gut epithelium in T cell differentiation." *J Exp Med* **173**(2): 471-81.

Haegebarth, A. and H. Clevers (2009). "Wnt signaling, lgr5, and stem cells in the intestine and skin." *Am J Pathol* **174**(3): 715-21.

Hardwick, J. C., L. L. Kodach, et al. (2008). "Bone morphogenetic protein signalling in colorectal cancer." *Nat Rev Cancer* **8**(10): 806-12.

Hanson, C. A. and J. R. Miller (2005). "Non-traditional roles for the Adenomatous Polyposis Coli (APC) tumor suppressor protein." *Gene* **361**: 1-12.

Harris, H., O. J. Miller, et al. (1969). "Suppression of malignancy by cell fusion." *Nature* **223**(5204): 363-8.

Hassan, N. J., A. N. Barclay, et al. (2004). "Frontline: Optimal T cell activation requires the engagement of CD6 and CD166." *Eur J Immunol* **34**(4): 930-40.

Hawkins, E. D. and S. M. Russell (2008). "Upsides and downsides to polarity and asymmetric cell division in leukemia." *Oncogene* **27**(55): 7003-17.

Hayday, A., E. Theodoridis, et al. (2001). "Intraepithelial lymphocytes: exploring the Third Way in immunology." *Nat Immunol* **2**(11): 997-1003.

He, X. C., J. Zhang, et al. (2004). "BMP signaling inhibits intestinal stem cell self-renewal through suppression of Wnt-beta-catenin signaling." *Nat Genet* **36**(10): 1117-21.

Helgeland, L., J. T. Vaage, et al. (1996). "Microbial colonization influences composition and T-cell receptor V beta repertoire of intraepithelial lymphocytes in rat intestine." *Immunology* **89**(4): 494-501.

Helming, L., J. Winter, et al. (2009). "The scavenger receptor CD36 plays a role in cytokine-induced macrophage fusion." *J Cell Sci* **122**(Pt 4): 453-9.

Helming, L. and S. Gordon (2009). "Molecular mediators of macrophage fusion." *Trends Cell Biol* **19**(10): 514-22.

Hermiston, M. L. and J. I. Gordon (1995). "In vivo analysis of cadherin function in the mouse intestinal epithelium: essential roles in adhesion, maintenance of differentiation, and regulation of programmed cell death." *J Cell Biol* **129**(2): 489-506.

Holland, A. J. and D. W. Cleveland (2009). "Boveri revisited: chromosomal instability, aneuploidy and tumorigenesis." *Nat Rev Mol Cell Biol* **10**(7): 478-87.

Hong, D., R. Gupta, et al. (2008). "Initiating and cancer-propagating cells in TEL-AML1-associated childhood leukemia." *Science* **319**(5861): 336-9.

Hooper, L. V., M. H. Wong, et al. (2001). "Molecular analysis of commensal host-microbial relationships in the intestine." *Science* **291**(5505): 881-4.

Hooper, L. V. and J. I. Gordon (2001). "Commensal host-bacterial relationships in the gut." *Science* **292**(5519): 1115-8.

Hooper, L. V., T. S. Stappenbeck, et al. (2003). "Angiogenins: a new class of microbicidal proteins involved in innate immunity." *Nat Immunol* **4**(3): 269-73.

Horn, E. J., A. Albor, et al. (2004). "RING protein Trim32 associated with skin carcinogenesis has anti-apoptotic and E3-ubiquitin ligase properties." *Carcinogenesis* **25**(2): 157-67.

Huang, H., B. M. Mahler-Araujo, et al. (2000). "APC mutations in sporadic medulloblastomas." *Am J Pathol* **156**(2): 433-7.

Ikeda, K. and T. Quertermous (2004). "Molecular isolation and characterization of a soluble isoform of activated leukocyte cell adhesion molecule that modulates endothelial cell function." *J Biol Chem* **279**(53): 55315-23.

Ireland, H., R. Kemp, et al. (2004). "Inducible Cre-mediated control of gene expression in the murine gastrointestinal tract: effect of loss of beta-catenin." *Gastroenterology* **126**(5): 1236-46.

Jackson, K. A., S. M. Majka, et al. (2001). "Regeneration of ischemic cardiac muscle and vascular endothelium by adult stem cells." *J Clin Invest* **107**(11): 1395-402.

Jensen, J., E. E. Pedersen, et al. (2000). "Control of endodermal endocrine development by Hes-1." *Nat Genet* **24**(1): 36-44.

Jezierska, A., W. Matysiak, et al. (2006). "ALCAM/CD166 protects breast cancer cells against apoptosis and autophagy." *Med Sci Monit* **12**(8): BR263-73.

Johansson, C. B., S. Youssef, et al. (2008). "Extensive fusion of haematopoietic cells with Purkinje neurons in response to chronic inflammation." *Nat Cell Biol* **10**(5): 575-83.

Joslyn, G., M. Carlson, et al. (1991). "Identification of deletion mutations and three new genes at the familial polyposis locus." *Cell* **66**(3): 601-13.

Jurjus, A. R., N. N. Khoury, et al. (2004). "Animal models of inflammatory bowel disease." *J Pharmacol Toxicol Methods* **50**(2): 81-92.

Kanki, J. P., S. Chang, et al. (1994). "The molecular cloning and characterization of potential chick DM-GRASP homologs in zebrafish and mouse." *J Neurobiol* **25**(7): 831-45.

Kaplan, J. H. and S. Lutsenko (2009). "Copper transport in mammalian cells: special care for a metal with special needs." *J Biol Chem* **284**(38): 25461-5.

Kaplan, K. B., A. A. Burds, et al. (2001). "A role for the Adenomatous Polyposis Coli protein in chromosome segregation." *Nat Cell Biol* **3**(4): 429-32.

Karin, M. (2005). "Inflammation and cancer: the long reach of Ras." *Nat Med* **11**(1): 20-1.

Karin, M. and F. R. Greten (2005). "NF-kappaB: linking inflammation and immunity to cancer development and progression." *Nat Rev Immunol* **5**(10): 749-59.

Karin, M. (2008). "The IkappaB kinase - a bridge between inflammation and cancer." *Cell Res* **18**(3): 334-42.

Kato, Y., Y. Tanaka, et al. (2006). "Involvement of CD166 in the activation of human gamma delta T cells by tumor cells sensitized with nonpeptide antigens." *J Immunol* **177**(2): 877-84.

Kayahara, T., M. Sawada, et al. (2003). "Candidate markers for stem and early progenitor cells, Musashi-1 and Hes1, are expressed in crypt base columnar cells of mouse small intestine." *FEBS Lett* **535**(1-3): 131-5.

Kiely, B., R. T. O'Donovan, et al. (2007). "Beta-catenin transcriptional activity is inhibited downstream of nuclear localisation and is not influenced by IGF signalling in oesophageal cancer cells." *Int J Cancer* **121**(9): 1903-9.

Kinzler, K. W. and B. Vogelstein (1996). "Lessons from hereditary colorectal cancer." *Cell* **87**(2): 159-70.

Klein, W. M., B. P. Wu, et al. (2007). "Increased expression of stem cell markers in malignant melanoma." *Mod Pathol* **20**(1): 102-7.

Klezovitch, O., T. E. Fernandez, et al. (2004). "Loss of cell polarity causes severe brain dysplasia in Lgl1 knockout mice." *Genes Dev* **18**(5): 559-71.

Knoblich, J. A. (2008). "Mechanisms of asymmetric stem cell division." *Cell* **132**(4): 583-97.

Koga, F., S. Kawakami, et al. (2003). "Impaired p63 expression associates with poor prognosis and uroplakin III expression in invasive urothelial carcinoma of the bladder." *Clin Cancer Res* **9**(15): 5501-7.

Kokkotou, E., A. C. Moss, et al. (2008). "Melanin-concentrating hormone as a mediator of intestinal inflammation." *Proc Natl Acad Sci U S A* **105**(30): 10613-8.

Kondo, M., I. L. Weissman, et al. (1997). "Identification of clonogenic common lymphoid progenitors in mouse bone marrow." *Cell* **91**(5): 661-72.

Korinek, V., N. Barker, et al. (1997). "Constitutive transcriptional activation by a beta-catenin-Tcf complex in APC-/- colon carcinoma." *Science* **275**(5307): 1784-7.

Korinek, V., N. Barker, et al. (1998). "Depletion of epithelial stem-cell compartments in the small intestine of mice lacking Tcf-4." *Nat Genet* **19**(4): 379-83.

Korinek, V., N. Barker, et al. (1998). "Two members of the Tcf family implicated in Wnt/beta-catenin signaling during embryogenesis in the mouse." *Mol Cell Biol* **18**(3): 1248-56.

Koster, M. I., S. Kim, et al. (2004). "p63 is the molecular switch for initiation of an epithelial stratification program." *Genes Dev* **18**(2): 126-31.

Koster, M. I., S. L. Lu, et al. (2006). "Reactivation of developmentally expressed p63 isoforms predisposes to tumor development and progression." *Cancer Res* **66**(8): 3981-6.

Kovacs, L. and C. S. Potten (1973). "An estimation of proliferative population size in stomach, jejunum and colon of DBA-2 mice." *Cell Tissue Kinet* **6**(2): 125-34.

Kristiansen, G., C. Pilarsky, et al. (2003). "ALCAM/CD166 is up-regulated in low-grade prostate cancer and progressively lost in high-grade lesions." *Prostate* **54**(1): 34-43.

Kroboth, K., I. P. Newton, et al. (2007). "Lack of adenomatous polyposis coli protein correlates with a decrease in cell migration and overall changes in microtubule stability." *Mol Biol Cell* **18**(3): 910-8.

Kuhn, R., J. Lohler, et al. (1993). "Interleukin-10-deficient mice develop chronic enterocolitis." *Cell* **75**(2): 263-74.

Kuhnert, F., C. R. Davis, et al. (2004). "Essential requirement for Wnt signaling in proliferation of adult small intestine and colon revealed by adenoviral expression of Dickkopf-1." *Proc Natl Acad Sci U S A* **101**(1): 266-71.

Kuphal, S., S. Wallner, et al. (2006). "Expression of Hugl-1 is strongly reduced in malignant melanoma." *Oncogene* **25**(1): 103-10.

Krause, D. S., N. D. Theise, et al. (2001). "Multi-organ, multi-lineage engraftment by a single bone marrow-derived stem cell." *Cell* **105**(3): 369-77.

Lagasse, E., H. Connors, et al. (2000). "Purified hematopoietic stem cells can differentiate into hepatocytes in vivo." *Nat Med* **6**(11): 1229-34.

Lechler, T. and E. Fuchs (2005). "Asymmetric cell divisions promote stratification and differentiation of mammalian skin." *Nature* **437**(7056): 275-80.

Lee, C. Y., B. D. Wilkinson, et al. (2006). "Brat is a Miranda cargo protein that promotes neuronal differentiation and inhibits neuroblast self-renewal." *Dev Cell* **10**(4): 441-9.

Lee, C. Y., K. J. Robinson, et al. (2006). "Lgl, Pins and aPKC regulate neuroblast self-renewal versus differentiation." *Nature* **439**(7076): 594-8.

Li, C., D. G. Heidt, et al. (2007). "Identification of pancreatic cancer stem cells." *Cancer Res* **67**(3): 1030-7.

Lickert, H., A. Kispert, et al. (2001). "Expression patterns of Wnt genes in mouse gut development." *Mech Dev* **105**(1-2): 181-4.

Lipkin, M. (1985). "Growth and development of gastrointestinal cells." *Annu Rev Physiol* **47**: 175-97.

Locke, M., C. L. Tinsley, et al. (2009). "TRIM32 is an E3 ubiquitin ligase for dysbindin." *Hum Mol Genet* **18**(13): 2344-58.

Logan, C. Y. and R. Nusse (2004). "The Wnt signaling pathway in development and disease." *Annu Rev Cell Dev Biol* **20**: 781-810.

Lu, X., X. Feng, et al. (2009). "Aberrant splicing of Hugl-1 is associated with hepatocellular carcinoma progression." *Clin Cancer Res* **15**(10): 3287-96.

Luna, L. G. (1968). *Manual of Histologic Staining Methods of the Armed Forces Institute of Pathology*. New York, McGraw-Hill Book Co.

Macpherson, A. J. and N. L. Harris (2004). "Interactions between commensal intestinal bacteria and the immune system." *Nat Rev Immunol* **4**(6): 478-85.

Madison, B. B., L. Dunbar, et al. (2002). "Cis elements of the villin gene control expression in restricted domains of the vertical (crypt) and horizontal (duodenum, cecum) axes of the intestine." *J Biol Chem* **277**(36): 33275-83.

Mantovani, A., T. Schioppa, et al. (2006). "Role of tumor-associated macrophages in tumor progression and invasion." *Cancer Metastasis Rev* 25(3): 315-22.

Martens, S. and H. T. McMahon (2008). "Mechanisms of membrane fusion: disparate players and common principles." *Nat Rev Mol Cell Biol* **9**(7): 543-56.

Maretto, S., M. Cordenonsi, et al. (2003). "Mapping Wnt/beta-catenin signaling during mouse development and in colorectal tumors." *Proc Natl Acad Sci U S A* **100**(6): 3299-304.

Masedunskas, A., J. A. King, et al. (2006). "Activated leukocyte cell adhesion molecule is a component of the endothelial junction involved in transendothelial monocyte migration." *FEBS Lett* **580**(11): 2637-45.

May, R., T. E. Riehl, et al. (2008). "Identification of a novel putative gastrointestinal stem cell and adenoma stem cell marker, doublecortin and CaM kinase-like-1, following radiation injury and in adenomatous polyposis coli/multiple intestinal neoplasia mice." *Stem Cells* **26**(3): 630-7.

Mekler, L. B. (1971). "[Hybridization of transformed cells with lymphocytes as 1 of the probable causes of the progression leading to the development of metastatic malignant cells]." *Vestn Akad Med Nauk SSSR* **26**(8): 80-9.

Mezzanzanica, D., M. Fabbi, et al. (2008). "Subcellular localization of activated leukocyte cell adhesion molecule is a molecular predictor of survival in ovarian carcinoma patients." *Clin Cancer Res* **14**(6): 1726-33.

Molenaar, M., M. van de Wetering, et al. (1996). "XTcf-3 transcription factor mediates beta-catenin-induced axis formation in Xenopus embryos." *Cell* **86**(3): 391-9.

Molla, M. and J. Panes (2007). "Radiation-induced intestinal inflammation." *World J Gastroenterol* **13**(22): 3043-6.

Mombaerts, P., J. Iacomini, et al. (1992). "RAG-1-deficient mice have no mature B and T lymphocytes." *Cell* **68**(5): 869-77.

Morin, P. J., B. Vogelstein, et al. (1996). "Apoptosis and APC in colorectal tumorigenesis." *Proc Natl Acad Sci U S A* **93**(15): 7950-4.

Morrison, S. J. and J. Kimble (2006). "Asymmetric and symmetric stem-cell divisions in development and cancer." *Nature* **441**(7097): 1068-74.

Moser, A. R., H. C. Pitot, et al. (1990). "A dominant mutation that predisposes to multiple intestinal neoplasia in the mouse." *Science* **247**(4940): 322-4.

Muncan, V., O. J. Sansom, et al. (2006). "Rapid loss of intestinal crypts upon conditional deletion of the Wnt/Tcf-4 target gene c-Myc." *Mol Cell Biol.*

Murtaugh, L. C., J. H. Chyung, et al. (1999). "Sonic hedgehog promotes somitic chondrogenesis by altering the cellular response to BMP signaling." *Genes Dev* **13**(2): 225-37.

Nakanishi, T., A. Kuroiwa, et al. (2002). "FISH analysis of 142 EGFP transgene integration sites into the mouse genome." *Genomics* **80**(6): 564-74.

Nelson, D. and R. Ganss (2006). "Tumor growth or regression: powered by inflammation." *J Leukoc Biol* **80**(4): 685-90.

Nern, C., I. Wolff, et al. (2009). "Fusion of hematopoietic cells with Purkinje neurons does not lead to stable heterokaryon formation under noninvasive conditions." *J Neurosci* **29**(12): 3799-807.

Nowell, P. C. (1976). "The clonal evolution of tumor cell populations." *Science* **194**(4260): 23-8.

Nygren, J. M., K. Liuba, et al. (2008). "Myeloid and lymphoid contribution to non-haematopoietic lineages through irradiation-induced heterotypic cell fusion." *Nat Cell Biol* **10**(5): 584-92.

Nygren, J. M., S. Jovinge, et al. (2004). "Bone marrow-derived hematopoietic cells generate cardiomyocytes at a low frequency through cell fusion, but not transdifferentiation." *Nat Med* **10**(5): 494-501.

O'Brien, C. A., A. Pollett, et al. (2007). "A human colon cancer cell capable of initiating tumour growth in immunodeficient mice." *Nature* **445**(7123): 106-10.

Oda, H., Y. Imai, et al. (1996). "Somatic mutations of the APC gene in sporadic hepatoblastomas." *Cancer Res* **56**(14): 3320-3.

Ohneda, O., K. Ohneda, et al. (2001). "ALCAM (CD166): its role in hematopoietic and endothelial development." *Blood* **98**(7): 2134-42.

Okamoto, R., T. Matsumoto, et al. (2006). "Regeneration of the intestinal epithelia: regulation of bone marrow-derived epithelial cell differentiation towards secretory lineage cells." *Hum Cell* **19**(2): 71-5.

Orlic, D., J. Kajstura, et al. (2001). "Bone marrow cells regenerate infarcted myocardium." *Nature* **410**(6829): 701-5.

Palermo, A., R. Doyonnas, et al. (2009). "Nuclear reprogramming in heterokaryons is rapid, extensive, and bidirectional." *Faseb J* **23**(5): 1431-40.

Pardal, R., M. F. Clarke, et al. (2003). "Applying the principles of stem-cell biology to cancer." *Nat Rev Cancer* **3**(12): 895-902.

Park, B. J., S. J. Lee, et al. (2000). "Frequent alteration of p63 expression in human primary bladder carcinomas." *Cancer Res* **60**(13): 3370-4.

Patel, D. D., S. F. Wee, et al. (1995). "Identification and characterization of a 100-kD ligand for CD6 on human thymic epithelial cells." *J Exp Med* **181**(4): 1563-8.

Pawelek, J. M. (2000). "Tumour cell hybridization and metastasis revisited." *Melanoma Res* **10**(6): 507-14.

Pawelek, J. M. (2005). "Tumour-cell fusion as a source of myeloid traits in cancer." *Lancet Oncol* **6**(12): 988-93.

Penman, G. A., L. Leung, et al. (2005). "The adenomatous polyposis coli protein (APC) exists in two distinct soluble complexes with different functions." *J Cell Sci* **118**(Pt 20): 4741-50.

Piazza, T., E. Cha, et al. (2005). "Internalization and recycling of ALCAM/CD166 detected by a fully human single-chain recombinant antibody." *J Cell Sci* **118**(Pt 7): 1515-25.

Picco, V., C. Hudson, et al. (2007). "Ephrin-Eph signalling drives the asymmetric division of notochord/neural precursors in Ciona embryos." *Development* **134**(8): 1491-7.

Pinto, D., A. Gregorieff, et al. (2003). "Canonical Wnt signals are essential for homeostasis of the intestinal epithelium." *Genes Dev* **17**(14): 1709-13.

Porter, E. M., C. L. Bevins, et al. (2002). "The multifaceted Paneth cell." *Cell Mol Life Sci* **59**(1): 156-70.

Potten, C. S., L. Kovacs, et al. (1974). "Continuous labelling studies on mouse skin and intestine." *Cell Tissue Kinet* **7**(3): 271-83.

Potten, C. S. (1977). "Extreme sensitivity of some intestinal crypt cells to X and gamma irradiation." *Nature* **269**(5628): 518-21.

Potten, C. S. (1990). "A comprehensive study of the radiobiological response of the murine (BDF1) small intestine." *Int J Radiat Biol* **58**(6): 925-73.

Potten, C. S., G. Owen, et al. (1990). "The temporal and spatial changes in cell proliferation within the irradiated crypts of the murine small intestine." *Int J Radiat Biol* **57**(1): 185-99.

Potten, C. S., C. Booth, et al. (2003). "Identification of a putative intestinal stem cell and early lineage marker; musashi-1." *Differentiation* **71**(1): 28-41.

Pull, S. L., J. M. Doherty, et al. (2005). "Activated macrophages are an adaptive element of the colonic epithelial progenitor niche necessary for regenerative responses to injury." *Proc Natl Acad Sci U S A* **102**(1): 99-104.

Rachkovsky, M., S. Sodi, et al. (1998). "Melanoma x macrophage hybrids with enhanced metastatic potential." *Clin Exp Metastasis* **16**(4): 299-312.

Radtke, F., H. Clevers, et al. (2006). "From gut homeostasis to cancer." *Curr Mol Med* **6**(3): 275-89.

Rennick, D., N. Davidson, et al. (1995). "Interleukin-10 gene knock-out mice: a model of chronic inflammation." *Clin Immunol Immunopathol* **76**(3 Pt 2): S174-8.

Reya, T. and H. Clevers (2005). "Wnt signalling in stem cells and cancer." *Nature* **434**(7035): 843-50.

Rizvi, A. Z., J. R. Swain, et al. (2006). "Bone marrow-derived cells fuse with normal and transformed intestinal stem cells." *Proc Natl Acad Sci U S A* **103**(16): 6321-5.

Roth, A., D. C. Drummond, et al. (2007). "Anti-CD166 single chain antibody-mediated intracellular delivery of liposomal drugs to prostate cancer cells." *Mol Cancer Ther* **6**(10): 2737-46.

Rubinfeld, B., I. Albert, et al. (1997). "Loss of beta-catenin regulation by the APC tumor suppressor protein correlates with loss of structure due to common somatic mutations of the gene." *Cancer Res* **57**(20): 4624-30.

Rupani, R., T. Handerson, et al. (2004). "Co-localization of beta1,6-branched oligosaccharides and coarse melanin in macrophage-melanoma fusion hybrids and human melanoma cells in vitro." *Pigment Cell Res* **17**(3): 281-8.

Sacco, A., R. Doyonnas, et al. (2008). "Self-renewal and expansion of single transplanted muscle stem cells." *Nature* **456**(7221): 502-6.

Sakamoto, I., S. Kishida, et al. (2000). "A novel beta-catenin-binding protein inhibits beta-catenin-dependent Tcf activation and axis formation." *J Biol Chem* **275**(42): 32871-8.

Sangiorgi, E. and M. R. Capecchi (2008). "Bmi1 is expressed in vivo in intestinal stem cells." *Nat Genet* **40**(7): 915-20.

Sansom, O. J., K. R. Reed, et al. (2004). "Loss of Apc in vivo immediately perturbs Wnt signaling, differentiation, and migration." *Genes Dev* **18**(12): 1385-90.

Sansom, O. J., V. S. Meniel, et al. (2007). "Myc deletion rescues Apc deficiency in the small intestine." *Nature* **446**(7136): 676-9.

Sato, T., R. G. Vries, et al. (2009). "Single Lgr5 stem cells build crypt-villus structures in vitro without a mesenchymal niche." *Nature*.

Schimanski, C. C., G. Schmitz, et al. (2005). "Reduced expression of Hugl-1, the human homologue of Drosophila tumour suppressor gene lgl, contributes to progression of colorectal cancer." *Oncogene* **24**(19): 3100-9.

Schuck, S. and K. Simons (2004). "Polarized sorting in epithelial cells: raft clustering and the biogenesis of the apical membrane." *J Cell Sci* **117**(Pt 25): 5955-64.

Schwamborn, J. C., E. Berezikov, et al. (2009). "The TRIM-NHL protein TRIM32 activates microRNAs and prevents self-renewal in mouse neural progenitors." *Cell* **136**(5): 913-25.

Scoville, D. H., T. Sato, et al. (2008). "Current view: intestinal stem cells and signaling." *Gastroenterology* **134**(3): 849-64.

Selinger, D. W., R. M. Saxena, et al. (2003). "Global RNA half-life analysis in Escherichia coli reveals positional patterns of transcript degradation." *Genome Res* **13**(2): 216-23.

Shibata, H., K. Toyama, et al. (1997). "Rapid colorectal adenoma formation initiated by conditional targeting of the Apc gene." *Science* **278**(5335): 120-3.

Sierra, J., T. Yoshida, et al. (2006). "The APC tumor suppressor counteracts beta-catenin activation and H3K4 methylation at Wnt target genes." *Genes Dev* **20**(5): 586-600.

Simpson, R. J. and A. T. McKie (2009). "Regulation of intestinal iron absorption: the mucosa takes control?" *Cell Metab* **10**(2): 84-7.

Sodi, S. A., A. K. Chakraborty, et al. (1998). "Melanoma x macrophage fusion hybrids acquire increased melanogenesis and metastatic potential: altered N-glycosylation as an underlying mechanism." *Pigment Cell Res* **11**(5): 299-309.

Sonoda, J. and R. P. Wharton (2001). "Drosophila Brain Tumor is a translational repressor." *Genes Dev* **15**(6): 762-73.

Soriano, P. (1999). "Generalized lacZ expression with the ROSA26 Cre reporter strain." *Nat Genet* **21**(1): 70-1.

Spees, J. L., S. D. Olson, et al. (2003). "Differentiation, cell fusion, and nuclear fusion during ex vivo repair of epithelium by human adult stem cells from bone marrow stroma." *Proc Natl Acad Sci U S A* **100**(5): 2397-402.

Staal, F. J. and H. C. Clevers (2005). "WNT signalling and haematopoiesis: a WNT-WNT situation." *Nat Rev Immunol* **5**(1): 21-30.

Storey, J. D. (2002). "A direct approach to false discovery rates." *Journal of the Royal Statistical Society, Series B* **64**: 479-498.

Su, L. K., G. Steinbach, et al. (2000). "Genomic rearrangements of the APC tumor-suppressor gene in familial adenomatous polyposis." *Hum Genet* **106**(1): 101-7.

Takemaru, K., S. Yamaguchi, et al. (2003). "Chibby, a nuclear beta-catenin-associated antagonist of the Wnt/Wingless pathway." *Nature* **422**(6934): 905-9.

Tang, F., C. Barbacioru, et al. (2009). "mRNA-Seq whole-transcriptome analysis of a single cell." *Nat Methods* **6**(5): 377-82.

Terada, N., T. Hamazaki, et al. (2002). "Bone marrow cells adopt the phenotype of other cells by spontaneous cell fusion." *Nature* **416**(6880): 542-5.

Tomita, K., A. van Bokhovenâ€ , et al. (2003). "Activated Leukocyte Cell Adhesion Molecule (ALCAM) Expression is Associated with a Poor Prognosis for Bladder Cancer Patients." *Urooncology* **3**(3): 121 - 129.

Topol, L., X. Jiang, et al. (2003). "Wnt-5a inhibits the canonical Wnt pathway by promoting GSK-3-independent beta-catenin degradation." *J Cell Biol* **162**(5): 899-908.

Tsuruga, T., S. Nakagawa, et al. (2007). "Loss of Hugl-1 expression associates with lymph node metastasis in endometrial cancer." *Oncol Res* **16**(9): 431-5.

Turner, J. R. (2009). "Intestinal mucosal barrier function in health and disease." *Nat Rev Immunol* **9**(11): 799-809.

Tyurina, Y. Y., V. A. Tyurin, et al. (2008). "Oxidative lipidomics of gamma-irradiation-induced intestinal injury." *Free Radic Biol Med* **44**(3): 299-314.

Uchida, N., Z. Yang, et al. (1997). "The characterization, molecular cloning, and expression of a novel hematopoietic cell antigen from CD34+ human bone marrow cells." *Blood* **89**(8): 2706-16.

van de Wetering, M., E. Sancho, et al. (2002). "The beta-catenin/TCF-4 complex imposes a crypt progenitor phenotype on colorectal cancer cells." *Cell* **111**(2): 241-50.

van der Flier, L. G., J. Sabates-Bellver, et al. (2007). "The Intestinal Wnt/TCF Signature." *Gastroenterology* **132**(2): 628-32.

van der Flier, L. G. and H. Clevers (2009). "Stem cells, self-renewal, and differentiation in the intestinal epithelium." *Annu Rev Physiol* **71**: 241-60.

van Es, J. H., P. Jay, et al. (2005). "Wnt signalling induces maturation of Paneth cells in intestinal crypts." *Nat Cell Biol* **7**(4): 381-6.

van Kempen, L. C., J. J. van den Oord, et al. (2000). "Activated leukocyte cell adhesion molecule/CD166, a marker of tumor progression in primary malignant melanoma of the skin." *Am J Pathol* **156**(3): 769-74.

Vassilopoulos, G., P. R. Wang, et al. (2003). "Transplanted bone marrow regenerates liver by cell fusion." *Nature* **422**(6934): 901-4.

Verma, A., N. K. Shukla, et al. (2005). "MEMD/ALCAM: a potential marker for tumor invasion and nodal metastasis in esophageal squamous cell carcinoma." *Oncology* **68**(4-6): 462-70.

Vermeulen, L., M. R. Sprick, et al. (2008). "Cancer stem cells--old concepts, new insights." *Cell Death Differ* **15**(6): 947-58.

Vignery, A. (2005). "Macrophage fusion: the making of osteoclasts and giant cells." *J Exp Med* **202**(3): 337-40.

Vignery, A. (2005). "Macrophage fusion: are somatic and cancer cells possible partners?" *Trends Cell Biol* **15**(4): 188-93.

Visvader, J. E. and G. J. Lindeman (2008). "Cancer stem cells in solid tumours: accumulating evidence and unresolved questions." *Nat Rev Cancer* **8**(10): 755-68.

Vogelstein, B. and K. W. Kinzler (2004). "Cancer genes and the pathways they control." *Nat Med* **10**(8): 789-99.

Wang, X., H. Willenbring, et al. (2003). "Cell fusion is the principal source of bone-marrow-derived hepatocytes." *Nature* **422**(6934): 897-901.

Wang, Z., M. Gerstein, et al. (2009). "RNA-Seq: a revolutionary tool for transcriptomics." *Nat Rev Genet* **10**(1): 57-63.

Wehkamp, J., H. Chu, et al. (2006). "Paneth cell antimicrobial peptides: topographical distribution and quantification in human gastrointestinal tissues." *FEBS Lett* **580**(22): 5344-50.

Weichert, W., T. Knosel, et al. (2004). "ALCAM/CD166 is overexpressed in colorectal carcinoma and correlates with shortened patient survival." *J Clin Pathol* **57**(11): 1160-4.

Weimann, J. M., C. B. Johansson, et al. (2003). "Stable reprogrammed heterokaryons form spontaneously in Purkinje neurons after bone marrow transplant." *Nat Cell Biol* **5**(11): 959-66.

Weiser, M. M. (1973). "Intestinal epithelial cell surface membrane glycoprotein synthesis. I. An indicator of cellular differentiation." *J Biol Chem* **248**(7): 2536-41.

Weiser, M. M. (1973). "Intestinal epithelial cell surface membrane glycoprotein synthesis. II. Glycosyltransferases and endogenous acceptors of the undifferentiated cell surface membrane." *J Biol Chem* **248**(7): 2542-8.

Weiss, L. (2000). "Metastasis of cancer: a conceptual history from antiquity to the 1990s." *Cancer Metastasis Rev* **19**(3-4): I-XI, 193-383.

Westfall, M. D. and J. A. Pietenpol (2004). "p63: Molecular complexity in development and cancer." *Carcinogenesis* **25**(6): 857-64.

Willenbring, H., A. S. Bailey, et al. (2004). "Myelomonocytic cells are sufficient for therapeutic cell fusion in liver." *Nat Med* **10**(7): 744-8.

Wirtz-Peitz, F., T. Nishimura, et al. (2008). "Linking cell cycle to asymmetric division: Aurora-A phosphorylates the Par complex to regulate Numb localization." *Cell* **135**(1): 161-73.

Wong, M. H., P. Oelkers, et al. (1994). "Expression cloning and characterization of the hamster ileal sodium-dependent bile acid transporter." *J Biol Chem* **269**(2): 1340-7.

Wong, M. H., M. L. Hermiston, et al. (1996). "Forced expression of the tumor suppressor adenomatosis polyposis coli protein induces disordered cell migration in the intestinal epithelium." *Proc Natl Acad Sci U S A* **93**(18): 9588-93.

Wong, M. H., B. Rubinfeld, et al. (1998). "Effects of forced expression of an NH2-terminal truncated beta-Catenin on mouse intestinal epithelial homeostasis." *J Cell Biol* **141**(3): 765-77.

Wong, M. H., J. R. Saam, et al. (2000). "Genetic mosaic analysis based on Cre recombinase and navigated laser capture microdissection." *Proc Natl Acad Sci U S A* **97**(23): 12601-6.

Wright, D. E., A. J. Wagers, et al. (2001). "Physiological migration of hematopoietic stem and progenitor cells." *Science* **294**(5548): 1933-6.

Xavier, R. J. and D. K. Podolsky (2007). "Unravelling the pathogenesis of inflammatory bowel disease." *Nature* **448**(7152): 427-34.

Xu, J. and J. I. Gordon (2003). "Inaugural Article: Honor thy symbionts." *Proc Natl Acad Sci U S A* **100**(18): 10452-9.

Yamashita, Y. M., A. P. Mahowald, et al. (2007). "Asymmetric inheritance of mother versus daughter centrosome in stem cell division." *Science* **315**(5811): 518-21.

Yamashita, Y. M., D. L. Jones, et al. (2003). "Orientation of asymmetric stem cell division by the APC tumor suppressor and centrosome." *Science* **301**(5639): 1547-50.

Yang, A., R. Schweitzer, et al. (1999). "p63 is essential for regenerative proliferation in limb, craniofacial and epithelial development." *Nature* **398**(6729): 714-8.

Yang, Y., S. Takeuchi, et al. (2005). "Methylation analysis of the adenomatous polyposis coli (APC) gene in adult T-cell leukemia/lymphoma." *Leuk Res* **29**(1): 47-51.

Yasumi, M., T. Sakisaka, et al. (2005). "Direct binding of Lgl2 to LGN during mitosis and its requirement for normal cell division." *J Biol Chem* **280**(8): 6761-5.

Yilmaz, Y., R. Lazova, et al. (2005). "Donor Y chromosome in renal carcinoma cells of a female BMT recipient: visualization of putative BMT-tumor hybrids by FISH." *Bone Marrow Transplant* **35**(10): 1021-4.

Yu, F., C. T. Kuo, et al. (2006). "Drosophila neuroblast asymmetric cell division: recent advances and implications for stem cell biology." *Neuron* **51**(1): 13-20.

Yu, J., M. A. Vodyanik, et al. (2006). "Human embryonic stem cells reprogram myeloid precursors following cell-cell fusion." *Stem Cells* **24**(1): 168-76.

Zwadlo, G., E. B. Brocker, et al. (1985). "A monoclonal antibody to a differentiation antigen present on mature human macrophages and absent from monocytes." *J Immunol* **134**(3): 1487-92.